

**Serbian Biochemical Society  
Seventh Conference**

*"Biochemistry of Control in Life and Technology"*

*Proceedings*

*Faculty of Chemistry  
Belgrade 2017*

# Serbian Biochemical Society

**President:** Marija Gavrović-Jankulović

**Vice-president:** Suzana Jovanović-Šanta

**General Secretary:** Milan Nikolić

**Treasurer:** Milica Popović

## Scientific Board

Milica Bajčetić

Duško Blagojević

Polina Blagojević

Jelena Bogdanović

Pristov

Nataša Božić

Ivona Baričević-Jones

Jelena Bašić

Tanja Ćirković

Veličković

Milena Ćurčić

Milena Čavić

Milena Despotović

Snežana Dragović

Marija Gavrović-  
Jankulović

Nevena Grdović

Lidija Israel-Živković

David R. Jones

Suzana Jovanović-Šanta

Ivanka Karadžić

Vesna Kojić

Jelena Kotur-

Stevuljević

Snežana Marković

Sanja Mijatović

Djordje Miljković

Marina Mitrović

Jelena Nestorov

Ivana Nikolić

Milan Nikolić

Miroslav Nikolić

Zorana Oreščanin-  
Dušić

Svetlana Paškaš

Andelka Petri

Edvard T. Petri

Natalija Polović

Tamara Popović

Željko Popović

Radivoje Prodanović

Niko Radulović

Ivan Spasojević

Karmen Stankov

Aleksandra Stanković

Tijana Stanković

Ivana Stojanović (ib)

Ivana Stojanović (ibiss)

Aleksandra Uskoković

Perica J. Vasiljević

Milan Zarić

Aleksandra Zeljković

Marko N. Živanović

Milan Žižić

## Proceedings

**Editor:** Ivan Spasojević

**Technical secretary:** Jelena Nestorov

**Cover design:** Zoran Beloševac

**Publisher:** Faculty of Chemistry, Serbian Biochemical Society

**Printed by:** Colorgrafx, Belgrade

Serbian Biochemical Society  
Seventh Conference

with international participation

Faculty of Chemistry, University of Belgrade  
10.11.2017. Belgrade, Serbia

***“Biochemistry of Control in Life and Technology”***

# PROGRAMME

- 10:00-10:10      Welcome message  
Marija Gavrović-Jankulović  
(President of the Serbian Biochemical Society)
- 10:10-10:40      Ario de Marco  
University of Nova Gorica, Vipava, Slovenia  
**Nanobodies: Towards rational design of immune-reagents**  
(FEBS3+ Lecture)
- 10:40-11:00      Vladimir P. Beškoski  
Faculty of Chemistry, University of Belgrade  
**Classical biochemistry / biotechnology and molecular  
biochemistry / biotechnology of environmental microorganisms in  
degradation of petroleum products and persistent organic  
pollutants**
- 11:00-11:20      Jakub Nowak  
NanoTemper Technologies, Krakow, Poland  
**Microscale thermophoresis and NanoDSF as advanced methods  
in life science research**
- 11:20-11:50      Coffee break
- 11:50-12:10      Marija Vidović  
Institute for Multidisciplinary Research, University of Belgrade  
**Sun as a stressor and/or regulator of plant metabolism: responses  
to UV radiation and high light**

- 12:10-12:30 Vladimir B. Mihailović  
Faculty of Science, University of Kragujevac  
**Phytochemical characterization and biological activities of some *Gentiana* plants from Serbia**
- 12:30-12:50 Marija Genčić  
Faculty of Science and Mathematics, University of Niš  
**Phytochemical re-examination of well-studied medicinal plants as an useful approach in the discovery of (novel) potentially bioactive natural products – The case of *Inula helenium* L.**
- 12:50-13:10 Dalibor Stanković  
The Vinča Institute of Nuclear Sciences, University of Belgrade  
**Nano-structured materials and their application in the detection of biological compounds**
- 13.10-13.40 Poster session
- 13.40-14.00 Cocktail
- 14:00-14:20 Ivana Beara  
Faculty of Sciences, University of Novi Sad  
**Battle against inflammation: polyphenols targeting selective inhibition of cyclooxygenase-2**
- 14:20-14:40 Tamara Saksida  
Institute for Biological Research “Siniša Stanković”, University of Belgrade  
**The role of macrophage migration inhibitory factor in the development of obesity and altered intestinal permeability**

14:40-15:00

Žanka Bojić Trbojević

Institute for the Application of Nuclear Energy - INEP, University of  
Belgrade

**Galectin-1 ligands in human trophoblasts**

15.00-15:20

Discussion and concluding remarks

## Poster Session

Ana Marija Balaž

Center of Chemistry, Institute of Chemistry, Technology and Metallurgy, University of Belgrade

**Semi-rational design of cellobiose dehydrogenase from *Phanerochaete chrysosporium* for increased oxidative stability and high-throughput screening of library mutants**

Sanja Berežni

Department of Chemistry, Biochemistry and Environmental Protection, Faculty of Sciences, University of Novi Sad

**Novel lignans from *Anthriscus sylvestris*: 3'-demethoxy podophyllotoxin and 3'-demethoxypodophyllotoxone**

Stefan Z. Blagojević

Department of Biology and Ecology, Faculty of Science, University of Kragujevac

**Statistical clustering of IC<sub>50</sub> values as bioactive substances cytotoxicity indicators on HCT-116 and SW-480 cell lines of colon cancer**

Petar Čanović

Department of Biochemistry, Faculty of Medical Sciences, University of Kragujevac

**Two newly synthesized ruthenium(II) polypyridyl complexes induce selective apoptosis of HeLa cancer cells via mitochondrial pathway**

Nikola Gligorijević

Institute for the Application of Nuclear Energy - INEP, University of Belgrade

**Influence of fibrinogen modifications on its interaction with insulin-like growth factor-binding protein 1**

Tamara Janković

Department of Medical Biochemistry, Faculty of Pharmacy, University of Belgrade

**In vitro comparison of antioxidative potential of differently substituted chalcones**

Jaroslav Katrlík

Institute of Chemistry, Slovak Academy of Sciences

**Determination of protein glycosylation using lectin-based protein microarrays**

Jelena Korać

Department of Life Sciences, Institute for Multidisciplinary Research, University of Belgrade

**Ligand and redox interactions of adrenaline with iron at physiological pH**

Gordana Kovačević

Innovation Center of the Faculty of Chemistry, University of Belgrade

**Protein engineering and development of high-throughput screening methods for glucose-oxidase gene library**

Branka Lončarević

Department of Chemistry, Institute of Chemistry, Technology and Metallurgy, University of Belgrade

**Application of microbial levan as a new component for production of graft copolymer with polystyrene**

Ivana Lukić

Department of Research and Development, Institute of Virology, Vaccine and Sera „Torlak“, Belgrade

**The role of heterologous immunity in resistance to ocular chlamydial infection**

Tatjana Majkić

Department of Chemistry, Biochemistry and Environmental Protection, Faculty of Sciences, University of Novi Sad

**Antioxidant and anti-inflammatory activity of Merlot wine**

Emilija Marinković

Institute of Virology, Vaccines and Sera - Torlak, Belgrade

**The effect of prophylactic treatment of recombinant banana on TNBS-induced colitis in BALB/C mice**

Nevena Marković

Institute of Chemistry, Technology and Metallurgy, University of Belgrade

**Synthesis of potential pharmaceutical active ingredients using omega-transaminase**

Ana Medić

School of Medicine, University of Belgrade

**Biodegradation of 2,6-di-tert-butylphenol by *Pseudomonas aeruginosa* strain**

Ivana Milenković

Department of Life Science, Institute for Multidisciplinary Research, University of Belgrade

**The influence of coated nanoCeO<sub>2</sub> on the phenol content in wheat and pea**

Ivan Mrkić

Innovation Centre of Faculty of Chemistry, University of Belgrade

**Newly designed soluble hemagglutinin-Der p 2 chimera is a potential candidate for allergen specific immunotherapy**

Ivana Nemeš

Department of Chemistry, Biochemistry and Environmental Protection, Faculty of Sciences, University of Novi Sad

**Chemical composition and antioxidant potential of hydromethanolic extracts of celery (*Apium graveolens* L.) cultivated at different locations in Vojvodina**

Danijela Nikodijević

Department for Biology and Ecology, Faculty of Science, University of Kragujevac

**Effects of the bee products on energy status and relative expression of biotransformation and apoptosis genes in healthy and colon cancer cells**

Teodora Obradović

Department of Medical Biochemistry, Faculty of Pharmacy, University of Belgrade

**Comparison of prooxidative properties of four different tyrosine kinase inhibitors**

Miloš Opačić

Department of Life Sciences, Institute for Multidisciplinary Research, University of Belgrade

**Imaging and regional distribution of copper, zinc, manganese and iron in sclerotic hippocampi of patients with mesial temporal lobe epilepsy**

Snežana Orčić

Department of Biology and Ecology, Faculty of Sciences, University of Novi Sad

**Environmental effect on metallothionein gene expression in honey bee (*A. mellifera*)**

Marijana Pavlović

Department of Experimental Oncology, Institute for Oncology and Radiology of Serbia, Belgrade

**Mechanism of action of novel ruthenium(III) complexes toward cisplatin resistant MDA-MB231 breast cells**

Vladana Petković

Vinča Institute of Nuclear Sciences, University of Belgrade

**Direct effects of  $\gamma$ -rays in MCF-7 breast cancer cells**

Diandra Pintac

Department of Chemistry, Biochemistry and Environmental Protection, Faculty of Sciences, University of Novi Sad

**Is wine price a guarantee for its healthful properties?**

Jovana J. Plavša

Department of Biology and Ecology, Faculty of Sciences, University of Novi Sad

**Identification of potential inhibitors of AKR1C3 and preparation for structural analyses**

Ivana Prodić

Faculty of Chemistry – Innovation Centre Ltd., University of Belgrade

**Whole grain of peanut digestomics according to harmonized static digestion protocol suitable for solid food and characterization of short digestion resistant fragments.**

Marija Stanojević

Institute for Pathological Physiology, Faculty of Medicine, University of Belgrade

**Minor depolarization mediates magnesium suppression of nonsynaptic epileptiform activity**

Nikola Tatalović

Department of Physiology, Institute for Biological Research “Siniša Stanković”,  
University of Belgrade

**The effects of ibogaine on uterine redox homeostasis and contractility**

Tamara Uzelac

Faculty of Chemistry, University of Belgrade

**Serum redox-homeostasis in half-marathons**

Teodora Vidonja Uzelac

Department of Physiology, Institute for Biological Research “Siniša Stanković”,  
University of Belgrade

**Ibogaine redox potential – the effects on antioxidant enzymes after ingestion**

Sanja Vujčić

Department of Medical Biochemistry, Faculty of Pharmacy, University of Belgrade

**Estimation of the overall cardiovascular risk in patients with acute myocardial infarction, stroke and polycystic ovary syndrome by DOI score (dyslipidemia, oxidative stress and inflammation) calculation**

Aleksandra Vukašinović

Department of Medical Biochemistry, Faculty of Pharmacy, University of Belgrade

**DOI score – novel biomarker for cardiovascular diseases**

Aleksandra Vukašinović

Department of Medical Biochemistry, Faculty of Pharmacy, University of Belgrade

**Telomerase stability study using Real-Time telomeric repeat amplification protocol**

Nevena Zelenović

Institute for Chemistry, Technology and Metallurgy, University of Belgrade

**Directed evolution of cellulase from *Trichoderma reesei* for higher activity and development of microtiter plate assay based on cellobiose dehydrogenase**

Aleksandra Žeradžanin

Department of Chemistry, Institute of Chemistry, Technology and Metallurgy, University of Belgrade

**Structural characterization of EPS produced by *Brachybacterium paraconglomeratum* sp. CH-KOV3**

---

## Foreword

Dear Colleagues

It is a great pleasure to welcome you to the 7<sup>th</sup> Conference of the Serbian Biochemical Society, entitled "Biochemistry of Control in Life and Technology".

Apparently, biochemistry is sprouting in Serbia. This year, we have over 30 young participants at the final year of PhD studies with poster presentations. The collaboration within FEBS3+ (Croatia, Hungary, Slovenia, and Serbia) Meeting Programme is containing with the invited lecture of our dear colleague Ario de Marco from the University of Nova Gorica. Traditionally, we invited eight potent scientists from four major universities in Serbia to deliver lectures at the Conference.

I would like to express my gratitude to the members of the Scientific Board who suggested lecturers and to all respected colleagues who accepted the invitation. I wish you all fruitful discussions within our biochemical hub.

*Editor of the Proceedings*  
*Ivan Spasojević*



## Proceedings

*Ario de Marco*

Nanobodies: Towards rational design of immune-reagents (19)

*Vladimir P. Beškosi*

Classical biochemistry / biotechnology and molecular biochemistry / biotechnology of environmental microorganisms in degradation of petroleum products and persistent organic pollutants (21)

*Jakub Nowak*

Microscale thermophoresis and NanoDSF as advanced methods in life science research (37)

*Marija Vidović*

Sun as a stressor and/or regulator of plant metabolism: responses to UV radiation and high light (39)

*Vladimir B. Mihailović*

Phytochemical characterization and biological activities of some *Gentiana* plants from Serbia (53)

*Marija Genčić*

Phytochemical re-examination of well-studied medicinal plants as an useful approach in the discovery of (novel) potentially bioactive natural products - The case of *Inula helenium* L. (65)

*Dalibor Stanković*

Nano-structured materials and their application in the detection of biological compounds (81)

*Ivana Beara*

Battle against inflammation: polyphenols targeting selective inhibition of cyclooxygenase-2 (91)

*Tamara Saksida*

The role of macrophage migration inhibitory factor in the development of obesity and altered intestinal permeability (101)

*Žanka Bojić Trbojević*

Galectin-1 ligands in human trophoblasts (109)

*Ana Marija Balaž*

Semi-rational design of cellobiose dehydrogenase from *Phanerochaete chrysosporium* for increased oxidative stability and high-throughput screening of library mutants (121)

*Sanja Berežni*

Novel lignans from *Anthriscus sylvestris*: 3'-demethoxy podophyllotoxin and 3'-demethoxypodophyllotoxone (125)

*Stefan Z. Blagojević*

Statistical clustering of IC<sub>50</sub> values as bioactive substances cytotoxicity indicators on HCT-116 and SW-480 cell lines of colon cancer (129)

*Petar Čanović*

Two newly synthesized ruthenium(II) polypyridyl complexes induce selective apoptosis of HeLa cancer cells via mitochondrial pathway (133)

*Nikola Gligorijević*

Influence of fibrinogen modifications on its interaction with insulin-like growth factor-binding protein 1 (135)

*Tamara Janković*

*In vitro* comparison of antioxidative potential of differently substituted chalcones (137)

*Jaroslav Katrlík*

Determination of protein glycosylation using lectin-based protein microarrays (141)

*Jelena Korać*

Ligand and redox interactions of adrenaline with iron at physiological pH (143)

*Gordana Kovačević*

Protein engineering and development of high-throughput screening methods for glucose-oxidase gene library (145)

*Branka Lončarević*

Application of microbial levan as a new component for production of graft copolymer with polystyrene (149)

*Ivana Lukić*

The role of heterologous immunity in resistance to ocular chlamydial infection (151)

*Tatjana Majkić*

Antioxidant and anti-inflammatory activity of Merlot wine (155)

*Emilija Marinković*

The effect of prophylactic treatment of recombinant banana on TNBS-induced colitis in BALB/C mice (157)

*Nevena Marković*

Synthesis of potential pharmaceutical active ingredients using omega-transaminase (159)

*Ana Medić*

Biodegradation of 2,6-di-tert-butylphenol by *Pseudomonas aeruginosa* strain ai (163)

*Ivana Milenković*

The influence of coated nanoCeO<sub>2</sub> on the phenol content in wheat and pea (165)

*Ivan Mrkić*

Newly designed soluble hemagglutinin-Der p 2 chimera is a potential candidate for allergen specific immunotherapy (169)

*Ivana Nemeš*

Chemical composition and antioxidant potential of hydromethanolic extracts of celery (*Apium graveolens* L.) cultivated at different locations in Vojvodina (171)

*Danijela Nikodijević*

Effects of the bee products on energy status and relative expression of biotransformation and apoptosis genes in healthy and colon cancer cells (173)

*Teodora Obradović*

Comparison of prooxidative properties of four different tyrosine kinase inhibitors (177)

*Miloš Opačić*

Imaging and regional distribution of copper, zinc, manganese and iron in sclerotic hippocampi of patients with mesial temporal lobe epilepsy (179)

*Snežana Orčić*

Environmental effect on metallothionein gene expression in honey bee (*A. mellifera*) (183)

*Marijana Pavlović*

Mechanism of action of novel ruthenium(III) complexes toward cisplatin resistant MDA-MB231 breast cells (185)

*Vladana Petković*

Direct effects of  $\gamma$ -rays in MCF-7 breast cancer cells (189)

*Diandra Pintać*

Is wine price a guarantee for its healthful properties? (191)

*Jovana J. Plavša*

Identification of potential inhibitors of AKR1C3 and preparation for structural analyses (193)

*Ivana Prodić*

Whole grain of peanut digestomics according to Harmonized static digestion protocol suitable for solid food and characterization of short digestion resistant fragments (195)

*Marija Stanojević*

Minor depolarization mediates magnesium suppression of nonsynaptic epileptiform activity (199)

*Nikola Tatalović*

The effects of ibogaine on uterine redox homeostasis and contractility (203)

*Tamara Uzelac*

Serum redox-homeostasis in half-marathons (207)

*Teodora Vidonja Uzelac*

Ibogaine redox potential - the effects on antioxidant enzymes after ingestion (211)

*Sanja Vujčić*

Estimation of the overall cardiovascular risk in patients with acute myocardial infarction, stroke and polycystic ovary syndrome by DOI score (dyslipidemia, oxidative stress and inflammation) calculation (213)

*Aleksandra Vukašinić*

DOI score - novel biomarker for cardiovascular diseases (217)

*Aleksandra Vukašinić*

Telomerase stability study using Real-Time telomeric repeat amplification protocol (221)

*Nevena Zelenović*

Directed evolution of cellulase from *Trichoderma reesei* for higher activity and development of microtiter plate assay based on cellobiose dehydrogenase (225)

*Aleksandra Žeradžanin*

Structural characterization of EPS produced by *Brachybacterium paraconglomeratum* sp. CH-KOV3 (227)

---

## Nanobodies: Towards rational design of immune-reagents

---

Ario de Marco\*

Laboratory for Environmental and Life Sciences, University of Nova Gorica, Vipava, Slovenia

\*e-mail: ario.demarco@ung.si

Antibodies are irreplaceable reagents in both research and clinical practice. Despite their relevance, the structural complexity of conventional mono- and polyclonal antibodies (IgG) has always been a limit for their engineering towards reagents optimized for specific applications, such as *in vivo* diagnostics and therapy. Furthermore, their isolation is time consuming, their production expensive, and their functionalization results often in heterogeneous macromolecule populations. These drawbacks promoted the search for both innovative antibody isolation strategies and alternative scaffolds. *In vitro* panning of pre-immune collections of recombinant antibody fragments allows for the simple and fast recovery of binders. Since they did not undergo somatic maturation, their affinity for targets can be insufficient but on the other hand they can be rapidly mutated by standard molecular biology techniques to generate second-generation antibodies among which to identify clones with improved characteristics. Both stochastic and rational methods have been proposed for the optimization process. Random mutagenesis followed by panning at stringent conditions has been successful used to select binders with improved physical characteristics. Rational methods try to identify *in silico* key residues involved in the regulation of specific antibody features, such as stability or binding affinity. The accuracy of these methods usually depends on the calculation resources. In this perspective, smaller molecules can be analyzed “better” than larger because of their restricted number of residues. Nanobodies of small dimensions have been long appreciated, since they enable better tissue penetration, shorter clearance time, higher yields. Now it becomes evident that this characteristic makes them also optimal objects for modeling.



---

# **Classical biochemistry / biotechnology and molecular biochemistry / biotechnology of environmental microorganisms in degradation of petroleum products and persistent organic pollutants**

---

Vladimir P. Beškoski\*

*Department of Biochemistry, Faculty of Chemistry, University of Belgrade, Belgrade, Serbia*

\**e-mail: vbeskoski@chem.bg.ac.rs*

In order to obtain successful biotechnological processes, it is necessary to analyse both microbiological and chemical parameters. The variety of methods includes classical biochemistry/biotechnology and molecular biochemistry/biotechnology. In this paper some of the methods that are being widely used for the analysis of *ex situ* bioremediation on the industrial scale are described. The analysis of microbial communities and individual isolates includes the determination of the number of microorganisms, individual groups, the characterization of growth on various substrates, enzymatic and lipid profiles and the 16S rRNA analysis, as well as sophisticated methods for the analysis of the protein profile for the characterization of certain isolates. Since the microbiological analysis alone is not sufficient to follow biotechnological processes and changes that occur during bioremediation, special attention has been paid to the analysis of pollutants from the simplest gravimetric analysis through the structural instrumental analysis such as GC-FID to GC-MS and the very sophisticated analysis, such as the comprehensive GCxGC-MS which can provide and enable one part of the metabolite analysis, i.e. metabolomics.

## **Environmental pollution**

Rapid growth and development of the industrial civilization has led to the pollution of the environment by a wide range of substances of different origin. Only 10% of the pollution comes from large incidents of spills that cause contamination of the seashore of the sea, lakes or watercourses and attract significant media attention. It is important to point out that pollutants from the location where they have been thrown away or spilled can easily get into the soil and water, and then into plants and animals and through the food chain also to humans. Although invisible to the naked eye, their toxic effects are cumulative, and the long-term exposure leads to a decline in immunity and cancer, and some act mutagenically and teratogenic, thus potentially endangering the health of the future generations. Some of the substances that are anthropogenically generated today are recognized as Persistent Organic Pollutants so their concentration in the environment but also the removal is attracting great attention today<sup>1,2</sup>.

Until recently, natural recycling capacities were considered unlimited. However, industrial development has led to the situation where the amount of the generated waste is exceeding the capacity of the nature for self-purification. Therefore, it is necessary to clean up polluted areas, "cure" them and return them to their original condition before pollution took place, that is, to remediate them. For this purpose, a number of methods have been devised and applied: physical, chemical, physico-chemical, in order to extract, control, and transform the harmful substances. However, for most of the methods currently in use, it is characteristic that as a result of their use, waste that requires a controlled disposal is generated.

The scope of this paper is to present classical biochemical / biotechnological and molecular biochemical / biotechnological procedures and methods that have been applied in order to monitor the success and realization of bioremediation procedures in real conditions at the industrial level.

## **Bioremediation**

One of the technologies that has achieved remarkable success in the world in terms of remediation of oil pollution is bioremediation - cleaning and curing primarily the soil as well as other ecosystems<sup>3</sup>. This is the most natural method of remediation that uses non-pathogenic microorganisms for which pollutants represent food. In this way, by the action of microorganisms naturally present in the soil, pollutants are transformed into substances that have no toxic effects on humans and on the environment, and then completely mineralized to carbon dioxide, water and biomass of microorganisms. The best microorganisms for bioremediation are those already present at the polluted site that needs to be remediated. The details of the bioremediation process of soil contaminated with petroleum and petroleum products, microorganisms, metabolic degradation paths as well as technologies are discussed more in the cited paper<sup>4</sup>.

## **Microorganisms**

The expectations that microbes are capable of performing successful bioremediation come from both the theory and the practical observation. Namely, it has been observed that a number of substances considered not to be biodegradable accumulate in the nature in a smaller amount than expected due to the degree of their release. This led to the conclusion that any organic, energy-rich compound is a potential food for microorganisms in the environment. Compounds initially resistant to biodegradation make selective pressure on microorganisms in their environment to evolve and acquire the ability to decompose them. In this way, these microorganisms acquire a selective advantage over the rest of the population that is not able to extract energy from these organic compounds. This concept was published more than 60 years ago and it was called the "hypothesis of microbial infallibility"<sup>5</sup>. According to the concept of the "microbial infallibility", there is no natural organic substance that is not degradable by some microorganism under certain circumstances.

Today it is widely accepted that bioremediation is a modern method that optimizes the growth conditions of microorganisms present in the ecosystem in order to increase the rate of biodegradation of hydrocarbons. It implies the use of microorganisms in order to reduce the complexity of organic molecules (biotransformation) or degradation to complete mineralization (biodegradation).

Some microorganisms degrade a number of petroleum components, but a mixed population-consortium, most often, allows a higher degree of degradation. Often the formation of the final product occurs in several steps in which the initial substrate transformation has occurred. Reactions are coordinated through the communication and coordination among different microorganisms where the product of the metabolism of one population is a substrate for the next in the sequence. This microbial consortium has two potential advantages. By reducing the intermediate of the reaction, the metabolic imbalance in microorganisms and the substrate decreases. It has been shown that the consortium can achieve complex degradation processes that individual populations are not able to achieve, but also to adapt more easily to changes in the ecosystem. Microorganisms in one consortium communicate with each other by exchanging metabolites or small signal molecules, so that the population and individual member of the population reacts to the presence of other members in the consortium. For bioremediation processes, it is believed that the optimal ones are the consortiums of zymogenous microorganisms that are naturally optimized for the given contamination and the sudden appearance of a new potential nutrient that has not been present in the environment<sup>6-8</sup>.

### **Bioremediation at the laboratory, on the pilot and the industrial level**

Laboratory bioremediation is carried out most often in Erlenmeyer flasks, at the optimum temperature and with the addition of nutrients and surfactants that will increase the oil pollutants solubility in water, thus increasing their availability to microorganisms. It is possible to realize bioremediation by using a microbial consortium, but also to test individual isolates for their ability to degrade complex substrates. Bioremediation at the laboratory level is mandatory prior to pilot tests, and it is carried out in order to isolate, characterize and select the optimal microbial consortium to be used on a larger scale. In this way, the laboratory provides useful information in terms of reducing concentrations of contaminants as well as individual fractions thereof, and also the information on the composition of the consortium and its metabolic potential for degradation of harmful substances. Bioremediation at the pilot level implies studies on a larger amount of contaminated soil and water (up to 10 m<sup>3</sup>), during which the conclusions from the laboratory level are confirmed and further examined by new factors that will enable successful scales up to the next level. Finally, bioremediation at the industrial level involves the realization of the remediation of a larger area (more than 10 m<sup>3</sup>) of contaminated soil, sediment and water.

The results of the study carried out during the *ex situ* bioremediation at the industrial level are presented below. The biopile dimensions were 75 x 20 x 0.4 m (length, width, height) and it contained about 600 m<sup>3</sup> of contaminated soil. After a uniform distribution of

materials, biomass and nutrients were applied. The biomass concentration was  $1.44 \times 10^7$  CFU/mL. The optimum C:N:P:K ratio (approx. 100:10:1:0.1) was provided by spraying the ammonium nitrate, diammonium phosphate and potassium chloride solutions using a tractor-driven agricultural sprayer. Addition of nutrients and biomass, i.e. reinoculation was conducted once a month followed by turning and mixing of a biopile.

At the beginning of the study, immediately after mixing but before the addition of nutrients and water, about 10 m<sup>3</sup> of soil from the biopile was separated and used as a control pile (CP). Chemical and microbiological parameters of the bioremediation process were followed immediately after the application of biomass (time zero, sample S-0) and every 50 days for the next 150 days (S-50, S-100, S-150). The details of the conducted industrial biotechnological process as well as the optimization of the process from laboratory to the industrial level are described in the cited papers<sup>7-14</sup>.

### **Analysis of chemical parameters during bioremediation processes**

In order to optimize biological degradation of pollutants, constant monitoring is necessary. It follows whether bioremediation takes place under the optimum conditions in terms of moisture content, pH, nutrients, rate of reduction of the concentration of the contaminant, the emission of easily volatile compounds, the migration of the contaminant into the soil, the increase in the polarity of the contaminant and migration into the aqueous phase.

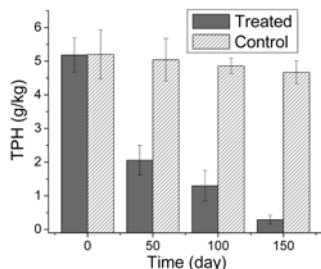
Chemical determination of the content of hydrocarbons of petroleum origin in soil is important to determine the endpoint of bioremediation with regard to the fulfilment of the legal and regulatory criteria, and together with microbiological indicators, serves to assess the biodegradation potential of contaminated soil. The most commonly used methods are gravimetric analysis, gas chromatography with flame ionization detector (GC-FID), gas chromatography with mass spectrometry (GC-MS), Fourier-transform infrared spectroscopy (FTIR) and high performance liquid chromatography (HPLC).

### **Gravimetric analysis of the Total Petroleum Hydrocarbons**

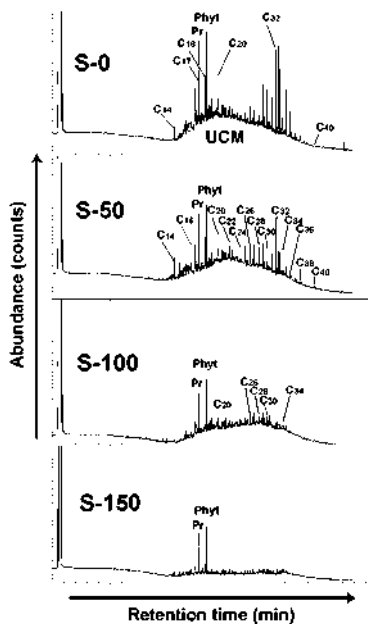
Gravimetric methods measure all hydrocarbons that can be extracted with the applied solvent and which are not removed during solvent evaporation. Standard gravimetric methods include the step of purifying with florisil to remove polar and biogenic materials. The detection limit is about 50 mg/kg of soil. This technique is not suitable for the measurement of light hydrocarbons that evaporate at temperatures below 70-85 °C. Gravimetric methods are commonly used for the determination of total petroleum hydrocarbons (TPH) in soil contaminated with large quantities of heavy oil fractions. The lack of gravimetric determination is reflected in the fact that this technique does not provide any information about the type of hydrocarbons present or about the presence of toxic molecules, nor does it provide specific information about the potential risk associated with contamination.

Figure 1 shows the trend of reducing TPH during the *ex situ* bioremediation study at the industrial level. The contamination level of TPH in S-0 was found to be 5.2 g/kg of soil.

With the application of zymogenous bacterial consortium and nutrients, the TPH level was reduced to 2.1, 1.3 and 0.3 g/kg of the soil after 50, 100 and 150 days respectively, meaning 60%, 75% and 94% of the TPH were biodegraded.



**Figure 1.** Reductions in TPH concentrations during bioremediation <sup>10</sup>.



**Figure 2.** Gas chromatograms of TPH during bioremediation <sup>10</sup>.

## Gas chromatography

All non-polar hydrocarbons extracted using the solvents (*n*-hexane or acetone/*n*-heptane) can be analysed using GC-FID. The concentration of hydrocarbons is determined by measuring the surface area of the chromatogram depending on the range of hydrocarbons to be measured. In addition to the total hydrocarbon content, information on the type of

petroleum hydrocarbons present as well as the degree of biodegradation is obtained. The detection limit is about 10 mg/kg dry soil. This method determines the hydrocarbons in the C<sub>10</sub> - C<sub>40</sub> range, which means that the volatile components that are eluted on GC column before the solvent will not be measured. Crude oil and many of its derivatives contain hydrocarbons with more than 40 C atoms so that they are beyond the measuring range of most GC methods and then gravimetry and Fourier-transform infrared spectroscopy (FTIR) methods are predominantly applied. For old oil pollution, it is characteristic that a large proportion of the present hydrocarbons cannot be easily explained by gas chromatography. The contaminant is usually weakly volatile at the time and has a high boiling temperature, and therefore, high temperature operating conditions in the GC column are also required. This technique cannot determine the polar components of naphtha such as nitrogen, sulphur and oxygen-containing (NSO) compounds, and water-soluble oxidation products. The application of this method is described in more detail in the cited papers <sup>10,15</sup>. As an illustration of GC-FID application, Figure 2 shows a gas chromatogram of the TPH of industrial *ex situ* bioremediation process.

Based on the GC analysis, it can be concluded that at the time 0 the content of the *n*-alkanes C<sub>17</sub> and C<sub>18</sub> was slightly lower comparing to pristane (C<sub>19</sub>) and phytane (C<sub>20</sub>). This indicates that the process of biodegradation has already begun and that the process of decomposition of hydrocarbons has already taken place. It is noticeable that a large part (about 50%) of *n*-alkanes in the C<sub>29</sub>-C<sub>36</sub> range has been biodegraded for the first 50 days. This is a direct consequence of the preparation of a specialized mixed consortium of zymogenous microorganisms, because as the sole source of carbon for the consortium growth in the bioreactor, mazut containing predominantly these hydrocarbons was used. The *n*-alkanes in the range of C<sub>14</sub>-C<sub>20</sub> were degraded for up to 100 days, followed by a complete degradation of C<sub>20</sub>-C<sub>36</sub> for 150 days. After 100 days, GC reveals a significant reduction in the Unresolved Complex Mixture. The GC analysis showed that the microbial consortium biodegraded and "consumed" all the components of a complex mixture of hydrocarbons, although different rates of degradation were observed.

## **Gas Chromatography with Mass Spectrometry**

GC-MS is routinely applied to identify individual hydrocarbon components. These methods have a high level of selectivity and the ability to verify the identity of the compound by analysing the retention time and the unique look of the mass spectrum. GC-MS allows confirmation of the presence of the target analyte and the identification of non-target analytes and it can be used to separate hydrocarbons into the class. The disadvantage of these methods is that the isomeric compounds have identical, while many different compounds can have similar mass spectra. Heavy oil fractions can contain thousands of components that cannot be separated in a gas chromatograph. Different compounds may have the same ions, which makes the identification process more difficult <sup>16</sup>. The monitoring of degradation of hydrocarbons in industrial conditions is much more complex than in laboratory conditions due to heterogeneity of the sample and heterogeneity of contamination. Due to the difficulty in quantifying hydrocarbons in bioremediation in

industrial conditions, the ratio of certain specific hydrocarbon compounds with a complex hydrocarbon mixture can be used to estimate the biodegradation of hydrocarbons. The importance of the GC-MS technique is discussed in detail in the cited publication<sup>17</sup>.

The fraction of saturated hydrocarbons is in most of the crude oils the dominant fraction comparing to aromatic hydrocarbons and NSO compounds<sup>18</sup>. The most represented are *n*-alkanes and isoprenoidal aliphatic alkanes. The *n*-alkanes in petroleum can be in different ranges, most commonly, C<sub>10</sub>-C<sub>35</sub>, and from isoprenoids the most significant are C<sub>19</sub>, pristane (2,6,10,14-tetramethyl-pentadecane) and C<sub>20</sub>, phytane (2,6,10,14-tetramethyl-hexadecane). For the purpose of more rigorous quantification of biodegradation, and after pristane and phytane are degraded, polycyclic hydrocarbon compounds of the type of sterane (C<sub>27</sub>-C<sub>29</sub>) and terpane (tri-, tetra- and pentacyclic; C<sub>19</sub>-C<sub>35</sub>) can be used as a preserved internal standard<sup>19</sup>. As an illustration for using GC-MS, in Figure 3, the fragmentograms of the isoprenoids (*m/z* 183) analysed in the Selected Ion Monitoring (SIM) mode are presented.

Reduction of the amount of isoprenoid molecules during the bioremediation process can be observed also on the basis of the obliquity of the peaks in the ion chromatograms *m/z* 183 characteristic for these molecules (samples S-0 and S-150; SIM method). In chromatogram *m/z* 183 of all samples, peaks of pristane and phytane are clearly differentiated and in the S-0 sample are most intense. In this sample, single peaks from the homologous series > C<sub>20</sub> isoprenoid are also visible, while in the S-150 sample they are completely biodegraded.

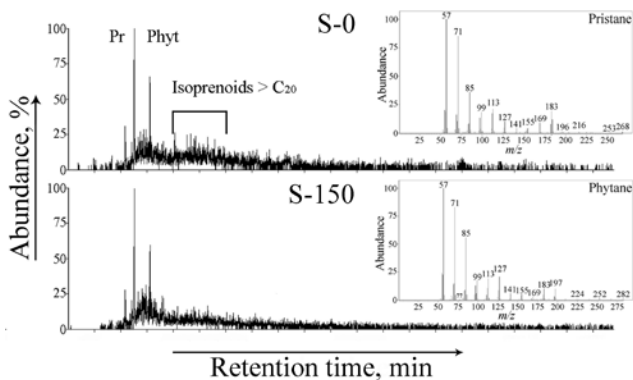


**Figure 3.** Fragmentograms of the isoprenoids (SIM, *m/z* 183) of the alkane fractions in the samples S-0 and S-150 (full mass spectra corresponding to peaks of pristane C<sub>19</sub> and phytane C<sub>20</sub> for S-0 sample are also presented); Pr: pristane; Phyt: phytane<sup>9</sup>.

### Comprehensive Two-Dimensional Gas Chromatography Mass Spectrometry

A method that provides for a more detailed insight into the chemical composition of the sample is certainly a comprehensive Two-Dimensional Gas Chromatography with a Mass Spectrometer detector (GCxGC-MS). This method allows the separation of the components of the mixture depending on the evaporation point (first dimension) and the

polarity (second dimension). In this way, a much more detailed insight into the composition of the analysed sample is obtained and it enables the analysis of the products of metabolism as well as the monitoring of the biodegradation of certain components of the mixture. The facts that isomeric compounds have identical, while many different compounds may have similar mass spectra based on which their accurate identification using GC-MS is made very difficult, are overcome by using GCxGC-MS. Heavy oil fractions can contain thousands of components that cannot be separated in a gas chromatograph, which nevertheless occurs through the use of a GCxGC. Bearing in mind that the detection limit is even ten times higher than in the usual GC, it is clear why this method is now considered the crown of gas chromatography<sup>20</sup>. The system is suitable for a variety of applications, including the analysis of complex matrices such as natural products that are hardly analysed by conventional GC or GC-MS, and grouping analysis based on two-dimensional chromatograph patterns (food, flavour & fragrance, environment, petrochemical etc.). Today this method is very welcomed for the monitoring of biotechnological processes in which the concentration of certain components of the mixture is reduced and the generation of new compounds occurs. Finally, this technique allows insight into the resulting metabolites and can be used for metabolomics studies. The significance and use of this technique in real-life examples, as well as the methodology, is described in detail in the papers cited<sup>19, 21-23</sup>.

As an illustration of the application of this method, in Figure 4, four three-dimensional chromatograms recorded in different bioremediation phases (0, 50, 100 and 150 days) are shown in which it is easy to monitor the decrease in the concentration of TPH and the reduction rate of concentration of certain components of the complex mixture of aromatic hydrocarbons.

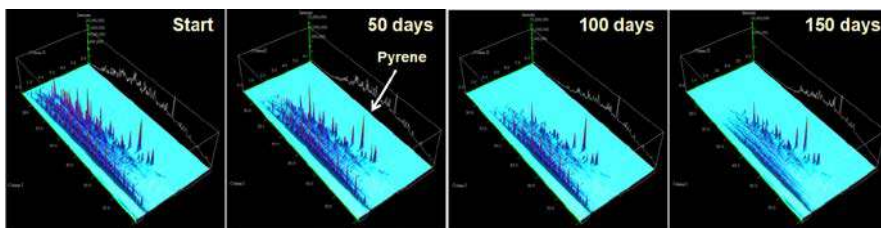


**Figure 4.** Comprehensive GCxGC-MS analysis<sup>24</sup>.

Chromatograms clearly show a decrease in the concentration of aliphatic and aromatic hydrocarbons during the bioremediation experiment that lasted for 6 months. Interestingly, in this case, the concentration of the polycyclic aromatic hydrocarbon of pyrene has been slightly reduced at the end of the process. For this reason, pyrene was observed as an internal standard in relation to which the rate of degradation of certain components was determined. By analysing the chromatogram in addition to *n*-alkanes, mono and polycyclic aromatic compounds, the presence of a biomarker compound is detectable and they are now clearly visible, all together on a single chromatogram. Some of these biomarker compounds are: C<sub>19</sub> - tricyclic terpene; C<sub>21</sub> - tricyclic terpene; C<sub>22</sub> - tricyclic terpene; C<sub>24</sub> -

tricyclic terpane; C<sub>25</sub> - tricyclic terpane; C<sub>24</sub> - tetracyclic terpane; C<sub>28</sub> -tricyclic terpane; C<sub>27</sub> - 18 $\alpha$ (H)-22,29,30-trisnorhopane; C<sub>29</sub> - 17 $\alpha$ (H),21 $\beta$ (H)-hopane; C<sub>27</sub> - 13 $\beta$ (H),17 $\alpha$ (H)-diasterane (20S). Also, compounds formed as a result of the interaction of microorganisms in aerobic conditions with petroleum hydrocarbons, primarily alcohol, aldehydes, and organic acids were detected.

### Analysis of microorganisms during bioremediation processes

Analyses of microorganisms before and during biotechnological procedures involve the determination of their number, particular groups using selective and differential media, their biochemical characterization, but also the characterization using molecular biology methods such as the determination of 16S rRNA and the protein profile of the isolate. Only after characterization microorganism can be further used in numerous biotechnological, bioremediation or biohydrometallurgical studies<sup>25,26</sup>.

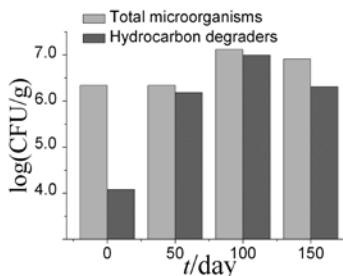


**Figure 5.** Changes in the number of total microorganisms and hydrocarbon degraders during the bioremediation process<sup>13</sup>.

### Number of microorganisms

The total number of microorganisms is most often determined in a representative composite soil sample, using a standard dilution series and a counting technique on nutrient agarized substrates. Hydrocarbon degraders can be determined in a similar manner, using a solid mineral substrate with the addition of a petroleum derivative such as diesel D2 or the corresponding hydrocarbon compound, as the only source of energy and carbon. Determination of the number of specific hydrocarbon oxidizing bacteria provides additional information on the potential degradation of hydrocarbons in the observed soil. The percentage share of hydrocarbon degraders in the total number of heterotrophic bacteria usually reflects the degree of the microbial adaptation. However, the technique of determining the number of microorganisms on the agarized substrate has several drawbacks, above all, the impossibility of determining non-culturally important microorganisms. As an illustration, Figure 5 shows a histogram of the changes in the number of total microorganisms and hydrocarbon degraders during the *ex situ* bioremediation process on the industrial scale.

It was concluded that following biostimulation and reinoculation, the number of hydrocarbon degrading microorganisms after 50 days had increased by as much as 100 times (from  $10^4$  to  $10^6$ ). Midway through the process, the proportion of oil hydrocarbon degraders in the total number of microorganisms had increased to 75%.

## Enzymatic activity of the soil

Microorganisms play an essential role in the reactions of substitution, dehydrogenation, dehalogenation, reduction, oxidation and hydrolysis of organic molecules, and processes are characterized as: degradation (biodegradation or biotransformation, chemical degradation or transformation), mineralization (end products are carbon dioxide, water and the inorganic components), detoxification and activation. It has been found that in bioremediation of petroleum hydrocarbons, lipases (LIP) and dehydrogenases (DH) are of particular importance. DG activity is a measure of general ability for the oxidation of various compounds. Biological oxidation of organic compounds is in fact a process catalysed by dehydrogenase enzymes. Because of this, these enzymes play an essential role in the oxidation of an organic substance, where hydrogen is transferred from an organic substrate to an electron acceptor. Many different specific enzymatic systems are involved in the soil dehydrogenase activity. These systems are an integral part of the soil microorganisms and largely reflect the biochemical activity of the soil. Since DH activity depends on the total microbiological activity of microorganisms in the soil, its values in different soils do not always reflect the total number of viable microorganisms isolated on the observed substrate. However, several factors affect the activity of DH in the soil, the presence of nitrates, nitrites and ions of iron that can inhibit dehydrogenase activity 27. LIP (triacylglycerol hydrolases) hydrolyse ester bonds of acylglycerol with the release of glycerol and fatty acids. In soil contaminated with oil, biodegradation products of hydrocarbons induce LIP activity. In Figure 6, the enzymatic activity of DH and urease and the activity of the lipase and phosphomonoesterase are shown. All enzyme activities are expressed in  $\mu\text{mol product/g dry soil per hour}$ , and dehydrogenase in  $\mu\text{g indonitrotetrazolium formazane (INTF) g}^{-1}\text{ h}^{-1}$ .

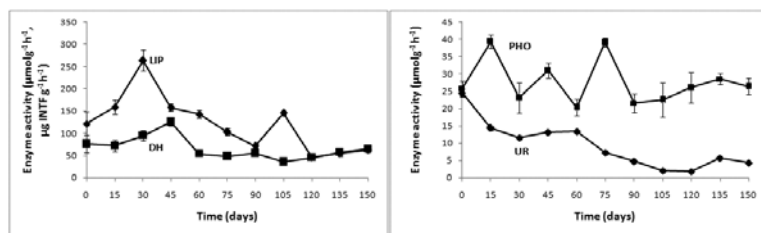


**Figure 6.** Time course of soil lipase and dehydrogenase activities (left), and time course of urease and phosphomonoesterase activities (right). Values are presented as means with standard deviations (n=6) <sup>28</sup>.

It has been found that the DH activity, as an indicator of general metabolic ability similar to a number of microorganisms is growing slowly in the initial period. The maximum value was achieved on the 50<sup>th</sup> day (125.9  $\mu\text{g INTF g}^{-1}\text{h}^{-1}$ ), followed by a slight decrease of the activity. In the second part of the observed period, the activity of this enzyme was in the range of 38-60  $\mu\text{g of g}^{-1}\text{h}^{-1}$ . The LIP activity increased rapidly to 33 days (263.58  $\mu\text{mol PNP g}^{-1}\text{h}^{-1}$ ), after which it decreased slightly and then slightly increased (145.3  $\mu\text{mol PNP g}^{-1}\text{h}^{-1}$ ). The activity of urease was maximal (24.5  $\mu\text{mol NH}_3 \text{g}^{-1}\text{h}^{-1}$ ) at the beginning and slowly decreased during the whole process. During the biodegradation process, enzymatic activities passed through two phases: the first phase in which the measured values were higher and where the maximum was either at the beginning or between the 50th and 65th days, and the second phase with the significantly reduced activity that encompasses the next three months. The reason for the existence of these two phases is probably reduced bioavailability as a result of the old contamination and accumulation of toxic products, which partly reduces enzymatic activity, although the number of microorganisms was not drastically reduced.

### **Biochemical characterization of hydrocarbon degrading microorganisms**

The analysis of the biochemical profile using commercial analytical profile index (API) tests is carried out according to the instructions of manufacturer BioMérieux Industry (Marcy l'Etoile, France). This analysis enables identification to the level of the genus and sometimes the species. In this case, from the consortium of hydrocarbon degrading microorganisms used in the process of industrial bioremediation, 30 pure strains were isolated and analysed. API 20NE, API RAPID, Coryne API, API 50 CHB, tests were used and microorganism profiles were analysed using species identification software. Biochemical characterization and API tests have confirmed the presence of various bacterial genera: *Pseudomonas sp.*, *Corynebacterium sp.*, *Sphingomonas sp.*, *Rhodococcus sp.*, *Achromobacter sp.*, *Bacillus sp.*, *Aeromonas sp.*, but also, *Stenotrophomonas sp.*, *Corynebacterium sp.*, *Burkholderia sp.*, *Nocardia sp.*, *Acinetobacter sp.*, *Flavobacterium sp.*, *Micrococcus sp.*, *Arthrobacter sp.*, *Alcaligenes sp.*, and *Mycobacterium sp.* Some of the results are presented in Table 1.

### **16S rRNA analysis of hydrocarbon degrading microorganisms**

The genomic DNA of each of the ten bacterium presented in the Table 1 was extracted. The 16S rRNA genes were amplified by PCR using 27F (5'-AGAGTTTGATCMTGGCTCAG-3'); and 1492R (5'-CGGCTACCTTGTTACGACTT-3') primers and amplified fragments were sequenced using the Applied Biosystems 3130 genetic analyser (Foster City, USA). The taxonomic analysis was conducted by the GenBank basic local alignment search tool (BLAST) program, and 16S rRNA gene sequences of the analysed strains were deposited in the NCBI GenBank. It was confirmed that API tests were reliable and isolated microorganisms based on 16S rRNA analysis were: *Pseudomonas aeruginosa* M-7, *Pseudomonas fluorescens* M2, *Corynebacterium*

*propinquum* J6, *Sphingomonas paucimobilis* BE<sup>'</sup>-4, *Pseudomonas luteola* BE<sup>'</sup>-9, *Rhodococcus erythropolis* BE<sup>'</sup>'-11A, *Achromobacter denitrificans* BE<sup>'</sup>'-11BB, *Rhodococcus rhodochrous* BE<sup>'</sup>''-10, *Bacillus licheniformis* BE<sup>'</sup>''- D, *Aeromonas hydrophila* BE<sup>'</sup>''- M. The results are presented in Table 1.

## MALDI-TOF MS analysis of hydrocarbon degrading microorganisms

Various traditional and modern microbiological methods enable the analysis and characterization of pure bacterial cultures. By using MALDI-TOF MS, biomolecules, such as proteins, peptides, oligosaccharides and oligonucleotides in the range of 400 to 350000 Da can be analysed within a few seconds. This method also provides for a direct analysis of the protein profile of intact (whole) cells and also as ethanol extracts.

Ten bacterial strains of hydrocarbon degraders previously analysed using API tests were further analysed using MALDI-TOF MS. Autoflex II Bruker Daltonics, and Microflex Bruker Daltonics MSTM, software flexControl, flexAnalysis and Maldi biotyper were used. Bacterial samples were analysed as intact (whole) cells and also as ethanol extracts. The spectral/protein profile was compared with a database of 3900 strains from over 2000 characterized microbial species. The process of sample preparation is described in the cited papers<sup>23, 25</sup>.

By comparing 16S rRNA identification with MALDI Biotyper software, a positive identification was obtained for only four samples. *Pseudomonas aeruginosa* M-7, *Sphingomonas paucimobilis* BE<sup>'</sup>-4, *Rhodococcus erythropolis* BE<sup>'</sup>'-11A, and *Aeromonas hydrophila* BE<sup>'</sup>''- M have been positively identified as a secure genus identification, probable species identification. However, Biotyper software was unable to identify the following genera: *Corynebacterium*, *Achromobacter* and *Bacillus*.

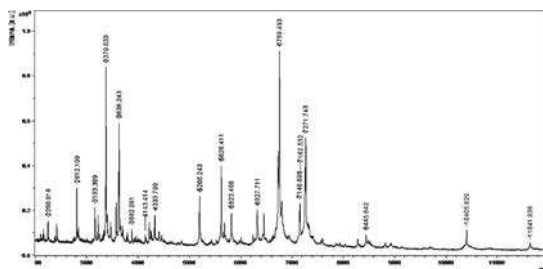


**Figure 7.** MALDI-TOF-MS analysis of the intact cells of hydrocarbon degrader<sup>23</sup>.

The results are provided in Table 1. It has been confirmed that the mass spectrum of evolutionarily closer bacteria isolated from the environment is more similar than that of phylogenetically distant bacteria. The similarity of the mass spectrum was in the range of 15% for evolutionary distances up, to more than 90% similarity of extremely close strains. It has been confirmed that the method is reliable for the differentiation and identification of genus and species. Ribosomal proteins, being dominant in the cell, are the target of this

analysis as well as other proteins copied in high numbers<sup>29</sup>. The mass spectrum obtained can be considered as a specific fingerprint of the bacterium analysed, because each particular protein has a unique pattern of *m/z* values. As an illustration of this method, Figure 7 presents the MALDI-TOF MS spectrum of intact whole cells of *Brachybacterium sp.* CH-KOV3 hydrocarbon degrading bacteria, a novel high levan producer. Details of this analysis are presented in the cited paper<sup>23</sup>.

**Table 1.** Results of biochemical characterization of microorganisms by commercial API tests, 16S rRNA and MALDI-TOF MS: (+++) Highly probable species identification; (++) Secure genus identification, probable species identification; (+) Probable genus identification; (-) Not reliable identification.

No.	Strain	API test	16S rRNA	MALDI-TOF MS
1.	M-7	<i>Pseudomonas aeruginosa</i>	<i>Pseudomonas aeruginosa</i>	++
2.	M2	<i>Pseudomonas fluorescens</i>	<i>Pseudomonas fluorescens</i>	-
3.	J6	<i>Corynebacterium sp.</i>	<i>Corynebacterium propinquum</i>	-
4.	BE <sup>2</sup> -4	<i>Sphingomonas paucimobilis</i>	<i>Sphingomonas paucimobilis</i>	++
5.	BE <sup>2</sup> -9	<i>Pseudomonas sp.</i>	<i>Pseudomonas luteola</i>	-
6.	BE <sup>22</sup> -11A	<i>Rhodococcus sp.</i>	<i>Rhodococcus erythropolis</i>	++
7.	BE <sup>22</sup> -11BB	<i>Achromobacter sp.</i>	<i>Achromobacter denitrificans</i>	-
8.	BE <sup>222</sup> -10	<i>Rhodococcus sp.</i>	<i>Rhodococcus rhodochrous</i>	-
9.	BE <sup>222</sup> -D	<i>Bacillus cereus</i>	<i>Bacillus licheniformis</i>	-
10.	BE <sup>222</sup> -M	<i>Aeromonas hydrophila</i>	<i>Aeromonas hydrophila</i>	++

## Proteomics in bioremediation

Proteomics-based studies are useful in determining the change in the composition and abundance of proteins, and in identifying key proteins involved in the physiological response of microorganisms when exposed to anthropogenic contaminants. Recently, the traditional proteomics approach has been used to detect the expression profile of proteins directly from samples of mixed microbial communities that reflects their actual functional activities in the given ecosystem. These microbial community proteomics, also termed metaproteomics have been significantly advanced due to technological developments in the two-dimensional gel electrophoresis coupled with mass spectrometry, together with the growth of the database in the protein sequence and structure<sup>30</sup>. The majority of published proteomic studies to date have employed conventional two-dimensional polyacrylamide gel electrophoresis (2D-PAGE), followed by mass spectrometry. MALDI-TOF MS is a technique that has been widely used to identify proteins of interest. However, 2D-PAGE is being replaced today by LC-MS/MS shotgun proteomic methods due to the automated approach and the larger number of proteins identified and quantitated. The identification of the peptide using MALDI-TOF MS or LC-MS/MS analysis is achieved by comparing them with a protein database of predefined peptides<sup>31</sup>.

As an illustration of the use of these methods in the environment biotechnology, we report an analysis of the change in the protein profile of hydrocarbon degrading isolate *Pseudomonas aeruginosa* M-7 when it is grown on the citrate base as the sole source of carbon and on the hydrocarbon extract from biopile for *ex situ* bioremediation. The bottom up proteomics analysis was performed on the HPLC coupled to "Q Exactive" Hybrid Quadrupole-Orbitrap Mass Spectrometer from Thermo, which is useful for untargeted or targeted screening and a broad range of qualitative and quantitative applications in drug discovery, proteomics, environmental and food safety, clinical research and forensic toxicology. Data were analysed using the MaxQuant/Perseus 1.5 software package. Differences between growth on citrate and hydrocarbons were determined using Student's t-test where p values lower than 0.01 were considered significant. This analysis of the proteomic profiles of *Pseudomonas aeruginosa* M-7 revealed 49 up-regulated proteins under hydrocarbons growth conditions with five of the proteins being found only in the hydrocarbons-grown cells. Citrate-grown cells showed 44 up-regulated proteins and four of them were found only in the citrate-grown cells. Up-regulated proteins belong to different metabolic pathways. This study is still in progress and we believe that it will give us a more detailed insight into the metabolic processes that take place in the cell, in order to optimize biotechnological *ex situ* bioremediation processes.

## Conclusion

In order to monitor the success of the applied bioremediation process, a multidisciplinary approach is required which includes the monitoring of chemical, biochemical and microbiological parameters that only together can provide a full picture of the process that takes place under real conditions. Modern instrumental methods such as GCxGC-MS provide an insight into the part of the newborn metabolites and the HPLC coupled to Q Exactive mass spectrometer provides insights into the changes in the protein profile due to the adaptation of microorganisms during growth at various sources of C atoms.

## Acknowledgements

This study was supported by the Ministry of Education and Science, Republic of Serbia, Project No. III 43004, FP7 project FCUB ERA and Japan International Cooperation Agency (JICA) Grassroot Project "Capacity Building for Analysis and Reduction Measures of Persistent Organic Pollutants in Serbia".

## References

1. Beškoski VP, et al. Perfluorinated compounds in sediment samples from the wastewater canal of Pančevo (Serbia) industrial area. *Chemosphere* 2013;91:1408-15.
2. Beškoski VP, et al. Distribution of perfluoroalkyl compounds in Osaka Bay and coastal waters of Western Japan. *Chemosphere* 2017;170:260-5.
3. Vidali M, Bioremediation. An overview. *Pure Appl Chem* 2001;73:1163-72.
4. Beškoski VP, Gojgić-Cvijović GĐ, Milić JS, Ilić MV, Miletić SB, Jovančičević BS, Vrvic MM. Bioremedijacija zemljišta kontaminiranog naftom i naftnim derivatima: mikroorganizmi, putanje razgradnje, tehnologije. *Hemijska Industrija* 2012;66:275-89.

5. Gayle EF. The Chemical Activities of Bacteria. Academic Press, London, 1952.
6. Gojgić-Cvijović G, et al. Isolation, selection and adaptation of zymogenous microorganisms: a basis of successful bioremediation, in Ljiljana Tanasijević (Ed.) Implementation of remediation in environmental quality improvement, Belgrade, 2006, pp 125-32.
7. Milić JS, Beškoski VP, Ilić MV, Ali SAM, Gojgić-Cvijović GĐ, Vrvic MM. Bioremediation of soil heavily contaminated with crude oil and its products: composition of the microbial consortium. J Serb Chem Soc 2009;74:455-60.
8. Miletić SB, Spasić SD, Avdalović J, Beškoski V, Ilić M, Gojgić-Cvijović G, Vrvic MM. The effect of humic acids on zymogenous microbial consortia growth. CLEAN - Soil, Air, Water 2014;42:1280-3.
9. Beškoski VP, Takić M, Milić J, Ilić M, Gojgić-Cvijović G, Jovančičević B, Vrvic MM. Change of isoprenoids, steranes and terpanes during *ex situ* bioremediation of mazut on industrial level. J Serb Chem Soc 2010;75:1605-16.
10. Beškoski VP, Gojgić-Cvijović G, Milić J, Ilić M, Miletić S, Šolević T, Vrvic MM. Ex situ bioremediation of a soil contaminated by mazut (heavy residual fuel oil) - A field experiment. Chemosphere 2011;83:34-40.
11. Jednak T, et al. Transformation and synthesis of humic substances during bioremediation of petroleum hydrocarbons. Int Biodeterior Biodegradation 2017;122:47-5.
12. Marić N, Ilić M, Miletić S, Gojgić-Cvijović G, Beškoski V, Vrvic MM, Papić P. Enhanced in situ bioremediation of groundwater contaminated by petroleum hydrocarbons at the location of the Nitex textiles, Serbia. Environ Earth Sci 2015;74:5211-9.
13. Novaković M, et al. Degradation of methyl-phenanthrene isomers during bioremediation of soil contaminated by residual fuel oil. Environ Chem Lett 2012;10:287-94.
14. Gojgić-Cvijović G, et al. Biodegradation of petroleum sludge and petroleum polluted soil by a bacterial consortium: a laboratory study. Biodegradation 2012;23:1-14.
15. Jovančičević B, Antić M, Pavlović I, Vrvic M, Beškoski V, Kronimus A, Schwarzbauer J. Transformation of petroleum saturated hydrocarbons during soil bioremediation experiments. Water Air and Soil Pollution 2008;190:299-307.
16. Jensen ST, Arvin E, Svensmark B, Wrang P. Quantification of compositional changes of petroleum hydrocarbons by GC/FID and GC/MS during long-term bioremediation experiment. Soil Sediment Contam 2000;9:549-77.
17. Beškoski VP, Gojgić-Cvijović G, Jovančičević B, Vrvic MM. Gas Chromatography in Environmental Sciences and Evaluation of Bioremediation, In: B. Salih, Ö. Çelikbıçak, (Eds) Gas Chromatography - Biochemicals, Narcotics and Essential Oils, InTech, Rijeka, 2012, pp. 3-28.
18. Peters KE, Walters CC, Moldowan JM. The biomarker guide. Cambridge Press, Cambridge, 2005.
19. Beškoski VP, et al. Biodegradation of isoprenoids, steranes, terpanes and phenanthrenes during in situ bioremediation of petroleum contaminated groundwater. CLEAN - Soil, Air, Water 2017;45:1600023.
20. Mondello L, Tranchida PQ, Dugo P, Dugo G. Comprehensive two-dimensional gas chromatography-mass spectrometry: a review. Mass Spectrom Rev 2008;27:101-24.
21. Kannan N, et al. Greener approaches to the measurement of polyaromatic hydrocarbons (PAHs) in unused and used crankcase motor oils from Malaysia. Environ Sci Pollut Res 2015, doi: 10.1007/s11356-015-5403-9.
22. Lama SM, Pampel J, Fellingner TP, Beškoski VP, Slavković-Beškoski LJ, Antonietti M, Molinari V. Efficiency of Ni-nanoparticles supported on a hierarchical porous nitrogen doped carbon for the hydrogenolysis of Kraft lignin in flow and batch systems. ACS Sustain Chem Eng 2017;5:2415-20.
23. Djurić A, et al. Brachy bacterium sp. CH-KOV3 isolated from an oil-polluted environment-a new producer of levan. Int J Biol Macromol 2017;104:311-21.
24. Ljesević M, et al. Microbial degradation of various aromatic compounds-evaluation by comprehensive two-dimensional gas chromatography-time-of-flight mass spectrometry (GCxGC-TOFMS). 26th Symposium on Environmental Chemistry Program and Abstracts, June 7-9, 2017, Shizuoka, Japan.

25. Avdalović J, Beškoski V, Gojgić-Cvijović G, Mattinen ML, Stojanović M, Zildžović S, Vrvic MM. Microbial solubilisation of phosphorus from phosphate rock by iron-oxidizing *Acidithiobacillus* sp. B2. *Minerals Eng* 2015;72:17-22.
26. Jeremic S, et al. Interactions of the metal tolerant heterotrophic microorganisms and iron oxidizing autotrophic bacteria from sulphidic mine environment during bioleaching experiments. *J Environ Manage* 2016;172:151-61.
27. Dibble JT, Bartha R. Effect of environmental parameters on the biodegradation of oil sludge. *Appl Environ Microbiol* 1979;37:729-39.
28. Beškoski VP. Proučavanje aktivnosti konzorcijuma zimogenih mikroorganizama zemljišta zagađenog naftom i njenim derivatima i njihova primena za bioremedijaciju, Doktorska disertacija, Hemijski fakultet, Beograd 2011, pp 1-270.
29. Ryzhov V, Fenselau C. Characterization of the protein subset desorbed by MALDI from whole bacterial cells. *Anal Chem* 2001;73:746-50.
30. Benndorf D, Balcke GU, Harms H, von Bergen M. 2007. Functional metaproteome analysis of protein extracts from contaminated soil and groundwater. *ISME J* 2007;1:224-34.
31. Mandalakis M, Panikov N, Dai S, Ray S, Karger BL. Comparative proteomic analysis reveals mechanistic insights into *Pseudomonas putida* F1 growth on benzoate and citrate. *AMB Express* 2013;3:64.

---

## Microscale thermophoresis and NanoDSF as advanced methods in life science research

---

**Jakub Nowak\***

*NanoTemper Technologies sp. z o.o., Krakow, Poland*

*\*e-mail: jakub.nowak@nanotemper.de*

The analysis of bio-molecular interactions, such as protein-protein, protein-nucleic acid or protein-small molecule, not only helps to develop therapeutics or diagnostics techniques, but it also provides important insights into cellular processes. Here we present MicroScale Thermophoresis (MST) for the investigation of affinities of biomolecular interactions. MST analyzes the directed movement of molecules in optically generated microscopic temperature gradients. This thermophoretic movement is determined by the entropy of the hydration shell around the molecules. Almost all interactions and any biochemical process relating to a change in size, charge and conformation of molecules alters this hydration shell and is thus detectable by MST. Measurements can be performed with purified molecules as well as in close-to-native conditions (lysate, serum). The readout of the method is fluorescence, derived either from fluorescently labeled interaction partners (via chemical dyes or fluorescent fusion proteins) or from intrinsic protein fluorescence.

The presentation will cover biophysical backgrounds of the technology, highlighting benefits of the MicroScale Thermophoresis platform, followed by specific examples of its application in characterizing biomolecular interaction in various scenarios.

The fluorescence of tryptophans in a protein is strongly dependent on its close surroundings. By following changes in fluorescence, chemical and thermal stability can be assessed in a truly label-free fashion. The dual-UV technology by NanoTemper allows for rapid fluorescence detection, providing an unmatched scanning speed and data point density. This yields ultra-high resolution unfolding curves which allow for detection of even minute unfolding signals. Furthermore, since no secondary reporter fluorophores are required, protein solutions can be analyzed independent of buffer compositions, and over a concentration range of 150 mg/ml down to 5 µg/ml. In addition, information on protein aggregation can be recorded in parallel, providing insight into colloidal stability of the sample. Therefore, nanoDSF is the method of choice for easy, rapid and accurate analysis of protein folding and stability, with applications in membrane protein research, protein engineering, formulation development and quality control.

The presentation will cover biophysical concepts of the technique showing benefits of the nanoDSF technology platform, and will be followed by specific examples of nanoDSF applications towards various experimental systems.



---

# Sun as a stressor and/or regulator of plant metabolism: responses to UV radiation and high light

---

Marija Vidović\*, Filis Morina, Sonja Veljović Jovanović

*Department of Life Science, Institute for Multidisciplinary Research, University of Belgrade, Belgrade, Serbia*

\*e-mail: marija@imsi.rs

In their natural environment, plants are constantly exposed to dynamic changes of solar radiation, which mainly consists of infrared (IR, >700 nm), photosynthetically active radiation (PAR, 400-700 nm) and minor portion of ultraviolet (UV) radiation (UV-B, 290-315 nm and UV-A, 315-400 nm). Sunlight is not only the primary source of energy in photosynthesis, it is also an important signal which regulates plant growth and development. During the period from the 1970s to 1990s, investigations on UV-B effects on organisms were in the centre of attention due to alarming depletion of stratospheric ozone layer and increased UV-B radiation reaching the Earth's surface. UV-B radiation has been perceived only as a stressor. A decade later, new data obtained using realistic UV-B doses and realistic UV-B:UV-A:PAR ratio, clearly show that UV-B is very important environmental cue and regulator of plant metabolism, rather than a stressor. In the recent years, great progress has been made in understanding the mechanisms of light signals' perception. However, the complications arise from the overlapping of the acclimative responses to UV-B radiation and high PAR intensity, imposing cross-tolerance to different components of solar radiation. Moreover, information on other constituents involved in the UV-B response, such as reactive oxygen species in relation to their tissue- and subcellular-localization is scarce. Our latest findings using leaf variegation as a model with metabolically contrasting tissues show specific responses to UV-B radiation and high light in relation to antioxidative metabolism, photosynthesis, carbohydrate metabolism, and distribution of phenolics.

## High light intensity

Light is the most important environmental factor for plants, as it provides the source of energy for plant life. Therefore, plants have developed complex mechanisms to perceive light quality, quantity, duration and direction, and to adjust their metabolism and development accordingly. Processes such as seed germination, seedling photomorphogenesis, chloroplast development and movement, phototropism, shade avoidance, circadian rhythms and flower induction are light-regulated.

Plants perceive light signals through several protein photoreceptors: five phytochromes (PHY A-E), which are sensitive to red and far-red light (600-750 nm), and two cryptochromes (CRY1 and CRY2), two phototropins (PHOT1 and PHOT2) and zeaxanthin proteins (ZTLs) for blue, and UV-A radiation (315-500 nm), while UV-B radiation is sensed by UV Resistant Locus 8 (UVR8)<sup>1,2</sup>. During the recent years, great efforts have

been made to characterize the organization of light-regulated transcriptional networks in the model plant *Arabidopsis thaliana*; particularly related to photomorphogenic responses. Every day, plants are exposed to varying photosynthetically active radiation (PAR) intensities in the field <sup>3,4</sup>. Under the low light intensity, photosynthetic efficiency is maximal, while its capacity is limited. With the increase in the light intensity, the rate of the light-dependent reaction, and therefore photosynthesis in general, increases proportionately; however, photochemical efficiency drops, until photosynthetic rate achieves the plateau. Above this point PAR intensity overcomes metabolic requirements and the capacity of dissipation mechanisms, finally resulting in increased rate of reactive oxygen species (ROS) generation, followed by the inhibition of photosynthesis and CO<sub>2</sub> assimilation <sup>5</sup>. This condition is called photooxidative stress. It is difficult to define which PAR intensity is a stressor for a particular plant species since this depends on the developmental stage, previous light adaptation, and on other environmental conditions, including drought, high salinity, nutrient deprivation, or temperature stress <sup>6</sup>. Even optimal PAR intensity might be a stressor in combination with conditions that limit CO<sub>2</sub> availability or decrease the rate of the Calvin-Benson cycle <sup>7</sup>. Under such conditions, down-regulation of photosystem II (PS II) is a major mechanism of photoprotection, as well as efficient dissipation of the excess of photon energy by a decrease of pH and zeaxanthin accumulation <sup>8</sup>. Molecular oxygen has an important role in energy dissipation under photoinhibitory conditions, as it serves as an electron acceptor in two photosynthetic processes, photorespiration and in the Mehler reaction coupled to the water-water cycle at photosystem I (PS I), where it is reduced to superoxide anion radical <sup>9,10</sup>.

Having in mind the effects of ROS generation in chloroplasts on overall cellular metabolism, we successfully established a model system with two metabolically contrasting tissues which are spatially closely related; variegated leaves which have both photosynthetically active (green sectors) and non-photosynthetically active (white sectors) cells. Under optimal light conditions, in the leaves of variegated *Pelargonium zonale*, differential subcellular distribution of low molecular antioxidants (ascorbate and glutathione) and spatial differences in distribution of enzymatic antioxidants, soluble sugars, and phenolics in the two tissue types have been revealed <sup>11,12</sup>. Under conditions which accelerate Mehler reaction in chloroplasts (*e.g.* high light, HL, exposure), H<sub>2</sub>O<sub>2</sub> significantly accumulated only in illuminated green sectors, and it has been restricted to the extracellular space of vascular and adjacent photosynthetically active cells and directly dependent on the activity of NADPH oxidase (Figure 1) <sup>13</sup>. Similar HL-induced H<sub>2</sub>O<sub>2</sub> accumulation in the (peri)vascular area has been reported in *A. thaliana* and *Mesembryanthemum crystallinum* <sup>14,15</sup>, which together with our results emphasize the tissue-specific response to HL and involvement of bundle sheet cells in rapid intercellular signal propagation during acclimatization to high light <sup>16</sup>.

In the mesophyll tissue of *P. zonale* plants under HL, efficient scavenging of H<sub>2</sub>O<sub>2</sub> in photosynthetic tissue has been attributed to catalase activity, while in the non-photosynthetic tissue peroxidases were involved in the antioxidative defence <sup>13</sup>. Although enzymes of ascorbate-glutathione cycle and total glutathione pool have been constitutively

higher in non-photosynthetic tissue, under progressive pro-oxidative conditions the reduction of oxidized glutathione has been more efficient in photosynthetic tissue, which is related to the photosynthetically-derived reducing equivalents.

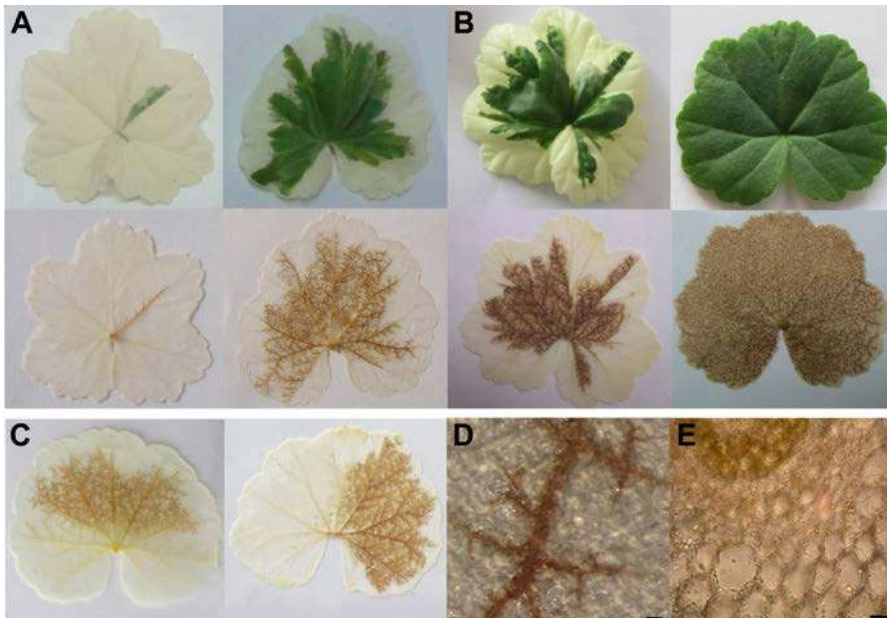


**Figure 1.** Accumulation of H<sub>2</sub>O<sub>2</sub> in *P. zonale* leaves detected by DAB ‘up-take’ method: A) after 1 h-exposure to high light (HL, >1100 μmol m<sup>-2</sup>s<sup>-1</sup> PAR); B) after 1 h-exposure to HL+100 μM paraquat. C) Light-dependent H<sub>2</sub>O<sub>2</sub> accumulation in green sectors has been confirmed by partial shielding of the bottom and lateral leaf halves during 1 h exposure to HL; D) green leaf sector 5× magnified (bar represents 1 mm); E) cross section of green leaf (peri)vascular tissue (100×, bar represents 50 μm). For detailed results see <sup>13</sup>.

Therefore, the question is what is the primary signal which triggered the unexpectedly strong response to HL in non-photosynthetically active tissue? This signal could be transferred from photosynthetic cells, but not through the involvement of extracellular H<sub>2</sub>O<sub>2</sub> originating from NADPH oxidase activity (Figure 1). On the other hand, it is possible that non-photosynthetic tissue responded to HL independently, provoked by some intrinsically generated factor.

Besides investigation of the tissue- and cell-specific tolerance to HL, extensive progress has recently been made towards characterizing rapid changes in nuclear gene expression triggered by HL <sup>17</sup>. These transcriptional changes are regulated in a photosynthesis-dependent manner and the signals generated in the chloroplasts are transported to the nucleus <sup>18</sup>. Moreover, chloroplastic signals can be transferred to neighbouring cells and

distal parts of the plant. Indeed, signals from reduced chloroplasts (optimal conditions) activate transport via plasmodesmata, which allows symplastic communication and exchange of molecules, while signals from oxidized plastids (paraquat-treated) inhibit this intercellular transport<sup>19</sup>. Light-provoked chloroplast retrograde signalling, mediated by the redox state of plastoquinone pool, regulates nuclear alternative splicing, which together with an unknown signalling molecule induce the same change further downstream, in the roots<sup>20</sup>. The intercessory signalling molecule is still not identified, although some evidence suggests it might be a certain redox-sensitive protein kinase.

Anthocyanins, red and blue pigments in flowers and fruits, have a role in attracting pollinators and in seed dispersal. With their strong absorption in the 260-280 nm and 500-550 nm ranges, anthocyanins absorb the green range of PAR, protecting photosynthetic apparatus in the leaves from light excess (excitation pressure) and from potential photooxidative stress<sup>21-23</sup>. Moreover, anthocyanidins are efficient antioxidants, and they can serve as an electron donor for class III peroxidases in H<sub>2</sub>O<sub>2</sub> scavenging, followed by re-reduction by ascorbate in vacuoles<sup>24</sup>.

Accumulation of the anthocyanins is one of the most recognizable HL-inducible symptoms, and that is why they have been included in the most of the studies exploring the mechanisms of plant responses to HL, particularly those involved in light-mediated redox chloroplast signalling.

What is the relationship between photosynthesis-dependant redox changes and anthocyanins accumulation under HL? Studies with mutants deficient in H<sub>2</sub>O<sub>2</sub> scavenging enzymes (chloroplastic ascorbate peroxidases, APX, and catalase) showed that high concentration of H<sub>2</sub>O<sub>2</sub> derived from chloroplasts and peroxisomes may be important for HL-dependent induction of anthocyanins<sup>25,26</sup>. In addition, Maruta and co-workers showed that chloroplastic H<sub>2</sub>O<sub>2</sub> generated under photooxidative stress induced by paraquat, enhanced the expression of anthocyanin biosynthesis and genes associated with its regulation even under lower PAR intensities<sup>27</sup>. Besides H<sub>2</sub>O<sub>2</sub>, other signals derived from photosynthesizing chloroplasts responsible for anthocyanin accumulation may be overreduction of the components of the photosynthetic electron transport chain (PETC), such as plastoquinone<sup>28</sup>. In favour of these findings, *Arabidopsis trol* mutant, with altered electron partitioning between energy-conserving and (energy)-dissipating pathways, has abolished production of anthocyanins comparing to wild type genotype<sup>29</sup>.

Very recently, by using HyPer2, a genetically encoded fluorescent H<sub>2</sub>O<sub>2</sub> sensor, it has been shown that H<sub>2</sub>O<sub>2</sub> accumulated in HL exposed chloroplasts, directly transfers from chloroplasts to nuclei, avoiding the cytosol, and enabling the photosynthetic control over the gene expression<sup>30</sup>. Moreover, the propensity of the main chloroplastic scavenger of H<sub>2</sub>O<sub>2</sub>: chloroplastic APX to inactivation by H<sub>2</sub>O<sub>2</sub> can be regarded as a signalling function<sup>31</sup>. The chloroplastic APXs (thylakoid bound-APX even more than the stromal APX) are very sensitive to inactivation in the presence of H<sub>2</sub>O<sub>2</sub> (>2 nM) under low ascorbate content (<20 μM)<sup>32</sup>.

Current progress in studying light response in plants shows that the role of visible light goes far beyond photosynthesis. It is clear that visible light can be perceived via several

photoreceptors, which specifically mediate regulation of important processes in the plant cell. However, there are non-specific mediators in the photosynthesizing chloroplasts, generated under HL (plastoquinone redox state, oxidized metabolites, H<sub>2</sub>O<sub>2</sub>), which are able to transfer the signal to the nucleus and regulate the expression of genes responsible for acclimative and protective responses.

## **UV-B radiation**

Ultraviolet radiation makes about 7% of the total solar radiation, consisting of UV-B (290-315 nm) and UV-A (315-400 nm) radiation<sup>33</sup>. First investigations of the influence of UV-B radiation on plant metabolism and growth indicated its harmful effects, including cyclobutane pyrimidine dimer formation in a DNA strand, enhanced ROS generation, oxidative stress and damage of cellular membrane and proteins, including D1 and D2 subunits of PS II, and Rubisco<sup>34,35</sup>. However, these detrimental effects have been attributed to unrealistic UV-B: UV-A: PAR ratios, high UV-B doses applied, unrealistic UV-B spectrum, plant history, as well as to combined effects of other environmental stressors (high light, drought, high temperature, nutrient deprivation)<sup>36,37</sup>. Today, it is accepted that ecologically relevant, low doses of UV-B radiation act as an important environmental cue and regulator of plant growth and development<sup>2,38,39</sup>.

In plant cells, UV-B radiation activates at least two independent signalling pathways that regulate the expression of different sets of genes, depending on its fluence rate<sup>40,41</sup>. One is UV-B stress response, and the second one is crucial for UV-B acclimation response, and it is triggered by UVR8, specific UV-B receptor<sup>42</sup>.

In the absence of UV-B radiation, UVR8 protein exists as a homodimer, maintained by cation- $\pi$  interactions between positively charged (arginine and lysine residues) and aromatic amino acids (tryptophan and tyrosine residues), and charge-stabilized hydrogen bonds at the dimer interface (Figure 2)<sup>43,44</sup>. Exposure to UV-B radiation induces excitation of Trp285 and Trp233 indole rings, resulting in the disruption of cation- $\pi$  interactions and UVR8 monomerization<sup>45</sup>. UV-B-mediated UVR8 monomers accumulate in the nucleus and interact with the protein COP1 (Constitutively Photomorphogenic 1). During the night, COP1, an E3 ubiquitin ligase, is responsible for targeting photomorphogenesis-promoting transcription factors (such as Elongated Hypocotyl 5, HY5 and HY5 Homolog, HYH) for proteolytic degradation. Under UV-B radiation, UVR8 monomers inhibit the association of COP1 with ubiquitin-proteasome apparatus and, thus, enable gene transcription mediated by HY5 and HYH (Figure 2)<sup>46</sup>. The accumulation of HY5 and/or HYH transcriptional factors in the nucleus is required for the expression of protective genes involved in the UV tolerance, including those for biosynthesis and metabolism of flavonoids and antioxidative defence, especially the glutathione metabolism (glutathione reductase, glutathione peroxidase, glutathione-S-transferase, peroxiredoxins and glutaredoxin)<sup>47,48</sup>.

Blue light and UV-A radiation inhibit COP1 via cryptochromes, disabling it to alter transcriptional factors like HY5 (Figure 2)<sup>49</sup>. For effective repression of photomorphogenesis induced by visible light, it is required that COP1 and accessory

proteins SPA (Suppressor of Phy A) form complexes with other components of the ubiquitin-proteasome system, while in UV-B response COP1 does not require SPA<sup>50</sup>. Contrasting to its negative role in the regulation of the visible light response, COP1 is an important positive regulator of responses to low UV-B doses (induction of UV-B responsive genes is impaired in mutants deficient in COP1), coordinating the HY5-dependent and the HYH-dependent pathways in signalling transduction. Therefore, acclimative responses to UV-B radiation and high PAR intensity may overlap, imposing cross-tolerance<sup>51,52</sup>. For example, high PAR-induced flavon-3-ols and hydroxycinnamates in epidermis may attenuate UV-B radiation<sup>53</sup>. Besides phenolics, blue light and UV-B radiation up-regulate photolyases, enzymes involved in the repair of cyclobutane pyrimidine dimers of DNA<sup>54,55</sup>. However, the exact mechanism by which COP1 integrates these different stimuli remains unknown. Two possibilities are proposed: either some unknown molecules/processes are involved in the UV-B response, or other functional domains of COP1, not necessarily the ones with E3 ligase activity, may interact with certain proteins<sup>38</sup>.

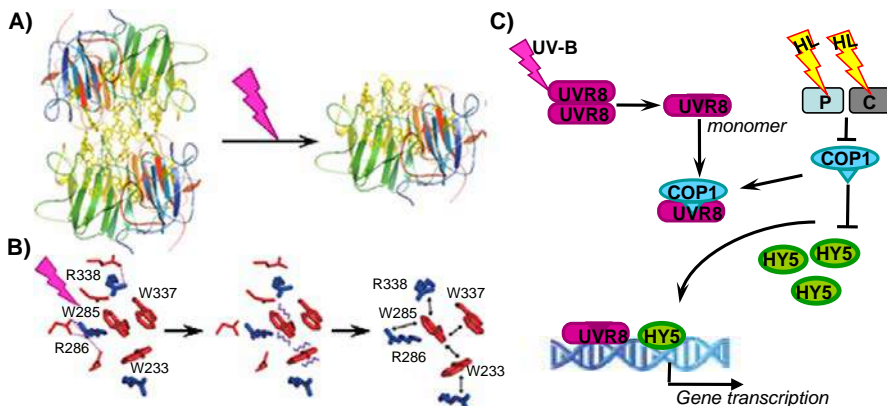


**Figure 2.** Schematic overview of UV-B radiation-induced activation of UVR8 receptor. A) UVR8 as a dimer in the absence of UV-B radiation. B) Important amino acids at the interface of two monomers and crucial cation- $\pi$ -interactions between two Arg (R338 and R286) and three Trp (W285, W233 and W337). UV-B-induced excitation of  $\pi$ -electrons of indole rings W285 and W233 (zig-zag purple lines), which prevents maintaining cation- $\pi$ -interactions and leads to monomerization of UVR8 dimer. C) The interaction between UVR8 monomer and COP1 - connection between visible light (HL) and UV-B perception. Detailed explanation is given in the text. P, phytochromes; K, cryptochromes. Adapted from<sup>2,45</sup>.

Nevertheless, activation of UVR8/COP1 pathway leads to the accumulation of secondary metabolites. In particular, accumulation of flavonoids and phenylpropanoids, alkaloids and terpenoids is considered as a hallmark of UV-B response in plants. Phenolic compounds are the most abundant secondary metabolites in plants, involved in a wide range of

developmental and regulatory processes, as well as in numerous biotic and abiotic stress responses<sup>56,57</sup>. Therefore, UV-B radiation improves plant adaptive capacity to drought, high temperatures, pathogen and insect attack, and nutrient deficiency conditions (reviewed in Vidović et al. 2017)<sup>39</sup>. Plants grown in the open field, exposed to natural UV-B doses, have higher nutritional and pharmacological value than plants grown in polytunnels and glasshouses, which are non-transparent to UV radiation<sup>58,59</sup>. These UV-B effects have a strong impact on the agricultural, pharmaceutical and food industries.

### **Interaction of UV-B radiation and high PAR on primary and secondary metabolism**

The importance of phenolic compounds on plant metabolism can be illustrated with the finding that over 20% carbon derived from the Calvin-Benson cycle is introduced to the shikimate pathway<sup>60</sup>. Biosynthesis of phenylpropanoids and flavonoid glycosides can be regarded as an additional energy escape valve under unfavourable conditions<sup>61</sup>. However, the exact relationship between photosynthesis and phenolic metabolism is insufficiently investigated.

Using leaf variegation enables the examination of source-sink interactions in relation to carbon (sugars, phenolics) allocation within the same leaf, providing the same microenvironment conditions. This is also an excellent model system for studying tissue-specific responses to photosynthesis-dependent H<sub>2</sub>O<sub>2</sub> generation. Since PAR, UV-A and UV-B radiation are interlaced under natural light conditions, employing variegated plants under strictly controlled and realistic conditions such as in Sun Simulators, enable relevant conclusions about specific responses to PAR and UV-B radiation. For illustration, high light in combination with UV-B radiation triggered stronger increase of APX and catalase activities and ascorbate accumulation than in the absence of UV-B radiation, only in green sectors of variegated *P. zonale* leaves (Figure 3). These findings indicate that that UV-B radiation and high PAR intensity synergistically stimulate antioxidative defence in green sectors of variegated *P. zonale* leaves<sup>11</sup>.

Reports on UV-B effects on photosynthetic machinery and stomatal conductance are inconsistent, due to various UV-B: UV-A: PAR ratios, different periods of exposure, plant metabolic state and previous plant exposure to UV-B radiation. A large number of studies have described deleterious, minimal or negligible effects of UV-B radiation on photosynthetic activity<sup>35,62</sup>.

The beneficial influence of ambient UV-B radiation on photosynthetic rate is rarely reported. The UVR8/COP1/HY5(HYH) signalling pathway leads to the expression of *SIG5* (which encodes sigma factor of plastidic RNA polymerase, involved in D2 protein biosynthesis) and induction of ELIP1 (Early-Light Inducible Protein 1), which may interact with D1 protein of PS I, and protect the photosynthetic apparatus from photooxidative stress<sup>48,63</sup>. In our study with variegated *Plectranthus coleoides* exposed to ecologically relevant UV-B radiation combined with high PAR, which simulates sunny spring conditions in mid-northern latitudes, rapid stimulation of CO<sub>2</sub> assimilation, was

observed already after four hours, and remained at the high level until the end of experiment<sup>64</sup>. In addition, after nine days of treatment, increased influx of electrons in alternative electron pathways was detected, compared with HL treatment with no UV-B radiation. Stimulation of photosynthesis might be related to an enhanced requirement for building blocks for biosynthesis of apigenin and cyanidin glycosides, particularly in the neighbouring non-photosynthetic cells (Figure 3).

Contrastingly to the results obtained with *P. coleoides*, in variegated *P. zonale* identical UV-B irradiances under the same experimental conditions, did not affect the photosynthetic rate<sup>11</sup>. Instead, UV-B radiation provoked carbon allocation from source (green) to sink (white) leaf tissue, decreasing trehalose concentration and, therefore, mediating regulation of starch degradation (Figure 3). Trehalose-6-phosphate is involved in carbon allocation to sink tissues (*e.g.* root), and in regulation of starch degradation<sup>65</sup>.

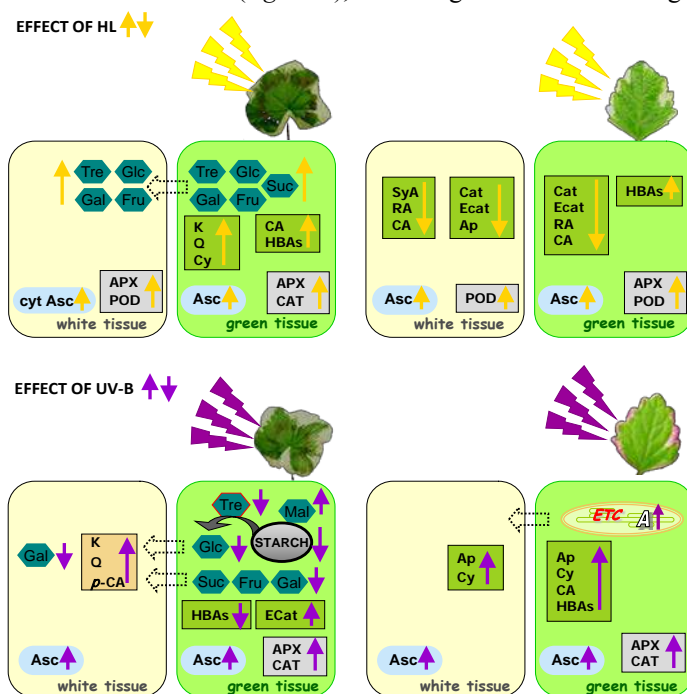


**Figure 3.** Schematic overview of the link between sugar, phenolic and antioxidative metabolism under high light (HL,  $1350 \mu\text{mol m}^{-2} \text{s}^{-1}$  PAR) and HL combined with ecologically relevant UV-B irradiance ( $0.9 \text{ W m}^{-2}$ ) combined with HL in green and white leaf sectors of variegated *P. zonale* (left) and *P. coleoides* (right). The influence of UV-B radiation on photosynthesis is emphasized. Arrow directions indicate increased or reduced metabolite content/enzyme activity. Ap, apigenin; APX, ascorbate peroxidase, CA, caffeic acid; CAT, catalase, Cat, catechin; Cy, cyanidin; Ecat, epicatechin; HBAs, hydroxybenzoic acids; K, kaempferol; *p*-CA, *p*-coumaric acid; POD, class III peroxidase; Q, quercetin; RA, rosmarinic acid; SyA, syringic acid. For details see<sup>11,64</sup>.

In these two studies with variegated species, UV-B-induced accumulation of phenylpropanoids and flavonoids has been closely related to, and regulated by photosynthesis. Flavonoids and anthocyanins (carbon-rich compounds) are mostly glycosylated in the plants, with two or three sugar moieties per aglycone, and their synthesis in the cells requires triosphosphates, ATP, NADPH and malonic acid. The link between photosynthesis and anthocyanin accumulation is even more clear in the case of variegated *Arabidopsis immutans* mutant, with 200 fold higher level of anthocyanin synthase transcripts in photosynthetic than in non-photosynthetic tissue<sup>66</sup>. Moreover, under HL, expression of anthocyanin regulatory transcription factors has been increased more than 100 times in green leaf sectors of *immutans* plants.

At the same time, these studies showed that UV-B differentially affected photosynthesis in the two variegated species (Figure 3). Favouring the carbon assimilation and electron partitioning towards phenylpropanoid pathway enabled increased flavonoid production in both leaf tissues of *P. coleoides* under UV-B radiation (Figure 3). Alternatively, in the leaves of *P. zonale*, UV-B radiation stimulated starch degradation and sugar transport from source to sink leaf tissue, providing the building blocks for biosynthesis of *p*-coumaric acid, kaempferol and quercetin glycosides, which have been induced in white tissue (Figure 3).

Taken together, the specific influence of UV radiation and of PAR alone, on plant metabolism is difficult to resolve, due to their interconnected character and due to other simultaneous factors in the field, which should not be neglected. However, it is obvious that signals dependent on photosynthesis are crucial in the regulation of biosynthesis of phenolic compounds, which are important not only for the plant-environment interactions, but are beneficial for human health and nutrition, as well. Moreover, the species-specific, and source-sink dependence of UV-B regulation of photosynthesis and associated processes, such as induction of flavonoids has to be considered. The targets of this regulation remain to be revealed.

## Conclusion and Future Perspectives

Naturally, PAR, UV-B and UV-A radiation are interlaced, and none should be taken as an isolated factor. The molecular mechanisms of functional integration of different light-mediated COP1-dependent pathways, in plants which grow under ambient conditions are still unknown. Besides photomorphogenic responses associated with COP1, high intensities of visible light can activate redox retrograde signalling pathways from chloroplasts, responsible for the acclimation responses. There is growing evidence that photosynthesis is involved in phenolics biosynthesis through redox changes in the electron transport chain, which include H<sub>2</sub>O<sub>2</sub> generation at PS I. In fact, it has been suggested that carbon-rich flavonoid glycosides act as energy escape valve under photooxidative stress. Comprehensive knowledge of the signalling pathways between plastids and other cellular compartments under optimal and stress conditions will provide new solutions for developing and engineering advanced plants with improved vigour and stress tolerance.

Furthermore, the specific effects of UV-B radiation on photosynthetic electron transport, CO<sub>2</sub> assimilation and associated processes still have to be elucidated. Investigation of the link between primary and secondary metabolism mediated by UV-B radiation presents a challenge for future studies.

## Acknowledgements

This study was supported by the Ministry of Education, Science and Technological Development, Republic of Serbia (Project No. III43010).

## References

1. Jiao Y, Lau OS, Deng XW. Light-regulated transcriptional networks in higher plants. *Nat Rev Genet* 2007;8:217-30.
2. Heijde M, Ulm R. UV-B photoreceptor-mediated signalling in plants. *Trends Plant Sci* 2012;17:230-37.
3. Mullineaux P, Karpinski S. Signal transduction in response to excess light: getting out of the chloroplast. *Curr Opin Plant Biol* 2002;5:43-8.
4. Lichtenthaler HK. Biosynthesis, accumulation and emission of carotenoids, alpha-tocopherol, plastoquinone, and isoprene in leaves under high photosynthetic irradiance. *Photosynth Res* 2007;92:163-79.
5. Li Z, Wakao S, Fischer BB, Niyogi KK. Sensing and responding to excess light. *Annu Rev Plant Biol* 2009;60:239-60.
6. Ort DR. When there is too much light. *Plant Physiol* 2001;125:29-32.
7. Baker NR. Chlorophyll fluorescence: a probe of photosynthesis *in vivo*. *Annu Rev Plant Biol* 2008;59:89-113.
8. Demmig-Adams B, Adams WW. The role of xanthophyll cycle carotenoids in the protection of photosynthesis. *Trends Plant Sci* 1996;1:21-6.
9. Asada K. The water-water cycle in chloroplasts: scavenging of active oxygens and dissipation of excess photons. *Annu Rev Plant Physiol Plant Mol Biol* 1999;50:601-39.
10. Noctor G, Veljovic-Jovanovic S, Driscoll S, Novitskaya L, Foyer CH. Drought and oxidative load in the leaves of C3 plants: a predominant role for photorespiration? *Ann Bot* 2002;89:841-850.
11. Vidović M, et al. Carbon allocation from source to sink leaf tissue in relation to flavonoid biosynthesis in variegated *Pelargonium zonale* under UV-B radiation and high PAR intensity. *Plant Physiol Biochem* 2015;93:44-55.
12. Vidović M, et al. Characterisation of antioxidants in photosynthetic and non-photosynthetic leaf tissues of variegated *Pelargonium zonale* plants. *Plant Biol* 2016;18:669-80.
13. Vidović M, Morina F, Prokić Lj, Milić-Komić S, Živanović B, Veljović Jovanović S. Antioxidative response in variegated *Pelargonium zonale* leaves and generation of extracellular H<sub>2</sub>O<sub>2</sub> in (peri)vascular tissue induced by sunlight and paraquat. *J Plant Physiol* 2016;206:25-39.
14. Mullineaux PM, Karpinski S, Baker NR. Spatial dependence for hydrogenperoxide-directed signaling in light-stressed plants. *Plant Physiol*. 2006;141:346-50.

15. Kuźniak E, et al. Photosynthesis-related characteristics of the midrib and the interveinal lamina in leaves of the C3-CAM intermediate plant *Mesembryanthemum crystallinum*. *Ann Bot* 2016;117:1141-51.
16. Mittler R, Blumwald E. The roles of ROS and ABA in systemic acquired acclimation. *Plant Cell* 2015;27:64-70.
17. Suzuki N, Koussevitzky S, Mittler R, Miller G. ROS and redox signalling in the response of plants to abiotic stress. *Plant Cell Environ* 2012;35:259-70.
18. Bobik K, Burch-Smith TM. Chloroplast signaling within, between, and beyond cells. *Front Plant Sci* 2015;6:781.
19. Stonebloom S, Brunkard JO, Cheung AC, Jiang K, Feldman L, Zambryski P. Redox states of plastids and mitochondria differentially regulate intercellular transport via plasmodesmata. *Plant Physiol* 2012;158:190-99.
20. Petrillo E, et al. A chloroplast retrograde signal regulates nuclear alternative splicing. *Science* 2014;344:427-30.
21. Neill SO, Gould KS. Anthocyanins in leaves: light attenuators or antioxidants? *Funct Plant Biol* 2003;30:865-73.
22. Hughes NM, Neufeld HS, Burkey KO. Functional role of anthocyanins in high-light winter leaves of the evergreen herb *Galax urceolata*. *New Phytol* 2005;168:575-87.
23. Guidi L, et al. UV radiation promotes flavonoid biosynthesis, while negatively affecting the biosynthesis and the de-epoxidation of xanthophylls: Consequence for photoprotection? *Environ Exp Bot* 2016;127:14-25.
24. Yamasaki H, Sakihama Y, Ikehara N. Flavonoid-peroxidase reaction as a detoxification mechanism of plant cells against H<sub>2</sub>O<sub>2</sub>. *Plant Physiol* 1997;115:1405-12.
25. Miller G, Suzuki N, Rizhsky L, Hegie A, Koussevitzky S, Mittler R. Double mutants deficient in cytosolic and thylakoid ascorbate peroxidase reveal a complex mode of interaction between reactive oxygen species, plant development, and response to abiotic stresses. *Plant Physiol* 2007;144:1777-85.
26. Vanderauwera S, et al. Genome-wide analysis of hydrogen peroxide-regulated gene expression in *Arabidopsis* reveals a high light-induced transcriptional cluster involved in anthocyanin biosynthesis. *Plant Physiol* 2005;139:806-21.
27. Maruta T, et al. Ferulic acid 5-hydroxylase 1 is essential for expression of anthocyanin biosynthesis-associated genes and anthocyanin accumulation under photooxidative stress in *Arabidopsis*. *Plant Sci* 2014;219:61-68.
28. Akhtar TA, Lees HA, Lampi MA, Enstone D, Brain RA, Greenberg BM. Photosynthetic redox imbalance influences flavonoid biosynthesis in *Lemna gibba*. *Plant Cell Environ* 2010;33:1205-19.
29. Vojta L, et al. TROL-FNR interaction reveals alternative pathways of electron partitioning in photosynthesis. *Sci Rep* 2015;5:10085.
30. Exposito-Rodriguez M, Laissue PP, Yvon-Durocher G, Smirnoff N, Mullineaux PM. Photosynthesis-dependent H<sub>2</sub>O<sub>2</sub> transfer from chloroplasts to nuclei provides a high-light signalling mechanism. *Nat Commun* 2017;8:49.

31. Dietz KJ. Thiol-based peroxidases and ascorbate peroxidases: why plants rely on multiple peroxidase systems in the photosynthesizing chloroplast? *Mol Cells* 2016;39:20-5.
32. Ishikawa T, Shigeoka S. Recent advances in ascorbate biosynthesis and the physiological significance of ascorbate peroxidase in photosynthesizing organisms. *Biosci Biotechnol Biochem* 2008;72:1143-54.
33. Kerr JB, Fioletov VE. Surface ultraviolet radiation. *Atmos-Ocean* 2008;46:159-84.
34. Jansen MAK, Gaba V, Greenberg BM. Higher plants and UV-B radiation: balancing damage, repair and acclimation. *Trends Plant Sci* 1998;3:131-35.
35. Lidon FJC, Reboredo FH, Leitã AE, Silva MMA, Duarte P, Ramalho JC. Impact of UV-B radiation on photosynthesis - an overview. *Emir J Food Agric* 2012;24:546-56.
36. Aphalo PJ, Albert A, Björn LO, McLeod A, Robson TM, Rosenqvist E. Beyond the visible: a handbook of best practice in plant UV photobiology. University of Helsinki, 2012.
37. Hideg É, Jansen MAK, Strid, Å. UV-B exposure, ROS, and stress: inseparable companions or loosely linked associates? *Trends Plant Sci* 2013;18:107-15.
38. Jenkins GI. Signal transduction in responses to UV-B radiation. *Annu Rev Plant Biol* 2009;60:407-31.
39. Vidović M, Morina F, Veljović Jovanović S. Stimulation of various phenolics in plants under ambient UV-B radiation. In: *UV-B Radiation: from environmental stressor to regulator of plant growth*. Wiley-Blackwell, West Sussex, UK, 2017;9-56.
40. Brosché M, Strid Å. Molecular events following perception of ultraviolet-B radiation by plants: UV-B induced signal transduction pathways and changes in gene expression. *Physiol Plant* 2003;117:1-10.
41. González Besteiro MA, Bartels S, Albert A, Ulm R. Arabidopsis MAP kinase phosphatase 1 and its target MAP kinases 3 and 6 antagonistically determine UV-B stress tolerance, independent of the UVR8 photoreceptor pathway. *Plant J* 2011;68:727-37.
42. Ulm R, Jenkins GI. Q&A: How do plants sense and respond to UV-B radiation? *BMC Biol* 2015;13:45.
43. Christie JM, et al. Plant UVR8 photoreceptor senses UV-B by tryptophan-mediated disruption of cross-dimer salt bridges. *Science* 2012;335:1492-96.
44. Heilmann M, Velanis CN, Cloix C, Smith BO, Christie JM, Jenkins GI. Dimer/monomer status and in vivo function of salt-bridge mutants of the plant UV-B photoreceptor UVR8. *Plant J* 2016;88:71-81.
45. Wu D, et al. Structural basis of ultraviolet-B perception by UVR8. *Nature* 2012;484:214-19.
46. Huang X, et al. Conversion from CUL4-based COP1-SPA E3 apparatus to UVR8-COP1-SPA complexes underlies a distinct biochemical function of COP1 under UV-B. *Proc Natl Acad Sci USA* 2013;110:16669-74.
47. Brown BA, Jenkins GI. UV-B signaling pathways with different fluence-rate response profiles are distinguished in mature Arabidopsis leaf tissue by requirement for UVR8, HY5, and HYH. *Plant Physiol* 2008;146:576-88.
48. Singh SK, Agrawal SB, Agrawal M. UVR8 mediated plant protective responses under low UV-B radiation leading to photosynthetic acclimation. *J Photochem Photobiol B Biol* 2014;137:67-76.

49. Yi C, Deng XW. COP1 - from plant photomorphogenesis to mammalian tumorigenesis. *Trends Cell Biol* 2005;15:618-25.
50. Chen H, et al. Arabidopsis CULLIN4-damaged DNA binding protein 1 interacts with Constitutively Photomorphogenic 1-Suppressor of PHYA complexes to regulate photomorphogenesis and flowering time. *Plant Cell* 2010;22:108-23.
51. Majer P, Hideg É. Existing antioxidant levels are more important in acclimation to supplemental UV-B irradiation than inducible ones: studies with high light pretreated tobacco leaves. *Emir J Food Agric* 2012;24:598-606.
52. Grifoni D, Agati G, Bussotti F, Michelozzi M, Pollastrini M, Zipoli G. Different responses of *Arbutus unedo* and *Vitis vinifera* leaves to UV filtration and subsequent exposure to solar radiation. *Environ Exp Bot* 2016;128:1-10.
53. Götz M, et al. PAR modulation of the UV-dependent levels of flavonoid metabolites in *Arabidopsis thaliana* (L.) Heynh. leaf rosettes: cumulative effects after a whole vegetative growth period. *Protoplasma* 2010;243:95-103.
54. Britt AB. Repair of DNA damage induced by solar UV. *Photosynth Res* 2004;81:105-12.
55. Ballaré CL, Caldwell MM, Flint SD, Robinson SA, Bornman JF. Effects of solar ultraviolet radiation on terrestrial ecosystems. Patterns, mechanisms, and interactions with climate change. *Photochem Photobiol Sci* 2011;10:226-41.
56. Gould KS, Lister C. Flavonoid functions in plants. In: *Flavonoids: chemistry, biochemistry and applications*. CRC Press Taylor & Francis, Boca Raton, USA. 2006;397-441.
57. Sedlarević A, et al. Comparative analysis of phenolic profiles of ovipositional fluid of *Rhinusa pilosa* (Mecynini, Curculionidae) and its host plant *Linaria vulgaris* (Plantaginaceae). *Arthropod Plant Interact.* 2016;10:311-22.
58. Jansen MAK, Hectors K, O'Brien NM, Guisez Y, Potters G. Plant stress and human health: Do human consumers benefit from UV-B acclimated crops? *Plant Sci* 2008;175:449-58.
59. Živanović B, et al. Contents of phenolics and carotenoids in tomato grown under polytunnels with different UV-transmission rates. *Turk J Agric For* 2017;41:113-20.
60. Jensen RA. The shikimate/arogenate pathway: link between carbohydrate metabolism and secondary metabolism. *Physiol Plant* 1986;66:164-68.
61. Hernández I, Van Breusegem F. Opinion on the possible role of flavonoids as energy escape valves: novel tools for nature's Swiss army knife? *Plant Sci* 2010;179:297-301.
62. Kataria S, Jajoo A, Guruprasad KN. Impact of increasing ultraviolet-B (UV-B) radiation on photosynthetic processes. *J Photochem Photobiol B Biol* 2014;137:55-66.
63. Rossini S, Casazza AP, Engelmann ECM, Havaux M, Jennings RC, Soave C. Suppression of both ELIP1 and ELIP2 in Arabidopsis does not affect tolerance to photoinhibition and photooxidative stress. *Plant Physiol* 2006;141:1264-73.
64. Vidović M, et al. UV-B component of sunlight stimulates photosynthesis and flavonoid accumulation in variegated *Plectranthus coleoides* leaves depending on background light. *Plant Cell Environ* 2015;38:968-79.
65. Smeekens S, Ma J, Hanson J, Rolland F. Sugar signals and molecular networks controlling plant growth. *Curr Opin Plant Biol* 2010;13:274-79.

66. Aluru MR, Zola J, Foudree A, Rodermeil SR. Chloroplast photooxidation-induced transcriptome reprogramming in *Arabidopsis immutans* white leaf sectors. *Plant Physiol* 2009;150:904-23.

---

# Phytochemical characterization and biological activities of some *Gentiana* plants from Serbia

---

Vladimir B. Mihailović\*

Department for Chemistry, Faculty of Science, University of Kragujevac, Kragujevac, Serbia

\*e-mail: vladam@kg.ac.rs

Medicinal plants and phytochemicals are often used in complementary and alternative medicines or as natural alternatives to synthetic drugs. In this sense, scientific data about their efficacy, safety and drug-discovery potentials are significant for modern pharmacy as an important gateway to novel discoveries for drug development as well as safe and effective use of traditional medicines. In spite of the wide use of *Gentiana* plants in ethnopharmacology, we investigated wild-growing *G. asclepiadea* and *G. cruciata*, members of the Gentianaceae family collected in Serbia. Phytochemical investigations revealed that these plants contain high amount of the bitter constituents which belong to the class of secoiridoid glycosides, with gentiopicrin as a main component followed by swertiamarine and sweroside. HPLC-MS studies also showed the presence of phenolic compounds in studied plants. Besides chemical composition of selected plants, our studies included biological investigations of their extracts, including antimicrobial, antioxidant, and hepatoprotective activities. Obtained results confirmed the hepatoprotective effects of aerial part and root extracts of *G. asclepiadea* and *G. cruciata* against carbon tetrachloride-induced liver injury in rats. Also, *G. asclepiadea* and *G. cruciata* extracts showed good antioxidant and antifungal activities. The observed results provide valuable information about phytochemistry of *Gentiana* plants, their pharmacological importance and support of the traditional use of these plants in the treatment of different liver diseases.

## Introduction

The family *Gentianaceae*, currently, includes 99 genera and over 1700 flowering species<sup>1</sup>. The plants of the family are many tropical and temperate trees, shrubs, and herbs<sup>2</sup>. *Gentianaceae* contain many species with interesting phytochemical properties. The genera *Blackstonia*, *Swertia*, *Centaurium*, *Gentiana*, and *Gentianella* are present in the flora of Serbia with the highest number of species in the genus *Gentiana*<sup>3</sup>. *Gentianaceae* contain many species widely used in traditional medicine and also as constituents in bitters and similar concoctions<sup>4</sup>. These are popular ingredients of many gastric herbal preparations and dietary supplements. Plants from *Gentiana* genus are also used in small amounts as

food and beverage flavoring agents, in antismoking products and even used as a substitute for hops in making beer<sup>5</sup>. Some plants from this family have a long tradition of use in Europe, dried flowering aerial parts of *Centaureum erythraea* (*Centaurei herba*) and the dried root of *Gentiana lutea* (*Gentianae radix*) have been reported in many European handbooks and Pharmacopoeias as medicines for gastrointestinal disorders<sup>6,7</sup>. The herbal substances and herbal preparations from *G. lutea* (great yellow gentian), such as an herbal tea, dry extract, tincture, and fluid extract have been found on the European market<sup>6</sup>. Due to overharvesting of *C. erythraea*, the number of wild populations and their sizes are decreasing<sup>8</sup>. Also, *G. lutea* is under wildlife protection in many countries<sup>6</sup>.

Besides great yellow gentian, widely distributed species of *Gentiana* throughout Europe are *Gentiana asclepiadea* L. and *G. cruciata* L.. *G. asclepiadea* is traditionally used as a medicine for hepatitis infections and the Serbian local name of this plant is a “grass of jaundice”. Herb and roots of this plant are also used in the traditional medicine as bitter tonics and gastric stimulants. *G. cruciata*, commonly called cross gentian, is also known as an appetite stimulant, for improving digestion, as well as component in preparations for gastroduodenal and liver protection<sup>9,10</sup>. Previous studies reported hepatoprotective, anti-inflammatory, cytotoxic, antitumor, antimicrobial, antioxidant, cholinesterase inhibitory, and immunomodulatory activities of *Gentiana* plant extracts<sup>11</sup>.

Phytochemical investigations of Gentianaceae species showed the presence of iridoids, xanthones, mangiferin, and C-glucoflavones in rhizomes, roots, stems, leaves, aerial parts, whole plants, and flowers of these species<sup>4</sup>. The iridoids (mainly secoiridoid glucosides) are typical chemical compounds from Gentianaceae plants presented in all species investigated. The secoiridoid glycosides identified in *Gentiana* species included mainly gentiopicroside (also known as gentiamarine and gentiopicrin), amarogentin, swertiamarine, and sweroside<sup>4,12</sup>. Xanthones (including mangiferin) and C-glucoflavones are not universally present in Gentianaceae<sup>4</sup>. Secoiridoid glycosides possess a wide spectrum of biological activities including antibacterial, antifungal<sup>13</sup>, anti-inflammatory, antitumor<sup>14</sup>, gastroprotective<sup>15</sup>, and hepatoprotective<sup>16,17</sup> activities. Also, phenolic compounds and xanthones from Gentianaceae species exhibited range of pharmacological activities, including antioxidant, antiproliferation, antifungal, and radioprotective<sup>11</sup>.

With the evidences of the bioactivities of *Gentiana* plants and the phytochemicals presented in these plants we continuously investigated chemical composition, antimicrobial and antioxidant potential of *G. asclepiadea* and *G. cruciata*. Considering the use of these plants in traditional medicine, our studies were also aimed to evaluate the *in vivo* hepatoprotective activity of *G. asclepiadea* and *G. cruciata* against hepatotoxicity induced by CCl<sub>4</sub> based on the traditional claim.

## Phytochemical analysis

For phytochemical analysis of selected *Gentiana* species collected in Serbia, we used methanolic extracts obtained from plants aerial parts and roots. Obtained extracts were characterized using spectrophotometric methods for quantification of phenolic compounds

and HPLC analysis for identification and quantification of secoiridoids and phenolic compounds. *G. asclepiadea* and *G. cruciata* extracts showed the presence of various quantities of total phenolic and flavonoids contents. The results showed that *G. cruciata* aerial part extract contained significantly higher total phenolic quantity than *G. asclepiadea* extracts. Contrary, *G. asclepiadea* aerial part extract had the highest total flavonoids content among all examined extracts (1 g of extract contained 51.98 mg of rutin equivalents). The concentrations of total phenolics and flavonoids were also higher in the aerial part than in root extracts of *G. asclepiadea* and *G. cruciata*<sup>18,19</sup>.

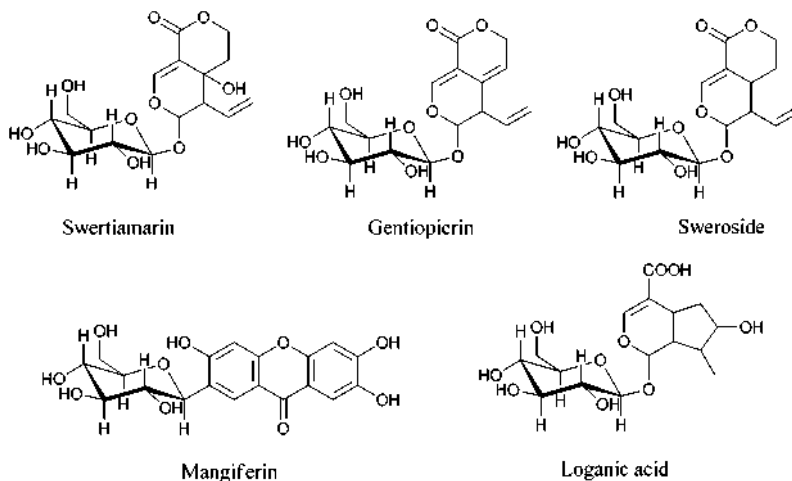


**Figure 1.** Iridoids, secoiridoids, and xanthones identified in investigated plant species.

In order to identify and quantify secoiridoids, mangiferin, and phenolic compounds, samples were subjected to HPLC-DAD and UHPLC-DAD/±HESI-MS/MS analysis. Identified secoiridoid glycosides in tested extracts are shown in Figure 1. Characteristic secoiridoid glycosides for *Gentianaceae* plant, swertiamarin, gentiopicrin and sweroside, were presented in all examined plant extract. According to obtained quantitative data, gentiopicrin was a dominant compound in all extracts with the highest concentration in *G. asclepiadea* extract. HPLC analyses showed higher concentration of gentiopicrin in roots of *G. asclepiadea* and *G. cruciata* than corresponding aerial part extracts. Concentration of gentiopicrin in examined extracts was in the range of 10.7 to 23.3 mg per g of dry extract. The concentrations of swertiamarin and sweroside were lower compared with gentiopicrin<sup>19,20,21</sup>. Mangiferin (Figure 1), a C-glucoxanthone, was identified only in *G. asclepiadea* aerial part extract<sup>19,20</sup>. Loganic acid (Figure 1), as the biosynthetic precursor of all iridoids and secoiridoids, was identified in aerial part and root extracts of *G. asclepiadea* and *G. cruciata*<sup>19</sup>.

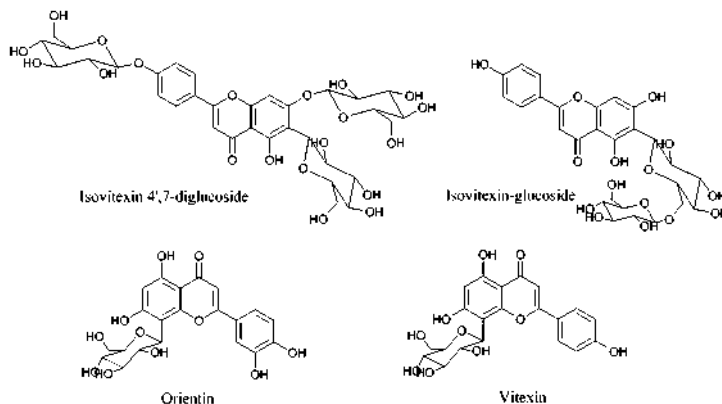


**Figure 2.** Phenolic compounds identified in investigated plant species.

Besides secoiridoid glycosides, UHPLC/±HESI-MS/MS analysis of methanolic extracts of *G. asclepiadea* and *G. cruciata* showed that extracts also contained more different phenolic compounds, mainly flavonoids (Figure 2). Widely distributed C-glucoflavones in Gentianaceae plants were identified in the extracts of two investigated *Gentiana* plants. Isovitexin 4',7-diglucoside, isovitexin-glucoside, orientin and vitexin (Figure 2) were putatively identified in both aerial part and root extracts of *G. asclepiadea*, while vitexin was identified in both investigated extracts of *G. cruciata*. Except vitexin, the root extract of *G. cruciata* contained isovitexin-glucoside, while *G. cruciata* aerial part extract contained isovitexin 4',7-diglucoside and orientin<sup>19</sup>. In previous studies, C-glucoflavones such as isoorientin, isovitexin, and their glucosides<sup>22</sup>, were identified in *G. asclepiadea* and *G. cruciata*. In our study, isovitexin 4',7-diglucoside, orientin and vitexin were identified for the first time in *G. asclepiadea* and *G. cruciata*.

### Antimicrobial activity

The methanolic extracts of aerial part and root of *G. asclepiadea* and *G. cruciata* were tested against a set of different bacterial and fungal strains. The obtained values for minimal inhibitory concentration (MIC) showed differences in activity of examined extracts. The highest antibacterial activity was observed for *G. asclepiadea* aerial part extract, with MIC values in the range of 0.2 to 1.6 mg/mL and with significantly lower MICs for Gram positive bacteria. Among Gram-negative bacterial species, only *E. coli* was sensitive to *G. asclepiadea* aerial part extract with a MIC of 0.8 mg/mL<sup>23</sup>. *G. cruciata* aerial part extract was almost ineffective in inhibition of bacterial growth showing bacteriostatic effects only for *E. faecalis* and *B. subtilis* (MICs were 8.0 and 4.0 mg/mL, respectively). *G. asclepiadea* and *G. cruciata* root extracts did not inhibit bacterial growth in concentration up to 10 mg/mL. *G. asclepiadea* aerial part extract also showed the lowest MIC values against selected fungal species. The most sensitive fungal species to this extract were two *Penicillium* species<sup>23</sup>. All investigated fungal species, except yeast *C.*

*albicans*, were resistant to *G. cruciata* aerial part extract. The root extracts were able to inhibit growth of most of tested fungal species with MIC values up to 10 mg/mL. For most fungal species, *G. cruciata* root extract showed lower MICs (0.156-0.625 mg/mL) than *G. asclepiadea* root extract (MIC 1.25-10.0 mg/mL). Better antifungal activities of the root extracts could be attributed to the higher presence of secoiridoid glycosides in the root than in the aerial part extract. The antifungal activity of secoiridoid glycosides was confirmed in previously published studies<sup>24,25</sup>. The better antimicrobial properties exhibited by *G. asclepiadea* aerial part extract may be due to the presence of mangiferin, xanthone presented only in this extract. Mangiferin was previously reported as antibacterial compound against a range of bacteria and methicillin-resistant *S. aureus*<sup>26,27</sup>.

### **Antioxidant activity**

The antioxidant activity of aerial parts and root extracts of *G. asclepiadea* and *G. cruciata* were determined using DPPH<sup>•</sup> and ABTS<sup>•+</sup> radical scavenging, reducing power, and lipid peroxidation assays. As shown in Figure 3, *G. asclepiadea* aerial part extract showed significantly ( $p < 0.05$ ) higher antioxidant activities in all applied methods than other examined extracts. Both aerial part extracts showed significantly ( $p < 0.05$ ) better antioxidant properties than root extracts with lower IC<sub>50</sub> values<sup>18,19</sup>. The better antioxidant activity of aerial part extracts is certainly related to a higher content of phenolics and flavonoids in these extracts compared to root extracts. The antioxidant activity of examined extracts was remarkably lower than the antioxidant activities of the well-known antioxidants, ascorbic acid and BHT.

The variation in the antioxidant properties of extracts could be attributed to the differences in their phytochemical profile. Regardless of a greater content of total phenolic compounds in *G. cruciata* aerial part extract, *G. asclepiadea* aerial part extract with a higher total flavonoids content showed better antioxidant potential. Also, better antioxidant activities of *G. asclepiadea* aerial part extract might depend on the presence of mangiferin in the extract which was not identified in other extracts. The antioxidant activity of mangiferin has been demonstrated as the free radical scavenger in many food and medicinal plants<sup>28</sup>. Regarding the fact that extracts with lower amounts of phenolic compounds and higher content of secoiridoides exhibited lower antioxidant activity, it may be concluded that the presence of secoiridoids did not have significant influence on antioxidant activities of extracts. According to the literature, swertiamarin, gentiopicrin and sweroside did not show antioxidant activity in DPPH assay<sup>13,29</sup>.

### **Hepatoprotective activity**

Considering the use of *Gentiana* plant in traditional medicine for the treatment of liver disease and previous reports that *Gentiana* plants rich in secoiridoid constituents, mainly gentiopicrin, are effective in protecting the liver against acetaminophen- and alcohol-induced liver damage<sup>30,31</sup>, we investigated hepatoprotective activity of methanolic extracts of aerial parts and roots of *G. asclepiadea* and *G. cruciata* against hepatotoxicity induced

by carbon tetrachloride (CCl<sub>4</sub>). Analyzed parameters and influence of examined extracts in liver protection against CCl<sub>4</sub> induced hepatotoxicity were illustrated in Figure 4. The main causes of acute liver injury by CCl<sub>4</sub> are generation of free radicals during its metabolism by the cytochrome P<sub>450</sub> (CYP) system. Trichloromethyl free radicals (‘CCl<sub>3</sub> or CCl<sub>3</sub>OO’), generated in this process<sup>32</sup>, immediately propagate a chain of lipid peroxidation leading to the breakdown of membrane structure and the consequent leakage of hepatic cell enzymes alanine aminotransferase (ALT), aspartate aminotransferase (AST), and alkaline phosphatase (ALP) into the bloodstream<sup>33</sup>.

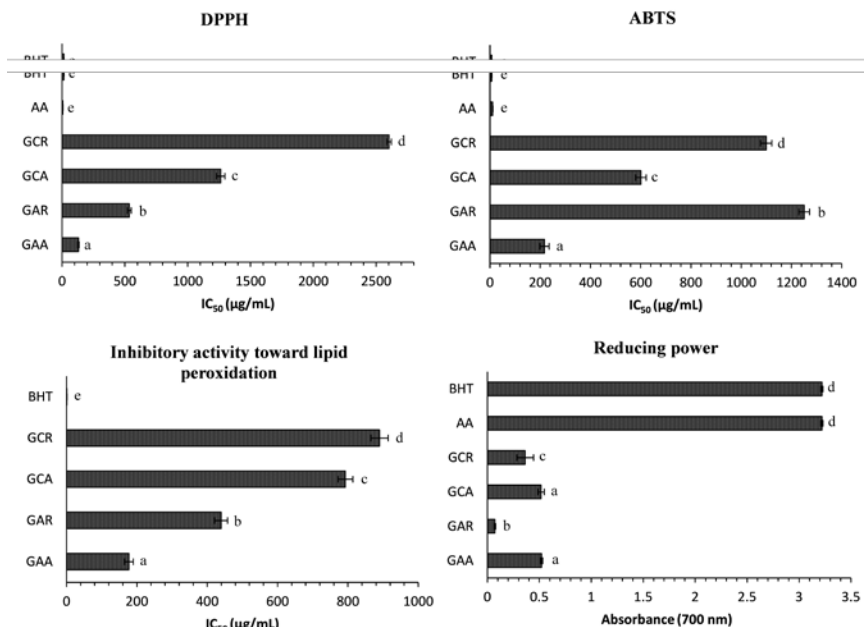


**Figure 3.** Antioxidative activity of *G. asclepiadea* and *G. cruciata* extracts<sup>18,19</sup>. GAA - *G. asclepiadea* aerial part extract, GAR - *G. asclepiadea* root extract, GCA - *G. cruciata* aerial part extract, GCR - *G. cruciata* root extract. Results were expressed as the means  $\pm$  SD from 3 independent determinations. Means with different letters are significantly different at  $p < 0.05$ .

In our studies, administration of CCl<sub>4</sub> to experimental group of rats caused significant increase of serum activities of AST, ALT and ALP enzymes and total bilirubin level, as well as a significant decrease of total protein level, compared to the untreated group. Experimental groups which orally received aerial part and root extracts of *G. asclepiadea* and *G. cruciata* in three different concentrations (100, 200 and 400 mg/kg of body weight (b.w.)) within 7 days prior to intraperitoneally administration of CCl<sub>4</sub> significantly normalize examined serum biochemical parameters compared to the CCl<sub>4</sub>-treated group (positive control). Comparing the results of serum biochemical parameters between the

groups, root extracts of both plants at the dose of 400 mg/kg b.w. reduced the activity of AST, ALT, and ALP more markedly, compared to aerial part extracts at the same dose. Serum biochemical parameters results also showed that *Gentiana* root extracts at the dose of 400 mg/kg b.w. possessed a same hepatoprotective level as well-known natural drug silymarin, applied in the dose of 100 mg/kg b.w. <sup>20,21</sup>.

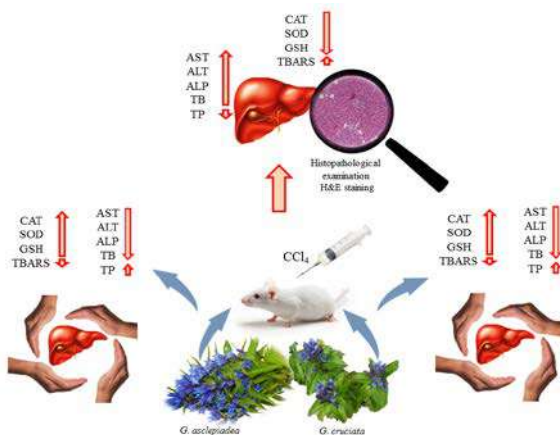


**Figure 4.** Hepatoprotective activity of *G. asclepiadae* and *G. cruciata* <sup>20,21</sup>. ALT - alanine aminotransferase, AST - aspartate aminotransferase, ALP - alkaline phosphatase, TB - total bilirubin, TP - total protein, CAT - catalase, SOD - superoxide dismutase, GSH - glutathione reduced, TBARS - thiobarbituric acid-reactive substance.

One of the possible mechanisms of hepatoprotective activities of medicinal plants is their antioxidant activity. As indicators of oxidative stress level in liver tissue in the investigation of the hepatoprotective activity of *G. asclepiadae* and *G. cruciata* extracts, we monitored the activities of catalase (CAT) and superoxide dismutase (SOD), as well as the levels of reduced glutathione (GSH) and thiobarbituric acid-reactive substance (TBARS) in rat liver homogenates. The administration of  $\text{CCl}_4$  to rats significantly decreased GSH, the activities of SOD and CAT, and increased the level of TBARS compared to the normal group. Pretreatment with *G. asclepiadae* extracts at concentrations of 200 and 400 mg/kg b.w. significantly regulated all examined oxidative stress parameters in liver, while extracts applied in concentration of 100 mg/kg b.w. did not have significant influence on all oxidative stress parameters compared with  $\text{CCl}_4$ -control group <sup>20</sup>. Considering obtained results for *G. cruciata* extracts, the most effective dose of aerial part and root extracts in the regulation of oxidative stress caused by  $\text{CCl}_4$  injection was 400 mg/kg b.w. *G. cruciata* extracts applied at doses of 100 and 200 mg/kg b.w. did not show significant regulation of all oxidative stress related parameters compared with  $\text{CCl}_4$ -model group. Silymarin showed more pronounced antioxidant effects against  $\text{CCl}_4$  induced hepatotoxicity compared to *G. cruciata* extracts <sup>21</sup>. Both examined plants showed

antioxidant potential, suggesting that they could modulate antioxidant defense system or prevent the formation and neutralize free radicals originated from CCl<sub>4</sub> metabolism.

Parallel with determination of biochemical parameters in serum and oxidative stress parameters in liver tissue from rats in different groups, the histopathological examination of the liver sections stained with haematoxylin-eosin were examined. According to histopathological results, CCl<sub>4</sub> induced ballooning degeneration (especially at the periphery of lobules), dilated portal spaces followed by infiltration of lymphocytes, focal and piecemeal necrosis. The pretreatment with all extracts in medium and high-dose markedly ameliorated the histological changes induced by CCl<sub>4</sub>. The pathomorphological changes were minor in groups pretreated with root extracts of both studied plants at the dose of 400 mg/kg b.w. compared with CCl<sub>4</sub>-model group. Appearances of some pathological hepatic lesions induced by the administration of CCl<sub>4</sub> were prevented in a better manner by these two extracts than by silymarin<sup>20,21</sup>.

Well known hepatoprotective compounds identified in all *Gentiana* extracts included in our experiments are gentiopicrin and swertiamarin<sup>16,17,34</sup>. The presence of these two active compounds in investigated *Gentiana* extracts may be the main contributing factor toward their hepatoprotective activity, but the total bioactivity of extracts might also depend of all phytochemicals present in extracts including phenolic compounds and mangiferin identified only in the aerial part extract of *G. asclepiadea* that is known to exhibit hepatoprotective effects<sup>35</sup>.

## Conclusion

The extracts of *G. asclepiadea* and *G. cruciata* plants displayed very similar biological activities, with some differences in their chemical composition. Higher gentiopicrin content was observed in *G. asclepiadea* extracts and mangiferin was identified in the aerial part extract, while *G. cruciata* aerial part extract possessed the highest total phenolic content. The differences in the chemical composition of investigated extracts can clarify that *G. asclepiadea* root extract (gentiopicrin-enriched extract) at the highest dose more effectively protect the liver from chemically induced toxicity compared with *G. cruciata*. *G. asclepiadea* also showed better antioxidant activities *in vitro* and *in vivo* than *G. cruciata*. Regardless of the differences between studied *Gentiana* plants, the results justify the use of these plants in traditional medicine in Serbia for the treatment of liver disease and suggesting that investigated plants could be attractive for pharmaceutical industry in forthcoming research. Also, both investigated plants possess remarkable biological activities, high secoiridoids content and could be used as a substitute for other endangered *Gentiana* species.

## Acknowledgements

This study was supported by the Ministry of Education, Science and Technology of the Republic of Serbia (project no. III 43004).

## References

1. Struwe L. Classification and Evolution of the Family Gentianaceae. In: Rybczyński JJ, Davey RM, Mikula A (eds) *The Gentianaceae - Volume 1: Characterization and Ecology*, Springer, Berlin, 2014, pp 13-35.
2. Singh A. Phytochemicals of Gentianaceae: A review of pharmacological properties. *Int J Pharm Sci Nanotech* 2008;1:33-6.
3. Josifović M. *Flora SR Srbije*, SASA, Belgrade, Serbia, 1973, pp. 419-420.
4. Jensen SR, Schripsema J. Chemotaxonomy and pharmacology of Gentianaceae. In: Struwe L, Albert VA (eds) *Gentianaceae systematics and natural history*, Cambridge University Press, Cambridge, 2002, pp. 573-631.
5. Hudecova A, et al. *Gentiana asclepiadea* protects human cells against oxidation DNA lesions. *Cell Biochem Funct* 2012;30:101-7.
6. European Medicines Agency (EMA), Assessment Report on *Gentiana lutea* L., radix (Doc. Ref.: EMA/HMPC/578322/2008). Committee on Herbal Medicinal Products, London, 2009.
7. European Medicines Agency (EMA), Assessment report on *Centaurium erythraea* Rafn. s.l., herba (Doc. Ref.: EMA/HMPC/277491/2015). Committee on Herbal Medicinal Products, London, 2015.
8. Šiler B, Avramov S, Banjanac T, Cvetković J, Nestorović Živković J, Patenković A, Mišić D. Secoiridoid glycosides as a marker system in chemical variability estimation and chemotype assignment of *Centaurium erythraea* Rafn from the Balkan Peninsula. *Ind Crops Prod* 2012;40:336-44.
9. Sarić M. *Lekovito Bilje Srbije*. SASA, Belgrade, Serbia, 1989.
10. Menković N, Šavikin K, Tasić S, Zbunić G, Stešević S, Milosavljević S, Vinček D. Ethnobotanical study on traditional uses of wild medicinal plants in Prokletije Mountains (Montenegro). *J Ethnopharmacol* 2011;133:97-107.
11. Pan Y, Zhao YL, Zhang J, Li WY, Wang YZ. Phytochemistry and pharmacological activities of the genus *Gentiana* (Gentianaceae). *Chem Biodiversity* 2016;13:107-50.
12. Aberham A, Pieri A, Croom Jr E, Ellmerer E, Stuppner H. Analysis of iridoids, secoiridoids and xanthenes in *Centaurium erythraea*, *Frasera caroliniensis* and *Gentiana lutea* using LC-MS and RP-HPLC. *J Pharm Biomed Anal* 2011;54:517-25.
13. Kumarasamy Y, Nahar L, Cox PJ, Jaspars M, Sarker SD. Bioactivity of secoiridoid glycosides from *Centaurium erythraea*. *Phytomedicine* 2003;10:344-7.
14. Ghisalberti EL. Biological and pharmacological activity of naturally occurring iridoids and secoiridoids. *Phytomedicine* 1998;5:147-63.
15. Niiho Y, et al. 2006. Gastroprotective effects of bitter principles isolated from *Gentian root* and *Swertia herb* on experimentally-induced gastric lesions in rats. *J Nat Med* 2006;60:82-8.
16. Kondo Y, Takano F, Hojo H. 1993. Suppression of chemically and immunologically induced hepatic injuries by gentiopicroside in mice. *Planta Med* 1993;60:414-6.
17. Lian LH, Wu YL, Wan Y, Li X, Xie WX, Nan JX. Anti-apoptotic activity of gentiopicroside in galactosamine/lipopolysaccharide-induced murine fulminant hepatic failure. *Chem Biol Interact* 2010;188:127-33.

18. Nićiforović N, Mihailović V, Mašković P, Solujić S, Stojković A, Pavlović Muratspahić D, Antioxidant activity of selected plant species; potential new sources of natural antioxidants. *Food Chem Toxicol* 2010;48:3125-30.
19. Mihailović V, et al. Comparative phytochemical analysis of *Gentiana cruciata* L. roots and aerial parts, and their biological activities. *Ind Crops Prod* 2015;73:49-62
20. Mihailović V, et al. Hepatoprotective effects of *Gentiana asclepiadea* L. extracts against carbon tetrachloride induced liver injury in rats. *Food Chem Toxicol* 2013;52:83-90.
21. Mihailović V, et al. Hepatoprotective effects of secoiridoid-rich extracts from *Gentiana cruciata* L. against carbon tetrachloride induced liver damage in rats, *Food Funct* 2014;5:1795-803.
22. Goetz M, Hostettmann K, Jacot-Gullarmod A. C-glucosides flavoniques et xanthoniques de *Gentiana cruciate*. *Phytochemistry* 1976;15:2015.
23. Mihailović V, Vuković N, Nićiforović N, Solujić S, Mladenović M, Mašković P, Stanković MS, Studies on the antimicrobial activity and chemical composition of the essential oils and alcoholic extracts of *Gentiana asclepiadea*. L. *J Med Plant Res* 2011;5:1164-74.
24. Tan RX, Wolfender JL, Ma WG, Zhang LX, Hostettman K. Secoiridoids and antifungal aromatic acids from *Gentiana algida*. *Phytochemistry* 1996;41:111-6.
25. Tan RX, Wolfender JL, Zhang LX, Ma WG, Fuzzati N, Marston A, Hostettman K. Acyl secoiridoids and antifungal constituents from *Gentiana macrophylla*. *Phytochemistry* 1996;42:1305-13.
26. Azebaze AGB, et al. Antimicrobial and antileishmanial xanthenes from the stem bark of *Allanblackia gabonensis* (Guttiferae). *Nat Prod Res* 2008;22:333-41.
27. Xin WB, Mao ZJ, Jin GL, Qin LP. Two new xanthenes from *Hypericum sampsonii* and biological activity of the isolated compounds. *Phytother Res* 2011; 25:536-9.
28. Zhi-quanW, Jia-gang D, Li Y. Pharmacological effects of mangiferin. *Chin Herb Med* 2011;3: 266-71.
29. Šiler B, et al. Centauries as underestimated food additives: antioxidant and antimicrobial potential. *Food Chem* 2014;147:367-76.
30. Wang AY, Lian LH, Jiang YZ, Wu YL, Nan JX. *Gentiana manshurica* Kitagawa prevents acetaminophen induced acute hepatic injury in mice via inhibiting JNK/ERK MAPK pathway. *World J Gastroenterol* 2010;21:384-91.
31. Lian LH, et al. *Gentiana manshurica* Kitagawa reverses acute alcohol-induced liver steatosis through blocking sterol regulatory element-binding protein-1 maturation. *J Agric Food Chem* 2010;58:13013-9.
32. Sheweita SA, Abd El-Gabar M, Bastawy M. Carbon tetrachloride-induced changes in the activity of phase II drug-metabolizing enzyme in the liver of male rats: role of antioxidants. *Toxicology* 2001;28:217-24.
33. Zhou D, Ruan J, Cai Y, Xiong Z, Fu W, Wei A. Antioxidant and hepatoprotective activity of ethanol extract of *Arachniodes exilis* (Hance) Ching. *J Ethnopharmacol* 2010;129:232-7.
34. Jaishree V, Badami S. Antioxidant and hepatoprotective effect of swertiamarin from *Enicostemma axillare* against D-galactosamine induced acute liver damage in rats. *J Ethnopharmacol* 2010;130:103-6.

35. Das J, Ghosh J, Roy A, Sil PC. Mangiferin exerts hepatoprotective activity against D-galactosamine induced acute toxicity and oxidative/nitrosative stress via Nrf2-NFjB pathways. *Toxicol Appl Pharmacol* 2012;260:35-47.



---

# Phytochemical re-examination of well-studied medicinal plants as an useful approach in the discovery of (novel) potentially bioactive natural products - The case of *Inula helenium* L.

---

Marija S. Genčić<sup>1\*</sup>, Niko S. Radulović<sup>1</sup>, Polina D. Blagojević<sup>1</sup>, Zorica Z. Stojanović-Radić<sup>2</sup>

<sup>1</sup>Department of Chemistry, Faculty of Science and Mathematics, University of Niš, Niš, Serbia

<sup>2</sup>Department of Biology, Faculty of Science and Mathematics, University of Niš

\*e-mail: denijum@yahoo.com

Medicinal plants have historically proven their value as a source of molecules with therapeutic potential, and nowadays still represent an important pool for the identification of novel drug leads. Over the years, some medicinal plants gain a status of well-studied species, from both phytochemical and pharmacological standpoint. However, constant progress in modern analytical techniques, separation methods and bioassays protocols, alongside with the change in plants secondary metabolites profiles that could be triggered by various genetic and ecological factors, increase the chance of finding new bioactive molecules even from these well-studied plant species. Herein we want point out how useful could be this re-examination approach in the case of *Inula helenium* L. (Asteraceae), a plant species with renowned ethnopharmacological usage especially in treatment of respiratory diseases and disorders. Our re-examination resulted in determination of the mode of action of *I. helenium* root essential oil against *Staphylococcus aureus* (common cause of skin and respiratory infections, and food poisoning), identification of three sesquiterpene lactones (alantolactone, isoalantolactone and diplophyllin) as main active principles and “location” of their pharmacophore. Bioassayed-guided fractionation of the oil also disclosed minor active constituent, rare sesquiterpene aldehyde elemenal, and a series of long-chain 3-methyl-2-alkanones, newly found plant secondary metabolites. To assess the structures of mentioned compounds we had to develop new NMR-based method and to apply small combinatorial library approach. Overall, it seems that structural fragment consisted of methylene double bond conjugated with carbonyl group (present in both sesquiterpene lactones and elemenal) represent a promising lead for antistaphylococcal agents development.

## From plant to pharmacy shelf – past, present and future

Ever since ancient times, in search for rescue for their disease, the people looked for medicines in nature. The healing properties of certain medicinal plants were identified, noted, and conveyed to the successive generations. The first written evidences of the use of plants as medicinal agents date back to 2600 BC and describe the existence of a

sophisticated medicinal system in Mesopotamia, comprising about 1000 plant-derived drugs<sup>1</sup>. However, it was not until the early 1800's that the active principles from plants were isolated, when the German apothecary assistant Friedrich Sertürner succeeded in isolating the analgesic and sleep-inducing agent from opium which he named morphium (morphine) after the Greek god of dreams, Morpheus. Morphine is also considered as the first natural product introduced for therapeutic use, marketed by Merck in 1826. This success triggered more intense examination of other medicinal herbs during the following decades of the 19<sup>th</sup> century and led to isolation of many bioactive natural products, primarily alkaloids (e.g. quinine, caffeine, nicotine, codeine, atropine, colchicine, cocaine, capsaicin) from their natural sources and some of them are still in use as drugs<sup>2</sup>. It could be said that it was at this point that the effectiveness of medicinal plants began to be attributed to science and not to magic or witchcraft. Subsequently, efforts were undertaken to produce natural products by chemical synthesis in order to facilitate production at higher quality and lower costs. Salicylic acid was the first natural compound produced by chemical synthesis in 1853, while the first semi-synthetic pure drug aspirin, based on a natural product salicin isolated from *Salix alba*, was introduced by Bayer in 1899<sup>3</sup>.

Natural products have provided considerable value to the pharmaceutical industry over the past half century. Until 2000, at least 119 chemical substances, derived from 90 plant species, were in use as drugs in one or more countries. Among these, 74% were discovered as a result of chemical studies directed at the isolation of the active substances from plants used in traditional medicine. In addition, about 10 new drugs originating from terrestrial plants launched on the market between 2000 and 2010<sup>3,4</sup>.

Although there are some limitation in natural product drug discovery programs, like accessibility of the plant material or a natural product that is identified to have a very promising bioactivity and becomes a pharmaceutical lead, they continue to be competitive with other drug discovery methods, and also to keep pace with the ongoing changes in the drug discovery process<sup>3,4</sup>. This unending interest in natural products research is mostly due to the failure of alternative drug discovery methods (e.g. combinatorial synthesis, computational design synthesis, target- or diversity-oriented synthesis) to deliver many lead compounds in key therapeutic areas such as immunosuppression, anti-infective, and metabolic diseases. On the other hand, the inherent potential of natural products in drug discovery lies in their structural diversity that is still largely untapped. Unfortunately, the chemical diversity and complexity developed during biosynthesis of natural products, is still unreachable by synthetic methods<sup>4</sup>.

### **Re-examination of well-studied medicinal plants?**

According to previous estimations only 6% of existing plant species have been systematically investigated pharmacologically, and only around 15% phytochemically. Thus, the future of natural products in drug discovery, thus, appears to be a tale of justifiable hope<sup>3,4</sup>. However, the questions arise: How to choose starting plant material? Should we follow some random screening approach or classical knowledge-based (ethnopharmacological) approach? In general, the random selection of plant material could

result in the identification of natural products with unexpected bioactivities that could not have been predicted based on the existing knowledge. However, the starting test samples (fractions or pure compounds) are usually available only in small amounts, limiting the number of bioassays in which they can be tested. As a result, random testing intrinsically suffers from a low hit-rate, while application of knowledge-based strategies increases the probability for the identification of relevant bioactive compounds out of a smaller number of test samples with the use of a limited number of carefully selected pharmacological assays <sup>2,5</sup>. Moreover, as rational drug discovery from plants started more than two centuries ago many medicinal plants may be considered as well-studied (from both phytochemical and pharmacological standpoints). Hence, should we continue to study these plant species? In recent years, the progress of modern analytical techniques, separation methods and bioassays protocols has enabled a more detailed phytochemical and pharmacological analysis, and facilitated the isolation, determination of the structure and bioactivity testing of molecules that are found in very small quantities in plant tissues <sup>2,6</sup>. This is one of the two main factors that led to the discovery of new bioactive secondary metabolites even in plant species that were previously phytochemically studied <sup>7</sup>. Another factor is changes in the profile of secondary metabolites of a plant species that can be effected by various genetic and ecological factors (such as the plant development phase, the habitat characteristic of the plant population, the presence of infection, insect attacks, etc.) <sup>8</sup>.

### ***Inula helenium* L. - from ethnopharmacological to potential medicinal uses**

*Inula helenium* L. ('oman' in Serbian), family Compositae, is a widespread perennial plant species native to southeast Europe and western Asia, and naturalised in Ireland, Britain and in north mid-west USA. The roots of *I. helenium* (as tea, infusion, powder, wine, syrup and balm) have been used as versatile traditional medicine in the treatment of variety of ailments, including asthma, bronchitis, tuberculosis, skin disorders, indigestion, chronic enterogastritis, infections and helminthic diseases. Recent pharmacological studies have demonstrated that root extracts of *I. helenium* possess strong anthelmintic, anti-inflammatory, antioxidant, anticancer and insecticidal activities <sup>9</sup>. It has been also confirmed that hexane, dichloromethane and methanol extracts are highly active against *Mycobacterium tuberculosis*, bacterium that causes tuberculosis <sup>10</sup>. Although only a limited number of studies have dealt so far with the antimicrobial activity of *I. helenium* root essential oil and extracts, it was found that the oil show a very broad spectrum of antimicrobial activities with the most outstanding potency against Gram-positive bacterium *Staphylococcus aureus* (including methicillin-resistant strains) and several *Candida* species <sup>11,12</sup>.

### **Sesquiterpene lactones as main bioactive secondary methabolites?**

Previous chemical studies of *I. helenium* have showed that roots contain up to 5% of the essential oil, thymol derivatives, triterpenes, sterols, and up to 44% of the polysaccharide inulin <sup>13,14</sup>. The dominant root volatiles are eudesmane-type sesquiterpene lactones such as

alantolactone and isoalantolactone. Several authors have been previously proposed that the pharmacological effects of this *Inula* spp. could be associated with the wide range of biological properties displayed by these sesquiterpenes, including anticancer, anti-inflammatory and antibacterial activities<sup>11,13–15</sup>.

### Insights to mechanism of antistaphylococcal activity of *I. helenium* volatile oil

The fact that *I. helenium* volatile oil and extracts possesses potent antistaphylococcal properties<sup>11,12</sup>, along with the lack of more detailed knowledge of the composition of its rather abundant in yield essential oil, prompted us to work more in this direction. A number of investigations dealing with the antimicrobial activity of essential oils and their constituents alone pointed to the common antimicrobial mode of action by targeting the cell membrane<sup>16</sup>. Thus, we decided to probe the antistaphylococcal activity (*S. aureus* ATCC 6538) of the *I. helenium* (IH) oil, as well as its effects on the cell membrane.

The yield of the essential oil was 1.4% (w/w). GC and GC/MS analyses enabled the identification of forty-five different compounds in the oil. The dominant constituents were three isomeric eudesmane-type sesquiterpene lactones [1–3]: alantolactone (55.8%), isoalantolactone (26.1%), and diplophyllin (5.1%; Figure 1). The cells of the *S. aureus* ATCC 6538 strain were inhibited from growth by IH oil at very low concentration of 13 µg/mL, while the bactericidal effect of the oil was observed at 26 µg/mL. The IH essential has been previously tested against *S. aureus* and the activity (MIC) of 600 µg/mL was reported.<sup>11</sup> The difference in the chemical compositions of the herein and previously studied oils (the levels of alantolactone and isoalantolactone were higher in our IH sample) could be, perhaps, used to explain the higher antibacterial activity of our IH sample. Alantolactone and isoalantolactone were reported to be strong antimicrobials, which even gave rise to MIC values of 32 µg/mL<sup>14</sup>. In addition, and to the best of our knowledge, diplophyllin haven't been reported so far as the *I. helenium* root volatile.

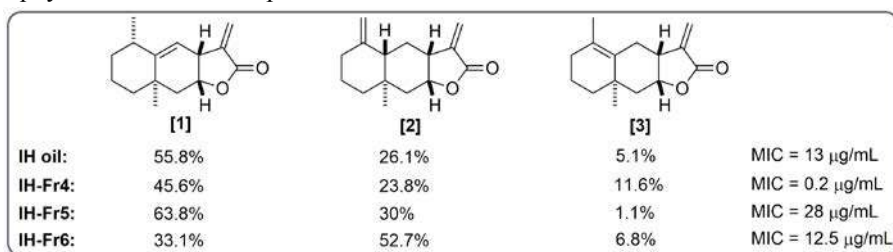


**Figure 1.** The structures of the major constituents of *Inula helenium* root essential oil: alantolactone [1], isoalantolactone [2] and diplophyllin [3] and the antistaphylococcal activities (MIC values) of the IH oil and the chromatographic fractions containing various amounts of these lactones.

Four spectrophotometric methods were employed in order to investigate the membrane-active nature of this essential oil. Absorbance (turbidity) measurements of the growing culture showed high inhibition at the MIC concentration, while the MBC concentration of the oil decreased the turbidity to zero after a period of 3.5 h (Figure 2A). To determine

whether *I. helenium* root essential oil stimulates the autolysis of the treated cells in suspension, measurements of the turbidity changes were performed at 600 nm. After 4 h, the percentage of the initial absorbance of *S. aureus* cells treated with IH oil dropped by 12.4% and 14.0% in the presence of MIC and MBC oil concentrations, respectively. The absorbance of the control decreased by only 3.8% during a 4-h period (Figure 2B). Additional tests, performed in order to detect disturbed membrane integrity, showed the release of phosphates, followed by large molecules (DNA and RNA; Figures 2C and 2D). *S. aureus* suspensions lost a significant amount of 260-nm-absorbing material, indicating severe damage of the cytoplasmic membrane of the treated cells.

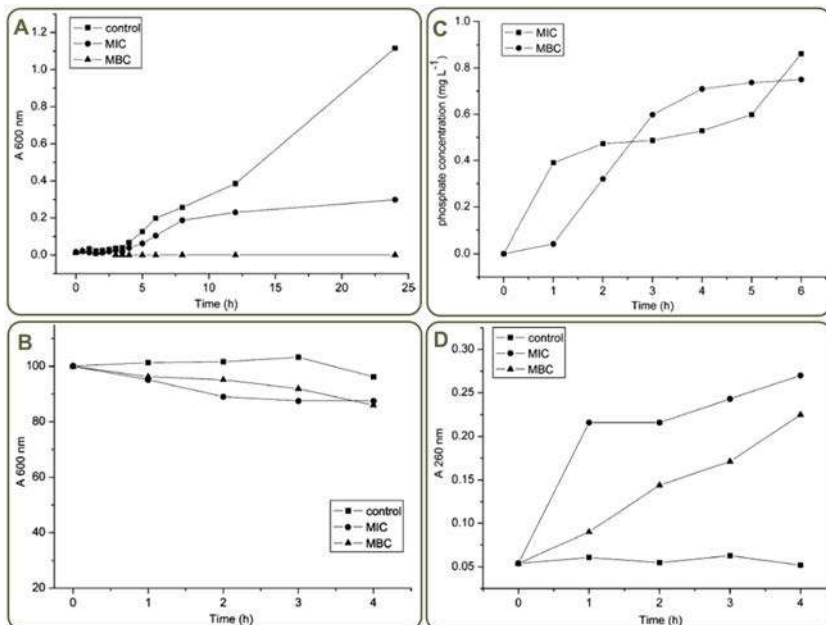


**Figure 2.** A. Growth of *Staphylococcus aureus* at 37 °C in Mueller-Hinton broth containing minimum inhibitory concentrations (MIC) and minimum bactericidal concentrations (MBC) of IH oil during 24 h of incubation. B. Autolysis of *S. aureus* cells in the presence of MIC and MBC concentrations of IH oil. C. Phosphate leakage from *S. aureus* cells induced by IH oil treatment. D. Appearance of 260-nm-absorbing material in the filtrates of *S. aureus* suspensions in phosphate-buffered saline treated with MIC and MBC concentrations of IH oil.

Finally, the SEM analysis showed that, after only 2 h post addition of the MIC concentration, marked cell clumping and shrinkage was noted (Figure 3A). On the other hand, after 6 h, the condition of the cells treated with an MBC oil concentration was worse when compared to those treated with the MIC oil concentration (Figure 3B). The presented SEM images show the lysis of the cells being very intensive at this length of time of treatment with MBC and that all cells were affected.

Overall, the presented results showed obvious membrane damage effects in the form of increased membrane permeability, which leads to cell autolysis, but it is also clear that the essential oil of *I. helenium* does not exhibit a fast bactericidal action. This suggests that changes in some other mechanisms (aside from the membrane action), such as energy transducing (ATP pool, membrane potential, pH gradient across the cytoplasmic membrane or potassium gradient) or synthetic processes inside the bacterial cells may also be involved. Further investigations on the *I. helenium* root essential oil mode of action are necessary in order to confirm or exclude these other mechanisms.

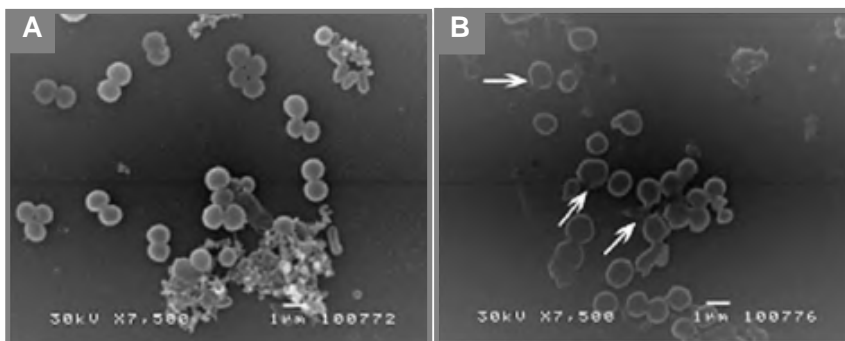


**Figure 3.** Scanning electron micrographs of *S. aureus* ATCC 6538 treated with IH oil: (A) disruption of membrane integrity after 2 h of treatment with MIC oil concentration and (B) lysis caused by MBC oil concentration after 6 h of treatment (the arrows indicate rupturing cells).

### **Bioassayed-guided fractionation of the oil disclosed the most potent oil' constituents**

With an idea that has been put forward more intensely recently on the fact that the net activity of a plant extract or essential oil is, in fact, the result of the work of several and only rarely one principle (several minor constituents on their own or working in unison with the major compounds) <sup>17,18</sup>, it provoked us to analyse meticulously the chemical composition of *I. helenium* root oil. In order to identify, with a higher degree of certainty, the active principles of the IH sample, some of which could even be minor oil constituents, IH oil was subjected to chromatographic separation by medium-pressure liquid chromatography (MPLC) and subsequently the antistaphylococcal activity of the oil fractions was determined. The fraction with the lowest MIC was mainly comprised of three sesquiterpene lactones ([1-3]; 81.0% in total; sample IH-Fr4; Figure 1). The activity of this fraction (MIC = 0.2 µg/mL) was significantly higher than that of the IH oil (MIC = 13 µg/mL; 87.0% of compounds [1-3]). It is interesting to note that an additional two fractions (IH-Fr5 and IH-Fr6) were also dominated with alantolactone, isoalantolactone, and diplophyllin. In fact, the sum of the relative amounts of these three compounds was even higher in the fractions IH-Fr5 (94.9%) and IH-Fr6 (92.6%). Nevertheless, the antimicrobial activities of IH-Fr5 (MIC = 28 µg/mL) and IH-Fr6 (MIC = 12.5 µg/mL) were comparable

to the activity of original oil (IH) and lower than that of IH-Fr4. One could even speculate that the highest relative amount of diplophyllin in IH-Fr4 (11.6%) is responsible for the observed decrease of the MIC value (the amounts of diplophyllin were much lower in IH [5.1%], IH-Fr5 [1.1%], and IH-Fr6 [6.1%]).

### Pharmacophore of main active constituents

With a goal to “locate” the pharmacophore of the major IH oil constituents, the oil was chemically modified. In general, it is thought that the occurrence of an  $\alpha,\beta$ -unsaturated lactone moiety is responsible for the high antimicrobial activity of a number of sesquiterpene lactones<sup>19</sup>. In order to test whether the loss of this Michael acceptor of the IH main constituents will result in a reduction/loss of the oil activity, IH was subjected to two chemoselective reductions: catalytic hydrogenation (which leads to the reduction of the two olefinic double bonds; sample IH-H<sub>2</sub>/Pd) and reaction with NaBH<sub>4</sub> (this leads to the reduction of aldehyde/ketone groups and/or olefinic bonds of the  $\alpha,\beta$ -unsaturated carbonyls sample IH-NaBH<sub>4</sub>). The structures of the expected dominant products of reduction (both methods) of alantolactone are depicted in Figure 4 (the analogous stands for isoalantolactone and diplophyllin). The major product of the catalytic hydrogenation of the IH sample was tetrahydroalantolactone ([2a]; 71.1%). This compound was most probably formed as the product of the total hydrogenation of all three main oil constituents [1-3]. The second most abundant compound (10.4%) was a saturated sesquiterpene acid, 12-eudesmic acid [2b], resulting from the further reduction of tetrahydroalantolactone. There was only a slight increase in the MIC (loss of activity; MIC = 28  $\mu\text{g}/\text{mL}$ ) for the sample IH-H<sub>2</sub>/Pd, in comparison to the untransformed oil (MIC = 13  $\mu\text{g}/\text{mL}$ ). This sample was additionally separated *via* an acid-base extraction. The obtained “acid” fraction (the main constituent [73.1%] was 12-eudesmic acid) showed no antistaphylococcal activity in the tested concentrations. This is in agreement with a previous study on the antifungal activity of the 12-eudesmic acid and structurally related compounds<sup>20</sup>. This points to the fact that the main IH-H<sub>2</sub>/Pd constituent, tetrahydroalantolactone isomer (with no  $\alpha,\beta$ -unsaturated carbonyl moiety or an isolated double bond; Figure 4), retains antimicrobial activity to a certain degree. It should be mentioned that it is not reasonable to expect that the minor IH-H<sub>2</sub>/Pd constituents (in the relative amount in which they are present in the sample) should exhibit such a high activity (MIC = 0.8  $\mu\text{g}/\text{mL}$ ).

The sample obtained after the reduction of the oil with NaBH<sub>4</sub> was subjected to MPLC. Two of the obtained fractions had (isomers of) dihydroalantolactone [1c], dihydroisoalantolactone [2c], and dihydrodiplophyllin [3c] (1,4-reduction products of [1-3]) as their major contributors (IH-NaBH<sub>4</sub>-Fr2 and IH-NaBH<sub>4</sub>-Fr3). However, the determined MIC values of these fractions were mutually significantly different (Figure 4). The relative amounts of the constituting isomeric dihydrolactones differed significantly in the two mentioned fractions, and this being the most probable reason for their different antistaphylococcal activities. In fact, the MIC value of IH-NaBH<sub>4</sub>-Fr3 was much lower than the MIC value determined for the pure oil. Bearing this in mind, one can conclude that, although the  $\alpha,\beta$ -methylene lactone moiety could be considered as the operative

pharmacophore in the case of the (iso)alantolactones, it is not the only structural fragment of the lactones that carries the high antimicrobial activity of this and similar compounds/mixtures of compounds. The fraction IH-NaBH<sub>4</sub>-Fr4, also noted to be a very strong inhibitor of bacterial growth, was comprised of isomeric eudesmen-8,12-diols [2d] (complete reduction of the  $\alpha,\beta$ -unsaturated carbonyl system), and also demonstrates that the lactone ring itself might not be the essential antimicrobial structural fragment of this class of compounds. It must be stressed, however, that the presence of two alcoholic groups in eudesmen-8,12-diols is at least partially responsible for the observed strong antistaphylococcal activity of the corresponding fraction.

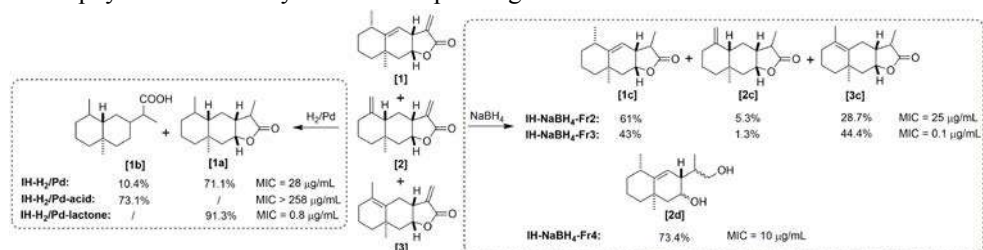


**Figure 4.** The reduction products of alantolactone [1], isoalantolactone [2] and diplophyllin [3]: tetrahydroalantolactone isomer [1a], 12-eudesmic acid [1b], dihydroalantolactone [1c], dihydroisoalantolactone [2c], dihydro diplophyllin [3c] and eudesmen-8,12-diol [2d], and their antimicrobial activities.

## Why is diplophyllin stronger antistaphylococcal agent than alantolactone and isoalantolactone?

Although lactones [1-3] are isomers with minor structural variation, differing only in the position of the isolated double bond, composition-activity relationship analyses revealed that the antimicrobial potential of diplophyllin is significantly higher than that of the other two isomers. Alongside the presence of some specific functional groups, three-dimensional structure (conformation) can play a significant role in the onset of biological/pharmacological activity of a certain compound<sup>21</sup>. The latter could be critical for optimal docking at the active site of the target biomolecules. Bearing this in mind, we assumed that the higher observed activity of diplophyllin, in comparison with alantolactone and isoalantolactone, could be due to their conformational differences. Thus, we decided to compute energetically favourable conformations of the dominant biologically active IH oil constituents, and seek possible differences between them.

Energetically favourable conformations of isomeric lactones [1-3] were calculated using MM+ and MMFF94 molecular mechanics and AM1 and PM3 semi-empirical methods, and mutually compared. The compounds were additionally described in terms of selected 2D and 3D molecular descriptors. It was found that alantolactone and isoalantolactone mainly adopt “U”-shaped conformations (>99%, calculated at 298 K; “closed” geometries; Figure 5), with the carbonyl moiety being rather sterically hindered by the axial C-14 methyl group. In contrast, the cyclohexene and lactone rings of diplophyllin are mutually

oriented in such a way to give the overall “S”-shape to the molecule (“open” geometry). These conformational differences, inherently influencing the optimal interaction of lactones [1-3] with the binding region of target biomolecules, could be, at least partially, responsible for the higher observed antistaphylococcal activity of diplophyllin in comparison with the other two isomeric lactones.

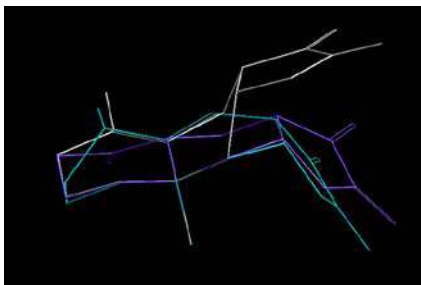


**Figure 5.** Comparison of the most energetically favorable conformation of alantolactone (pale blue colored), isoalantolactone (deep blue colored) and diplophyllin (white coloured).

### Bioassayed-guided fractionation of the oil also dislosed minor active pinciples

The chromatographic separation of the IH oil enabled the detection (and identification) of some additional minor constituents, originally undetected in the GC and GC-MS runs of the unfractionated oil. A minor fraction (3.5 %) of the oil that eluted with 5% diethyl ether in hexane containing a sesquiterpene aldehyde (RI = 1578) exhibited a very high activity against *S. aureus* (MIC = 0.8 µg/mL). The only oil fraction that had a lower MIC value (0.2 µg/mL) than that was the most active fraction consisted of alantolactone, isoalantolactone, and diplophyllin. The mentioned sesquiterpene aldehyde was accompanied with nine additional constituents (**S<sub>1</sub>-S<sub>9</sub>**) with a characteristic mass spectral fragmentation pattern (Figure 6). The base peaks at  $m/z$  72 (McLafferty fragment) and the relatively abundant fragments at  $m/z$  43 (acyl ion) hinted that the structures of the nine compounds corresponded to a series of 3-methyl-2-alkanones<sup>22</sup>. Additionally, the difference of 14 amu (one CH<sub>2</sub> group) between the molecular ions of any two consecutive compounds in the gas chromatogram, separated by *ca.* 100 RI units, pointed to the existence of a C<sub>11</sub>-C<sub>19</sub> homologous series (Figure 6).

A detailed literature survey showed that long-chain 3-methyl-2-alkanones had rarely been reported in samples of natural origin, with no reference to their existence in the Plant Kingdom. 3-Methyl-2-decanone was found in territorial marking fluids of the male Bengal tiger, *Panthera tigris*<sup>23</sup>, whereas this compound and its homologue (3-methyl-2-undecanone) were detected in the normal urine of male wolves, *Canis lupus*<sup>24</sup>. Three longer chain homologues, 3-methyl-2-tridecanone, 3-methyl-2-tetradecanone and 3-methyl-2-pentadecanone, were found in Dufour glands' secretions of a species of desert-dwelling ants of the *Cataglyphis bicolor* group<sup>25</sup>. Motivated by the interesting properties of these ketones and their limited natural occurrence, the tentative structure assignment

was confirmed by comparing the chromatographic and spectral properties of these, up to now unknown, *I. helenium* constituents to that of synthetic 3-methyl-2-alkanones. We opted for synthesis since their isolation seemed virtually impossible from the complex oil matrix and due to their low relative content, as well as, to gain the opportunity to ascertain to what extent these compounds contribute to the high antistaphylococcal activity of the fraction in question.

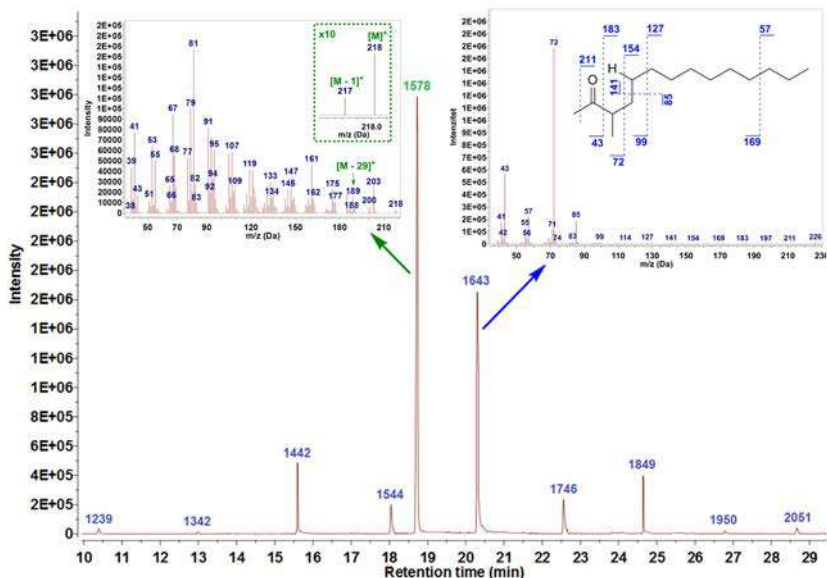


**Figure 6.** TIC chromatogram of a GC-MS run of a fraction (5% diethyl ether in hexane) of *I. helenium* root essential oil showing peaks with retention indices (blue colored) corresponding to a series of 3-methyl-2-alkanones and an unidentified sesquiterpene aldehyde (green colored), as well as the mass spectra of the aldehyde and of 3-methyltetradecan-2-one (S5).

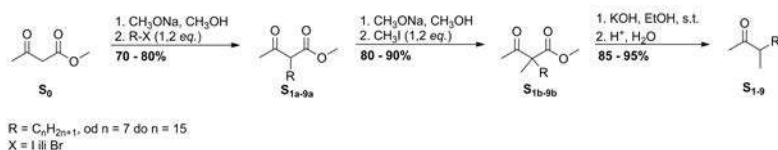


**Figure 7.** Synthetic route to 3-methyl-2-alkanones (S1-S9).

The commercially available methyl acetoacetate ( $S_0$ ) was the starting material and three step transformations of this molecule to appropriate 3-methyl-2-alkanones  $S_{1-9}$  have been achieved in 50-65% overall yields (as depicted in Figure 7). The structural assignments of target molecules were achieved by spectral means ( $^1\text{H}$  and  $^{13}\text{C}$  NMR, IR, MS). After the

co-injection of these nine synthesized compounds with the root essential oil of *I. helenium*, the originally proposed hypothesis was unambiguously corroborated and compounds S<sub>1-9</sub> were proven to be members of the C<sub>11</sub>-C<sub>19</sub> homologous series of 3-methyl-2-alkanones. All nine 3-methyl-2-alkanones were found herein for the first time in the Plant Kingdom. Additionally, four of them (C<sub>13</sub>, C<sub>17</sub>-C<sub>19</sub>) are reported here to occur in a living organism for the first time. For the quantification of 3-methyl-2-alkanones in the plant material we build up GC-FID calibration curves as  $(A_s/A_i) = f(C_s/C_i)$ . The content of 3-methyl-2-alkanones determined per 100 g of dry *I. helenium* roots was within the range 0.08-24.2 mg.

The contribution of the identified 3-methyl-2-alkanones to the overall antimicrobial action of the original fraction of IH oil was evaluated in microdilution assays against six pathogenic bacterial and two fungal strains. Surprisingly, 3-methyl-2-alkanones did not show any anti-staphylococcal activity in the concentrations tested. Furthermore, 3-methyl-2-alkanones manifested selectivity toward just one fungal strain - *Candida albicans* (MIC= 3.7 mg/mL). This implies that the very high activity against *S. aureus* of this oil fraction comes from the still unidentified sesquiterpene aldehyde with a mass spectrum resembling that of bicyclogermacrenal. The observed anti-candidal activity of 3-methyl-2-alkanones (*C. albicans* is a yeast species that can be found in the soil<sup>26,27</sup>) suggests that these compounds could be plant-root defence metabolites against attack of such pathogens and a number of previous studies on related compounds confirm this<sup>28-30</sup>.

### **Application of new structural elucidation methodology for determining identity of antistaphylococcal sesquiterpene aldehyde**

In order to identify this sesquiterpene aldehyde, a larger quantity of the essential oil was fractionated by chromatography on SiO<sub>2</sub>. Repeated usage of a non-polar eluent led to sample A, which weighted *ca.* 5 mg, enriched with the compound in question. The GC-MS analysis of this sample revealed that it contained roughly 85% of the sesquiterpene accompanied with geranyl (8%) and neryl isobutanoates (5%), as the main contaminants. Extensive NMR measurements of sample A were done in order to try to gain as much structural data on the sesquiterpene aldehyde as possible directly from the mixture. Also, for some low-intensity signals it was unambiguously confirmed to belong to the two main impurities, geranyl and neryl isobutanoates, by comparison with the corresponding chemical shifts in <sup>1</sup>H NMR spectra of authentic standards. However, these detailed analyses of 1D- and 2D-NMR spectra of this original complex sample allowed access to a very limited amount of structural data for the unknown aldehyde (2,4-dimethylhexa-1,5-diene-3,4-diyl fragment and methacrolein moiety were identified; Figures 8B and 8C, respectively). The region of <sup>1</sup>H NMR spectrum up to 3 ppm was especially complex to analyse since it contained a number of highly overlapped signals.

Having in mind that this sesquiterpene contains an aldehyde group, which is considered a good Lewis base, it was decided to try to simplify the proton spectrum in the high field region by an NMR-monitored titration with lanthanide-induced shift reagent (LSR). The formation of an adduct with LSR could possibly enable the assignment of the proton from the CH group at  $\delta_C$  36.5 ( $\delta_H$  2.55) attached to the acrolein moiety-the coordination site of

LSR, *i.e.* a significant downfield shift should be expected. *tris*(6,6,7,7,8,8,8-Heptafluoro-2,2-dimethyl-3,5-octanedionato)europium(III) ( $\text{Eu}(\text{fod})_3$ ) was chosen as LSR because it combines the maximum shift capacity with minimum broadening of the shifted resonances, good solubility in chloroform with absence of interfering chelate resonances in the usual range of NMR frequencies. The incremental addition of  $\text{Eu}(\text{fod})_3$  resulted in a great simplification of the  $^1\text{H}$  NMR spectrum of sample A as a number of signals were observed to move to lower field. While the shifts of the first fragment (Figure 8B) proton signals, located near the coordination site, were expected, the effect of  $\text{Eu}(\text{fod})_3$  on the protons from the vinyl, isopropenyl and the second CH group ( $\delta_{\text{C}}$  52.5 and  $\delta_{\text{H}} \approx 2.10$ ) from the second fragment were unforeseen (Figure 9).

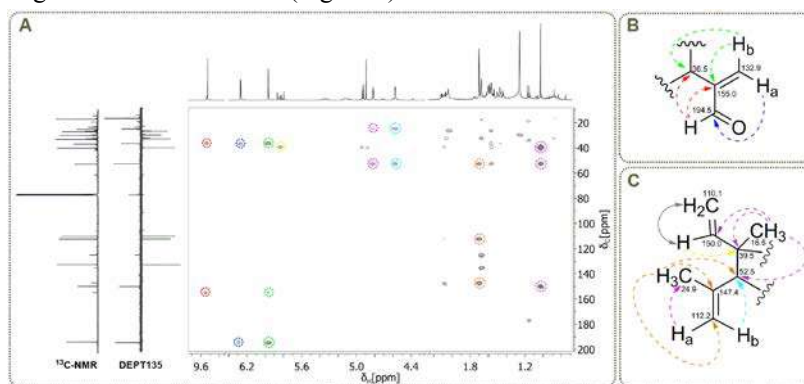


**Figure 8.** A. Expansion of the HMBC spectrum of sample A with key cross peaks marked with appropriate coloring to match that in B. and C. B. and C. Structural fragments with marked observed HMBC interactions (dashed colored arrows). Gray double ended arrow represents a 1H-1H COSY interaction.

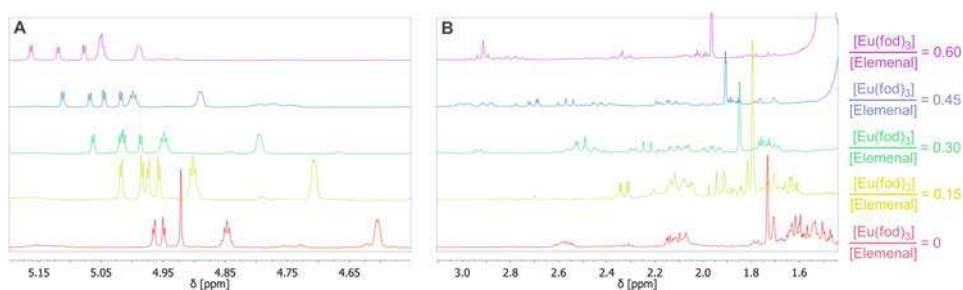


**Figure 9.** The shifts of signals after incremental additions of  $\text{Eu}(\text{fod})_3$  corresponding to (A) the olefinic protons with  $\delta_{\text{H}} < 5$  ppm in the unshifted spectrum, and (B) the enlargement of the area with the aliphatic protons with  $\delta_{\text{H}}$  between 1.45 and 2.60 ppm in the unshifted spectrum.

Overall, simplification of the NMR spectra in terms of signal overlap and removal of chemical shift degeneracy, allowed the mining of crucial data from the shifted NMR spectra. 2D NMR spectra ( $^1\text{H}$ - $^1\text{H}$ -COSY, NOESY, HSQC and HMBC) of the sample

mixed with  $\text{Eu}(\text{fod})_3$ , proved to be particularly valuable in this respect. The obtained additional information revealed that the compound in question was a rare sesquiterpene - elemenal (elema-1,3,11(13)-trien-12-al). However, there is a doubt about natural origin of elemenes as it is believed that elemenes are formed by a Cope rearrangement of the corresponding germacranes. This hypothesis is supported by recent reinvestigation of *Saussurea lappa* Clarke fresh root essential oil and extract composition which indicated that (-)-elemenal, along with (-)- $\beta$ -elemene and (-)-elema-1,3,11(13)-trien-12-ol, is most possibly a heat-induced artefact formed from the corresponding germacrane derivatives by Cope rearrangement during drying of the roots, and/or manufacture of the oil and/or GC analysis.<sup>31</sup>

Alongside the total NMR assignments of elemenal, the data obtained after incremental additions of lanthanide shift reagents (vinyl-allylic couplings, nOe cross peaks and shift gradient ( $\Delta E$ ) values) enabled the assessment of conformation that this sesquiterpene aldehyde most probably adopts in its complex with  $\text{Eu}(\text{fod})_3$ . MM2 calculations revealed that this is not the energetically most favorable conformation of elemenal and that it is dictated by the geometric requirements of Cope rearrangement of the appropriate germacradienal. In order to additionally justify the conclusions regarding the stereochemistry of the elemenal- $\text{Eu}(\text{fod})_3$  complex, we performed a conformational analysis using the lanthanide-probe method (Figure 10).

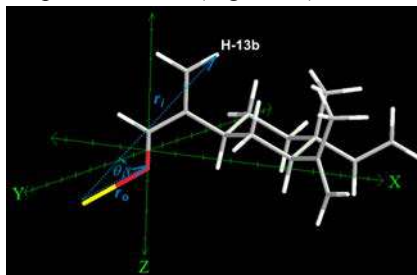


**Figure 10.** The most likely conformation of elemenal- $\text{Eu}(\text{fod})_3$  complex (placed in Cartesian coordinate system) obtained by lanthanide probe method ( $r_o = 2.328 \text{ \AA}$ ,  $\alpha_o = 120^\circ$  and  $\beta_o = 180^\circ$ ). The parameters required for the calculation of  $\Delta_{\text{cal}}$  values according to McConnell-Robertson equation are illustrated for proton H-13b;  $r_i$  is the distance between the europium and this nucleus, and  $\theta_i$  is the angle made by the vector corresponding to  $r_i$  and the vector  $r_o$  representing the Eu-O bond.

Interestingly,  $\beta$ -elemene is widely considered as a potential novel natural anticancer plant drug and some formulations for pharmacological uses based on this compound have been patented and are currently in application for clinical studies in USA<sup>32</sup>. A recent study revealed that  $\beta$ -elemenal was appreciably more potent than  $\beta$ -elemene in suppressing nonsmall cell lung cancer growth and proliferation. Thus,  $\beta$ -elemenal may have great potential as an anticancer alternative to  $\beta$ -elemene in treating lung cancer and other tumors

33

## Acknowledgements

This study was supported by the Ministry of Education, Science and Technological Development of Serbia (Project No. 172061).

## References

1. Bauer Petrovska B. Historical review of medicinal plants' usage. *Pharmacogn Rev* 2012;6:1-5.
2. Atanasov AG, et al. Discovery and resupply of pharmacologically active plant-derived natural products: A review. *Biotechnol Adv* 2015;33:1582-614.
3. Newman DJ, Cragg GM, Snader KM. The influence of natural products upon drug discovery. *Nat Prod Rep* 2000;17:215-34.
4. Brahmachari G. Natural Products in Drug Discovery: Impacts and Opportunities – An Assessment. In: Brahmachari G (ed) *Bioactive Natural Products*, World Scientific, Singapore, 2011, pp 1-199.
5. Rates SMK. Plants as source of drugs. *Taxon* 2001;39:603-13.
6. Harvey AL. Natural products in drug discovery. *Drug Discov Today* 2008;13:894–901.
7. Radulović N, Đorđević N, Denić M, Martins Gomes Pinheiro M, Dias Fernandes P, Boylan F. A novel toxic alkaloid from poison hemlock (*Conium maculatum* L., Apiaceae): Identification, synthesis and antinociceptive activity. *Food Chem Toxicol* 2012;50:274-9.
8. Queiroz EF, Marston A, Hostettmann K. Contemporary Methodological Approaches in the Search for New Lead Compounds from Higher Plants. In: Elisabetsky E, Etkin NL (eds) *Ethnopharmacology, Encyclopedia of Life Support Systems (EOLSS)*, Developed under the Auspices of the UNESCO, Eolss Publishers, Oxford, 2005, Available at <http://www.eolss.net>.
9. Seca AM, Grigore A, Pinto DC, Silva AM. The genus *Inula* and their metabolites: from ethnopharmacological to medicinal uses. *J Ethnopharmacol* 2014;154:286-310.
10. Cantrell CL, Fischer NH, Urbatsch L, McGuire MS, Franzblau SG. Antimycobacterial crude plant extracts from South, Central, and North America. *Phytomedicine* 1998;5:137-45.
11. Deriu A, et al. Antimicrobial activity of *Inula helenium* L. essential oil against Gram-positive and Gram-negative bacteria and *Candida* spp. *Int J Antimicrob Agent* 2008;31:581-92.
12. O'Shea S, Lucey B, Cotter L. In vitro activity of *Inula helenium* against clinical *Staphylococcus aureus* strains including MRSA. *Br J Biomed Sci* 2009;66:186-9.
13. Stojakowska A, Kedzia B, Kisiel W. Antimicrobial activity of 10-isobutyryloxy-8,9-epoxythymol isobutyrate. *Fitoterapia* 2005;76:687-90.
14. Li Y, et al. Antitumour activities of sesquiterpene lactones from *Inula helenium* and *Inula japonica*. *Z Naturforsch C* 2012;67:375-380.
15. Zhao YM, Zhang ML, Shi QW, Kiyota H. Chemical constituents of plants from the genus *Inula*. *Chem Biodivers* 2006;3:371-384.
16. Hammer KA, Carson CF. Antibacterial and Antifungal Activities of Essential Oils. In: Thormar H (ed) *Lipids and Essential Oils as Antimicrobial Agents*, John Wiley & Sons, Ltd, Chichester, 2010, pp 255-306.

17. Stojanović-Radić Z, Čomić L, Radulović N, Dekić M, Randelović V, Stefanović O. Chemical composition and antimicrobial activity of *Erodium* species: *E. ciconium* L., *E. cicutarium* L., and *E. absinthoides* Willd. (Geraniaceae). *Chem Papers* 2010;64:368-77.
18. Radulović N, Dekić M, Stojanović Radić Z, Palić R. Chemical composition and antimicrobial activity of the essential oils of *Geranium columbinum* L. and *G. lucidum* L. (Geraniaceae). *Turk J Chem* 2011;35:1-14.
19. Cantrell CL, Pridgeon JW, Fronczek FR, Becnel JJ. Structure-activity relationship studies on derivatives of eudesmanolides from *Inula helenium* as toxicants against *Aedes aegypti* larvae and adults. *Chem Biodivers* 2010;7:1681-97.
20. Shtacher G, Kashman Y. 12-Carboxyeudesma-3,11(13)-diene. Novel sesquiterpenic acid with a narrow antifungal spectrum. *J Med Chem* 1970;13:1221-3.
21. Radulović N, Bogdanović G, Blagojević P, Dekić V, Vukićević R. Could X-ray analysis explain for the differing antimicrobial and antioxidant activity of two 2-arylamino-3-nitro-coumarins? *J Chem Crystallograph* 2011;41:545-51.
22. Francke W. Structure elucidation of some naturally occurring carbonyl compounds upon coupled gas chromatography/mass spectrometry and micro-reactions. *Chemoecology* 2010; 20:163-9.
23. Burger BV, et al. Chemical characterization of territorial marking fluid of male Bengal tiger, *Panthera tigris*. *J Chem Ecol* 2008;34:659-71.
24. Raymer J, Wiesler D, Novotny M, Asa C, Seal US, Mech LD. Chemical scent constituents in urine of wolf (*Canis lupus*) and their dependence on reproductive hormones. *J Chem Ecol* 1986;12:297-314.
25. Gökçen OA, Morgan ED, Dani FR, Agosti D, Wehner R. Dufour gland contents of ants of the *Cataglyphis bicolor* group. *J Chem Ecol* 2002;28:71-87.
26. Marples MJ. Some observations on the ecology of *Candida albicans*, a potential mammalian pathogen. *New Zeal J Ecol* 1966; 13:29-34.
27. Hube B. From commensal to pathogen: stage- and tissue specific gene expression of *Candida albicans*. *Curr Opin Microbiol* 2004;7:336-41.
28. McDowell PG, Lwande W, Deans SG, Waterman P. Volatile resin exudate from stem bark of *Commiphora rostrata*: Potential role in plant defence. *Phytochemistry* 1988;7:2519-21.
29. Fridman E, et al. Metabolic, genomic, and biochemical analyses of glandular trichomes from the wild tomato species *Lycopersicon hirsutum* identify a key enzyme in the biosynthesis of methylketones. *Plant Cell* 2005;17:1252-67.
30. Ntalli NG, Manconi F, Leonti M, Maxia A, Caboni P. Aliphatic ketones from *Ruta chalepensis* (Rutaceae) induce paralysis on root knot nematodes. *J Agric Food Chem* 2011;59:7098-103.
31. de Kraker JW, Franssen MC, de Groot A, Shibata T, Bouwmeester HJ. Germacrene from fresh costus roots. *Phytochemistry* 2001;8:481-7.
32. Barrerro AF, et al. Efficient synthesis of the anticancer  $\beta$ -elemene and other bioactive elemenes from sustainable germacrene. *Org Biomol Chem* 2011;9:1118-1125.
33. Li QQ, Wang G, Huang F, Li JM, Cuff CF, Reed E. Sensitization of lung cancer cells to cisplatin by  $\beta$ -elemene is mediated through blockade of cell cycle progression: antitumor efficacies of  $\beta$ -elemene and its synthetic analogs. *Med Oncol* 2013;30:488-98.



---

# Nano-structured materials and their application in the detection of biological compounds

---

Dalibor M. Stanković\*, Miloš Ognjanović, Bratislav Antić

*The Vinča Institute of Nuclear Sciences, University of Belgrade, Belgrade, Serbia*

\*e-mails: daliborstankovic@vin.bg.ac.rs; dalibors@chem.bg.ac.rs

Nanoscale materials nowadays represent a widely investigated research area. With the development of controlled synthesis and uniform materials characteristics, their high potential is being realized to the maximum. The results presented in this short review clearly point out that an expansive amount of structural, chemical and electrochemical data about materials is available in field of electroanalytical chemistry and chemical sensors and biosensors. It is shown that adequate material synthesis with unique characteristics can improve detection of biological active compounds in terms of simplicity, sensitivity and selectivity.

## Introduction

State-of-the-art research in this field is focused on the application of novel synthesized nanomaterials as electrode materials. Common solid-state electrodes showsatisfactory characteristics for the quantification of biologically active components, but also hasome drawbacks, including adsorption of tested compounds on electrode surface. This signifies surface cleaning and electrode renewal would be necessary, but since these practices are difficult or impossible to implement, electrode use is limited to one measurement. These facts have encouraged the application of different novel nanomaterials for solid electrodes and investigation of their performance in real sample analysis.

The combing of different materials at nanoscale, opens numerous possibilities to fabricate different surface with unique properties. These materials, in recent years, have shown high potential in the field of electrochemistry and electroanalytical chemistry of biologically active compounds. The aim of this work is to show recent progress and application of nanostructured materials as electrochemical sensors and biosensors<sup>1</sup>.

## Electrochemical sensors for detection of biologically active compounds

**Carbon and carbon-based materials.** Carbon is widely present in the field of electroanalytical chemistry in the several forms including carbon paste electrode (CPE), screen printed carbon electrode (SPCE) and glassy carbon (GC) electrode known for many decades. Recently, new allotropes of carbon, as extremely versatile materials exhibiting a large number of unique properties, have been intensively studied in this field. Most known materials in this group are graphene, graphene oxide (GO), reduced graphene oxide (RGO), graphene nanoplatelets (GNP), graphene nanoribbons (GNS) and different carbon

nanotubes, which can be divided as single- and multi-wall carbon nanotubes. In addition, hybrid carbon materials have been synthesized, characterized, and applied by many researchers in the detection of biomolecules. These materials are known as “doped” or “decorated” carbon materials.

**Modification of carbon paste electrode - application for detection of riboflavin, gallic acid and simultaneous detection of catechol and hydroquinone.** Carbon paste electrodes are widely used as electrode material for the development of various electrochemical sensors and biosensors. Such electrodes can be simply modified. The main advantages of carbon paste electrode are: (i) easy preparation; (ii) reproducible surface; and (iii) low residual current in a wide potential window. Modification of carbon paste electrode can be performed in two different ways - modification of surface and modification paste with different amounts of modifiers to exploit all advantages of the electrode, such as renewable surface. Here we present the uses of several nanomaterials for detection of different important molecules.

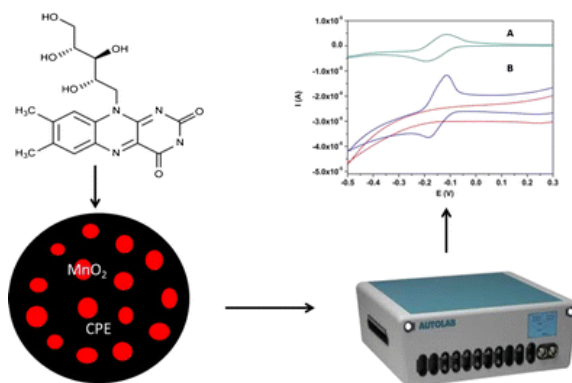


**Figure 1.** Schematic illustration of the system for detection of riboflavin using modified  $\text{MnO}_2/\text{CPE}$  electrode.

### **Manganese dioxide-modified carbon paste electrode for voltammetric determination of riboflavin**

A number of studies have developed modifications of several carbon electrodes using different types of modifiers, such as  $\text{MnO}_2$ ,  $\text{Fe}_3\text{O}_4$ ,  $\text{FeO}$ ,  $\text{SnO}_2$ ,  $\text{CuO}$ ,  $\text{Fe}_2\text{O}_3$  which are can be very sensitive to acids and basis media, oxides of platinum group metals, complexes of copper, nickel, iron and chromium or/and also nanocomposites of these modifiers. The aim of modifications is to lower overpotential for the oxidation or reduction of analytes, in comparison with unmodified electrodes. The obtained analytical responses are significantly higher and show considerable reproducibility.  $\text{MnO}_2$  based electrodes are very popular for all mentioned characteristics. They show high catalytic effects at appropriate potential for sensing the target analyte. In this study a simple and cheap

procedure for the determination of Vitamin B2 at low concentrations based on a manganese dioxide bulk-modified carbon paste electrode ( $\text{MnO}_2/\text{CPE}$ ) was proposed <sup>2</sup>. Schematic illustration of the work is presented in Figure 1.

It is noted that the current corresponding to  $\text{MnO}_2/\text{CPE}$  electrode is at about two times higher value when compared to the unmodified electrode. This is mainly attributed to the higher active surface area of  $\text{MnO}_2$  particles present on the surface of modified CPE electrodes. The current response obtained for the modified electrode approves the effect of  $\text{MnO}_2$  in the electrode structure. The results show a dynamic range for concentrations from 0.02 to 9  $\mu\text{M}$  and detection limit of 15 nM. This confirms that this electrode represents a satisfactory replacement for commercial electrodes. This sensor shows low detection limit, wide linear range with good sensitivity and reproducibility, and comparable or better characteristics for the quantification of VB2, compared to previous reports.

**Optimized chemical composition of  $(\text{Mg},\text{Fe})_3\text{O}_4/\text{glassy carbon paste electrodes with enhanced sensitivity toward detection of gallic acid and estimation of total antioxidant activity}$** . Ferrites with the general formula  $\text{MFe}_2\text{O}_4$  ( $\text{M} = \text{Mg}, \text{Zn}, \text{Co}, \text{Mn}, \text{Cu}, \text{Cr}, \text{Ni}$ ), both in nanoform and bulk, are being intensively investigated for potential applications in many branches of technology. Their promising characteristics can be probably attributed to their chemical composition and structure, where two cation sites (8a) and (16d) are occupied by different metals. Usually in nano-ferrites, a cation is found on both sites. Their broad application has required development of controlled methods of synthesis, which would supply targeted characteristics of materials such as selectivity, stability and sensitivity. The other possibility to improve physical properties of ferrites is partial substitution of cations by 3d and 4f elements. One of the goals of this study was to investigate the effect of  $\text{Fe}^{2+}$  to  $\text{Mg}^{2+}$  substitution in  $\text{Fe}_3\text{O}_4$ , over a wide concentration range, in order to develop new materials ( $\text{Mg}_x\text{Fe}_{3-x}\text{O}_4$  where  $x = 0, 0.1, 0.2, 0.4, 0.6, 0.8$  and 1) for potential application as electrochemical sensors <sup>3</sup>. Schematic illustration of this idea is given at Figure 2.

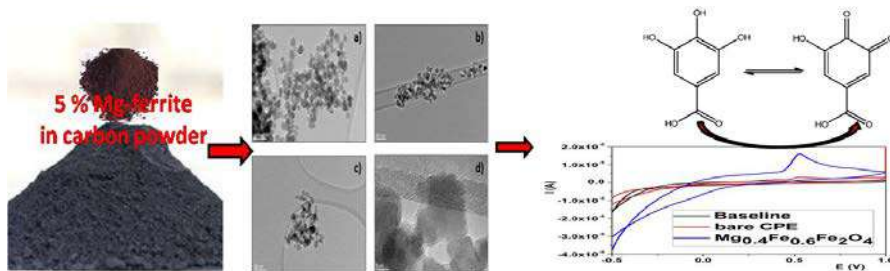


**Figure 2.** Schematic illustration of the system for detection of gallic acid using modified CPE electrode.

Each of  $\text{Mg}_x\text{Fe}_{3-x}\text{O}_4$  was used to prepare composite  $\text{Mg}_x\text{Fe}_{3-x}\text{O}_4/\text{glassy carbon paste}$ , which was investigated as potential electrode for gallic acid detection and estimation of the total antioxidant activity of liquids. It was found that the analytical performance of the  $\text{Mg}_x\text{Fe}_{3-x}\text{O}_4/\text{glassy carbon paste}$  depends on  $\text{Mg}_x\text{Fe}_{3-x}\text{O}_4$  nanoparticles. The increase of magnesium

concentration up to the value of  $x = 0.4$  in  $Mg_xFe_{3-x}O_4$ /glassy carbon paste results in increased oxidation current of gallic acid. However, further increase in the  $x$  value causes a decrease of the current. An electroanalytical procedure was established and analytical performances of proposed  $Mg_{0.4}Fe_{2.6}O_4$ /glassy carbon paste was monitored using previously optimized experimental conditions. It was found the procedure can be applied for detection of low content of gallic acid with satisfactory selectivity in the presence of the most common natural occurring compounds. In this study it was shown that controlled synthesis with partial substitution in the material structure can improve its characteristics, probably due to synergetic effect of both presented metals. This opened a new approach for application of such compounds in electroanalysis.

**Effects of cobalt doping level of ferrites in enhancing sensitivity of analytical performances of carbon paste electrode for simultaneous determination of catechol and hydroquinone.** Cobalt ferrites (Co/Ferrites) represent a promising candidate for electrode material due to their stable electronic properties and mechanical strength that has been attributed to the anti-parallel spins of  $Fe^{3+}$  and  $Co^{2+}$  ions from tetrahedral and octahedral sites respectively. These nanoparticles increase electrochemical performances and provides significant improvements of electrodes that can be used in sensors and biosensors for important metals and biological active substances. Also, this material shows low toxicity, easy preparation pathway, long term stability, low cost and safety<sup>4</sup>.

In this work, cobalt ferrite (CoFerrite) composites were synthesized and the electrochemical properties were studied by fabricating a simple and sensitive electrochemical dihydroxybenzene sensor based on CoFerrite modified carbon paste electrode (CoFerrite/CPE) (Figure 3). These electrodes exhibited highly sensitive performance for simultaneous determination of catechol (CC) and hydroquinone (HQ), fast voltammetric response, as well as good selectivity. It was shown that the electrocatalytic activity of such materials strongly depends on the level of substituted Co in the ferrite nanoparticles. The sensor was also applied to simultaneous determination of CC and HQ in tap water with satisfactory results.

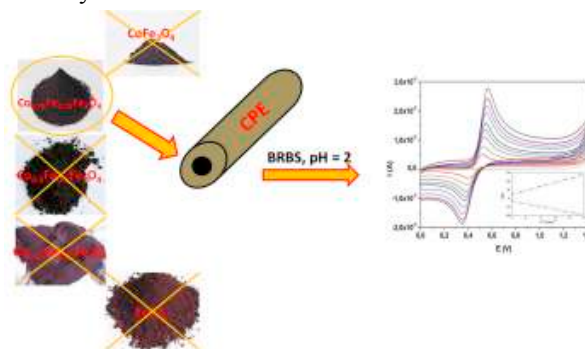


**Figure 3.** Schematic illustration of the system for detection of catechol and hydroquinone using modified CPE electrode.

For the quantification of both tested compounds amperometric detection and differential pulse voltammetry were used. Calibration curves were constructed by plotting oxidation peak current against concentration of analyte and it was shown that both techniques possess satisfactory results using proposed electrode. LODs were lower than 1  $\mu\text{M}$  and wide linear ranges for both compounds were achieved. Results obtained in this study were comparable or better than those found in the literature for simultaneous detection of these compounds. In comparison with study for magnesium ferrites it was found that higher concentration of cobalt in ferrite structure shows best electrochemical response. These results imply importance of detailed studies in this field and high dependence of material structure and electrochemical characteristics.

**Modification of glassy carbon electrode - application for detection of gallic acid in wines and nitrites in water samples.** In recent years, one of the widely investigated materials in the field of electrochemical sensors is reduced graphene oxide (rGO). This material can be obtained by reduction of graphene oxide using different methods, including chemical, electrochemical, and microwave-assisted. Pristine graphene oxide, due to high amounts of disrupted  $\text{sp}^2$  bonds, possesses lower electrical conductivity in comparison to rGO. Nanostructured materials yield excellent conductivity and high electrocatalytic activity. Titanium nitride, due to its exceptional combination of chemical, physical, and mechanical properties, and excellent electrical conductivity ( $4 \times 10^3$  to  $5.55 \times 10^4 \text{ S cm}^{-1}$ ), attracts much attention for its potential application in various fields such as lithium ion storage, supercapacitors, catalysis and biosensors. Commercially available wolfram carbide has a low surface ( $2.1 \text{ m}^2 \text{ g}^{-1}$ ) but also shows good characteristics and potential in the field of electrochemistry. Due to these properties, newly synthesized hybrid structures titanium nitride- and wolfram carbide-doped reduced graphene oxide were used for modification of glassy carbon electrode for detection of gallic acid<sup>5</sup>. Schematic illustration of this idea is given in Figure 4.

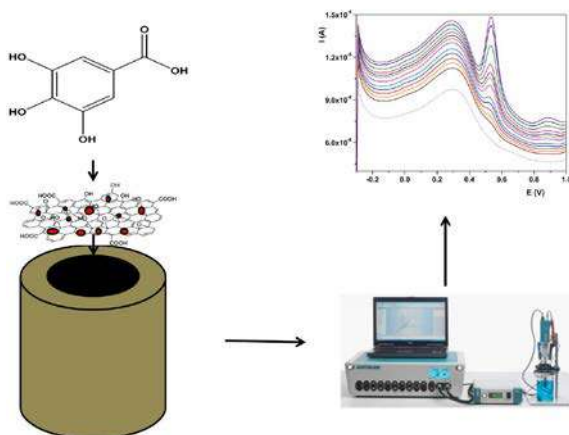


**Figure 4.** System for detection of gallic acid using modified GC electrode.

With this approach, two electrodes based on modification of the GC electrode were prepared for quantification of gallic acid in sweet wines. Two newly proposed compounds, based on reduced graphene oxide doped either with titanium nitride or wolfram carbide, were synthesized and applied for this purpose. Involvement of titanium nitride or wolfram carbide in the modifier structure played a crucial role in the fabrication of sensor. Obtained characteristics improved detection of this compound in terms of sensitivity as well as selectivity. Also, this study shows that application of modifiers solves adsorption problems of carbon electrodes, one of main goals of lot of researchers.

**Determination of nitrite in tap water: A comparative study between cerium, titanium and selenium dioxide doped reduced graphene oxide modified glassy carbon electrodes.** In this study a comparative study between three different novel synthesized materials, cerium, titanium and selenium dioxide doped reduced graphene oxide, was done toward detection of nitrite in tap water, with schematic illustration in Figure 5. It was found that best response and analytical performance were achieved with cerium dioxide reduced graphene oxide modified glassy carbon electrode. The materials were synthesized and characterized with transmission electron microscopy, electrochemical impedance spectroscopy and UV-vis spectroscopy. Inclusion of different dopants in the graphene structure for novel materials to modify solid electrodes was found to enhance the catalytic effect toward nitrite detection<sup>6</sup>.

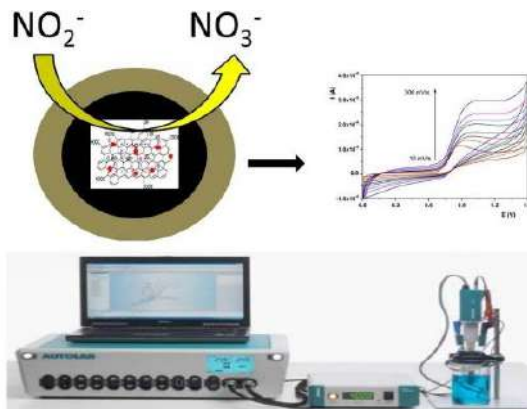


**Figure 5.** System for detection of nitrites using modified decorated graphene modified GC electrode

### Electrochemical biosensors based on nano-structured materials

Novel nano-materials found wide application in field of electrochemical biosensors. With their involving in electrochemical biosensors performance of these devices were strongly improved, dominantly selectivity, sensitivity, life time as well as producing costs. Most of the biosensors investigated up to date detect glucose level, due to its importance in diabetes, a disease with unequibrated glucose levels affecting roughly 422 millions of

people worldwide. One can distinguish three generations of electrochemical glucose biosensors according to the response mechanisms. The first generation makes use of oxygen as an electron acceptor; the electrochemical detection relies either on monitoring the co-substrate,  $O_2$ , or the intermediate of the enzymatic reaction,  $H_2O_2$ . Sensors working on this principle are prone to errors from oxygen deficiency. Other limitations, such as high overpotentials for the oxidation or reduction of the target analyte may be overcome by mediators to some extent. The second generation uses synthetic electron acceptors rather than oxygen; their presence in samples is better controllable but they are still liable for errors and limitations due to interfering compounds and the enzyme itself. Direct electron transfer between an electrode surface and the enzyme is usually not possible due to the protein shell, which acts as a barrier for the electrical communication between the co-enzyme and the electrode surface. “Wiring” of enzyme provides a direct electron shuttle between the electrode surface and the active center of the enzyme resulting in sensors of the so-called third generation. Development of new materials, which with controlled synthesis procedure possess exact structure and properties, opened new field of non-enzymatic biosensors (in literature known as “reagentless” biosensors).

**Second generation of biosensors.** Schematic illustration of glucose sensing devices is shown in Figure 6. Second generation obviously is based on mediators, such as nanomaterials with different characteristics. This field is widely investigated, but increase in the knowledge in the field of materials offer improvement in glucose detection and development of novel approach in glucose sensing, such as third sensor generation and “reagentless” glucose biosensors <sup>7</sup>.

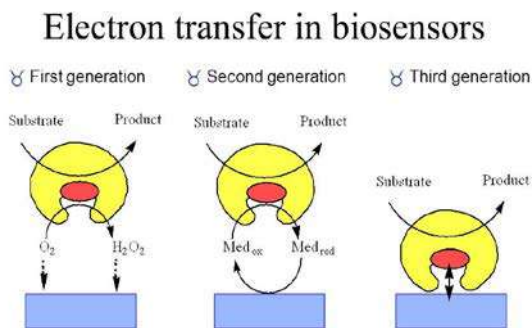


**Figure 6.** Schematic illustration of historical development of glucose biosensors.

**Wiring of glucose oxidase with graphene nanoribbons: an electrochemical third generation glucose biosensor.** A reagentless third generation electrochemical glucose biosensor was fabricated based on wiring of a template enzyme, glucose oxidase (GOx), with graphene nanoribbons (GN) in order to create direct electron transfer between the co-factor (flavin adenine dinucleotide, FAD) and the electrode. The strategy (Figure 7) involved: (i) isolation of the apo-enzyme by separating off its co-enzyme; (ii) preparation of graphene nanoribbons (GN) by oxidative unzipping of multi-walled carbon nanotubes;

(iii) adsorptive immobilization of GNs on the surface of a screen printed carbon electrode (SPCE); (iv) covalent attachment of FAD to the nanoribbons; (v) recombination of the apo-enzyme with the covalently bound FAD to the holoenzyme; and (vi) stabilization of the bio-layer with a thin membrane of Nafion. Screen printed carbon electrodes were chosen as a proper platform because they are very robust, mechanically and chemically more stable and inert than carbon paste electrodes. Compared to glassy carbon the heterogeneous nature of the screen-printed film offers higher hydrophilicity due to the presence of a polymer (polyester or similar); this feature seems positive towards graphene nanoribbons which contain many oxygen-containing groups after chemical oxidative unzipping from multiwall carbon nanotubes.

Graphene nanoribbons are derived from graphene and bear still its advantageous characteristics for designing sensors and biosensors. They seem to be a proper material for acting like a cable to shuttle electrons from the active center to the electrode surface due to their geometry and electric conductivity. The biosensor (GN/FAD/apo-GOx/Nafion/SPCE) for the determination of glucose was operated at a potential of +0.475 V vs Ag/AgCl/{3 M KCl} in flow-injection mode with oxygen-free phosphate buffer (0.1 mol·L<sup>-1</sup>, pH 7.5) as a carrier. Results, obtained in oxygen- and mediator-free medium, provide a good proof for the direct electron transfer between the redox active site of GOx (FAD) and the electrode surface via nanoribbons, which is underlined by varying the glucose concentration with sensors containing the recombined enzyme<sup>8</sup>.

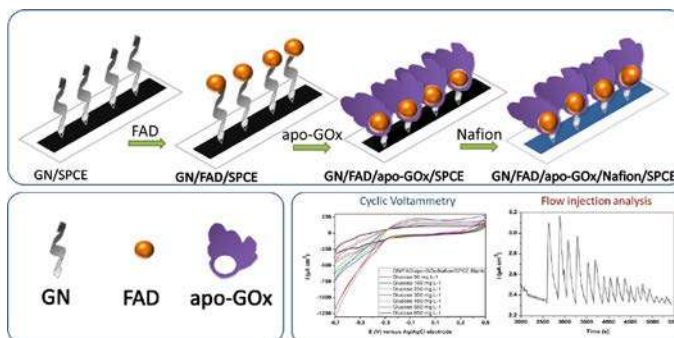


**Figure 7.** Reconstitution of the holoenzyme GOx on a screen-printed carbon electrode and glucose detection

**Reagentless glucose biosensor based on zinc substituted magnetite.** In a new approach based on two-step procedure, co-precipitation method followed by hydrothermal treatment in a microwave field, Zn-substituted Fe<sub>3</sub>O<sub>4</sub> nanoparticles (Zn<sub>x</sub>Fe<sub>3-x</sub>O<sub>4</sub>, x = 0-1.0) were synthesized. Results of XRD, ICP-OES and TEM analysis clearly demonstrate that nanoparticles are single phase, crystallizing in the spinel structure type (*S.G. Fd3m*) with crystallite size in the range of 2-20 nm, which strongly depends on Zn concentration. The produced nanoparticles were used for fabrication of modified carbon paste electrodes as a novel system for the electrochemical non-enzymatic glucose detection. It was found that

increasing of zinc concentration in used nanoparticles up to the value of  $x = 0.56$  ( $\text{Zn}_{0.56}\text{Fe}_{2.44}\text{O}_4$ ) was followed with an increase of a performance of the modified carbon paste electrode toward glucose detection. Linear working range from 0.1 to 2 mM was obtained with detection limit at a value of 0.03 mM<sup>9</sup>.

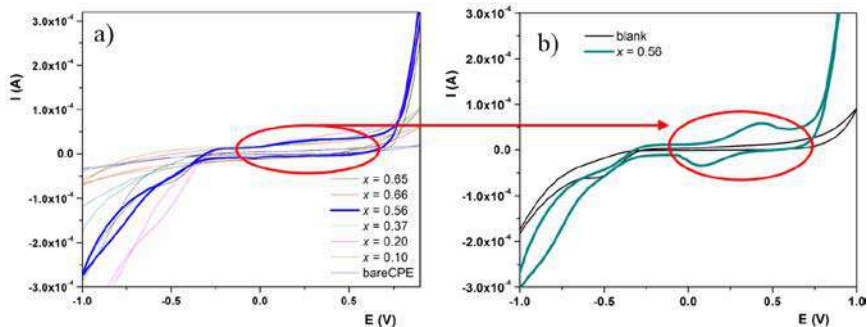


**Figure 8.** Cyclic voltammograms in presence and absence of 0.01 M of glucose using  $\text{Zn}_x\text{Fe}_{3-x}\text{O}_4$  (with  $x = 0, 0.10, 0.20, 0.37, 0.56, 0.66$  and  $0.65$ ) modified glassy carbon paste electrode in 0.1 M NaOH supporting electrolyte. (b) Cyclic voltammograms in presence of 0.1 M of glucose using  $\text{Mg}_{0.56}\text{Fe}_{2.44}\text{O}_4$  modified glassy carbon paste electrode in 0.1 M NaOH supporting electrolyte.

Obtained analytical characteristics of selected electrode were investigated using amperometric detection in 0.1 M NaOH as supporting electrolyte at potential of 0.5 V (Figure 8). The comparable LOD and operating range obtained with this approach clearly indicate that the magnetic nanoparticles with exact Zn content were found as optimum for using for modification of carbon electrodes. In conclusion, it can say the synthesized  $\text{Zn}_x\text{Fe}_{3-x}\text{O}_4$  were exploited for the first time in connection with amperometric technique to elaborate the novel and advanced electrochemical protocols for simple, low cost and reagentless analytical determination of glucose.

## Conclusion

The application of new types of materials is gaining a number of unique properties in electrochemical behavior. Such materials may be applied in in electrochemical sensors and biosensors, as well as in other fields such as optic, electronic, environmental. Controlled synthesis procedure, adequate uses and careful study can offer promising characteristics of such materials as well as opening of new fields of research.

## Acknowledgments

This work was supported by Magbiovin project (FP7-ERACHairs-Pilot Call-2013, Grant agreement: 621375), by the Ministry of Education, Science and Technology, the Republic of Serbia (Project No. OI 172030).

## References

1. Laurila T, Sainio S, Caro MA. Hybrid carbon based nanomaterials for electrochemical detection of biomolecules. *Progr Mater Sci* 2017;88:499-594.
2. Mehmeti E, Stanković DM, Chaiyo S, Švorc L, Kalcher K. Manganese dioxide-modified carbon paste electrode for voltammetric determination of riboflavin. *Microchim Acta* 2016;183:1619-24.
3. Stanković DM, et al. Optimized chemical composition of (Mg,Fe)<sub>3</sub>O<sub>4</sub>/glassy carbon paste electrodes with enhanced sensitivity toward detection of gallic acid and estimation of total antioxidant activity, *under review*.
4. Lakić M, Vukadinović A, Kalcher K, Nikolić AS, Stanković DM. Effect of cobalt doping level of ferrites in enhancing sensitivity of analytical performances of carbon paste electrode for simultaneous determination of catechol and hydroquinone. *Talanta* 2016;161:668-74.
5. Stanković DM, Ognjanović M, Martin F, Švorc L, Mariano JFML, Antić B. Design of titanium nitride- and wolfram carbide-doped RGO/GC electrodes for determination of gallic acid, *Anal Biochem* doi: 10.1016/j.ab.2017.10.018.
6. Stanković DM, Mehmeti E, Zavašnik J, Kalcher K. Determination of nitrite in tap water: A comparative study between cerium, titanium and selenium dioxide doped reduced graphene oxide modified glassy carbon electrodes. *Sensors Actuators B: Chem* 2016;236:311-7.
7. Yoo E-H, Lee S-Y. Glucose biosensors: An overview of use in clinical practice. *Sensors* 2010;10:4558-76.
8. Mehmeti E, Stanković DM, Chaiyo S, Zavasnik J, Žagar K, Kalcher K. Wiring of glucose oxidase with graphene nanoribbons: an electrochemical third generation glucose biosensor. *Microchim Acta* 2017;184:1127-34
9. Stanković D, Ognjanović M, Ming Y, Zhang H, Jancar B, Dojčinović B, Prijović Z, Antić B. Reagentless glucose biosensor based on zinc substituted magnetite, *under review*.

---

## **Battle against inflammation: polyphenols targeting selective inhibition of cyclooxygenase-2**

---

**Ivana N. Beara\***

*Department of Chemistry, Biochemistry and Environmental Protection, Faculty of Sciences, University of Novi Sad, Novi Sad, Serbia*

*\*e-mail: ivana.beara@dh.uns.ac.rs*

Upon activation of enzyme phospholipase A<sub>2</sub> by different inflammatory stimuli, arachidonic acid is released from membrane phospholipids and can be converted to structurally diverse eicosanoids in three directions, determined by three classes of enzymes: cyclooxygenases (COX), lipoxygenases, and epoxygenases. Besides in inflammation and pathologic conditions, including pain, cardiovascular disease and cancer, these lipids evince various biological activities in normal physiology - vasodilatation, vasoconstriction, ovulation, platelet and renal function, etc. The key step of COX pathway implies activities of COX-1 and -2. Ever since enrolment of COX-2 in numerous pathologial processes was recognized, it became significant therapeutic target for inflammation. Common non-steroidal anti-inflammatory drugs (NSAID) inhibit both COX-1 and -2, and this non-selective mechanism is crucial for unwanted, side-effects of NSAID. Also, selective COX-2 inhibitors have some disadvantages. Consequently, there is certain need to find new inhibitors, that can provide adequate therapeutic potential with minor side effects. Contemporary search for COX-2 selective inhibitors is focused on some natural products, particularly polyphenols.

### **Arachidonic acid metabolism**

A complex network of inflammatory response is directed by numerous mediators, and the control of their production is assumed to be an efficient target for anti-inflammatory therapy. In this sense, convenient approach to the inflammation modulation is influence on the production of inflammatory mediators - eicosanoids, generated in arachidonic acid metabolism. Besides in inflammation and pathologic conditions, including pain, cardiovascular disease and cancer, these lipids evince various biological activities in normal physiology - vasodilatation, vasoconstriction, ovulation, platelet and renal function, etc <sup>1,2</sup>. Upon activation of enzyme phospholipase A<sub>2</sub> (PLA<sub>2</sub>) by different inflammatory stimuli, arachidonic acid is released from membrane phospholipids and can be converted to structurally diverse eicosanoids by three pathways determined by three classes of enzymes: cyclooxygenases (COX), lipoxygenases (LOX) and epoxygenases.

The key step of COX pathway implies activities of COX-1 and COX-2, also known by the name prostaglandin H synthase-1 and -2 (PGHS-1/2), which corresponds to the nomenclature convention<sup>3</sup>. COX-1 and -2 are bifunctional enzymes, since they possess both cyclooxygenase and peroxidase activities. Although PLA<sub>2</sub> activity is required to initiate arachidonic acid pathway, the overall regulation of the type and amount of inflammatory mediators in a specific cell is dependent on the expression levels of COX-1, COX-2, and terminal synthase enzymes. Reaction catalyzed by COX starts with the formation of the cyclic endoperoxide prostaglandin G<sub>2</sub> (PGG<sub>2</sub>) from arachidonic acid (cyclooxygenase activity), which is then reduced to PGH<sub>2</sub> by the peroxidase activity. PGH<sub>2</sub> is subsequently metabolized to terminal prostaglandins: PGE<sub>2</sub>, PGI<sub>2</sub> (prostacyclin), PGD<sub>2</sub>, PGF<sub>2α</sub>, as well as thromboxane A<sub>2</sub> (TXA<sub>2</sub>) by corresponding prostaglandin and thromboxane synthases<sup>1</sup>. These PGs could be found in different cells and tissues where exert different activities: PGE<sub>2</sub> and PGI<sub>2</sub> in the gastric mucosa - gastroprotection, PGE<sub>2</sub> and PGI<sub>2</sub> in the kidney - salt and water excretion, PGE<sub>2</sub> in joints - inflammation and pain, PGI<sub>2</sub> in endothelial cells - platelet inhibition and vasodilation, PGE<sub>2</sub> in the central nervous system - pain and fever, TXA<sub>2</sub> in platelets - platelet activation, vasoconstriction<sup>4</sup>.

Even though COX-1 and COX-2 have identical structures and catalyze same reactions, they have distinct functions and are encoded by distinct genes whose expression is regulated by different mechanisms. While COX-1 is constitutively expressed in virtually all cells, and is responsible for platelet aggregation, gastric cytoprotection and renal water balance, COX-2 is highly up regulated in the macrophages, monocytes, fibroblasts and endothelial cells during inflammation<sup>1,2</sup>. Ever since enrolment of COX-2 in numerous pathological processes was recognized, it became significant therapeutic target for inflammation. Term "selective" COX-2 inhibitor generally refers to the selective inhibition of COX-1/2 activity, rather than the selective inhibition of their expression. A brief overview of the structure-activity relationship of COX-1/2 selective inhibition and some natural products, particularly some polyphenols will be presented in this paper.

## **COX-1 and COX-2 structure and function**

Human COX-1 and COX-2 are homodimers consisting of 576 and 581 amino acids, respectively. They are mainly located on the luminal side of the endoplasmatic reticulum membrane and nuclear envelope, but can be also found in lipid bodies, mitochondria, filamentous structures, vesicles and nucleus<sup>3</sup>. Their crystal structures are well-known<sup>4,5</sup>. The presence of three high mannose oligosaccharides facilitates protein folding, while a fourth oligosaccharide, present only in COX-2, regulates its degradation. Each subunit of the dimer has three domains: the epidermal growth factor domain (residues 34-72) involved in dimerization via hydrophobic interactions, the membrane binding domain (residues 73-116), and the catalytic domain. The large catalytic domain makes about 80% of the protein, and contains the sites for cyclooxygenase and peroxidase reactions. These active sites are distinct, but structurally and functionally interconnected<sup>5</sup>.

COX active site is positioned at the top of a long, hydrophobic channel that originates in the membrane binding domain. Access of the lipid substrate (arachidonic acid) to the

active site is provided through this hydrophobic tunnel, where Arg120 is essential for substrate binding. When arachidonic acid binds to the cyclooxygenase active site, its carboxyl group is sited at the lower, narrow part of the channel, while carbon-13 is placed closely to Tyr385, the critical catalytic amino acid for the cyclooxygenase reaction<sup>5</sup>.

The peroxidase active site is located opposite from the membrane binding domain and consists of the heme positioned at the bottom of a shallow gap. The conversion of arachidonic acid starts with the transfer of an electron to the heme from Tyr385, when a tyrosyl radical in the cyclooxygenase active site is generated. This radical is placed suitably to abstract the pro-*S* hydrogen from carbon-13 of arachidonic acid, initiating the cyclooxygenase reaction and formation of C11-C15 delocalized pentadienyl radical, that sequentially reacts with two molecules of O<sub>2</sub>, yielding the bicyclic PGG<sub>2</sub> peroxy radical. Reduction of the peroxy radical to the 15-hydroperoxide PGG<sub>2</sub> regenerates the tyrosyl radical. Further peroxidase activity implies reduction of the hydroperoxyde PGG<sub>2</sub> to the corresponding alcohol - PGH<sub>2</sub><sup>5</sup>.

Differences in three amino acids between COX-1 and COX-2 primary sequence are key reason for their different activities. Namely, Ile434, His513 and Ile532 present in COX-1 corresponds to Val434, Arg513 and Val523 in COX-2, which cause change in relative volume of active site making the side pocket in COX-2 that is absent in COX-1<sup>6</sup>. Since COX-1 and COX-2 have similar *K<sub>m</sub>* values with arachidonic acid, it is considered that these minor differences cause significantly diverse pharmacological and biological activities. The difference in the size and shape of the two active sites led to the development of the COX-2 selective inhibitors<sup>2,5</sup>.

### **Non-steroidal anti-inflammatory drugs (NSAID) and coxibs**

Common non-steroidal anti-inflammatory drugs (NSAID), such as aspirin (salicylate), ibuprofen and naproxen (propionic acid derivatives), meloxicam and piroxicam (enolic acid derivatives), mefenamic acid (fenamates), indomethacin, diclofenac and sulindac (acetic acid derivatives) lead to inhibition of both COX-1 and -2, usually by blocking access of arachidonic acid to the COX active site. NSAID inhibit COX differently: most carboxylate-containing NSAID are binding to Arg120, while Ser530 is target residue for acetylsalicylic acid and phenylacetic acid (diclofenac)<sup>7</sup>. This non-selective mechanism is crucial for unwanted, side-effects of NSAID.

Namely, COX-1 is the only isoform expressed in mature platelets and is the most highly expressed COX isoform in the gastric mucosa. Inhibition of COX-1 by nonselective NSAID increases the risk of unwanted gastrointestinal symptoms, mucosal damage and bleeding. For example, at low doses (30 to 160 mg/day), acetylsalicylic acid irreversibly inhibits COX-1 in platelets, and because they do not have nucleus further production of COX-1 is impossible. The consequent permanent reduction in TXA<sub>2</sub> production in platelets results in the antithrombotic effect of acetylsalicylic acid. Same process occurs in the gastric mucosa where cells can synthesize more COX-1 so the inhibition has less influence and the risk for side effects is lower. Also, low-doses of acetylsalicylic acid have

minimal effect on COX-2-mediated synthesis of PGI<sub>2</sub> in endothelial cells, which are nucleated and respectively synthesize more COX-2. But, at higher doses, the action of acetylsalicylic acid is similar to those of other nonselective NSAID and can cause severe side effects<sup>4</sup>. Therefore, strong efforts were made to develop COX-2-selective NSAID - coxibs. The coxibs inhibit only the COX-2-mediated pathways. Therapeutic goal of coxibs is achieved by blocking PGE<sub>2</sub> formation and thus reducing inflammation and pain, without influence on COX-1-mediated gastric PGE<sub>2</sub> production and preserving its gastroprotective actions. Unfortunately, it was found that selective coxibs elevate the risk for myocardial infarction and stroke<sup>8</sup>. Some of them, such as rofecoxib (Vioxx) and valdecoxib were withdrawn from the market<sup>4,5</sup>.

Present data evidenced that COX-2 may be constitutively expressed by endothelial cells, as well as in brain, kidney and pancreas. The inhibition of endothelial vascular protective PGI<sub>2</sub> by COX-2 selective agents may cause serious adverse cardiovascular disorders. At some lower extent, PGI<sub>2</sub> synthesis is also inhibited by high dose of acetylsalicylic acid and other NSAID. In addition, renal PGE<sub>2</sub> and PGI<sub>2</sub> production can also be affected by NSAID, resulting in sodium and water retention, as well as elevation of blood pressure<sup>4</sup>.

Due to many coxibs disadvantages, there is certain need to find new, selective COX-2 inhibitors that can provide adequate therapeutic potential with minor side effects. Therefore, contemporary search for COX-2 selective inhibitors is focused on some natural products, particularly polyphenols.

### **Polyphenols as COX inhibitors**

Polyphenols are secondary plant metabolites abundant in fruits, vegetables, but also cereals. Common structural feature of polyphenols are aromatic rings, each bearing one or more hydroxyl groups. Their classification is based on the number of phenol rings and the way how these rings are bonded: the phenolic acids, flavonoids, stilbenes, and lignans. Among wide range of biological activities, including antioxidant, antimicrobial, antiviral, anticancer, immunomodulatory, etc., anti-inflammatory properties of polyphenols are also remarked<sup>9-11</sup>. One of the mechanisms explaining anti-inflammatory activity of polyphenols is modulation of enzymes activities included in arachidonic acid metabolism, PLA<sub>2</sub>, COX and LOX, on both transcriptional and enzyme levels. For example, one of the first evidence was that quercetin inhibited PLA<sub>2</sub> from human neutrophils<sup>12</sup>, followed by findings that luteolin, galangin and morin can inhibit COX<sup>13</sup>. Since then, many polyphenols were tested and it was confirmed that they possess therapeutic potential by targeting arachidonic acid pathway<sup>9,10,14</sup>. Regarding cyclooxygenase inhibitory activity, some interesting conclusions on structural characteristics of flavonoids responsible for activity were reached.

It has been found that the C2-C3 double bond is essential for the COX-1 inhibitory activity, since it provides the planarity of the molecule and its interaction with the enzyme. For the presence of 3-OH group in C ring it is not clearly determined weather it can

diminish activity<sup>15</sup> or has no effect<sup>16</sup>. The example of good COX-1 inhibitor<sup>16</sup>, flavone 1 is shown in Figure 1.

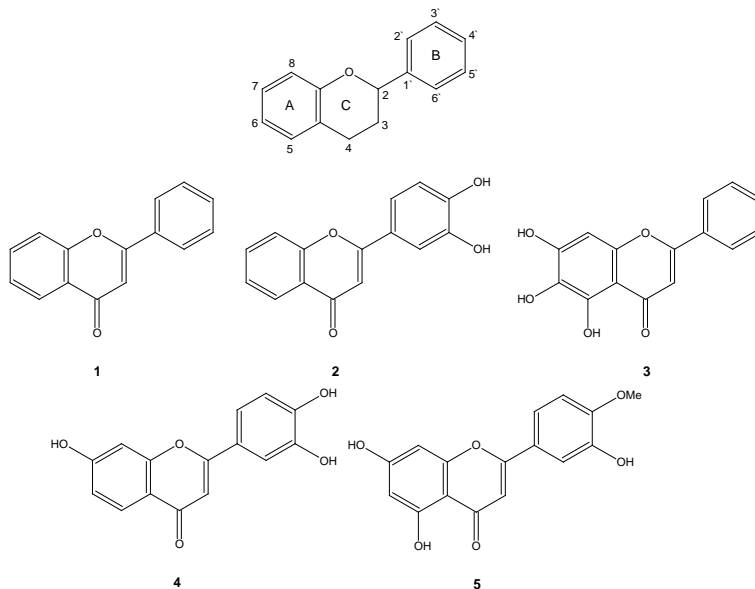


**Figure 1.** General structure of flavonoids, potent COX-1 inhibitors (1), COX-2 inhibitors (2,3), and selective COX-1/2 inhibitors (4,5)

The most active COX-2 inhibitors have 4-oxo group in C ring. C2-C3 double bond also enhances activity, as well as 5- and 7-OH groups<sup>17</sup>. Also, catechol group in B ring (3', 4'-dihydroxyl moiety) lowers potency of COX-2 inhibitors, while more than two hydroxyl residues on B ring leads to the loss of inhibitory activity<sup>17</sup>. However, this conclusion was not correlated with results of Ribiera et al.<sup>16</sup>, where opposite conclusions were addressed. Nevertheless, docking study showed that catechol moiety contributes to the establishment of hydrogen bonds with Tyr385 and Ser530 in hydrophobic pocket of enzyme, but the overall activity can be rather caused by the ability of these flavonoids to scavenge or inhibit the production of pro-oxidant reactive species implicated in overexpression of COX-2<sup>17,18</sup>. The examples of good COX-2 inhibitors<sup>16,17</sup>, flavone 2 and 3 (baicalein) are shown in Figure 1. In general, the glycosides of various flavonoids exhibit lower activity than their corresponding aglycones and it can be at least partially accounted to their lower permeability through cell membrane<sup>17</sup>. Regarding potential selectivity on COX-1/2, some interesting conclusions were also reached. A study undertaken in human whole blood system for series of flavonoids showed that less substituted flavonoids were more active for COX-1 than for COX-2. This is due to smaller volume of COX-1 active site and fact that interactions of less substituted molecule may be more favourable than those of more substituted and larger molecule<sup>16</sup>. The examples of potent selective COX-2 inhibitors, according to Ribeiro et al.<sup>16</sup>, are flavonoids 4 and 5.

Having all this structural properties in mind, flavonoids inhibition activity towards COX could be predicted to some extent. However, plant extracts are mixtures of numerous compounds, and testing their activity, particularly selectivity is certain challenge. Interestingly, some plant extracts could also be selective, as it was demonstrated for chamomile extract<sup>19</sup>. Several model-systems for COX-1 and COX-2 inhibition potential, as well as selectivity, were developed.

### ***In vitro* assays for screening COX-1 and COX-2 activity**

Various *in vitro* experimental models are used to test COX-1 and COX-2 activity, including enzymes of animal or human origin, native or recombinant, purified, in microsomal preparations or in different cell types. Regarding cell-based assays, as a source of COX-1 washed platelets and monocytes are commonly used, while COX-2 inhibition can be determined in macrophages, monocytes, chondrocytes, synoviocytes etc. Additionally, induction agents of COX-2 can also vary (bacterial lipopolysaccharide, various cytokines, such as interleukin-1 or tumor necrosis factor), as well as technique used for detection of COX-2 (and COX-1) metabolites derived from endogenous or exogenous arachidonic acid (EIA, RIA, liquid chromatography)<sup>20</sup>. To determine COX-1/2 selectivity and considering presence of adequate enzyme, combination of different cell lines are used, usually platelets and macrophages. But, IC<sub>50</sub> varies greatly, as well as COX-1/2 IC<sub>50</sub> ratios, and results should not be compared directly. Additionally, activities of COX-1 and COX-2 can be measured in isolated human monocytes or whole-blood, that is considered as the matrix most approximate to the physiological conditions and where both isoenzymes are present<sup>16,21,22</sup>. To avoid some ethical issues regarding blood collection, and diminish influence and unreliability due to use of different origin of cells, we propose a novel model-system based on COX-1/2 availability in same cell line: U937 monocytes are used to determine COX-1 inhibition potential, while derived macrophages are used to test COX-2 inhibition.

### **Our results**

As a part of our ongoing studies concerning biological potential of some red wines and its relation to their phenolic profile, novel model-system to determine COX-1/2 activity was applied. In brief, human U937 monocytes ( $1 \times 10^6$  cells/mL), as a source of COX-1, were pretreated with wine samples for 2 h. Afterward, arachidonic acid (10  $\mu$ M) was added and cells were incubated for 10 min<sup>23,24</sup>. Extraction of products and internal standard (PGB<sub>2</sub>) was done according to Beara et al<sup>25</sup>. Quantification of produced PGE<sub>2</sub> and TXA<sub>2</sub> in cell lysate was done by LC-MS/MS<sup>26</sup>. Same procedure was done for COX-2 activity, but macrophages were used ( $1 \times 10^6$  U937 monocytes/mL were differentiated into macrophages in the presence of PMA (100 nM)) and COX-2 was induced by LPS (0.5  $\mu$ g/mL, 20 h), after pretreatment with wine samples. The results are presented in Table 1. Furthermore, LC-MS/MS technique was applied to evaluate the quantitative content of 45 phenolics in

wine samples, including 16 phenolic acids, 25 flavonoids, 3 coumarins, 1 stilbenoid, 2 lignans and one organic acid<sup>27</sup>.

**Table 1.** PGE<sub>2</sub> and TXA<sub>2</sub> response ratios in probe and in control

Product response ratios in probe / Product response ratios in control							
	control	Aspirin (25 µM)	Gallic acid (25 µM)	Resveratrol (25 µM)	Catechin (25 µM)	San Trifone wine (300 mg/mL)	Petrovic wine (300 mg/mL)
monocytes							
PGE <sub>2</sub>	1.00 ± 0.14 <sup>a</sup>	0.86 ± 0.06 <sup>a</sup>	1.14 ± 0.21 <sup>a</sup>	1.07 ± 0.11 <sup>a</sup>	0.80 ± 0.11 <sup>a</sup>	1.49 ± 0.13 <sup>b</sup>	1.01 ± 0.07 <sup>a</sup>
TXA <sub>2</sub>	1.00 ± 0.17 <sup>a</sup>	0.35 ± 0.03 <sup>b</sup>	1.41 ± 0.22 <sup>a</sup>	0.74 ± 0.02 <sup>a</sup>	0.43 ± 0.05 <sup>b</sup>	1.52 ± 0.01 <sup>a</sup>	1.29 ± 0.08 <sup>a</sup>
macrophages							
PGE <sub>2</sub>	1.00 ± 0.06 <sup>a</sup>	0.69 ± 0.01 <sup>b</sup>	0.58 ± 0.02 <sup>b</sup>	0.87 ± 0.00 <sup>a</sup>	0.90 ± 0.00 <sup>a</sup>	0.80 ± 0.05 <sup>b</sup>	0.68 ± 0.02 <sup>b</sup>
TXA <sub>2</sub>	1.00 ± 0.05 <sup>a</sup>	0.29 ± 0.01 <sup>b</sup>	0.59 ± 0.07 <sup>b</sup>	0.27 ± 0.04 <sup>b</sup>	0.58 ± 0.20 <sup>b</sup>	0.68 ± 0.04 <sup>b</sup>	0.57 ± 0.05 <sup>b</sup>

Response ratios - metabolite peak area/internal standard peak area

Values are means ± SD of three repetitions. Means within each row with different letters (a, b) differ significantly from control (p < 0.05).

In general, phenolic profile of samples (data not shown) could be, at least partially, correlated with shown activities. We also show results for some polyphenolic compounds, other than flavonoids (gallic acid and resveratrol), since their presence can be strongly implicated in biological activities of wines. Overall, our experiment showed that established system could be used to test both common anti-inflammatory activity by means of COX-2 inhibition, as well as COX-1/2 selectivity of plant extracts or isolated compounds.

## Conclusion

The resolution of inflammatory process is particular challenge for many researches. Having in mind that many known therapeutics, such as coxibs, can exert side-effects, use of natural products in treatment of inflammation is a concept that can provide new possibilities and opportunities in terms of safety drugs.

## Acknowledgements

The Ministry of Education and Sciences Republic of Serbia (Grant No. 172058) supported this research. We thank dr Snežana Kojić, Institute of Molecular Genetics and Genetic Engineering, University of Belgrade for providing U937 cells.

## References

1. Smith W. The eicosanoids and their biochemical mechanism of action. *Biochem J* 1989;259:315-24.

2. Morita I. Distinct functions of COX-1 and COX-2. *Prostaglandins Other Lipid Mediat* 2002;68-69:165-75.
3. Chandrasekharan N, Simmons D. The cyclooxygenases. *Gen Biol* 2004;5:241:1-7.
4. Cairns J. The coxibs and traditional nonsteroidal anti-inflammatory drugs: a current perspective on cardiovascular risks. *Can J Cardiol* 2007;23:125-31.
5. Rouzer C, Marnett L. Cyclooxygenases: structural and functional insights. *J Lipid Res* 2009;50:S29-34.
6. Gierse J, McDonald J, Hauser S, Rangwala S, Koboldt C, Seibert K. A single amino acid difference between cyclooxygenase-1 (COX-1) and -2 (COX-2) reverses the selectivity of COX-2 specific inhibitors. *J Biol Chem* 1996;271:15810-14.
7. Firestein G, Budd R, Gabriel S, McInnes I, O'Dell J. Prostaglandins, Leukotrienes, and Related Compounds. In: Harris ED, Kelley N, William MA. *Kelley's Textbook of Rheumatology*. Elsevier, Saunders, 2013, pp340-58.
8. Grosser D, et al. Biological basis for the cardiovascular consequences of COX-2 inhibition: therapeutic challenges and opportunities. *J Clin Invest* 2006;116:4-15.
9. García-Lafuente A, Guillamón E, Villares A, Rostagno M, Martínez J. Flavonoids as anti-inflammatory agents: Implications in cancer and cardiovascular disease. *Inflamm Res* 2009;58:537-52.
10. Ribeiro D, Freitas M, Lima J, Fernandes E. Proinflammatory pathways: The modulation by flavonoids. *Med Res Rev* 2015;5:877-936.
11. Mitjavila M, Moreno J. The effects of polyphenols on oxidative stress and the arachidonic acid cascade. Implications for the prevention/treatment of high prevalence diseases. *Biochem Pharmacol* 2012;84:1113-22.
12. Lee T-P, Matteliano M, Middleton E. Effect of quercetin on human polymorphonuclear leukocyte lysosomal enzyme release and phospholipid metabolism. *Life Sci* 1982;31:2765-74.
13. Bauman J, von Bruchhausen F, Wurm G. Flavonoids and related compounds as inhibitors of arachidonic acid peroxidation. *Prostaglandins* 1980;20:627-39.
14. Yarla N, Bishayee A, Sethi G, Reddanna P, Kalle A, Dhananjaya B, Dowluru K, Chintala R, Duddukuri G. Targeting arachidonic acid pathway by natural products for cancer prevention and therapy. *Semin Cancer Biol* 2016;40-41:48-81.
15. Wang H, et al. Cyclooxygenase active bioflavonoids from Balaton™ tart cherry and their structure activity relationships. *Phytomedicine* 2000;7:15-9.
16. Ribeiro D, Freitas M, Tomé S, Silva A, Laufer S, Lima J, Fernandes E. Flavonoids inhibit COX-1 and COX-2 enzymes and cytokine/chemokine production in human whole blood. *Inflammation* 2015;38:858-870.
17. Takano-Ishikawa Y, Goto M, Yamaki K. Structure-activity relations of inhibitory effects of various flavonoids on lipopolysaccharide-induced prostaglandin E<sub>2</sub> production in rat peritoneal macrophages: Comparison between subclasses of flavonoids. *Phytomedicine* 2006;13:310-7.
18. Mello P, Gadhwal M, Joshi U, Shetgiri P. Modeling of COX-2 inhibitory activity of flavonoids. *Int J Pharm Pharm Sci* 2011;3:33-40.
19. Srivastava J, Pandey M, Gupta S. Chamomile, a novel and selective COX-2 inhibitor with anti-inflammatory activity. *Life Sci* 2010;85:663-69.
20. Pairet M, van Ryn J. Experimental models used to investigate the differential inhibition of cyclooxygenase-1 and cyclooxygenase-2 by non-steroidal anti-inflammatory drugs. *Inflamm Res* 1998;47:S93-101.
21. Laufer S, Luik S. Different methods for testing potential cyclooxygenase-1 and cyclooxygenase-2 inhibitors. *Methods Mol Biol* 2010;644:91-116.
22. Demasi M, Caughey G, James M, Cleland L. Assay of cyclooxygenase-1 and 2 in human monocytes. *Inflamm Res* 2000;49:737-43.
23. Penglis P, Cleland L, Demasi M, Caughey G, James M. Differential regulation of prostaglandin E<sub>2</sub> and thromboxane A<sub>2</sub> production in human monocytes: implications for the use of cyclooxygenase inhibitors. *J Immunol* 2000;165:1605-11.
24. Wong E, et al. Characterization of autocrine inducible prostaglandin H synthase-2 (PGHS-2) in human osteosarcoma cells. *Inflamm Res* 1997;46:51-9.

25. Beara I, Orčić D, Lesjak M, Mimica-Dukić N, Peković B, Popović M. Liquid chromatography/tandem mass spectrometry study of anti-inflammatory activity of plantain (*Plantago L.*) species. *J Pharm Biomed Anal* 2010;52:701-6.
26. Lesjak M, Beara I, Orčić D, Ristić J, Anačkov G, Božin B, Mimica-Dukić N. Chemical characterisation and biological effects of *Juniperus foetidissima* Willd. 1806. *LWT - Food Sci Techn* 2013;53:530-9.
27. Orčić D, Francišković M, Bekvalac K, Svirčev E, Beara I, Lesjak M, Mimica-Dukić N. Quantitative determination of plant phenolics in *Urtica dioica* extracts by high-performance liquid chromatography coupled with tandem mass spectrometric detection. *Food Chem* 2014;143:48-53.



---

# The role of macrophage migration inhibitory factor in the development of obesity and altered intestinal permeability

---

Tamara Saksida\*, Dragica Gajić, Ivan Koprivica, Ivana Nikolić, Milica Vujičić, Stanislava Stošić-Grujičić, Ivana Stojanović

*Department of Immunology, Institute for Biological Research Siniša Stanković, University of Belgrade, Belgrade, Serbia*

\*e-mail: cvjetica@ibiss.bg.ac.rs

Macrophage migration inhibitory factor (MIF) is a molecule expressed both by the immune cells, like T, B lymphocytes and macrophages, and non-immune cells, like adipocytes, hepatocytes and beta cells of pancreatic islets. It has actions in the innate and adaptive immunity, such as a part in regulating the interleukin-17 expression and production, but also in the development of chemically induced type 1 diabetes in mice. This paper summarizes our results on the role of MIF in the development of obesity and type 2 diabetes, done *in vitro* on beta cell models and murine pancreatic islets, as well as *in vivo*, when mice with MIF deletion (MIF-KO) and their wild type (wt) counterparts were on a high fat diet. It is considered that obesity can develop as a consequence of altered intestinal permeability, so potential leakage of the intestinal barrier is investigated in the MIF-KO and wt mice. Also, the interplay between MIF and regulatory T cells, as an important regulator of inflammation in the adipose tissue, is explored at the level of visceral adipose tissue.

## Introduction

Macrophage migration inhibitory factor (MIF) is a cytokine that is ubiquitously expressed, both by the immune and non-immune cells. Importantly, MIF is expressed by pancreatic beta cells and by adipose tissue cells. It is well known for its pro-inflammatory effects on other immune cells: MIF promotes the inflammatory response by inducing the expression of macrophage surface receptors (Toll-like receptor 4, receptor for TNF- $\alpha$  and for interleukin (IL)-1) and by increasing the release of other pro-inflammatory mediators (TNF- $\alpha$ , prostaglandin-E2, cytochrome oxidase-2). Besides from its actions on innate immunity, MIF is implicated in adaptive immunity as it is released by T lymphocytes, it promotes B- and T-cell proliferation and induces expression of CD25 (IL-2R). Also, MIF is recognized as a negative regulator of the immunosuppressive actions of glucocorticoids. In line with this, MIF has been implicated in the development of many acute inflammatory and auto-immune diseases, as well as chronic inflammatory metabolic disorders. Work in our laboratory showed that MIF has a critical role in the immune-mediated beta-cell destruction in the animal model of human type 1 diabetes mellitus<sup>1</sup>. Lymphocytes from mice treated with the MIF inhibitors exhibited reduction of both islet antigen-specific

proliferative responses and adhesive cell-cell interactions. Neutralization of MIF down-regulated the *ex vivo* secretion of the proinflammatory mediators, TNF- $\alpha$ , IFN- $\gamma$ , and nitric oxide, while augmenting production of the antiinflammatory cytokine, IL-10. MIF can act via its receptor CD74, and controls the recruitment of inflammatory cells via CXCR2 and CXCR4 signaling. Furthermore, MIF can exert pro-inflammatory effects through its enzymatic tautomerase and oxidoreductase activity. MIF is a stimulator of another potent pro-inflammatory cytokine, IL-17<sup>2</sup>, so it could be positioned on the top of a pro-inflammatory cascade. T helper type 17 (Th17) cells produce IL-17 and have a critical role in immunity to extracellular bacteria and the pathogenesis of several autoimmune disorders. The effect of MIF on IL-17 production was dependent on p38, extracellular signal-regulated kinase, Jun N-terminal kinase and Janus kinase 2/signal transducer and activator of transcription 3, and not on nuclear factor-kappaB and nuclear factor of activated T cells signaling<sup>2</sup>. Several lines of evidence provide indications that MIF, besides its role in inflammation, may have a role in energy metabolism. As mentioned, MIF is expressed in metabolically active tissues such as the adipose tissue and the liver. Its expression by adipocytes is regulated by glucose and insulin and it has been shown to have catabolic effects in muscle. Importantly, MIF co-localizes with insulin within the secretory granules of pancreatic beta cells. Our investigations established that MIF binds insulin within beta cell and that pre-incubation of recombinant MIF with insulin promotes the formation of insulin hexamers<sup>3</sup>. Based on these results, it is presumed that MIF enables proper insulin folding which results in insulin full activity.

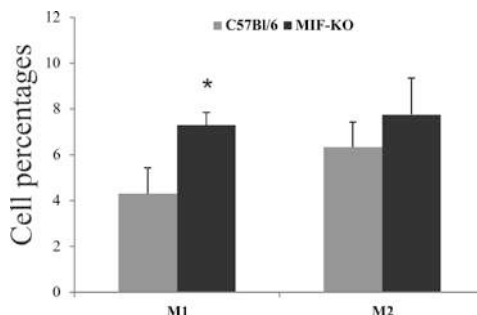


**Figure 1.** Percentages of M1 (F4/80<sup>+</sup>CD40<sup>+</sup>) and M2 (F4/80<sup>+</sup>CD206<sup>+</sup>) macrophages in visceral adipose tissue of MIF-KO and C57Bl/6 mice measured by flow cytometry. Results obtained from 6 animals per group.\*p<0.05 represents statistically significant difference versus C57Bl/6 mice.

## MIF in obesity and type 2 diabetes

Human studies have shown a positive association between obesity and circulating MIF levels, generally reporting increased circulating MIF in obese individuals compared with healthy lean controls. Also, MIF mRNA expression in the mononuclear cells is elevated in the obese subjects<sup>4</sup>. So, having all this in mind it was of interest to investigate its role in the development of obesity and type 2 diabetes. Starting point were the *in vitro* investigations done on pancreatic islets and insulinoma cell lines, as models for beta cells

of pancreatic islets. When these cells are exposed to high concentrations of saturated fatty acid, palmitic acid, as they are exposed during the progression of these diseases, they succumb to apoptotic death<sup>5</sup>. The cells can be protected by the inhibition of MIF: whether chemical inhibition (ISO-1) is employed, or whether neutralizing anti-MIF antibody is used, or whether we use small interfering RNAs, or it is deleted at gene level (usage of cells from MIF-KO mice), the end result is the same: taking MIF out the equation rescues beta cells from toxic fatty acid insult. Protection from the induced apoptosis is mediated by altered activation of the caspase pathway and had correlated with changes in the level of Bcl-2 family members<sup>5</sup>. Interestingly, ablation of MIF is protective even in the circumstances of the exposure to high glucose concentrations<sup>6</sup>. Diabetes patients or pre-diabetic individuals cannot regulate glucose metabolism and have variations in blood glucose concentration, which is considered as another harmful stimulus for beta cells. *In vitro* investigation that mimics this situation is the exposure of beta cells to high glucose concentrations. Again, MIF neutralization or deletion is a rescue for beta cells<sup>6</sup>. So, one could hope for a similar situation to happen *in vivo*. In order to test this, MIF-KO and wild type control mice were feed a high fat diet. Such an approach is a model for diet induced obesity and type 2 diabetes. High fat feeding of C57Bl/6 mice was accompanied with an up-regulation of MIF in pancreatic islets<sup>5</sup>. On the other hand, MIF-KO mice developed obesity even without high fat food. Starting from the 6<sup>th</sup> months of their lives they have higher body mass compared to wild type controls<sup>7</sup>. Also, even without high fat feeding they develop glucose intolerance and hyperglycemia. What could underlie such a phenomenon? MIF and glucocorticoids are on a balance: MIF is (so far) the only cytokine that can antagonize anti-inflammatory actions of GCs. On the other hand, when GCs are high, as they are in Cushing's disease, the patients exhibit obesity and metabolic syndrome. So, we measured corticosterone in sera of our MIF-KO colony<sup>8</sup>. In the situation of innate absence of MIF, GCs were higher than in wild type controls. Furthermore, when MIF-KO mice were treated with GC antagonist, RU486, they handled more efficiently glucose burden, measured by the *i.p.* glucose tolerance test. Also, treating mice with the antagonist restored euglycemia<sup>8</sup>. This could be one possible explanation for the observed discrepancy of *in vitro* and *in vivo* results. In the simplified *in vitro* situation MIF ablation may be sufficient to protect beta cells from toxic insults such as fatty acids or glucose, but in the more complicated setting of *in vivo* investigation, one must account for other factors, such as hormones, redundancy of cytokines, etc.

### **What happens at the level of target tissue, adipose tissue?**

During the progression of obesity adipose cells experience hypertrophy and hyperplasia, to cope with the high energy demands forced upon them with the intake of high caloric diet. In a lean individual adipose tissue is held in a quiescent state by the action of both the innate and adaptive immune systems, notably the anti-inflammatory macrophages (type 2 macrophages) and T regulatory (Treg) cells. But, as obesity progresses this fat depot takes on a pro-inflammatory tenor, hosting a variety of innate and adaptive effector-cell types, such as neutrophils, pro-inflammatory macrophages, CD8<sup>+</sup> T lymphocytes and Th1 cells.

Obesity increases adipose tissue macrophage numbers and these macrophages, not adipocytes, produce majority of cytokines in response to obesity. Namely, these are the pro-inflammatory, type 1 macrophages. Indeed, visceral adipose tissue of MIF-KO mice had significantly higher proportion and number of type 1 macrophages, compared to wild type controls (Figure 1). At the same time with the increase in macrophage numbers, obesity is accompanied by a significant drop in the population of Treg cells in visceral adipose tissue but not elsewhere; and systemic reduction or augmentation of Treg cells increases or decreases adipose-tissue inflammation and insulin resistance, respectively<sup>9,10</sup>, thus showing a significant role for Treg cells in metabolic processes. Interestingly, visceral adipose tissue of MIF-KO mice harbored significantly more Treg cells than the visceral adipose tissue of C57Bl/6 mice (Figure 2).

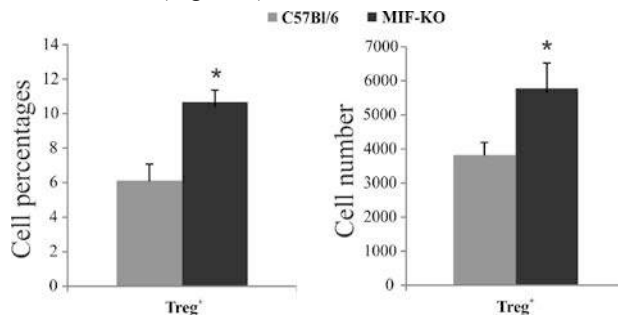


**Figure 2.** Cell percentages and number of Treg cells in the visceral adipose tissue MIF-KO and C57Bl/6 mice. Treg subpopulation analyzed by flow cytometry as a proportion of FoxP3<sup>+</sup> cells within CD4<sup>+</sup>CD25<sup>high</sup> cells. Results obtained from 3 animals per group.\*p<0.05 represents statistically significant difference versus C57Bl/6 mice.

In order to answer why these cells were so abundantly present in the adipose tissue, we measured their proliferation with BrdU test. The animals received an *i.p.* injection of BrdU, a deoxy analog of thymidine that incorporates to DNA during replication. After 24h proliferation of Treg cells residing in visceral adipose tissue, denoted with FoxP3 transcription factor, was measured on a flow cytometer. As Treg cells of MIF-KO mice had comparable proliferation as the cells of C57Bl/6 mice (Figure 3) we can conclude that the reason for the Treg abundance in the visceral adipose tissue of MIF-KO mice is not their increased *in situ* proliferation. Instead, it might be that the migration of Treg cells to the adipose tissue in MIF-KO mice is increased or that Treg cells are developing by conversion from conventional CD4<sup>+</sup> cells. These hypotheses are to be investigated in the future. The functionality of these Treg cells is further questioned, as in spite of their abundance the MIF-KO mice are obese. We tested the IL-10 production of Treg cells in adipose tissue, because IL-10 is the main cytokine of Treg's suppressive action. Indeed, Treg cells isolated from visceral adipose tissue of MIF-KO mice had significantly lower percentages and numbers of IL-10<sup>+</sup> cells (Figure 4). These findings imply a connection between the Treg cells and MIF in the adipose tissue that should be further delineated.

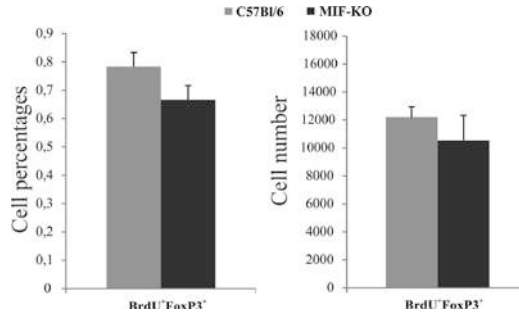


**Figure 3.** Cell percentages and number of cells positive for BrdU and FoxP3 in the visceral adipose tissue MIF-KO and C57Bl/6 mice. Mice received an *i.p.* injection of BrdU (400mg/kg body weight) and after 24 hours cells were analyzed on a flow cytometer. Results obtained from 3 animals per group.

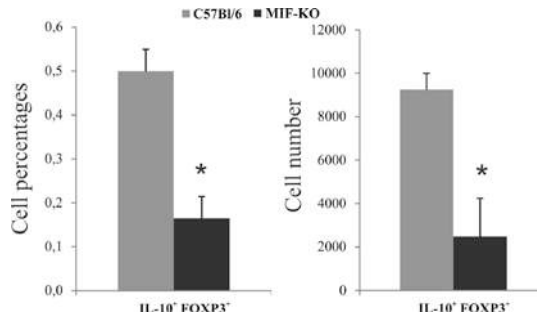


**Figure 4.** Cell percentages and number of cells positive for IL10 and FoxP3 in the visceral adipose tissue MIF-KO and C57Bl/6 mice measured by flow cytometry. Results obtained from 3 animals per group. \* $p < 0.05$  represents statistically significant difference versus C57Bl/6 mice.

### How can one connect obesity and intestinal permeability?

Obesity is a health problem of the modern age, it is connected with the way people live (sedentary) and eat (high fat food). High caloric food is a burden for the organism itself, as the organism must process and store the ingested energy. Apart from the obvious hypertrophy and hyperplasia of adipocytes that fat food imposes, such type of food can change the composition of microbiota. There are animal studies that investigated effects of high-fat diets on the intestinal permeability and on the composition of gut microbiota. Consistently, energy-rich high-fat diets enhanced intestinal permeability. This increased intestinal permeability reflected disturbances of the gastrointestinal barrier. When gut barrier is dysfunctional it enables the entry of toxins from the intestinal lumen, such as LPS— a structural part of gram-negative bacteria cell walls. As a consequence, these high blood endotoxins levels can trigger local inflammation or gain access to circulation and induce systemic inflammation through cytokine release. Continuous infusion of endotoxins

or a high endotoxin level induced by a high-fat diet was shown to trigger the development of obesity and insulin resistance<sup>11</sup>. The authors coined the term metabolic endotoxemia, to differentiate it from the higher endotoxinemic levels found in sepsis. To test intestinal permeability of MIF-KO mice, we applied FITC-dextran *per os* to the obese MIF-KO mice. Indeed, MIF-KO mice had a higher incidence of increased intestinal permeability (7 out of 10 tested mice) than C57Bl/6 mice. These results suggest that MIF absence provoked an increase in intestinal permeability that could be linked to increased obesity of MIF-KO mice.

## Conclusion

MIF is a pleiotropic molecule with versatile functions. Its role in the development of diabetes and obesity is doubtless. On one hand, MIF deletion/inhibition may be protective for beta cells in the early stages of obesity/type 2 diabetes progression, but its ablation does not seem favorable at the level of adipose tissue. Intestinal permeability is impaired without MIF and this could contribute to the observed adiposity in MIF-KO mice. If Treg cells are indeed less functional without MIF, then the potentiation of MIF may be a novel approach to enhance Treg cells.

## Acknowledgements

This work was supported by the Ministry of Education, Science and Technological development of the Republic of Serbia (#173013).

## References

1. Cvetkovic I, et al. Critical role of macrophage migration inhibitory factor activity in experimental autoimmune diabetes. *Endocrinology* 2005;146:2942-51.
2. Stojanović I, Cvjetičanin T, Lazaroski S, Stosić-Grujčić S, Miljković D. Macrophage migration inhibitory factor stimulates interleukin-17 expression and production in lymph node cells. *Immunology* 2009;126:74-83.
3. Vujčić M, Senerović L, Nikolić I, Saksida T, Stosić-Grujčić S, Stojanović I. The critical role of macrophage migration inhibitory factor in insulin activity. *Cytokine* 2014;69:39-46.
4. Sánchez-Zamora YI, Rodríguez-Sosa M. The role of MIF in type 1 and type 2 diabetes mellitus. *J Diabetes Res* 2014;2014:804519.
5. Saksida T, Stosić-Grujčić S, Timotijević G, Sandler S, Stojanović I. Macrophage migration inhibitory factor deficiency protects pancreatic islets from palmitic acid-induced apoptosis. *Immunol Cell Biol* 2012;90:688-98.
6. Stojanović I, Saksida T, Timotijević G, Sandler S, Stosić-Grujčić S. Macrophage migration inhibitory factor (MIF) enhances palmitic acid- and glucose-induced murine beta cell dysfunction and destruction *in vitro*. *Growth Factors* 2012;30:385-93.
7. Serre-Beinier V, et al. Macrophage migration inhibitory factor deficiency leads to age-dependent impairment of glucose homeostasis in mice. *J Endocrinol* 2010;206:297-306.
8. Nikolić I, Vujčić M, Saksida T, Berki T, Stosić-Grujčić S, Stojanović I. The role of endogenous glucocorticoids in glucose metabolism and immune status of MIF-deficient mice. *Eur J Pharmacol* 2013;714:498-506.
9. Feuerer M, et al. Lean, but not obese, fat is enriched for a unique population of regulatory T cells that affect metabolic parameters. *Nat Med* 2009;15:930-9.

10. Eller K, et al. Potential role of regulatory T cells in reversing obesity-linked insulin resistance and diabetic nephropathy. *Diabetes* 2011; 60:2954-62.
11. Cani PD, et al. Metabolic endotoxemia initiates obesity and insulin resistance. *Diabetes* 2007;56:1761-72.



---

## Galectin-1 ligands in human trophoblasts

---

Žanka Bojić-Trbojević<sup>1\*</sup>, Milica Jovanović Krivokuća<sup>1</sup>, Ivana Stefanoska<sup>1</sup>, Nikola Kolundžić<sup>1</sup>, Aleksandra Vilotić<sup>1</sup>, Toshihiko Kadoya<sup>2</sup>, Ljiljana Vićovac Panić<sup>1</sup>

<sup>1</sup>Laboratory for Biology of Reproduction, Institute for the Application of Nuclear Energy - INEP, University of Belgrade, Belgrade, Serbia

<sup>2</sup>Department of Biotechnology, Maebashi Institute of Technology, Maebashi, Gunma, Japan

\*e-mail: zana@inep.co.rs

Interactions of sugar binding proteins galectins have been long considered relevant for various reproductive processes, including embryo implantation. The first galectin family member discovered and identified in the female reproductive system was galectin-1 (gal-1). The involvement of gal-1 in multiple processes during establishment, development and maintenance of pregnancy is unique. Several studies point to its role in modulation of maternal immune response, and trophoblast cell functions. In cell models gal-1 was shown to modulate trophoblast invasive properties, which is accomplished through interaction with ligands at the cell surface and in the extracellular matrix. Data from literature, including our own, point to several trophoblast glycoproteins as gal-1 ligands, such as oncofetal fibronectin, laminin,  $\beta_1$  integrin and mucins. Each of these gal-1 ligands has recognized signalling potential profoundly influencing cell functionality. Given the matricellular nature of gal-1, these interactions may include not only lectin-glycan, but also protein-protein interactions. In human placenta, we speculate that this complex interplay between gal-1 and its identified trophoblast ligands might be important for the regulation of trophoblast cell adhesion, migration and invasion. Although an increasing number of studies searched for identity of gal-1 ligand candidates, insight into the molecular mechanisms of their interactions and influence on trophoblast cell function are still lacking. In clinical studies, altered gal-1 is often associated with pregnancy pathologies.

### Introduction

Highly controlled and specific interactions between trophoblast and uterine epithelium are required for implantation of competent blastocyst and formation of functional placenta. During early stages of pregnancy, trophoblast cells differentiate along two distinct pathways - villous and extravillous<sup>1</sup>. By acquiring migratory and invasive characteristics, extravillous trophoblast cells invade maternal decidua and its vasculature. Accumulated data have shown that trophoblast invasion depends on complex and dynamic crosstalk

between various cell adhesion molecules and components of extracellular matrix (ECM) including heavily glycosylated proteins, such as laminin and oncofetal fibronectin <sup>2,3</sup>. Moreover, it is widely accepted that trophoblast invasion, as prerequisite for normal placental and embryonic development, is a process in which both glycode and glycan-binding proteins likely play important roles <sup>4-6</sup>. In addition to ECM molecules, members of the sugar binding proteins - galectins (gals), gal-1 in particular, has been shown to influence adhesive, migratory and invasive behaviour of trophoblast cells *in vitro*, partially through interactions with glycoconjugates <sup>7</sup>. Despite the increasing number of studies investigating potential gal-1 ligand candidates involved in this processes, knowledge about the biochemical nature of the interactions and their importance for trophoblast cell function, and, consequently relevance for pregnancy outcome is still lacking.

### **Galectin-1: an overview**

Galectins are defined as a family of sugar-binding proteins with an affinity for  $\beta$ -galactosides and significant sequence similarity of the carbohydrate-recognition domain (CRD) <sup>8</sup>. They participate in diverse functions, including immunomodulation, cell differentiation and death, proliferation, signaling, cell adhesion, migration and invasion. Among the 16 different galectins' CRDs identified, gal-1 is the family member best studied so far <sup>9</sup>. It exists as a noncovalent homodimer composed of two CRDs, which recognize a wide range of glycans. For functional activity, gal-1 requires reducing microenvironment <sup>8-10</sup>. However, presence of six cysteine residues per gal-1 monomer, makes this protein sensitive to oxidation which consequently leads to loss of lectin activity. Although gal-1 lacks recognizable secretion signal sequence and has characteristics of a typical cytoplasmic protein, it is well known that it can be found at the cell membrane as well as in the ECM <sup>11</sup>. Therefore, it could act both inside cells, mainly via sugar independent interactions, and out of cells through lectin activity <sup>12</sup>. Numerous studies have shown that ECM components - laminin (LN), oncofetal fibronectin (onfFN), thrombospondin, vitronectin, osteopontin provide the glycotopes for gal-1 binding, in a  $\beta$ -galactoside- and dose-dependent manner <sup>13-15</sup>. Clearly, gal-1 as multivalent carbohydrate-binding protein could bind many ligands (Table 1), but the biological relevance of these interactions remains to be elucidated.

Galectin-1 was the first galectin isolated, purified and cloned from the human placenta <sup>28</sup>. The presence of gal-1 has been shown in human female reproductive tract, as well as at the maternofetal interface <sup>29</sup>. Among placental trophoblast cells, it is immunolocalized in the syncytiotrophoblast, cytotrophoblast of middle and distal cell columns of the anchoring villi, and in the endometrium and decidua of early gestation <sup>30-32</sup>. Besides gal-1, two other members of gal family, gal-3 and -8 are expressed in extravillous cell columns, and throughout the invasive pathway <sup>30,33,34</sup>. Galectin-1 is also expressed by isolated trophoblast in cell culture and trophoblast cell lines, as the predominantly expressed galectin at the trophoblast cell membrane <sup>7,30,35,36</sup>.

**Table 1.** Gal-1 binding partners

Binding partners	Binding type	Tissue/Cell types	Functions/References
Osteopontin	P-C	VSMC	↑ adhesion <sup>15</sup>
Thrombospondin	P-C	VSMC	↑ adhesion <sup>15</sup>
Vitronectin	P-C	VSMC	ECM assembly <sup>13,15</sup>
Laminin	P-C	ovarian carcinoma, Leydig cells, placenta	↑ adhesion <sup>16-18</sup>
Fibronectin	P-C	ovarian carcinoma, placenta	↑ adhesion <sup>16,17</sup>
Glycosaminoglycan	P-C	VSMC	Modulation of ECM assembly, ↓ adhesion <sup>15</sup>
β <sub>1</sub> integrin, α <sub>1</sub> β <sub>1</sub>	P-C	Skeletal and vascular SMC	Adhesion, FAK activation <sup>13,15,19,20</sup>
α <sub>3</sub> β <sub>1</sub>	P-C	epithelial carcinoma cells	Inhibits ras-MEK-ERK pathway <sup>20</sup>
CD45	P-C	T, B cells	Induction of cell death <sup>21, 22</sup>
Mucin	P-C	epithelial glycocalyxes of gastric and intestinal mucosa	NS <sup>23</sup>
CA-125	P-C	HeLa cells	Gal-1 export? <sup>24</sup>
Actin	P-P	brain	NS <sup>25</sup>
H-Ras	P-P	HeLa, HEK293, Rat-1, 293T cells	Selective activation of Raf-1-ERK pathway <sup>26,27</sup>

P-C protein-carbohydrate interaction, P-P protein-protein interaction; VSMC - vascular smooth muscle cell; FAK-focal adhesion kinase; NS-not specified; ↓ decreases and/or inhibits; ↑ increases and /or favors; ? uncertain.

The activity of gal-1 in establishing, development and maintenance of human pregnancy could be described as polyvalent (Figure 1). Several studies described gal-1 as a tolerogenic, pro-angiogenic and growth regulatory protein driving maternal adaptations<sup>37-39</sup>. Moreover, gal-1 has been associated with early pregnancy loss, preeclampsia and gestational trophoblastic disease, i.e. some of the serious pathological conditions involving trophoblast<sup>40-42</sup>. Recent work from our laboratory confirmed functional relevance of gal-1 for trophoblasts invasiveness *in vitro*, partially due to its interactions with β-galactoside containing ligands on the cell surface or in the ECM<sup>7</sup>. Namely, blocking extracellular function of endogenous gal-1 in primary cytotrophoblasts and extravillous HTR-8/SVneo cells either by inhibitory sugar lactose or by function blocking anti-gal-1 antibody, substantially reduced cell invasion. Furthermore, supplementation with stabilized gal-1 (CS-gal-1) in which six cysteine residues are replaced with serine was more potent in stimulating trophoblast invasion than oxidized form of recombinant human gal-1 (Ox-gal-1).

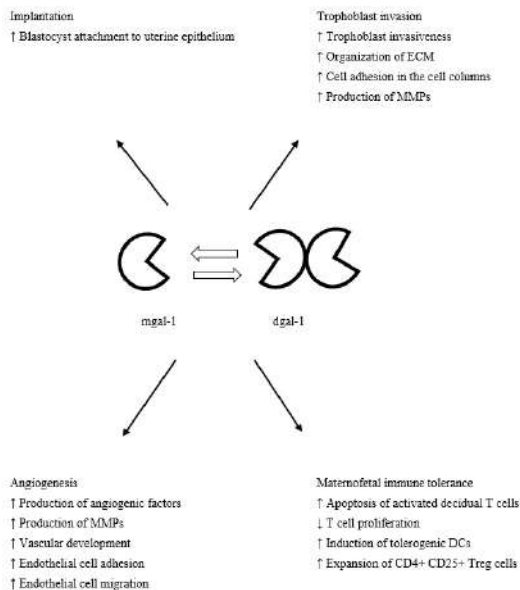


**Figure 1.** Multiple gal-1 roles in implantation, trophoblast invasion, angiogenesis and maternofetal immune tolerance. Mgal-1, monomeric gal-1; dgal-1, dimeric gal-1; MMP, matrix metalloproteinase; DC, dendritic cell.

## Trophoblast glycans

Glycosylation is one of the most frequent posttranslational modifications, affecting protein folding, localization and function. There are three main glycosylation types - N- and O-linked glycosylation and glypiation<sup>43</sup>. Carbohydrate functional groups have been shown to participate in many cellular processes, including embryo implantation<sup>44</sup>. In human placenta, N-glycan profile of cell membrane glycoconjugates was investigated throughout gestation<sup>45</sup>, as well as in different trophoblast cell types<sup>44</sup>. Glycomic analysis revealed differential glycosylation of syncytiotrophoblast (STB), cytotrophoblast (CTB) and EVT cells. Elevated levels of biantennary N-glycans in STB and CTB and low levels of polylectosamine structures were detected. Some of these glycans were sialylated, primarily by  $\alpha$ 2,3 linked sialic acid. The same types of N-glycans were detected in EVT, though in differing proportions. The level of bisecting N-glycans was reduced, with higher amounts of polylectosamines in EVT, compared to other trophoblast cell types. Moreover, N-glycans associated with EVT were exclusively capped with  $\alpha$ 2,3 sialic acid<sup>44</sup>. These results suggest a possibility that interaction at the maternofetal interface could be influenced by the differential glycosylation of human trophoblasts subpopulations. Although O-glycosidic linked glycans of placental proteins (primarily mucins) were investigated, data regarding O-glycan profile are still missing. In addition to the insight

into the glycosylation pattern of the placental cell membrane, deciphering glycoprotein specific glycotopes should be of particular interest for understanding trophoblast function.

### **Galectin-1 binding partners in trophoblast**

Understanding relevance of galectins for invasive properties of normal and transformed trophoblast has been a long standing interest of this group. Owing to ability of gal-1 to bind and cross-link multiple  $\beta$ -galactoside containing cell surface ligands, it has been found associated with many glycoconjugates. Literature data demonstrate that gal-1 mediated functions and ligand interactions can vary with the cell type studied, and need to be determined for the cell type of interest. Regarding human trophoblast so far, our own and other published data point to several trophoblast glycoproteins as gal-1 ligands, which include onfFN, LN,  $\beta_1$  integrin and MUC1/mucins.

### **LN and onfFN of the extracellular matrix**

As in other tissues, ECM of the fetomaternal interface is thought to participate in trophoblast adhesion to maternal uterine tissues and subsequent trophoblast invasion, a process that leads to remodelling of the decidua. The ECM is composed of supramolecular glycoproteins. The major ECM components include proteoglycans, collagenous and elastic fibers, glycoproteins such as LN and onfFN and matricellular proteins<sup>46</sup>. Laminin and onfFN, typical ECM glycoproteins, have been the first proposed endogenous gal-1 ligands in human placenta<sup>16,47,48</sup>. Within the oligosaccharides of both LN and onfFN there are gal-1 binding structures - bi-, tri- and tetraantennary complex type N-glycans with high content of poly-N-acetylglucosamine<sup>16</sup>. Gal-1 binding to these two ECM glycoproteins was shown in several studies using affinity chromatography<sup>16,47</sup>. Moreover, colocalization of gal-1, LN and onfFN within ECM in human placental tissue, BeWo choriocarcinoma cells and isolated trophoblast in cell culture suggests lectin involvement in ECM organization and/or control of ECM-integrin interaction<sup>30</sup>.

### **$\beta_1$ integrin**

Several lines of evidence have shown that cell adhesion molecules such as integrins, through interactions with corresponding ECM molecules, could generate signals for EVT migration and invasion. Differentiation of first trimester trophoblast cells into an invasive EVT phenotype is accompanied by a switch in their integrin repertoire<sup>3</sup>. Along the invasive differentiation pathway, integrin  $\alpha_6\beta_4$  is lost, while expression of  $\alpha_5\beta_1$  is up-regulated. Additionally, integrin  $\alpha_1\beta_1$  appears at the distal cell columns and cytotrophoblast invading decidua<sup>49,50</sup>.

Integrins are decorated with N- and O-glycans, important for both integrin structure and function. Numerous investigations have reported presence of different  $\beta_1$  glycoforms, which interestingly had also been associated with a physiological change in cytotrophoblast invasiveness through gestation<sup>4,51,52</sup>. High levels of polyglucosamine

carbohydrate structures have been detected in cytotrophoblast  $\beta_1$  heterodimers, including  $\alpha_5\beta_1$  fibronectin receptor and  $\alpha_1\beta_1$  laminin/collagen receptor<sup>4</sup>. The type and degree of  $\beta_1$  glycosylation seems to be receptor specific, and, in the case of fibronectin receptor, coincided with reduction of cytotrophoblast invasiveness with advancement of pregnancy<sup>4</sup>. In  $\alpha_5\beta_1$  purified from human placenta, analysis of N-glycans revealed 35 different oligosaccharide structures, which were more than 80% sialylated primarily with  $\alpha_2,3$  sialic acid at the non-reducing galactose residues<sup>53</sup>. As glycoproteins with high poly lactosamine content, integrins are potential ligands of  $\beta$ -galactoside binding lectins - galectins. Several experiments in different cell types reported interaction of gal-1 with  $\alpha_7\beta_1$ ,  $\alpha_5\beta_1$  and  $\beta_1$  integrins<sup>14,20,54</sup>. Our recent study demonstrated interaction of endogenous gal-1 and  $\beta_1$  integrins in trophoblast, predominantly in intracellular compartments and at the plasma membrane of extravillous HTR-8/SVneo cells, but not with  $\alpha_1$  and  $\alpha_5$  subunits<sup>55</sup>. Furthermore, the gal-1/ $\beta_1$  integrin complex has been shown sensitive to enzyme and chemical treatments, indicating carbohydrate dependent interaction. Despite a complex interaction of gal-1 and  $\beta_1$  integrin, these molecules are not coexported in trophoblast cells *in vitro*<sup>55</sup>.

### **MUC1/mucin(s)**

Mucins are defined as abundantly glycosylated proteins that can confer normal physiological protection and lubrication to epithelial surfaces. Based on their cellular localization mucins are grouped into two different categories, secreted and membrane-bound. Mucins are also expressed by trophoblast. To date, only membrane-bound mucins have been investigated. In human term placenta MUC1 and MUC15 proteins, and *MUC3*, *MUC13*, *MUC17* and *MUC20* mRNA have been detected<sup>56</sup>. Presence and localization of MUC1 were investigated using different antibodies specific for various epitopes on the molecule. The antibody used detected either MUC1 epitope within long extracellular mucin domain containing variable tandem repeats (VNTR) or MUC1 associated glycans. Although MUC1 has been observed in placenta, isolated trophoblast and choriocarcinoma cell lines, dissonant findings regarding distribution and staining intensity were obtained<sup>57-59</sup>. During gestation, increased MUC1 expression predominantly by the STB and less in EVT was shown using antibodies specific for under- and hypoglycosylated MUC1<sup>58</sup>. Other specific glycotopes carried by MUC1, CA 15-3 and CA19-9, were also detected in EVT<sup>60</sup>. Demonstrated CA 15-3 expression in the first and second trimester invasive trophoblast, is in keeping with the study of Shyu et al., regarding staining intensity and the relative number of stained trophoblast cells<sup>58</sup>. In contrast, using polyclonal anti-bovine submaxillar mucin antibodies (anti-BSM) our recent study demonstrated moderate to strong MUC1/mucin(s) staining of first trimester placental villi<sup>61</sup>. Using various antibodies that recognize different MUC1 epitopes, expression of this glycoprotein was detected in freshly isolated trophoblast cells, extravillous HTR-8/SVneo cells, BeWo, JAR and JEG-3 choriocarcinoma cells<sup>57,59,61</sup>. Immunocytochemical studies using either antibodies specific for cytoplasmic MUC1 domain or for MUC1 glycotope revealed strong membrane MUC1 and cytoplasmic staining. A recent study in addition detected MUC1

extracellular domain within trophoblast nuclei using different antibodies specific for VNTR only<sup>59</sup>. Obviously, the staining pattern depends on antibody used, and the influence of glycosylation on epitope recognition by MUC1 extracellular domain specific antibodies and the variability of MUC1 glycosylation in different cells must be considered. Of the membrane mucin family, MUC 15 was also studied in human trophoblast<sup>56</sup>. This mucin is predominantly found at the apical STB membrane, and is absent from EVT. Studies of placental mucin glycosylation pattern are scarce in literature. Histochemical studies and lectin-blotting however suggest probable presence of short mucin-type O-glycans, such as Thomsen-Friedenreich antigen (Gal $\beta$ 1,3GalNAc, TF antigen) and Tn antigen (GalNAc)<sup>57,62</sup>. Some of these glycotopes terminate with sialic acid, mainly linked by the  $\alpha$ 2,3 bond and less by  $\alpha$ 2,6 bond<sup>62</sup>.

In recent years, functional properties of MUC1/mucins present in trophoblast have been increasingly investigated. Overexpression of MUC1 decreased adhesion of extravillous HTR-8/SVneo cells to different ECM components<sup>63</sup>. Furthermore, we recently showed enhanced aggregation of HTR-8/SVneo cells when BSM, similar to MUC1 with respect to the presence of glycans such as TF and sialylTn antigens, was added to cells in culture<sup>64</sup>. The same study showed reduced migration of extravillous HTR-8/SVneo cells, in the presence of BSM, which could be prevented by the specific antibody<sup>64</sup>. Active roles in trophoblast invasion have been suggested for both MUC1 and MUC15, since their overexpression suppressed invasion of choriocarcinoma cells<sup>56,58</sup>. Consistent with this finding, invasion of HTR-8/SVneo cells was also negatively affected by the MUC1 overexpression, through inhibition of  $\beta_1$  integrin activity and downstream signaling<sup>63</sup>.

Abundant mucin glycosylation with multiple O-glycan chains can lead to interaction with galectins, among other binding partners. Recently, interaction of gal-1 and MUC1/ mucins was confirmed in trophoblast cell culture<sup>64</sup>. In functional test, when the cell migration was performed in the presence of both exogenously added molecules, gal-1 and mucin(s) interacted in such a way that the increased presence of gal-1 restored cell migration, originally decreased by added BSM<sup>64</sup>. Moreover, the interaction between MUC1/mucin and gal-1 was abrogated in the presence of lactose, pointing to the lectin-type interactions between these molecules.

### **Interaction of gal-1 with ligands in trophoblast - functional relevance**

In many cases functional relevance of gal-1 interaction with numerous glycoconjugates is not clear. Gal-1 association with the  $\beta_1$  integrin reported recently, however, might affect integrin ligand binding and trophoblast cell function (Figure 2).

It is not possible to specify at this time whether gal-1 interaction is limited to  $\beta_1$  monomer or whether gal-1/ $\beta_1$  complex serves to aid dimer formation. Invasive EVT cells are known to express gal-1,  $\beta_1$  integrins, onffn and LN, among other molecules involved in complex cross-talk. Since ECM proteins are physiological regulators of integrin outside-in signaling and are known gal-1 ligands, modification of  $\beta_1$  integrin availability by gal-1 for binding

with ECM may affect crosslinking between these molecules in trophoblast. This interaction thus might be important for trophoblast cell adhesion, migration and invasion. Considerably more is known regarding influence of gal-1 interaction with MUC1/mucin(s) on trophoblast function. Each of these proteins was shown to affect trophoblast invasion *in vitro*, MUC1 decreasing it, and gal-1 inducing an increase<sup>7,58</sup>. Under physiological conditions, when both molecules are expressed by EVT, interaction may balance pro- and anti-invasive-actions of the two molecules (Figure 2). High decidual gal-1 expression, could shift the balance in favor of migration and invasion, explaining trophoblast invasion *in vivo*.

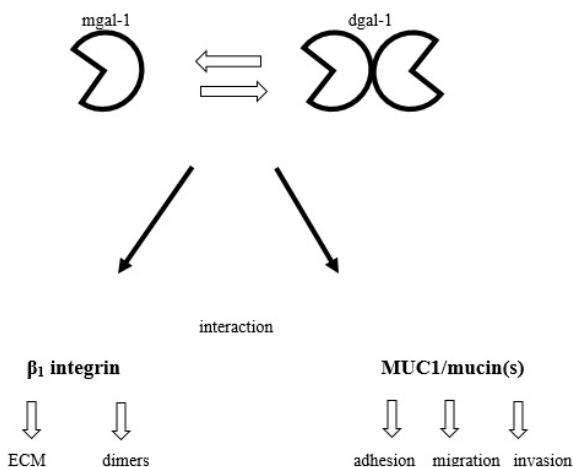


**Figure 2.** Schematic representation of effects resulting from interactions of monomeric gal-1 (mgal-1) or dimeric gal-1 (dgal-1) with MUC1/mucin(s) and  $\beta_1$  integrin in human trophoblast. Gal-1 binding to  $\beta_1$  integrin could affect ECM binding and signaling via integrin and formation and stabilization of integrin dimers, while interaction with mucin(s) may influence trophoblast function.

## Conclusion

Despite the significant breakthroughs in understanding gal-1 function in trophoblast in the past decade, investigation of gal-1 binding partners is still in its early stages. A combination of several approaches will be required to identify gal-1 interacting partners, but understanding physiological significance of these interactions is a major challenge. Future studies will likely involve both biochemical and genetic approaches in the precise mapping of gal-1 domains on one hand, and glycan structures on the other, involved in these interactions. Moreover, there is a strong possibility that altered glycosylation could influence placental proteins in (patho) physiological conditions during gestation, and their functions through change in affinity or ability for gal-1-binding. However, to what degree

abberant glycosylation contributes to improper interaction and poor pregnancy outcome in clinically relevant conditions is an issue for further investigation.

## Acknowledgements

This work was supported by the Ministry of Education, Science and Technological Development of the Republic of Serbia, grant 173004.

## References

1. Morrish DW, Dakour J, Li H. Functional regulation of human trophoblast differentiation. *J Reprod Immunol* 1998;39:179-95.
2. Aplin JD, Haigh T, Jones CJP, Church HJ, Vićovac Lj. Development of cytotrophoblast columns from explanted first-trimester human placental villi: role of fibronectin and integrin  $\alpha 5\beta 1$ . *Biol Reprod* 1999;60:828-38.
3. Damsky CH, et al. Integrin switching regulates normal trophoblast invasion. *Development* 1994;120:3657-66.
4. Moss L, Prakobphol A, Wiedmann T-W, Fisher SJ, Damsky CH. Glycosylation of human trophoblast integrins is stage and cell-type specific. *Glycobiology* 1994;4:567-75.
5. Genbacev OD, et al. L-selectin-mediated adhesion at the maternal-fetal interface. *Science* 2003;299:405-8.
6. Zhou Y, Genbacev O, Fisher SJ. The human placenta remodels the uterus by using a combination of molecules that govern vasculogenesis or leukocyte extravasation. *Ann N Y Acad Sci* 2003;95:73-83.
7. Kolundžić N, Bojić-Trbojević Ž, Kovačević T, Stefanoska I, Kadoya T, Vićovac Lj. Galectin-1 is part of human trophoblast invasion machinery - A functional study *in vitro*. *PLoS One* 2011; 6:e28514.
8. Barondes SH, Cooper DN, Gitt MA, Leffler H. Galectins. Structure and function of a large family of animal lectins. *J Biol Chem* 1994;269:20807-10.
9. Cummings RD, Liu FT. Galectins. In: Varki AC, Cummings RD, Esko JD, Freeze HH, Stanley P, Bertozzi CR, Hart GW, Etzler ME (eds) *Essentials of Glycobiology*. Cold Spring Harbor Laboratory Press, New York, 2009, pp 475-88.
10. Guardia CM, Caramelo JJ, Trujillo M, Méndez-Huergo SP, Radi R, Estrin DA, Rabinovich GA. Structural basis of redox-dependent modulation of galectin-1 dynamics and function. *Glycobiology* 2014;24:428-41.
11. Hughes RC. Secretion of the galectin family of mammalian carbohydrate binding proteins. *Biochim Biophys Acta* 1999;1473:172-85.
12. Camby I, Le Mercier M, Lefranc F, Kiss R. Galectin-1: a small protein with major function. *Glycobiol* 2006;16:137R-57R.
13. Moiseeva EP, Soring EL, Baron JH, de Bono DP. Galectin-1 modulates attachment, spreading and migration of cultured vascular smooth muscle cells via interaction with cellular receptors and components of extracellular matrix. *J Vasc Res* 1999;36:47-58.
14. Moiseeva EP, Williams B, Goodall AH, Samani NJ. Galectin-1 interacts with beta-1 subunit of integrin. *Biochem Biophys Res Commun* 2003;310:1010-6

15. Moiseeva EP, Williams B, Samani NJ. Galectin1 inhibits incorporation of vitronectin and chondroitin sulphate B into the extracellular matrix of human vascular smooth muscle cells. *Biochim Biophys Acta* 2003;1619:125-32.
16. Ozeki Y, Matsui T, Yamamoto Y, Funahashi M, Hamako J, Titani K. Tissue fibronectin is an endogenous ligand for galectin-1. *Glycobiol* 1995;5:255-61.
17. van den Brule F, Califice S, Garnier F, Fernandez PI, Berchuck A, Castronovo V. Galectin-1 accumulation in the ovary carcinoma peritumoral stroma is induced by ovary carcinoma cells and affects both cancer cell proliferation and adhesion to laminin-1 and fibronectin. *Lab Invest* 2003;83:377-86.
18. Martinez VG, et al. Galectin-1, a cell adhesion modulator, induces apoptosis of rat Leydig cells in vitro. *Glycobiology* 2004;14:127-37.
19. Gu M, Wang W, Song WK, Cooper DN, Kaufman SJ. Selective modulation of the interaction of  $\alpha_7\beta_1$  integrin with fibronectin and laminin by L-14 lectin during skeletal muscle differentiation. *J Cell Sci* 1994;107:175-81.
20. Fisher C, et al. Galectin-1 interacts with the  $\alpha 5\beta 1$  fibronectin receptor to restrict carcinoma cell growth via induction of p21 and p27. *J Biol Chem* 2005;280:37266-77.
21. Pace KE, Hahn HP, Pang M, Nguyen JT, Baum LG. CD7 delivers a pro-apoptotic signal during galectin-1-induced T cell death. *J Immunol* 2000;165:2331-4.
22. Pace KE, Lee, C, Stewart PL, Baum LG. Restricted receptor aggregation into membrane microdomains occurs on human T cells during apoptosis induced by galectin-1. *J Immunol* 1999;163:2801-11.
23. Wasano K, Hirakawa Y. Recombinant galectin-1 recognizes mucin and epithelial cell surface glycolcalyces of gastrointestinal tract. *J Histochem Cytochem* 1997;45:275-83.
24. Seelenmayer C, Wegenhangel S, Lechner J, Nickel W. The cancer antigen CA125 represents a novel counter receptor for galectin-1. *J Cell Sci* 2003;116:1305-18.
25. Joubert R, Caron M, Avellano-Adalid V, Mornet D, Bladier D. Human brain lectin: a soluble lectin that binds actin. *J Neurochem* 1992;58:200-3.
26. Prio IA, Muncke C, Parton RG, Hancock JF. Direct visualization of Ras proteins in spatially distinct cell surface microdomains. *J Cell Biol* 2003;160:165-70.
27. Rotblat B, Niv H, André S, Kaltner H, Gabius HJ, Kloog Y. Galectin-1 (L11A) predicted from a computed galectin-1 farnesyl-binding pocket selectively inhibits Ras-GTP. *Cancer Res* 2004;64:3112-8.
28. Hirabayashi J, Kasai K. Human placenta beta-galactoside-binding lectin. Purification and some properties. *Biochem Biophys Res Commun* 1984;122:938-44.
29. Bevan BH, Kilpatrick DC, Liston WA, Hirabayashi J, Kasai K. Immunohistochemical localization of a b-D-galactoside-binding lectin at the human maternofetal interface. *Histochem J* 1994;26:582-6.
30. Vićovac Lj, Janković M, Čuperlović M. Galectin-1 and -3 in cells of the first trimester placental bed. *Hum Reprod* 1998;13:730-5.
31. Maqui E, van den Brule FA, Castronovo V, Foidart JM. Changes in the distribution pattern of galectin-1 and galectin-3 in human placenta correlates with the differentiation pathways of trophoblasts. *Placenta* 1997;18:433-9.
32. von Wolff M, Wang X, Gabius HJ, Strowitzki T. Galectin fingerprinting in human endometrium and decidua during the menstrual cycle and in early gestation. *Mol Hum Reprod* 2005;11:189-94.

33. Van den Brule FA, Price J, Sobel ME, Lambotte R, Castronovo V. (1994) Inverse expression of two laminin binding proteins, 67LR and galectin-3, correlates the invasive phenotype of trophoblastic tissue. *Biochem Biophys Res Commun* 1994;201:388-93.
34. Kolundžić N, Bojić-Trbojević Ž, Radojčić Lj, Petronijević M, Vićovac Lj. Galectin-8 is expressed by villous and extravillous trophoblast of the human placenta. *Placenta* 2011;32:909-11.
35. Bojić-Trbojević Ž, Janković M, Vićovac L. Influence of IGF-I on adhesion, proliferation and galectin-1 production in JAR and JEG-3 choriocarcinoma cell lines. *Arch Oncol* 2005;13:7-11.
36. Bojić-Trbojević Ž, Božić M, Vićovac Lj. Steroid hormones modulate galectin-1 in the trophoblast HTR-8/SVneo cell line. *Arch Biol Sci* 2008;60:11-23.
37. Blois SM, Conrad ML, Freitag N, Barrientos G. Galectins in angiogenesis: consequences for gestation. *J Reprod Immunol* 2015;108:33-41.
38. Barrientos G, Freitag N, Tirado-Gonzales I, Unverdorbens L, Jeschke U, Thijssen VLJL, Blois SM. Involvement of galectin-1 in reproduction: past, present and future. *Hum Reprod Update* 2014;20:175-93.
39. Tirado-Gonzalez I, et al. Galectin-1 influences trophoblast immune evasion and emerges as a predictive factor for the outcome of pregnancy. *Mol Hum Reprod* 2013;19:43-53.
40. Božić M, Petronijević M, Milenković S, Atacković J, Lazić J, Vićovac Lj. Galectin-1 and galectin-3 in the trophoblast of the gestational trophoblastic disease. *Placenta* 2004;25:797-802.
41. Jeschke U, et al. Expression of galectin-1, -3 (gal-1, gal-3) and the Thomsen-Friedenreich (TF) antigen in normal, IUGR, preeclamptic and HELLP placentas. *Placenta* 2007;28:1165-73.
42. Liu AX, et al. Proteomic analysis of the alteration of protein expression in the placental villous tissue of early pregnancy loss. *Biol Reprod* 2006;75:414-20.
43. Spiro RG. Protein glycosylation: nature, distribution, enzymatic formation, and disease implications of glycopeptide bonds. *Glycobiol* 2002;12:43R-56R.
44. Chen Q, et al. Evidence for differential glycosylation of human trophoblast cell types. *Mol Cell Proteom* 2016;15:1857-66.
45. Robajac D, Masnikosa R, Vanhooren V, Libert C, Miković Ž, Nedić O. The N-glycan profile of placental membrane glycoproteins alters during gestation and aging. *Mech Ageing Devel* 2014;138:1-9.
46. da Anuniação A, Mess AM, Orechio D, Aguiar BA, Favaron PO, Miglino MA. Extracellular matrix in epitheliochorial, endotheliochorial and haemochorial placentation and its potential application for regenerative medicine. *Reprod Domest Anim* 2017;52:3-15.
47. Sato S, Hughes R. Binding specificity of a baby hamster kidney lectin for H type I and II chains, poly-lactosamine glycans and appropriately glycosylated forms of laminin and fibronectin. *J Biol Chem* 1992;267:6983-90.
48. Zhou Q, Cummings RD. L-14 lectin recognition of laminin and its promotion of in vitro cell adhesion. *Arch Biochem Biophys* 1993;300:6-17.
49. Aplin, JD. Expression of integrin  $\alpha 6\beta 4$  in human and its loss from extravillous cells. *Placenta* 1993;14:203-15.
50. Damsky CH, Fitzgerald ML, Fisher SJ. Distribution patterns of extracellular matrix components and adhesion receptors are intricately modulated during first trimester cytotrophoblast differentiation along the invasive pathway, *in vivo*. *J Clin Invest* 1992;89:210-22.
51. Seales EC, Jurado GA, Singhal A, Bellis, SL. Ras oncogene directs expression of a differentially sialylated, functionally altered beta1 integrin. *Oncogene* 2003;22:7137-45.
52. Semel AC, Seales EC, Singhal A, Eklund EA, Cooley KJ, Bellis SL. Hyposialylation of integrin stimulates the activity of myeloid fibronectin receptors. *J Biol Chem* 2002;277:32830-6.

53. Nakagawa H, Zheng M, Hakomori S, Tsukamoto Y, Kawamura Y, Takahashi N. Detailed oligosaccharide structures of human integrin  $\alpha 5\beta 1$  analyzed by a three-dimensional mapping techniques. *Eur J Biochem* 1996;237:76-85.
54. Gu M, Wang W, Song WK, Cooper DN, Kaufman SJ. Selective modulation of the interaction of  $\alpha 7\beta 1$  integrin with fibronectin and laminin by L-14 lectin during skeletal muscle differentiation. *J Cell Sci* 1994;107:175-81.
55. Bojić-Trbojević Ž, Jovanović Krivokuća M, Stefanoska I, Kolundžić N, Vilotić A, Kadoya T, Vićovac Lj. Integrin  $\beta 1$  is bound to galectin-1 in human trophoblast. *J Biochem* 2017; doi:10.1093/jb/mvx061/4157559.
56. Shyu MK, et al. Mucin 15 is expressed in human placenta and suppresses invasion of trophoblast-like cells in vitro. *Hum Reprod* 2007;22:2723-32.
57. Jeschke U, Richter DU, Hammer A, Briese V, Friese K, Karsten U. Expression of the Thomsen-Friedenreich antigen and its putative carrier protein mucin1 in the human placenta and in trophoblast cells in vitro. *Histochem Cell Biol* 2002;117:219-26.
58. Shyu MK, et al. MUC1 expression is increased during human placental development and suppresses trophoblast-like cell invasion in vitro. *Biol Reprod* 2008;79:233-9.
59. Kumar P, Lindberg L, Thirkill TL, Jennifer WJ, Martsching L, Douglas GC. The MUC1 extracellular domain subunit is found in nuclear speckled and associated with spliceosomes. *PLoS ONE* 2012;7:e42712.
60. Bojić-Trbojević Ž, Krivokuća MJ, Vrzić-Petronijević S, Petronijević M, Vićovac L. Expression of tumor associated antigens CA 15-3 and CA 19-9 in trophoblast of the normal human placenta. *Eur J Gynecol Oncol* 2012;33:281-4.
61. Bojić-Trbojević Ž, Jovanović Krivokuća M, Kolundžić N, Petronijević M, Vrzić-Petronijević S, Golubović S, Vićovac Lj. Galectin-1 binds mucin in human trophoblast. *Histochem Cell Biol* 2014;142:541-53.
62. Paszkiewicz-Gadek A, Porowska H, Sredzinska K. Expression of MUC1 mucin in full-term pregnancy human placenta. *Adv Med Sci* 2008;53:54-8.
63. Shyu MK, et al. MUC1 expression is elevated in severe preeclamptic placentas and suppresses trophoblast cell invasion via  $\beta 1$ -integrin signaling. *J Clin Endocrinol Metab* 2011;96:3759-67.
64. Bojić-Trbojević Ž, Jovanović Krivokuća M, Kolundžić N, Kadoya T, Radojčić Lj, Vićovac Lj. Interaction of extravillous trophoblast galectin-1 and mucin(s)-is there a functional relevance? *Cell Adh Migr* 2015;10:179-88.

---

## **Semi - rational design of cellobiose dehydrogenase from *Phanerochaete chrysosporium* for increased oxidative stability and high-throughput screening of library mutants**

---

**Ana Marija Balaz<sup>1\*</sup>, Raluca Ostafe<sup>2</sup>, Rainer Fischer<sup>2</sup>, Radivoje Prodanović<sup>3</sup>**

<sup>1</sup>*Center of Chemistry, Institute of Chemistry, Technology and Metallurgy, University of Belgrade, Belgrade, Serbia*

<sup>2</sup>*Fraunhofer Institute for Molecular Biology and Applied Ecology (IME), Aachen, Germany*

<sup>3</sup>*Faculty of Chemistry, University of Belgrade*

\**e-mails: ambalaz@gmail.com; anam@chem.bg.ac.rs*

Cellobiose dehydrogenase (CDH, EC 1.1.99.18) from *Phanerochaete chrysosporium* belongs to a group of oxidoreductases and has the ability to degrade different components of woody plants<sup>1</sup>. CDH is secreted by wood degrading, phytopathogenic and saprotrophic fungi and this widespread appearance implies its important function and makes it an important enzyme for applications in industrial and biotechnological processes, as well as biosensors and biofuel cells<sup>1</sup>. CDH is also used in industry for bleaching cotton and in food industry for lactose detection<sup>2</sup>. CDH is a monomeric enzyme consisting of two domains, a flavin domain containing FAD as a cofactor and a smaller heme b containing cytochrome domain, connected via a flexible linker<sup>3</sup>. The physiological role of CDH is reflected in the degradation of cellulose and lignin in cooperation with other cellulolytic enzymes, because CDH catalyzes the oxidation of cellobiose (Glc -  $\beta$  - 1,4 Glc) and other  $\beta$  - 1,4 - linked disaccharides and oligosaccharides to the corresponding lactones<sup>1,2</sup>. Enzymes used in biosensors and for bleaching cotton should have high stability, especially toward reactive oxygen species. In order to improve the oxidative stability of CDH, we have mutated CDH and tested its stability in the presence of hydrogen peroxide. After successful cloning of the CDH gene in the pYES2 vector, saturation mutagenesis was used to create library mutants where three methionine residues were mutated. The residual activity of mutants was measured after the enzyme incubation in 0.3 M hydrogen peroxide for 0, 2 and 6 h. After analysis of a large number of mutants, it was observed that three mutants are showing higher oxidative stability compared to the wild-type enzyme. Residual activities of these mutants after 6 h of incubation in the hydrogen peroxide were over 50%, whereas the wild-type has 30%. Selected mutants were expressed in *S. cerevisiae* and purified on a DEAE column. Purity and activity of the enzymes were detected on the electrophoresis gel, oxidative stability of purified mutants was measured once again and characterization of these mutants was done.

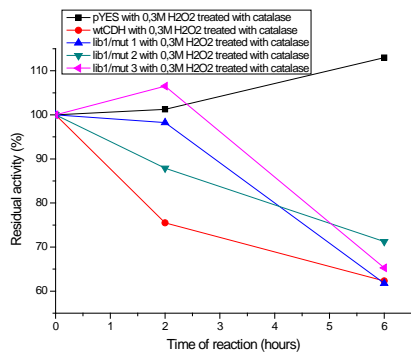


**Figure 1.** Residual activity of library 1 mutants at times of incubation in 0.3 M H<sub>2</sub>O<sub>2</sub>.

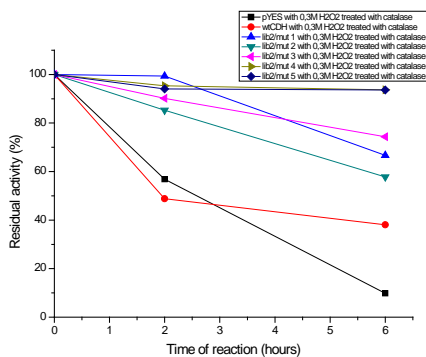


**Figure 2.** Residual activity of library 2 mutants at times of incubation in 0.3 M H<sub>2</sub>O<sub>2</sub>.

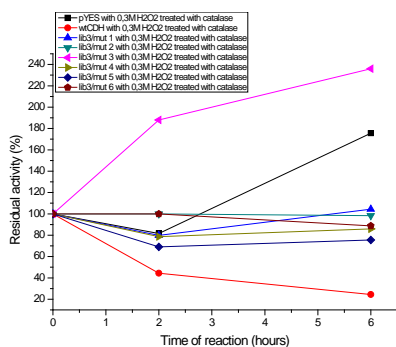


**Figure 3.** Residual activity of library 3 mutants at times of incubation in 0.3M H<sub>2</sub>O<sub>2</sub>.

Mutants showing increased oxidative stability were sequenced and we have decided to combine these mutations with each other in order to make combined mutants that will be tested for oxidative stability. Screening library mutants for improved features in microtitar plates is a long time process, in order to shorten the time necessary for screening libraries with 106 mutants we are developing fluorescent assay for flow cytometry.

## **Acknowledgements**

This study was supported by funds from the Ministry of Education and Science, Republic of Serbia by the project number NO46010 and DAAD founding organization. One part of this PhD thesis was done at Fraunhofer institute, RWTH University, Aachen, Germany in collaboration with Prof. Rainer Fischer and Raluca Ostafe.

## **References**

1. Eriksson KE, Blanchette RA, Ander P. Microbial and Enzymatic Degradation of Wood and Wood Components. Springer Series in Wood Science, Springer-Verlag, Berlin, 1990.
2. Henriksson G, Ander P, Pettersson B, Pettersson G. Cellobiose dehydrogenase (cellobiose oxidase) from *Phanerochaete chrysosporium* as a wood-degrading enzyme. Studies on cellulose, xylan and synthetic lignin. *Appl Microbiol Biotechnol* 1995;42:790-6.
3. Hallberg MB, Bergfors T, Bäckbro K, Pettersson G, Henriksson G, Divne C. A new scaffold for binding haem in the cytochrome domain of the extracellular flavocytochrome cellobiose dehydrogenase. *Structure* 2000;8:79-88.



---

## Novel lignans from *Anthriscus sylvestris*: 3'-demethoxy podophyllotoxin and 3'-demethoxypodophyllotoxone

---

Sanja Berežni, Dejan Orčić\*, Milica Basarić, Dragan Miladinov, Filip Šibul, Neda Mimica-Dukić

*Department of Chemistry, Biochemistry and Environmental Protection, Faculty of Sciences, University of Novi Sad, Novi Sad, Serbia*

\*e-mail: [dejan.orcic@dh.uns.ac.rs](mailto:dejan.orcic@dh.uns.ac.rs)

Lignans exhibit a wide range of biological activities<sup>1</sup>, thus representing promising natural drugs. One of the best known aryltetralin lignans, podophyllotoxin, has been used for two millenia for treatment of tumors, and some of its semi-synthetic derivatives - etoposide, etopophos and teniposide - are nowadays used as chemotherapeutic medications<sup>2</sup>. Mechanism of cytotoxic action depends on structure - some features favor tubuling growth inhibition, while others result in binding to DNA-topoisomerase II complex and increased cleavage or reduced religation of DNA chains<sup>3</sup>.

*Anthriscus sylvestris* (L.) Hoffm. (wild chervil) is a wild-growing plant from Apiaceae family. It is a rich source of diverse lignans, mostly dibenzobutyrolactones and aryltetralins<sup>4,5</sup>. Some of them are known for extremely potent cytotoxic activity<sup>6,7</sup> (IC<sub>50</sub> in MTT assay ranging from sub-ng/mL to µg/mL) and antiinflammatory activity, but majority have never been evaluated. In this paper, the isolation of two novel aryltetralin lignans from *A. sylvestris* is described, alongside their structural elucidation by UV, ESI-MS and NMR.

Air-dried roots of *A. sylvestris* from Fruška gora (492 g) were extracted with MeOH by percolation (5×1 L). Lignans were enriched by water-CHCl<sub>3</sub> partitioning, followed by acetonitrile-hexane partitioning of CHCl<sub>3</sub> layer, yielding 13.5 g of acetonitrile fraction rich in lignans. Using flash chromatography (silicagel, hexane-acetone gradient), it was fractionated into F1-F9, with fractions F6-F8 containing lignans. F7 and F8 were fractionated by flash chromatography (silicagel, hexane-EtOAc gradient) into F7.1-F7.10 and F8.1-F8.7. Fractions F7.5 (126 mg) and F8.4 (310 mg), confirmed by LC-MS to contain novel compounds, were fractionated by semi-preparative HPLC (Zorbax XDB-C18, water-MeOH gradient) into F7.5.1-F7.5.18 and F8.4.1-F8.4.11.

Fraction F7.5.6 (4.4 mg) was further purified by semi-prep HPLC, yielding 2.2 mg of compound labelled P382C (purity 91 %). UV spectrum exhibits maxima at 326 nm, 282 nm, 238 nm and 200 nm, indicating extended delocalization - unsaturated dibenzobutyrolactone<sup>6</sup>, or 7-oxo-aryltetraline. In ESI-MS spectrum<sup>2</sup>, two minor peaks corresponding to consecutive loss of 2H<sub>2</sub>O from [M+H]<sup>+</sup> indicate lactone ring<sup>5</sup>. The absence of abundant water loss indicates absence of alcoholic OH<sup>5</sup>. Crotonolactone loss

from  $[M+H]^+$  may indicate unsaturation at C7. Fragments with  $m/z$  245, 201, 143 and 115 are also found in podophyllotoxone MS<sup>2</sup> spectrum, and correspond to  $[M+H-ArH]^+$  ion (and consecutive losses of CO<sub>2</sub>, CO+CH<sub>2</sub>O and CO) of a lignan with methylenedioxy-substitution at condensed system<sup>5</sup>. From  $M_{mi}$  of ArH loss, it can be concluded that pendant ring is either dimethoxy or, less likely, hydroxy, methylenedioxy-substituted. <sup>1</sup>H NMR confirmed 7-oxo-aryltetralin structure with dimethoxylated pendant ring and *cis*-configuration of C7' and C8'. Thus, P382C is 3'-demethoxypodophyllotoxone (Figure 1) or, unlikely, its 8-epimer (*isopicro*-isomer).

Fractions F8.4.6 and F8.4.7 were further purified by semi-prep HPLC, yielding 47.1 mg of compound labelled P384A (purity 98 %). Accurate  $M_{mi}$  indicated molecular formula of C<sub>21</sub>H<sub>20</sub>O<sub>7</sub>. The absence of UV maxima above 300 nm indicates aryltetralin or saturated dibenzobutyrolactone. Abundant  $[M+H-ArH]^+$  ion at  $m/z$  247.06059 confirms aryltetralin structure with hydroxy, methylenedioxy-substitution at condensed ring system. Thus, the pendant ring has to be dimethoxylated, i.e. P384A is 3'-demethoxypodophyllotoxin or its diastereoisomer. <sup>1</sup>H NMR experiments (<sup>1</sup>H, <sup>13</sup>C, HSQC, HMBC, COSY, NOESY) confirmed stereochemistry of 3'-demethoxypodophyllotoxin (Figure 1).

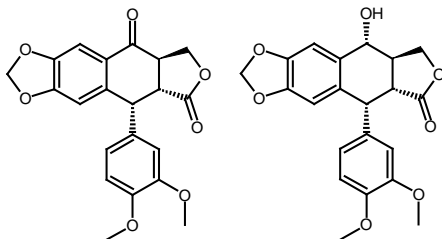


**Figure 1.** Structures of 3'-demethoxypodophyllotoxone and 3'-demethoxypodophyllotoxin.

## Acknowledgements

This study was supported by a research grant from the Ministry of Education and Science, Republic of Serbia (Grant No. 172058), and was partially done at Fakultät für Chemie & Pharmazie, Universität Regensburg, Germany.

## References

1. Cunha RW, Andrades Silva ML, Sola Veneziani RC, Ambrosio SR, Bastos JK. Lignans: Chemical and Biological Properties. In: Rao V (Ed.) *Phytochemicals - A Global Perspective of Their Role in Nutrition and Health*. Intech, Rijeka, Croatia, 2012, pp. 213-34
2. Gordaliza M, Garcia PA, Miguel del Corral JM, Castro MA, Gomez-Zurita MA. Podophyllotoxin: distribution, sources, applications and new cytotoxic derivatives. *Toxicol* 2004;44:441-59.
3. Lee K-H, Xiao Z. Podophyllotoxins and Analogs. In: Cragg GM, Kingston DGI, Newman DJ. (eds) *Anticancer Agents from Natural Products*. CRC Press, Boca Raton, 2005.

4. Olaru TO, Nitulescu MG, Ortan A, Dinu-Pirvu CE. Ethnomedicinal, phytochemical and pharmacological profile of *anthriscus sylvestris* as an alternative source for anticancer lignans. *Molecules* 2015;20:15003-22.
5. Hendrawati O, Woerdenbag HJ, Michiels PJA, Aantjes HG, Van Dam A, Kayser O. Identification of lignans and related compounds in *Anthriscus sylvestris* by LC-ESI-MS/MS and LC-SPE-NMR. *Phytochemistry* 2011;72:2172-9.
6. Ikeda R, Nagao T, Okabe H, Nakano Y, Matsunaga H, Katano M, Mori M. Antiproliferative constituents in Umbelliferae plants. III. Constituents in the root and the ground part of *Anthriscus sylvestris* Hoffm. *Chem Pharm Bull* 1998;46:871-4.
7. Ikeda R, Nagao T, Okabe H, Nakano Y, Matsunaga H, Katano M, Mori M. Antiproliferative constituents in Umbelliferae plants. IV. Constituents in the fruits of *Anthriscus sylvestris* Hoffm. *Chem Pharm Bull* 1998;46:875-8.



---

## Statistical clustering of IC<sub>50</sub> values as bioactive substances cytotoxicity indicators on HCT-116 and SW-480 cell lines of colon cancer

---

Stefan Z. Blagojević<sup>1\*</sup>, Boris Furtula<sup>2</sup>, Aleksandra G. Nikezić<sup>1</sup>, Milena G. Milutinović<sup>1</sup>, Marko N. Živanović<sup>1</sup>, Snežana D. Marković<sup>1</sup>

<sup>1</sup>*Department of Biology and Ecology, Faculty of Science, University of Kragujevac, Kragujevac, Serbia*

<sup>2</sup>*Department of Chemistry, Faculty of Science, University of Kragujevac*

\**e-mail: stefanblagojevickg@gmail.com*

Colon cancer is one of the most common tumors <sup>1</sup>. One of the most important aspects in strategy for cancer treatment and design of antitumor medicines is isolation and/or modification of bioactive substances originating from natural sources, as well as the synthesis of new chemical compounds that will act cytotoxic, proapoptotic and antimetastatic to tumor cells, and will not harm the healthy ones. Intensive research in this field, and the large number of cytotoxicity results obtained for various active substances, and their use in the prevention and treatment of colon cancer lead to the need to perform clustering and statistical processing of these data <sup>2,3</sup>.

The aim of this study is statistical clustering and data processing for IC<sub>50</sub> values as indicators of the cytotoxic effects of natural and chemically synthesized bioactive substances on colon cancer cells (HCT-116 and SW-480).

Statistical clustering and processing of IC<sub>50</sub> values were executed based on the results of the research performed within the Laboratory for Cell and Molecular Biology, Faculty of Science, University of Kragujevac for the period 2010-2017. In this research, 55 different treatments for HCT-116 and 35 for SW-480 cell line were examined.

General hypotheses for data processing are: (i) The cytotoxicity of bioactive substances differs in relation to their origin: isolated from natural sources (extracts of plants, fungi and lichens - natural extracts, NE) and chemically synthesized substances (CHS). (ii) The cytotoxicity of NE and CHS differs in relation to the type of cancer cells which are treated: HCT-116 and SW-480. (iii) The cytotoxicity NE and CHS in the treatment of HCT-116 and SW-480 cells differs in relation to the time of treatment: 24 and 72 h. (iv) The cytotoxicity of NE in the treatment of HCT-116 and SW-480 cells after 24 and 72 h differs in relation to the source of NE: plants, fungi, lichens.

Table 1 shows that there is no statistically significant difference in the cytotoxicity (IC<sub>50</sub> values) of bioactive substances of natural extracts and chemical substances in relation to the type of cancer cells which are treated: HCT-116 and SW-480. Table 1 shows that there is no difference in the cytotoxicity of bioactive substances in HCT-116 and SW-480 cells.

**Table 1.** Values for basic descriptive statistics, analysis of variance and correlations for NE and CHS IC<sub>50</sub> values related to the incubation period 24 and 72 h and to the type of cell line.

	Cell Line	<i>mean ± SE</i>		N	p	r
		24h	72h			
NE	HCT-116	140±20	120±20	45/47	0.280	0.38
	SW-480	100±20	130±20	24/29	0.327	0.68
	N	45/24	10/31			
	p	0.132	0.580			
CHS	HCT-116	200±50	100±20	8/8	0.101	0.74
	SW-480	120±30	60±15	6/6	0.108	0.99
	N	8/6	8/6			
	p	0.237	0.179			

Results are shown as mean ± SE for 24 and 72 hours, N - Number of data, p < 0.05, r > 0.85 - significant correlation

Table 2 shows that there is a statistically significant difference in the cytotoxicity of NE in the treatment of HCT-116 cells after 24 h in relation to the source of NE.

**Table 2.** Values for basic descriptive statistics, analysis of variance and correlations for NE IC<sub>50</sub> values in treatment of HCT-116 and SW-480 cells after 24 and 72 hours in relation to the source of NE: Plants, Fungi and Lichens.

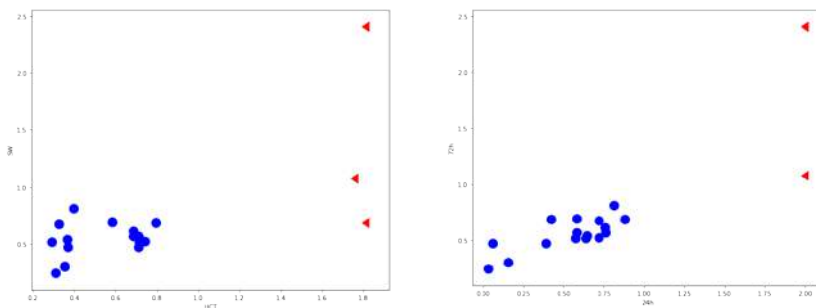
Comparison		<i>mean ± SE</i>			N	P
		Plants	Fungi	Lichens		
HCT-116	Plants/Fungi/Lichens 24 h	120±20	260±4	140±30	34/2/9	0.020
	Plants/Fungi/Lichens 72 h	120±20	150±50	100±30	36/2/9	0.789
SW-480	Plants/Fungi/Lichens 24 h	100±20	170±2	80±10	18/2/4	0.374
	Plants/Fungi/Lichens 72 h	110 ±30	250±80	140±30	20/3/6	0.209

Table 3 shows that there is a statistically significant difference in the cytotoxicity of bioactive substances from plants extract after 72 h incubation period in relation to HCT-116 and SW-480 cells and in SW-480 cells compared to treatment time: 24 and 72 h

**Table 3.** Values for basic descriptive statistics, analysis of variance and correlations for IC<sub>50</sub> values of bioactive substances from Plants extract related to the incubation period 24 and 72 hours and related to the type of cell line HCT-116 and SW-480.

Cell Line	<i>mean ± SE</i>		N	P	r
	24h	72h			
HCT-116	86±17	61±10	11/14	0.188	0.49
SW-480	64±14	27±6	14/14	0.021	0.80
N	11/14	14/14			
P	0.303	0.005			

By clustering data for  $IC_{50}$  values, two separate groups/clusters were obtained. Figure 1 shows that these clusters are categorized by treatments with good and poor cytotoxic effects. Clustering the  $IC_{50}$  value was done based on two criteria: (a) selected plant treatments after 72 h related to HCT-116 and SW-480 cells; (b) selected plant treatments on SW-480 cells related to the incubation period: 24 and 72 h.



**Figure 1.** Left: Clustering between the  $IC_{50}$  value of plant-based treatment for 72 h between different cell lines: HCT-116 and SW-480. Right: Clustering between the  $IC_{50}$  values of plant-based treatment on SW-480 colon cancer cells related to the incubation period: 24 and 72 h.

The presented results provide a good basis for further research of molecular mechanisms of antitumor activity of bioactive substances isolated from natural sources and for the synthesis of new chemical compounds that will act cytotoxic, as well as in the potential application of these treatments supplements in antitumor therapy.

## References

1. Zdravković D, Bilanović D, Randelović T, Zdravković M, Tošković B. Implication of late diagnosis for survival of patients with colorectal carcinoma. *Vojnosanit Pregl* 2009;66:135-140.
2. Čurčić M. Molekularni mehanizmi apoptoze u ćelijama karcinoma kolona nakon in vitro tretmana ekstraktima lekovitih biljaka. Doktorska disertacija. Prirodno-matematički fakultet, Univerzitet u Kragujevcu, 2014.
3. Chen HJ, Inbaraj BS, Chen BH. Determination of phenolic acids and flavonoids in *Taraxacum formosanum* kitam by liquid chromatography-tandem mass spectrometry coupled with a post-column derivatization technique. *Int J Mol Sci* 2012;13:260-85.



---

## Two newly synthesized ruthenium(II) polypyridyl complexes induce selective apoptosis of HeLa cancer cells via mitochondrial pathway

---

Petar Čanović\*, Ivanka Zelen, Marina Mitrović, Milan Zarić, Ivana Nikolić

*Department of Biochemistry, Faculty of Medical Sciences, University of Kragujevac, Kragujevac, Serbia*

\*e-mail: petar.c89@gmail.com

One of the most used anticancer drugs is cisplatin, but because of its serious side effects, clinical applications of cisplatin are limited. In the field of non-platinum complexes the most promising are ruthenium complexes, showing activity in tumors which had developed resistance to cisplatin. Ruthenium complexes with polypyridyl ligands have emerged as leading candidates for use as anticancer agents<sup>1,2</sup>.

Therefore, in our investigation we examined the cytotoxicity of two newly synthesized polypyridyl ruthenium(II) complexes, [Ru(Cl-Ph-tpy)(phen) Cl]Cl (1) and [Ru(Cl-Ph-tpy)(o-bqdi)Cl]Cl (2) (where Cl-Ph-tpy = 4'-(4-chlorophenyl)-2,2':6',2''-terpyridine, phen = 1,10-phenanthroline, o-bqdi = o-benzoquinonediimine) against human HeLa cancer cells and non-cancer, human fibroblast cells MRC-5. The cytotoxicity of cisplatin against these cells has also been examined due to its clinical use.

The cytotoxicity of two new polypyridyl ruthenium(II) complexes on HeLa and MRC-5 cells was determined by MTT assay. The type of cell death induced by these compounds was verified by Annexin V/7AAD assay. Intracellular localisation and expression of apoptotic proteins including Bax, Bcl-2, cytochrome c and caspase-3 were determined by flow cytometry.

Both ruthenium complexes showed high cytotoxic activity against cancers HeLa cells and had no or little influence on viability of human fibroblast MRC-5 cells. Ruthenium complex 2 significantly decreased viability after 72 h of treatment of HeLa cells, with IC<sub>50</sub> value of  $6,4 \pm 1,3$   $\mu$ M. Additionally, ruthenium complex 2 showed higher cytotoxic activity against HeLa cells compared to the cytotoxicity of cisplatin. Both complexes decreased viability of HeLa cells by inducing apoptosis. Our findings demonstrated that both ruthenium complexes induced the activation of proapoptotic Bax and decreased the expression of antiapoptotic Bcl-2 protein, released cytochrome c from mitochondria into cytosol and cleaved/activated caspase-3, which subsequently induced apoptosis of HeLa cells. Our findings suggest that ruthenium(II) complexes selectively induced apoptosis of HeLa cells via mitochondrial pathway *in vitro* and that these compounds might have a promising role as a potential future anticancer drugs.

## References

1. Wan D, Lai SH, Zeng CC, Zhang C, Tang B, Liu YJ. Ruthenium(II) polypyridyl complexes: Synthesis, characterization and anticancer activity studies on BEL-7402 cells. *J Inorg Biochem* 2017;173:1-11.
2. Čanović P, et al. Impact of aromaticity on anticancer activity of polypyridyl ruthenium(II) complexes: synthesis, structure, DNA/protein binding, lipophilicity and anticancer activity. *J Biol Inorg Chem* 2017 doi: 10.1007/s00775-017-1479-7.

---

## **Influence of fibrinogen modifications on its interaction with insulin-like growth factor-binding protein 1**

---

**Nikola Gligorijević\***

*Institute for the Application of Nuclear Energy - INEP, University of Belgrade, Belgrade, Serbia*

*\*e-mail: nikolag@inep.co.rs*

Fibrinogen or factor I is the main protein involved in coagulation and wound healing. Fibrinogen is a homodimer with  $(\alpha\beta\gamma)_2$  structure, having a molecular mass of 340 kDa. This molecule is phosphorylated and glycosylated. Both of these post-translational modifications are important for its proper function. In fibrinogen, only  $\beta$  and  $\gamma$  chains are N-glycosylated, each of them having one place for glycosylation. Upon thrombin action, fibrinogen is transformed into fibrin which forms insoluble clot. Not only that this clot provides a patch at the site of injury but also actively participates in its maintenance and fibrinolysis. Physiological roles of fibrinogen and fibrin would be impossible if they do not interact with many proteins including those from the insulin-like growth (IGF) system, such as IGF-binding protein 3 (IGFBP-3) <sup>1</sup>, and recently discovered interaction with IGFBP-1 <sup>2</sup>.

IGFBP-1 is the third most abundant IGF-binding protein in the circulation, whose concentration fluctuates during a day and is dependent on insulin. The rise of insulin lowers IGFBP-1 concentration; however in prolonged poorly regulated diabetes this regulation is lost. IGFBP-1 can have both IGF-stimulating and IGF-inhibitory effect, depending on its phosphorylation status. Highly phosphorylated IGFBP-1, which is dominant in the circulation, has higher affinity for IGF than less phosphorylated or non-phosphorylated IGFBP-1, which are more abundant in the amniotic fluid. Besides IGF related function, IGFBP-1 has also IGF-independent effects. The protein has a RGD (Arg-Gly-Asp) sequence that enables it to bind to  $\alpha_5\beta_1$  integrin. This interaction stimulates cell migration, so IGFBP-1 has beneficiary effect on wound healing. For that reason, its interaction with fibrinogen was further studied.

By analysing fibrinogen, isolated from human plasma, IGFBP-1 was detected as its binding partner. This interaction was confirmed by several immuno-affinity methods <sup>1</sup>, and it enables IGFBP-1 delivery at the site of injury. IGFBP-1 can stimulate wound healing either by locating IGF at the site of injury or through its interaction with  $\alpha_5\beta_1$ . It was shown that IGFBP-1 fragments can also have stimulatory effect on cellular migration. Plasmin, serine protease that is responsible for fibrin degradation, can also degrade IGFBP-1 and created fragments may have beneficiary effect on cells at the site of injury.

Fibrinogen is a protein that is susceptible to different pathological modifications such as oxidation and glycation, which may affect its affinity towards IGFBP-1. Both of these modifications occur in diabetes mellitus type 2 (DM 2). It was detected both *in vivo* and *in vitro* that modification of fibrinogen with glucose or methylglyoxal, reactive molecule whose concentration increases in DM 2 and is responsible for the formation of advanced glycation endproducts (AGEs), reduces the amount of fibrinogen/IGFBP-1 complexes. Reduction is even greater in the case of fibrin, which was shown to form complexes with IGFBP-1 as well. The reduced affinity of fibrinogen for IGFBP-1 due to glyco-oxidative modification accompanying diabetes can potentially shift the equilibrium to liberate more IGFBP-1 (and possibly IGF-I) capable of platelet activation during coagulation, so contributing to the hypercoagulation state together with many other factors <sup>3</sup>.

Tertiary structure of fibrinogen is altered in older persons compared to younger and middle aged, as was observed by spectrofluorimetry. N-glycosylation pattern of fibrinogen is also significantly changed due to aging. These changes may influence fibrinogen affinity towards IGFBP-1. Our results have shown that there are no changes in the amount of fibrinogen/IGFBP-1 complexes during healthy aging process <sup>4</sup>, although the concentration of IGFBP-1 is significantly higher in older persons (up to two times). This finding suggests that fibrinogen affinity constant for IGFBP-1 may be lower in older individuals.

Different relation was observed when fibrinogen isolated from patients with liver cirrhosis was studied. Again, the structure of fibrinogen is altered, and the concentration of IGFBP-1 is up to four times higher in patients with cirrhosis than in healthy individuals, but cirrhosis is accompanied by significantly higher quantities of fibrinogen/IGFBP-1 complexes. At the moment, it is still not clear whether the increase in the amount of complexes is only the consequence of the IGFBP-1 concentration gradient or the affinity of fibrinogen for IGFBP-1 due to cirrhosis is also affected.

## Acknowledgements

This work was supported by the Ministry of Education, Science and Technological Development of the Republic of Serbia, Grant No. 173042.

## References

1. Campbell PG, Durham SK, Hayes JD, Suwanichkul A, Powell DR. Insulin-like growth factor-binding protein-3 binds fibrinogen and fibrin. *J Biol Chem* 1999;274:30215-21.
2. Gligorijević N, Nedić O. Interaction between fibrinogen and insulin-like growth factor-binding protein-1 in human plasma under physiological conditions. *Biochemistry-Moscow* 2016;81:135-140.
3. Gligorijević N, Penezić A, Nedić O. Influence of glyco-oxidation on complexes between fibrin(ogen) and insulin-like growth factor-binding protein-1 in patients with diabetes mellitus type 2. *Free Radic Res* 2017;51:64-72.
4. Nedić O, Šunderić M, Gligorijević N, Malenković V, Miljuš G. Analysis of four circulating complexes of insulin-like growth factor binding proteins in human blood during aging. *Biochemistry-Moscow* 2017;82:1200-6.

---

## ***In vitro* comparison of antioxidative potential of differently substituted chalcones**

---

**Tamara Janković<sup>1\*</sup>, Branko Subošić<sup>1</sup>, Jelena Kotur-Stevuljević<sup>1</sup>, Branka Ivković<sup>2</sup>**

<sup>1</sup>*Department of Medical Biochemistry, Faculty of Pharmacy, University of Belgrade, Belgrade, Serbia*

<sup>2</sup>*Department of Pharmaceutical Chemistry, Faculty of Pharmacy, University of Belgrade*

\**e-mail: tasha9933@yahoo.com*

An imbalance between oxidants and antioxidants in favour of the oxidants, potentially leading to damage, is termed oxidative stress. Free radicals are formed as products of normal aerobic cellular metabolism. Antioxidants (AO), either enzymatic or non-enzymatic, are the ones that can reduce diverse effects which pro-oxidants can lead to, such as damage of DNA, proteins and lipids<sup>1</sup>. Chalcones (1.3-diaryl-2-propen-1-ones) are flavonoids that are widely biosynthesized in plants, and as flavonoids, chalcones also play an important role in defense against pathogens and insects. A longstanding scientific research has shown that chalcones also display other interesting biological properties such as antioxidant, cytotoxic, anticancer, antimicrobial, antihistaminic and anti-inflammatory activities<sup>2</sup>. Chemically, they consist of open-chain flavonoids in which the two aromatic rings are joined by a three carbon  $\alpha,\beta$ -unsaturated carbonyl system, that is responsible for bioactivity of compounds<sup>3</sup>.

The aim of this study was to compare the antioxidant potential within chalcones during *in vitro* induced oxidative stress. Oxidative stress was induced in serum samples of healthy individuals with 0.25 mmol/L tert-butyl hydro peroxide (TBH), and then we monitored the effects of various concentrations of chalcones on oxidative stress parameters: total antioxidant status (TAS), total oxidant status (TOS), total activity of sulfhydryl group (SHgr) and pro-oxidants antioxidants balance (PAB), then we calculated antioxidative index (AOI = TAS/TOS) and ratio between PAB and SH groups<sup>4</sup>. We used ANOVA repeated measures to compare oxidative-stress status of samples within chalcones, then with TBH and DMSO.

Our results showed significant difference in antioxidative potential between chalcones, and also compared to oxidant (TBH) and control (DMSO) samples. Chalcones named H11-H15 showed higher AOI values, in samples without oxidant, shown in Figure 1. Still in samples with TBH, chalcones named H11-H15 showed significantly higher AOI values, that can be observed in Figure 2.

Antioxidative index is a parameter that speaks in favor of better antioxidant ability of a compound. Elevated AOI and TAS values were detected in the samples to which chalcones

H11-H15 were added, which can be explained by the electronic effects of functional groups in the structure of these chalcones.

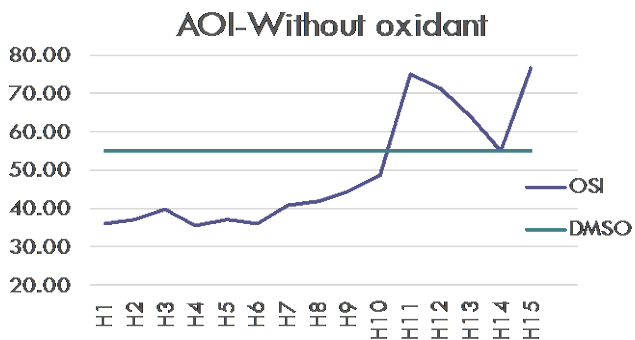


**Figure 1.** Antioxidative index in samples without oxidant

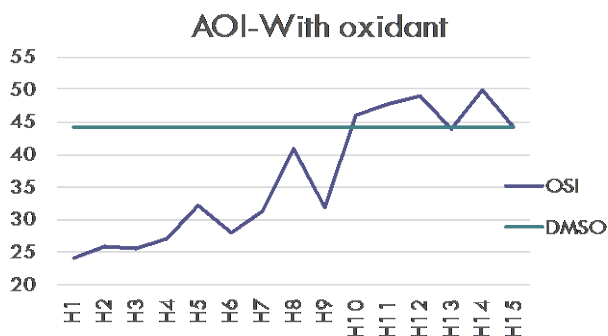


**Figure 2.** Antioxidative index in samples with oxidant

The increase in electron density in the molecule, achieved by groups with positive resonant and inductive effects (phenolic-H14 and H15, methyl-H10 and H11), enhances its antioxidant ability. The presence of the aromatic nitro group (H12 and H13) contributes to the reactivity of nitrochalcone in reactions with formed superoxide anions. The presence of  $\alpha,\beta$ -unsaturated ketones and hydroxy groups in these chalcone compounds is considered essential for their antioxidant properties<sup>5</sup>. Groups that reduce electronic density in the molecule (halogen elements) reduce its antioxidant potential as well as the results obtained in this study and confirmed. Elevated TOS values were found in samples of chalcones labeled H1-H6, which have a halogen element in the structure (chlorine and fluorine). Also, it has been observed that chalcones with the substituents in the *para* position show higher antioxidant potential than chalcones with substituents in the *meta* or the *ortho*

position. We suppose that steric disturbances of substituents in *meta* and *ortho* positions are the cause of poorer antioxidant activity.

## References

1. Lubrano V, Balzan S. Enzymatic antioxidant system in vascular inflammation and coronary artery disease. *World J Exp Med* 2015;5:218-24.
2. Batovska DI, Todorova TI. Trends in utilization of the pharmacological potential of chalcones. *Curr Clin Pharmacol* 2010;5:1-29.
3. Ni L, Meng CQ i Sikorsk JA. Recent advances in therapeutic chalcones. *Expert Opin Ther Patents* 2004;14:1669-91.
4. Kotur-Stevuljević J. Totalni oksidantno-antioksidantni status kod pacijenata sa koronarnom arterijskom bolešću. V Congress of Pharmacists of Serbia, Beograd 2010.
5. Gacche R. Antioxidant and anti-inflammatory related activities of selected synthetic chalcones: Structure-activity relationship studies using computational tools. *Chem Pharm Bull* 2008;56:897-901.



---

## Determination of protein glycosylation using lectin-based protein microarrays

---

Jaroslav Katrlík<sup>1\*</sup>, Martina Križáková<sup>1</sup>, Zuzana Pakanová<sup>1</sup>, Marek Nemčovič<sup>1</sup>, Peter Baráth<sup>1</sup>, Ján Mucha<sup>1</sup>, Goran Miljuš<sup>2</sup>, Miloš Šunderić<sup>2</sup>, Dragana Robajac<sup>2</sup>, Olga Nedić<sup>2</sup>

<sup>1</sup>*Institute of Chemistry, Slovak Academy of Sciences, Bratislava, Slovakia*

<sup>2</sup>*Institute for the Application of Nuclear Energy - INEP, University of Belgrade, Belgrade, Serbia*

\**e-mail: katrlik@yahoo.com*

Glycosylation of proteins is one of the most important co- and post-translational modifications affecting almost all biological functions. Altered glycosylation is associated with a range of physiological and pathological processes. Changes in glycan structures of proteins and cell surfaces are in relationship with many biological functions (pathogen-host interactions, immune system, stem cells, fertilization, etc.), with various diseases (e.g. cancer, inflammatory diseases, neurological diseases, psychiatric diseases, congenital diseases of glycosylation) and also with structure and function of pathogens. We are focused on development and application of affinity bioanalytical techniques analysing glycans based on protein microarray biochips with fluorescence detection for biomedicine, biology and biotechnology. These methods have great potential in the detection of microorganisms, development and testing of vaccines and biopharmaceuticals, stem cell research, study of fertilization process and mainly in discovering and testing glyco-biomarkers which can be sensitive markers of many diseases including cancer<sup>1,2</sup>. As biorecognition elements are used lectins, special proteins recognizing particular glycan structures, or anti-carbohydrate antibodies both enabling glycoprofiling of proteins, cells and tissues. (Glyco)protein microarrays in the combination with lectins or other glycan binding probes enable effective high-throughput glyco-profiling of samples and screening/analysis of glyco-biomarkers. We have developed lectin-based protein microarray platforms used for the study of glyco-biomarkers of some diseases as e.g. colorectal cancer (CRC) and congenital disorder of glycosylation (CDG) in various kinds of samples. The samples were spotted and incubated with panel of biotinylated lectins. In the case of CDG, spotted were serum samples and isolated transferrin from CDG patient, patient's parents and healthy control. We observed significant differences in lectin reactivity in patient samples vs. both patient's parents and healthy control for both kinds of samples. The most significant differences were observed in the case of mannose binding lectins. Analysis of isolated transferrin showed higher differences between patient vs. control samples than analysis of serum samples. Identification of glycan structures on samples by N- glycoprofiling using MALDI-TOF MS and LC-MS/MS methods confirmed

glycosylation changes detected by microarray. In the case of CRC, the samples included sera (from healthy persons and patients with CRC), cytosol/membrane proteins fractions (from non-tumor and tumor colon tissue), and insulin-like growth factor-binding protein 3 (IGFBP-3) and IGF receptors (IGF1R and IGF2R) isolated from non-tumor and tumor colon tissue. Glycan analysis of serum samples revealed increased sialylation in patients with CRC, which is a common feature for many tumor types. Glycan analysis of IGFBP-3 pointed to specific glycosylation pattern of this glycoprotein, suggesting further investigation to find out whether IGFBP-3 is glycosylated in a tissue-specific manner, since it seems to be glycosylated in a tumor-specific manner. The changes in glycans on IGF1R could possibly affect ligand binding, whereas changes in glycans on IGF2R do not seem to induce such effect. Determination of pathophysiological consequences of altered glycosylation of IGF1R and IGF2R, however, needs additional research. Although analytical systems based on lectin-glycan interactions does not allow accurate identification of glycan structures, the lectin-based protein microarray platform is suitable for rapid screening to detect glycosylation changes or abnormalities for a large number of samples making this method very useful in glyco-biomarker research. Identification of glycan structures by MS methods suitably complements and enable confirming data obtained using lectin-based protein microarray<sup>3</sup>.

## Acknowledgements

This work was supported by the bilateral project APVV SK-SRB-2016-0023. This publication is the result of the project implementation: Centre for materials, layers and systems for applications and chemical processes under extreme conditions – Stage II, ITMS No. 26240120021 supported by the Research & Development Operational Programme funded by the ERDF.

## References

1. Pinho SS. et al. Glycosylation in cancer: mechanisms and clinical implications. *Nat Rev Cancer* 2015;15:540-55.
2. Drake PM. et al. Sweetening the pot: adding glycosylation to the biomarker discovery equation. *Clin Chem* 2010;56:223-6.
3. Zámorová M. et al. Analysis of changes in the glycan composition of serum, cytosol and membrane glycoprotein biomarkers of colorectal cancer using a lectin-based protein microarray. *Anal Methods* 2017;9:2660-6.

---

## Ligand and redox interactions of adrenaline with iron at physiological pH

---

Jelena Korać<sup>1\*</sup>, Dalibor Stanković<sup>2</sup>, Marina Stanić<sup>1</sup>, Danica Bajuk-Bogdanović<sup>3</sup>, Milan Žižić<sup>1</sup>, Jelena Bogdanović Pristov<sup>1</sup>, Sanja Grgurić-Šipka<sup>4</sup>, Ana Popović-Bijelić<sup>3</sup>, Ivan Spasojević<sup>1</sup>

<sup>1</sup>*Department of Life Sciences, Institute for Multidisciplinary Research, University of Belgrade, Belgrade, Serbia*

<sup>2</sup>*Department of Analytical Chemistry, Innovation center of the Faculty of Chemistry, University of Belgrade*

<sup>3</sup>*Faculty of Physical Chemistry, University of Belgrade*

<sup>4</sup>*Department of General and Inorganic Chemistry, Faculty of Chemistry, University of Belgrade*

\**e-mail: jskorac@gmail.com*

Adrenaline (Adr) is catecholamine that is released by the sympathetic nervous system and adrenal medulla. It is involved in several physiological functions, including regulation of blood pressure, vasoconstriction, cardiac stimulation, and regulation of the blood glucose levels<sup>1</sup>. Transients of high levels of Adr in the bloodstream have been recognized for a long time as a cause of cardiovascular problems that develop under chronic exposure to psychosocial and physical stress<sup>2,3</sup>. A number of studies have found a connection between the excess of Adr, cardiotoxic effects, and oxidative stress, that is irrespective of adrenergic receptors stimulation<sup>2-4</sup>. The mechanism behind this involves Adr (coordinate and redox) interactions with iron, which are still not clear. Two main concepts have been proposed - Adr autooxidation and redox interactions with iron, the most abundant transition metal in human plasma<sup>5</sup>. Fe<sup>3+</sup> is known to build complexes with catechols<sup>6</sup>, but data on Fe<sup>3+</sup> coordinate interactions with Adr at physiological pH are missing. In addition to its (patho)physiological role, Adr is of interest from the aspect of development of catecholamine-rich biopolymers with adhesive properties and metelloorganic frameworks<sup>7,8</sup>. The adhesion and other properties materials are based on the cross-linking via coordinate bonds with Fe<sup>3+</sup> at pH > 7. Finally, ligands might dramatically alter the redox potential of Fe<sup>3+</sup>/Fe<sup>2+</sup> couple<sup>9</sup>. It has been shown that specific ligands with high affinity for Fe<sup>3+</sup>, including some catechols, might promote the oxidation and increase the reactivity of Fe<sup>2+</sup> with molecular oxygen<sup>10</sup>.

The aim of our study was to examine the nature of Adr interactions with Fe<sup>3+</sup> and Fe<sup>2+</sup>: stoichiometry, sites of coordinate bonds formation and structure of complex(es), and redox activity, at pH 7.4 and different concentration ratios. The coordinate and redox interactions were investigated using UV/Vis spectrophotometry, low temperature EPR, Raman

spectroscopy, cyclic voltammetry, and oximetry. The stability of Adr in the studied reactions was monitored by HPLC.

At pH 7.4, Adr forms complexes with  $\text{Fe}^{3+}$ , in the 1:1, and 3:1 stoichiometry, depending on (high or low) Adr/ $\text{Fe}^{3+}$  concentration ratio. The high-spin  $\text{Fe}^{3+}$  1:1 and 3:1 complexes show different symmetries, with the 3:1 complex displaying higher EPR spectral anisotropy. Raman spectroscopy showed that oxygen atoms on the catechol ring represent the sites of coordinate bond formation in the bidentate Adr- $\text{Fe}^{3+}$  complex. The bonds appear to be stronger in the 1:1 complex, and not to share the same plane with the ring. On the other hand, Adr and  $\text{Fe}^{2+}$  build a complex that acts as a strong reducing agent. In the presence of  $\text{O}_2$ , this leads to the production of  $\text{H}_2\text{O}_2$ , and to a facilitated formation of Adr/ $\text{Fe}^{3+}$  complexes. Adr is not oxidized in this process, *i.e.* iron is not an electron shuttle but electron donor. Catalyzed oxidation of  $\text{Fe}^{2+}$  in the presence of Adr represents a plausible chemical basis of stress-related damage of heart cells. In addition, our results imply that the application/pre-binding of  $\text{Fe}^{2+}$  followed by oxidation at  $\text{pH} > 7$  might be a simple alternative strategy for promotion of cross-linking in catecholamine-rich biopolymers frameworks.

## Acknowledgements

This study was supported by the Ministry of Education, Science and Technological Development of the Republic of Serbia, grant number OI173017.

## References

1. Álvarez-Diduk R, Galano A. Adrenaline and noradrenaline: Protectors against oxidative stress or molecular targets? *J Phys Chem B* 2015;119:3479-91.
2. Singal PK, Beamish RE, Dhalla NS. Potential oxidative pathways of catecholamines in the formation of lipid peroxides and genesis of heart disease. *Adv Exp Med Biol* 1983;161:391-401.
3. Meerson FZ. Disturbances of metabolism and cardiac function under the action of emotional painful stress and their prophylaxis. *Basic Res Cardiol* 1980;75:479-500.
4. Persoon-Rotherth M, van der Valk-Kokshoorn EJ, Egas-Kenniphaas JM, Mauve I, van der Laarse A. Isoproterenol-induced cytotoxicity in neonatal rat heart cell cultures is mediated by free radical formation. *J Mol Cell Cardiol* 1989;21:1285-91.
5. Mladěnka P. et al. The novel iron chelator, 2-pyridylcarboxaldehyde 2-thiophenecarboxyl hydrazone, reduces catecholamine-mediated myocardial toxicity. *Chem Res Toxicol* 2009;22:208-17.
6. Avdeef A, Sofen SR, Bregante TL, Raymond KN. Coordination chemistry of microbial iron transport compounds. 9. Stability constants for catechol models of enterobactin. *J Am Chem Soc.* 1978;100:5362-70.
7. Tran DT, et al. Enhanced electrocatalytic performance of an ultrafine AuPt nanoalloy framework embedded in graphene towards epinephrine sensing. *Biosens Bioelectron* 2017;89:750-57.
8. Sever MJ, Weisser JT, Monahan J, Srinivasan S, Wilker JJ. Metal-mediated cross-linking in the generation of a marine-mussel adhesive. *Angew Chem Int Ed Engl* 2004;3:448-50.
9. Rizvi MA, Mane M, Khuroo MA, Peerzada GM. Computational survey of ligand properties on iron(III)-iron(II) redox potential: exploring natural attenuation of nitroaromatic compounds. *Monatsh Chem* 2017;148:655.
10. Park JS, Wood PM, Davies MJ, Gilbert BC, Whitwood AC. A kinetic and ESR investigation of iron(II) oxalate oxidation by hydrogen peroxide and dioxygen as a source of hydroxyl radicals. *Free Radic Res* 1997;27:447-58.

---

# Protein engineering and development of high-throughput screening methods for glucose-oxidase gene library

---

Gordana Kovačević<sup>1\*</sup>, Radivoje Prodanović<sup>2</sup>

<sup>1</sup>Innovation Center of the Faculty of Chemistry, University of Belgrade, Belgrade, Serbia

<sup>2</sup>Faculty of Chemistry, University of Belgrade

\* e-mail: gordanak@chem.bg.ac.rs

Glucose oxidase (GOx) stands out as important industrial enzyme, used in food preservation, textile bleaching, glucose biosensors and enzymatic biofuel cells. It catalyzes oxidation of  $\beta$ -D-glucose producing  $\delta$ -gluconolactone and hydrogen-peroxide. While presence of hydrogen peroxide is important in food preservation and textile bleaching, it has harmful effects in biosensors and biofuel cells <sup>1,2</sup>. It has been shown that glucose oxidase loses activity during prolonged use, and it was suggested that reason for that was oxidative damage caused by hydrogen peroxide. The main culprit for the oxidative inactivation is methionine, as that is the amino acid most susceptible to oxidation even by mild reactive oxygen species <sup>3</sup>. Therefore, GOx mutants with higher activity or stability have important role in the development of biosensors and biofuel cells. Finding enzyme mutants with improved activity or stability can be time-consuming if appropriate medium or high-throughput screening methods (HTS) are not available.



**Figure 1.** Positions of the methionine residues (C $\alpha$ -atoms) plotted on the GOx crystal structure.

Figure 1 shows all methionine residues of GOx from *Aspergillus niger* as potential hot spots for protein redesign. We prepared the saturation mutant libraries at the position of each of the selected methionines and developed a yeast surface display based technique for

screening the oxidative stability. We cloned in *Pichia pastoris*, expressed and purified the two most prominent single mutants and the appropriate double mutant. The single methionine mutations in the proximity of the active site culminated in a two and four-fold increase in the reaction rate, and 1.5 and 2.5 times higher oxidative stability compared to the wild-type GOx. For the corresponding double mutant, we observed a one-fold increase in the reaction rate in comparison with the wild-type enzyme and a similar oxidative stability as for the single mutants. Our findings indicate that the exchange of a single methionine residue close to the active site cavity can be beneficial for both catalytic activity and oxidative stability of GOx.

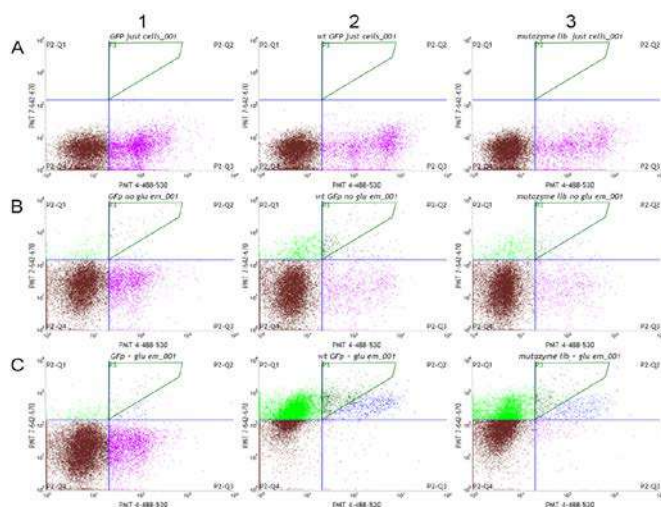


**Figure 2.** FACS analysis of *S.cerevisiae* EB100 cells. A: Non-treated cells expressing GFP (1), wtGOx-GFP (2), Gox-lib with GFP (3); B: Cells recovered from single water-in-oil emulsions after reaction with DyLight650 tyramide and without glucose, expressing GFP (1), wtGOx-GFP (2), Gox-lib with GFP (3); C: Cells recovered from single water-in-oil emulsions after reaction with DyLight650 tyramide and glucose, expressing GFP (1), wtGOx-GFP (2), Gox-lib with GFP (3).

GOx mutant libraries were successfully screened and sorted using HTS system based on fluorescent labeling of yeast cell expressing glucose oxidase on its surface<sup>4</sup>. For this purpose, we cloned wild-type and A2 mutant GOx in GFP-pCTCON2 vector and expressed it on the surface of *S.cerevisiae* EB100 cells. Expressed GOx-GFP chimera maintained differences in catalytic activity between wild-type and mutant GOx, and fluorescence of GFP was preserved. GOx mutant libraries were made by random mutagenesis. Fluorescent labeling of cells was done in water-in-oil emulsions using red fluorescent DyLight650-tyramide, peroxidase and glucose as substrate. After recovering cells from emulsion, they were screened and positive cells were gated on a fluorescence double plot (fluorescence emissions were detected using 530 and 670 nm filters) as can be seen on Figure 2. Sorted cells (P3 gate) were plated on selective media, and percentage of

positive cells was detected using agar plate assay. We managed to sort cells expressing GOx-GFP with higher activity and to enrich sorted population around 40%. From sorted libraries we indentified several GOx mutants with higher activity than the wild-type enzyme. Using GFP as a marker of protein expression level for FACS screening enabled us to sort cells expressing more active GOx without fluorescent antibody labeling of the expressed enzyme.

### **Acknowledgements**

This study was supported by funds from the Ministry of Education and Science, Republic of Serbia by the project No. ON172049 and DAAD funding organisation.

### **References**

1. Bankar SB, Bule MV, Singhal RS, Ananthanarayan L. Glucose oxidase – An overview. *Biotechnol Adv* 2009;27:489-501.
2. Leskovac V, Trivić S, Wohlfahrt G, Kandrač J, Peričin D. Glucose oxidase from *Aspergillus niger*: The mechanism of action with molecular oxygen, quinones, and one-electron acceptors. *Int. J. Biochem. Cell Biol* 2005;37:731-50.
3. Manning MC, Chou DK, Murphy BM, Payne RW, Katayama DS. Stability of protein pharmaceuticals: an update. *Pharm Res* 2010;27:544-75.
4. Ostafe R, Prodanović R, Nazor J, Fischer R. Ultra-high-throughput screening method for the directed evolution of glucose oxidase. *Chem Biol* 2014;21:414-21.



---

# Application of microbial levan as a new component for production of graft copolymer with polystyrene

---

Branka Lončarević<sup>1\*</sup>, Marija Lješević<sup>1</sup>, Gordana Gojgic-Cvijović<sup>1</sup>, Dragica Jakovljević<sup>1</sup>, Vladimir Nikolić<sup>2</sup>, Miroslav M. Vrvic<sup>3</sup>, Vladimir P. Beškoski<sup>3</sup>

<sup>1</sup>Department of Chemistry, Institute of Chemistry, Technology and Metallurgy, University of Belgrade, Belgrade, Serbia

<sup>2</sup>Innovation Center, Faculty of Chemistry, University of Belgrade

<sup>3</sup>Department of Biochemistry, Faculty of Chemistry, University of Belgrade

\* e-mail: brankakekez@chem.bg.ac.rs

Polysaccharides based on fructose, also called fructans, are synthesized from sucrose by some plant species and many bacteria, fungi and *Archaea*. Levan is an exopolysaccharide composed of fructose units and has numerous applications in personal care and cosmetics, medicine and food industry<sup>1,2</sup>. Polystyrene is the most widespread polymer for plastic production due to its low costing and easy production. Degradation of polystyrene is long-term process, therefore incorporating natural polymers is the desirable approach<sup>3</sup>.

In the present study, levan-polystyrene graft copolymer (L-g-PS) was synthesized, characterized and influence of reaction time on grafting reaction at two temperatures was investigated. Levan was isolated after cultivation *Bacillus licheniformis* NS032. Syntheses of L-g-PS were performed by the free radical reaction using K<sub>2</sub>S<sub>2</sub>O<sub>8</sub> as initiator<sup>4</sup>. Grafting reactions proceeded in nitrogen atmosphere, at 55°C and 70°C and reaction time ranged between 15 and 210 min. FTIR spectra and XRD patterns were recorded using a Thermo Nicolet 6700 Spectrophotometer and Philips PW-1710 automated diffractometer, respectively.

The formation of L-d-g-PS was confirmed by FTIR spectra which displayed the presence of all characteristic peaks for both component and X-ray diffractograms which showed amorphous nature of copolymer. Compared to other reaction parameters, the temperature of 70°C and time of 45 min was more optimal showing higher percentage of grafting.

## Acknowledgements

This study was supported by Ministry of Education, Science and Technological Development of the Republic of Serbia through Scholarship for PhD students Program and Project III 43004.

## References

1. Öner TE, Hernández L, Combie J. Review of Levan polysaccharide: From a century of past experiences to future prospects. *Biotechnol Adv* 2016;34:827-44.

2. Srikanth R, Sudhar Reddy HSSC, Siddartha G, Ramaiah JM, Uppuluri BK. Review on production, characterization and applications of microbial levan. *Carbohydr Polym* 2015;120:102-14.
3. Sheikh N, Akhavan A, Ataeviarjovi E. Radiation grafting of styrene on starch with high efficiency. *Radiat Phys Chem* 2013;85:189-92.
4. Kekez et al. Synthesis and characterization of a new type of levan-graft-polystyrene copolymer. *Carbohydr Polym* 2016;154:20-9.

---

## The role of heterologous immunity in resistance to ocular chlamydial infection

---

Ivana Lukić<sup>1\*</sup>, Aleksandra Inić-Kanada<sup>2</sup>, Elisabeth Stein<sup>2</sup>, Emilija Marinković<sup>1</sup>, Ana Filipović<sup>1</sup>, Radmila Đokić<sup>1</sup>, Talin Barisani-Asenbauer<sup>2</sup>, Marijana Stojanović<sup>1</sup>

<sup>1</sup> Department of Research and Development, Institute of Virology, Vaccine and Sera „Torlak“, Belgrade, Serbia

<sup>2</sup> OCUVAC - Center of Ocular Inflammation and Infection, Institute of Specific Prophylaxis and Tropical Medicine, Center for Pathophysiology, Infectiology and Immunology, Medical University of Vienna, Vienna, Austria

\* e-mail address: [anavimasaj@gmail.com](mailto:anavimasaj@gmail.com)

Trachoma is a chronic keratoconjunctivitis caused by recurrent infection with intracellular bacterium *Chlamydia trachomatis* (Ct), serovars A, B, Ba and C, and represents the leading cause of preventable blindness worldwide<sup>1</sup>. The disease was endemic in Europe and the United States until well into the 20<sup>th</sup> century and has been disappeared from these regions as a result of improved living conditions and health care. In addition, the decline in trachoma incidence parallels the introduction of mandatory vaccination.

Our hypothesis is that mandatory vaccination against tetanus contributes to the immunity against ocular Ct infection and in that way supported trachoma elimination from Europe and the USA. The following evidence support this hypothesis: 1) vaccination against tetanus could positively affect the outcome of the infection caused by heterologous microorganisms<sup>2-7</sup>, 2) there is a high structural similarity at the level of short peptide sequences between tetanus toxin (TT) and Ct major outer membrane protein, which is marked as the most promising antigen to be incorporated in the vaccine against Ct, 3) the higher level of antibodies specific for chlamydial antigens has been detected in immunized individuals (immunization against tetanus included) comparing to non-immunized subjects<sup>8</sup>.

Eight anti-tetanus monoclonal antibodies (MAbs) were preliminary tested for binding to CtA, CtB, and *Chlamydia caviae* (natural chlamydial pathogen in guinea pigs)<sup>9</sup>. MAb26 and MAb5, which bind CtA, CtB and *Chlamydia caviae* (Cc) in a direct ELISA, were selected for further research. MAb26 binds tetanus toxin (TT) with lower affinity comparing to MAb51 and, contrary to MAb51, is not able to provide protection against TT intoxication<sup>9</sup>. However, MAb26 has been superior to MAb51 in binding to chlamydial antigens (Figure 1A). The cross-reactivity of MAb26 and MAb51 toward chlamydial proteins, especially those having molecular weights below 50 kDa, has been confirmed by Western blot. In comparison with MAb51, the binding of MAb26 to TT has been profoundly inhibited by preincubation with CtA, CtB and Cc. This finding correlated with

higher potential of MAb26 to inhibit *in vitro* infection of human epithelial cell line (HCjE) by CtB (Figure 1B). Furthermore, MAb26 diminished intensity of ocular pathology in guinea pigs infected with Cc in the peak of the disease in comparison with either MAb51-treated guinea pigs or sham-control (\* $p$ <0.05, two-way ANOVA test). Guinea pigs treated with MAb26 have also had a shorter recovery time (Figure 1C).

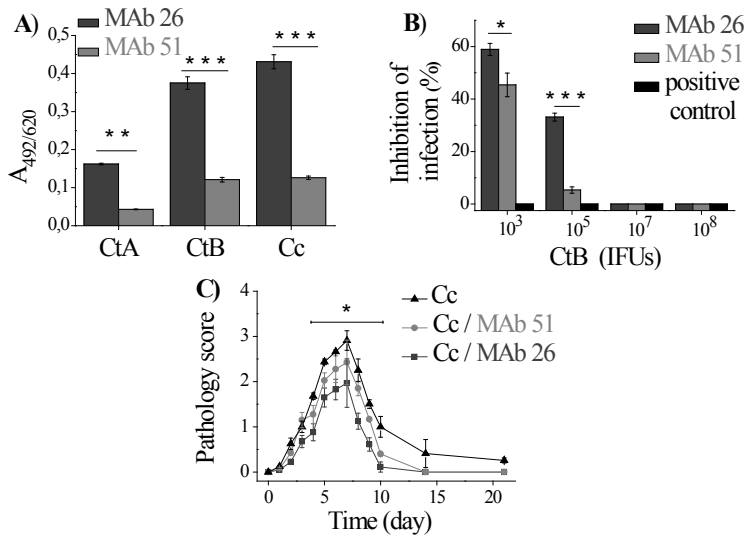


**Figure 1.** Binding of MAb26 and MAb51 to CtA, CtB and Cc and their impact on *in vitro* and *in vivo* chlamydial infections. (A) Binding of MAb26 and MAb51 (10  $\mu$ g/ml) to CtA, CtB, Cc (10<sup>6</sup> IFUs/ml) was assessed by a direct ELISA. (B) The potential of MAb26 and MAb51 (5  $\mu$ g/ml) to prevent infection by various doses of CtB was evaluated *in vitro* in HCjE cells. (C) The *in vivo* protective potential of MAb26 and MAb51 was assessed in the model of inclusion conjunctivitis in guinea pigs. Guinea pigs (n=3 per group) were infected (day 0) by 1 x 10<sup>4</sup> IFU of CC (positive control) or with 1 x 10<sup>4</sup> IFU of CC pre-incubated with MAb26 or MAb51 (10  $\mu$ g/ml, 1h, RT). Upon infection, the local treatment by corresponding MAb (10  $\mu$ g/ml, 25  $\mu$ l/eye) was performed daily until day 7 post-infection. Guinea pigs were monitored until the resolution of infection (day 21). Statistical significance of the observed differences was determined by two-way ANOVA test (\*  $p$ <0.05, \*\* $p$ <0.005, \*\*\* $p$ <0.001).

Our results suggest that immunization against tetanus promotes secretion of TT-specific antibodies, which are not capable to confer protection against TT intoxication but, due to cross-reactivity, could improve immunity to heterologous antigens from *Chlamydia*.

## Acknowledgement

This research has been supported by Ministry of Education, Science and Technological Development of the Republic of Serbia (Grant No. 172049) and by the “Laura Bassi Centers of Expertise” program

of the Austrian Federal Ministry of Economy through the Austrian Research Promotion Agency (Grant No. 822768)

## References

1. Hu V, Harding-Esch E, Burton M, Bailey R, Kadimpeul J, Mabey D. Epidemiology and control of trachoma: systematic review. *Trop Med Int Health* 2010;15:673-91.
2. Benn CS, Netea MG, Selin LK, Aaby P. A small jab - a big effect: nonspecific immunomodulation by vaccines. *Trends Immunol* 2013;34:431-9.
3. Flanagan KL, van Crevel R, Curtis N, Shann F, Levy O. Heterologous (“nonspecific”) and sex-differential effects of vaccines: Epidemiology, clinical trials, and emerging immunologic mechanisms. *Clin Infect Dis* 2013;57:283-9.
4. Kandasamy R, et al. Non-specific immunological effects of selected routine childhood immunisations: systematic review. *BMJ* 2016;355:i5225.
5. Gil A, Kenney LL, Mishra R, Watkin LB, Aslan N, Selin LK. Vaccination and heterologous immunity: educating the immune system. *Trans R Soc Trop Med Hyg* 2015;109:62-9.
6. Van Regenmortel MH. From absolute to exquisite specificity. Reflections on the fuzzy nature of species, specificity and antigenic sites. *J Immunol Methods* 1998;216:37-48.
7. Agergaard J, et al. Serological evidence for Chlamydia pneumoniae infection following diphtheria-tetanus-pertussis booster vaccination. *J Inf Dis Immunity* 2010;2:1-14.
8. Stine J, et al. Chlamydia antibody response in healthy volunteers immunized with nonchlamydial antigens: A randomized, double-blind, placebo-controlled study. *Clin Inf Dis* 2003;36:586-91
9. Lukic I, et al. Key protection factors against tetanus: Anti-tetanus toxin antibody affinity and its ability to prevent tetanus toxin e ganglioside interaction. *Toxicon* 2015;103:135-44.



---

## Antioxidant and antiinflammatory activity of Merlot wine

---

**Tatjana Majkić\*, Ksenija Dobrokes, Martin Spevak, Dejan Orčić, Neda Mimica-Dukić, Marija Lesjak, Ivana Beara**

*Department of Chemistry, Biochemistry and Environmental Protection, Faculty of Sciences, University of Novi Sad, Novi Sad, Serbia*

\*e-mail: [tatjana.majkic@dh.uns.ac.rs](mailto:tatjana.majkic@dh.uns.ac.rs)

A number of studies confirmed health benefits of moderate wine consumption. It can contribute to the reduced risk of chronic, cardiovascular and neurodegenerative diseases, as well as cancer. It is considered that red wine exerts more protective effects than white wine, due to higher content of polyphenolic compounds<sup>1</sup>. One of the most famous grape variety which is used for producing red wine around the world is Merlot. Despite huge market popularity, there is little data about biological activity of this variety grown in Serbia.

As a part of broad investigation of biological potential of wine from Vojvodina, the aim of this study was to evaluate antioxidant and antiinflammatory activity of Merlot wine from three different wineries: Čoka (Subotica), Veranda (Irig) and Šukac (Sremska Kamenica). The antioxidant activity of samples was analyzed using tests related to NO<sup>•</sup> scavenging effect and the potential of lipid peroxidation inhibition. Antiinflammatory activity was determined as a potential to inhibit production of prostaglandin E<sub>2</sub> and thromboxane A<sub>2</sub> in inflammatory process. Namely, macrophages (derived from U937 monocytes) were pretreated with wine samples and inflammation was induced by LPS. Quantification of produced eicosanoids in cell lysate was done by LS-MS/MS<sup>2,3</sup>. Besides, total content of phenols, flavonoids, tannins and anthocyanins were determined spectrophotometrically in all wine samples<sup>4,5</sup>.

Merlot from Čoka winery had the best antioxidant activity, that was correlated with the highest total phenolic and flavonoid content. Slightly weaker antioxidant potential exhibited Merlot from Šukac winery, which had the highest content of tannins and anthocyanins. Wine from Veranda winery had the lowest content of all determined compounds, as well as antioxidant activity. In general, all analysed samples showed moderate antiinflammatory potential, but statistically significant differences were not found between their activities.

In this short report novel and valuable data about biological activity of Merlot wine from Serbia are presented. Obtained results confirmed that the Merlot wine is a rich source of phenolic compounds and natural antioxidants. Moreover, they indicate that compounds from Merlot wine could be regarded as a potential antiinflammatory agents.

## Acknowledgements

This study was supported by The Ministry of Education, Sciences and Technological Development of the Republic of Serbia (OI 172058).

## References

1. Tauchen J, Marsik P, Kvasnicova M, Maghradze D, Kokoska L, Vanek T, Landa P. *In vitro* antioxidant activity and phenolic composition of Georgian, Central and West European wines. *J Food Comp Anal* 2015;41:113-21.
2. Beara I, Orčić D, Lesjak M, Mimica-Dukić N, Peković B, Popović M. Liquid chromatography/tandem mass spectrometry study of anti-inflammatory activity of plantain (*Plantago* L.) species. *J Pharm Biomed Anal* 2010;52:701-6.
3. Lesjak M, Beara I, Orčić D, Ristić J, Anačkov G, Božin B, Mimica-Dukić N. Chemical characterisation and biological effects of *Juniperus foetidissima* Willd. 1806. *Food Sci Technol* 2013;53:530-9.
4. Beara I, et al. Plantain (*Plantago* L.) species as novel sources of flavonoid antioxidants. *J Agric Food Chem* 2009;57:9268-73.
5. Lee J, Durst R, Wrolstad R. Determination of total monomeric anthocyanin pigment content of fruit juices, beverages, natural colorants, and wines by the pH differential method: collaborative study. *J AOAC Int* 2005;88:1269-78.

---

## The effect Of prophylactic treatment of recombinant banana on TNBS-induced colitis in BALB/C mice

---

Emilija Marinković<sup>1\*</sup>, Radmila Djokić<sup>1</sup>, Ana Filipović<sup>1</sup>, Ivana Lukić<sup>1</sup>, Dejana Kosanović<sup>1</sup>, Aleksandra Inić-Kanada<sup>2</sup>, Marija Gavrović-Jankulović<sup>3</sup>, Marijana Stojanović<sup>1</sup>

<sup>1</sup>*Institute of Virology, Vaccines and Sera - Torlak, Belgrade, Serbia*

<sup>2</sup>*The Laura Bassi Center of Expertise, Medical University Vienna, Vienna, Austria*

<sup>3</sup>*Department of Biochemistry, Faculty of Chemistry, University of Belgrade, Belgrade, Serbia*

\**e-mail: emilymarinkovic84@gmail.com*

Banana lectin (BanLec) is a mannose-specific lectin that belongs to the jackalin superfamily. Immunomodulatory activity of BanLec has been shown in various human and murine systems<sup>1-3</sup>. In our research, we used recombinantly produced BanLec (rBanLec) which structurally and functionally highly resemble to its naturally occurring counterparts<sup>2,3</sup>. Besides, rBanLec is recognized as modulator of local immune response in the murine colon<sup>4</sup>. The aim of this study was to investigate prophylactic effect of rBanLec on murine model of colitis induced by 2,4,6-trinitrobenzene sulfonic acid (TNBS).

Experimental colitis was induced in BALB/c mice by a single intrarectal (i.r.) administration of 2.5 mg TNBS/50% EtOH. Mice were treated with rBanLec (i.r. 100 µL rBanLec/PBS, rBanLec concentrations: 0.1 µg/mL, 1 µg/mL, and 10 µg/mL; groups assigned rBL0.1, rBL1, and rBL10, respectively) 24h prior to induction of colitis. Colitic BALB/c mice (TNBS group) not subjected to rBanLec treatment were referent. Mice treated only with 50% EtOH (i.r. 100 µL; EtOH group) were negative control of the experiment. The disease severity (evaluated according weight loss) and inflammatory response were examined at the peak of pathology (the 3<sup>rd</sup> day upon TNBS administration).

Comparing to TNBS group, a significant reduction in disease severity was recorded in rBL1 ( $P < 0.005$ ) and rBL10 ( $P < 0.0005$ ) groups (Figure 1A). The reduced inflammation-associated damage (neutrophil infiltration and colon shortening) of colonic tissues of rBL1 and rBL10 mice was marked as well. It was revealed by confocal microscopy that colonic tissue from rBL1 and rBL10 mice contained less CD11b<sup>+</sup> cells than tissue of TNBS mice. In line with the observed reduction in inflammation-associated damage of colon, local MPO activity, NO production, IL-12 and TNF- $\alpha$  production, and T-bet and ROR-t expression were significantly diminished in rBL1 and rBL10 mice in comparison to the referent ones.

Unexpectedly, the local levels of anti-inflammatory cytokines, IL-10 and TGF- $\beta$ , were also reduced in rBL1 and rBL10 mice comparing to TNBS ones. Statistical analyses implied

that for the overall outcome local concentration of particular cytokine might be less important than its contribution to the local cytokine milieu. In our model system, the severity of pathology positively correlated to the ratio of local TNF- $\alpha$  and IL-10 concentrations (Pcc=0.827, P=0.05; Figure 1B).

Obtained results show that rBanLec pre-treatment could lessen the colon pathology in TNBS-induced colitis in mice. rBanLec, in a positive dose-dependent manner, modulates local immune milieu in colon in a way to diminish deleterious potential of subsequently induced inflammatory response.

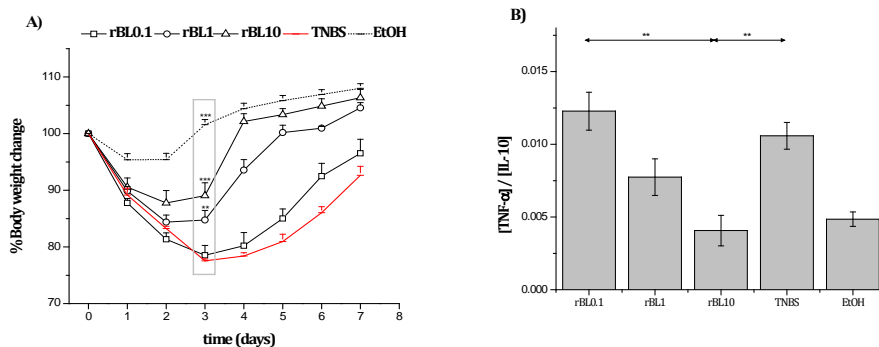


**Figure 1.** Changes in body weight upon induction of experimental colitis in mice and the ratio of local concentrations of TNF- $\alpha$  and IL-10 at the peak of disease. (A) The changes in body weight over the course of disease are presented as percentages of the initial body weight (n = 10 mice/group). (B) The local concentrations of TNF- $\alpha$  and IL-10 were evaluated at peak of disease (colon samples collected 3 days upon colitis induction). Concentrations of cytokines were determined in supernatant of colon homogenates by sandwich ELISA. The mean [TNF- $\alpha$ ]/[IL-10]  $\pm$  SE per group (n=10) are presented. Statistical significance of the observed differences were evaluated by T-test (TNBS group was referent: \*\*P < 0.005, \*\*\*P < 0.001).

## Acknowledgements

This study was supported by by the Ministry of Education, Science and Technological Development of the Republic of Serbia (Grant No. 172049).

## References

1. Peumans WJ, et al. Fruit-specific lectins from banana and plantain. *Planta* 2000;211:546-4.
2. Gavrović-Jankulović M, Poulsen K, Brckalo T, Bobić S, Linder B, Petersen A. A novel recombinantly produced banana lectin isoform is a valuable tool for glycoproteomics and a potent modulator of the proliferation response in CD3<sup>+</sup>, CD4<sup>+</sup>, and CD8<sup>+</sup> populations of human PBMCs. *Int J Biochem Cell Biol* 2008;40:929-41.
3. Stojanovic M, et al. In vitro stimulation of Balb/c and C57BL/6 splenocytes by a recombinantly produced banana lectin isoform result in both a proliferation of T cells and an increased secretion of interferon-gamma. *Int Immunophar* 2010;10:120-9.
4. Marinkovic E, Lukic I, Kosanovic D, Inic-Kanada A, Gavrovic-Jankulovic M, Stojanovic M. Recombinantly produced banana lectin isoform promotes balanced pro-inflammatory response in the colon. *J Funct Foods* 2016;20:68-78.

---

## Synthesis of potential pharmaceutical active ingredients using omega-transaminase

---

Nevena Marković<sup>1\*</sup>, Suzana Jovanović Šanta<sup>2</sup>, Radivoje Prodanović<sup>3</sup>

<sup>1</sup>*Institute of Chemistry, Technology and Metallurgy, University of Belgrade, Belgrade, Belgrade*

<sup>2</sup>*Faculty of Natural Sciences, University of Novi Sad, Novi Sad, Serbia*

<sup>3</sup>*Faculty of Chemistry, University of Belgrade*

\**e-mail: markovicnevena6@gmail.com*

Transaminases (EC 2.6.1.X) are enzymes which catalyze reversible transfer of amino group from amino acids to  $\alpha$ -keto acids by using pyridoxal-5'-phosphate as a coenzyme. There is a huge interest for the application of  $\omega$ -transaminases in industrial production of chiral amines and alkaloids since those compounds are extensively used in pharmaceutical, agricultural, and chemical industries. Application of  $\omega$ -transaminases in asymmetric synthesis of these compounds enables efficient production of biologically active amines, due to their catalytic properties for synthesis with a high level of enantioselectivity, substrate promiscuity (they are capable to aminate keto acids, aldehydes and ketones), high turnover number, no requirement for regeneration of external cofactors, and among other cheaper, simpler and green process of production<sup>1,2</sup>.

We are developing biocatalytic route for the synthesis of amino steroids by using  $\omega$ -transaminase, (R)-selective, ATA-117 enzyme variant from *Arthrobacter* sp<sup>3</sup>. It can be observed that enzyme expression was done in *Echerichia coli* BL21 D3 pLysS (Figure 1), and HPLC analysis of enzyme activity and specificity toward 15 structurally different steroid compounds was performed. (R)-methylbenzylamine was used as amino group donor and pyridoxal-5'-phosphate as cofactor. Activity of the enzyme was measured in bacterial lysate based on the absorbance of acetophenone, that is formed during the transamination reaction of (R)-methylbenzylamine. Figures 2 and 3 are showing chromatograms of acetophenone standard and products of reaction performed with enzyme expressed in *E. coli* and 16,17-epoxypregnenolone. Reactions were analysed on reversed phase column NucleosilC18. Based on the results, we have selected four steroid compounds for which enzyme showed highest activity and with a potential for biological activity. The next step was optimisation of the reaction conditions with a low cost amino donor isopropylamine, and isolation and characterisation of a pure amino steroid products. Until now we have managed to enzymatically synthesize and purify one amino steroid which should be further analysed by spectral characterization and its biological activity will be determined.

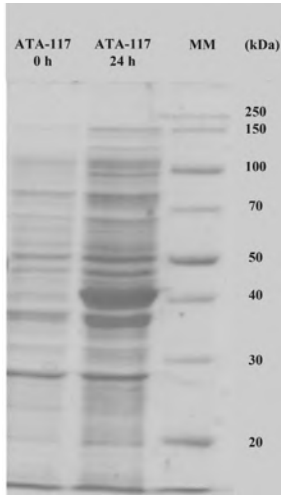


**Figure 1.** SDS-PAGE of ATA-117 expressed in *E. coli* BL21 DE3 pLysS compared against proteins in bacterial lysat before the induction of enzyme expression.

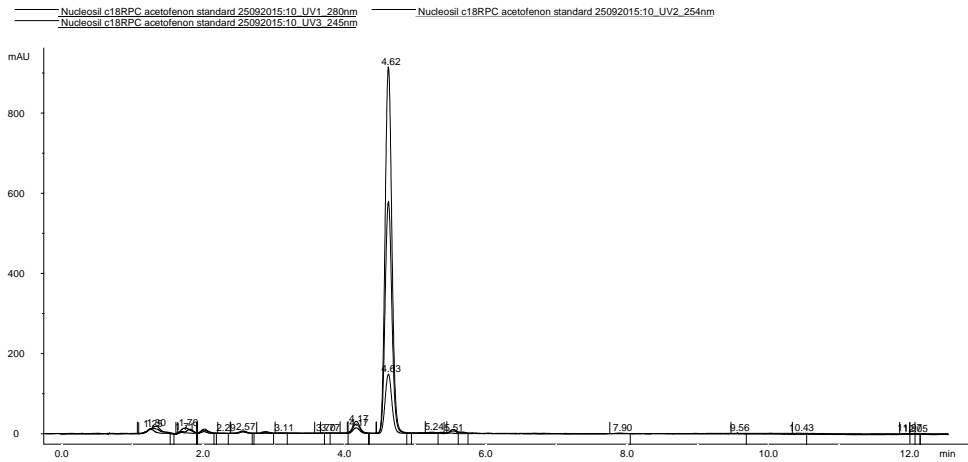


**Figure2.** Chromatogram of acetophenone (20 mM) in buffer solution (100 mM HEPES, pH 8.0)-retention time 4.62 min.

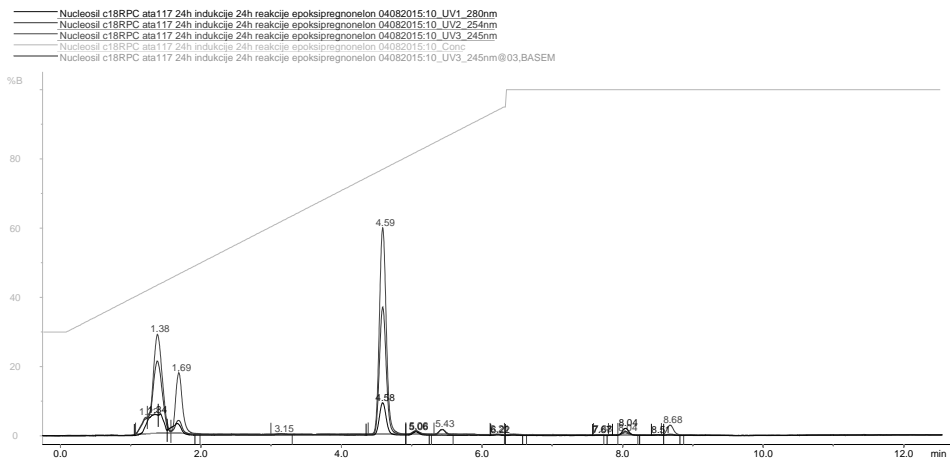


**Figure 3.** Chromatogram of reaction performed with induced enzyme (24h of reaction) and 16,17-epoxyprogrenolone-retention time of acetophenone 4.59 min

## Acknowledgements

This study was supported by Grant ON173017 sponsored by the Ministry of Education and Science, Republic of Serbia.

## References

1. Cassimjee KE.  $\omega$ -Transaminase in Biocatalysis: Methods, Reactions and Engineering. Doctoral thesis. KTH Royal Institute of Technology, School of Biotechnology, Stockholm, 2012.
2. Svedendahl M. Lipase and  $\omega$ -Transaminase: Biocatalytic Investigations. Doctoral thesis. KTH Royal Institute of Technology, School of Biotechnology, Stockholm, 2010.
3. Richter N, Simon RC, Kroutil W, Ward JM, Hailes HC. Synthesis of pharmaceutically relevant 17- $\alpha$ -amino steroids using an  $\omega$ -transaminase. Chem Commun 2014;50:6098-100.



---

## Biodegradation of 2,6-di-tert-butylphenol by *Pseudomonas aeruginosa* san ai

---

Ana Medic<sup>1\*</sup>, Ksenija Stojanović<sup>2</sup>, Ivanka Karadžić<sup>1</sup>

<sup>1</sup>School of Medicine, University of Belgrade, Belgrade, Serbia

<sup>2</sup> Faculty of Chemistry, University of Belgrade

\*e-mail: ana.medic@med.bg.ac.rs

2,6-Di-tert-butylphenol (2,6-DTBP) is hazardous and very toxic to aquatic life. The release into the natural environment as well as in surface water is possible during manufacturing processes and by leaching from final products <sup>1</sup>. Biodegradation is regarded as a promising alternative method to remove 2,6-DTBP from polluted area. The strain *P. aeruginosa* san ai was isolated from industrial mineral metal-cutting oil <sup>2</sup>, and it has ability to produce biotechnologically important substances <sup>3</sup>, and to be used for remediation of heavy metal pollution <sup>4</sup>. The main objective of this study was to estimate capability of *P. aeruginosa* to degrade 2,6-DTBP. The effects of different initial concentration of 2,6-DTBP and pH values of medium on bacterial growth and metabolism as well as biodegradation efficiency was examined.

*P. aeruginosa* san ai was cultivated for 7 days under aerobic conditions in liquid mineral salt medium supplemented with 2,6-DTBP (2, 10, 100, 400 mg/L) as a sole carbon source at different pH values (5.0 - 8.0). Intracellular protein profiles were monitored by SDS-PAGE. Respiration of culture exposed to 2,6-DTBP was measured and efficiency of mineralization of 2,6-DTBP was estimated.

*P. aeruginosa* san ai completely degraded lower concentrations (2, 10 mg/L) of 2,6-DTBP while higher concentrations (100 and 400 mg/L) were degraded 68,34% and 17,84%, respectively. The results demonstrate a high capacity of the strain not only to survive but also to degrade efficiently the toxic compound. As the concentration of 2,6-DTBP determined in the wastewater was referred to be about 4.0 mg/L<sup>1</sup>, it is expected that 2,6-DTBP would be effectively removed by strain *P. aeruginosa* san ai from the even more polluted water. *P. aeruginosa* san ai could degrade 2,6-DTBP in a wide range of pH values (from 5.0 to 8.0). The maximum DTBP degradation and cell growth were observed at pH 5.0. The percent degradation of 2,6-DTBP at pH 5.0, 7.0 and 8.0 was 96,76%, 77,01% and 58,97%, respectively. Protein profiles of cell biomass of *P. aeruginosa* san ai grown on 2,6-DTBP and sunflower oil as a sole carbon source obtained by SDS-PAGE electrophoresis undoubtedly show differences in the metabolism depending on source of carbon.

In view of the effective degradation of 2,6-DTBP the strain of *P. aeruginosa* san ai can be considered as a good candidate for application in bioremediation of environments accidentally polluted by different phenolic compounds.

## References

1. OECD/SIDS. Screening Information Data Set (SIDS) of OECD High Production Volume Chemicals Programme, 1994.
2. Karadžić I, Masui A, Fujiwara N. Purification and characterization of a protease from *Pseudomonas aeruginosa* growth in cutting oil. *J Biosci Bioeng* 2004;98:145-52.
3. Rikalović M, Abdel-Mawgoud AM, Déziel E, Gojgić-Cvijović G, Nestorović Z, Vrvic M, Karadžić I. Comparative analysis of rhamnolipids from novel environmental isolates of *Pseudomonas aeruginosa*. *J Surfact Deterg* 2013;16:673-82.
4. Avramović N, Nikolić-Mandić S, Karadžić I. Influence of rhamnolipids, produced by *Pseudomonas aeruginosa* NCAIM(P), B001380 on their Cr(VI) removal capacity in liquid medium. *J Serb Chem Soc* 2013;78:639-51.

---

## The influence of coated nanoCeO<sub>2</sub> on the phenol content in wheat and pea

---

Ivana Milenković<sup>1\*</sup>, Manuel Algarra<sup>2</sup>, Slađana Spasić<sup>1</sup>, Aleksandra Mitrović<sup>1</sup>, Vladimir Beškoski<sup>3</sup>, Ksenija Radotić<sup>1</sup>

<sup>1</sup>*Department of Life Sciences, Institute for Multidisciplinary Research, University of Belgrade, Belgrade, Serbia*

<sup>2</sup>*Department of Inorganic Chemistry, Faculty of Sciences, University of Málaga, Málaga, Spain*

<sup>3</sup>*Department of Biochemistry, Faculty of Chemistry, University of Belgrade*

\**e-mail: ivana.milenkovic@imsi.rs*

The use of nanomaterials in various commercial products and industrial processes has increased. Although the application of nanoparticles has great importance, some of them can be risky to human health and the environment. The unregulated usage of nanoparticles can result in excessive accumulation in sediments, soils, air and aquatic environments, endangering terrestrial plants<sup>1</sup>.

Cerium oxide nanoparticles (nanoCeO<sub>2</sub>) have been extensively investigated due to the excellent oxygen storage capacities on the basis of the redox transition between Ce<sup>3+</sup> and Ce<sup>4+</sup> and formation of oxygen vacancies on their surface<sup>2</sup>. The effect of nanoCeO<sub>2</sub> on individual organisms and the ecosystem in general are not sufficiently explored and the literature on the toxicity of nanoCeO<sub>2</sub> in edible plants is contradictory. NanoCeO<sub>2</sub> is very stable in soil and different environmental media and has been found to transfer within plant tissues unaltered. It is very likely that it interacts with plants in nanoparticulate forms<sup>3</sup>.

In this research we used CeO<sub>2</sub>, naked and coated with three different carbohydrates (glucose, pullulan or levan), to study their effect on phenol content, as an important indicator of plant stress<sup>4,5</sup>, in aboveground plant organs in wheat and pea. NanoCeO<sub>2</sub> was synthesized using self-propagating room temperature method by the procedure of Matović et al<sup>6</sup>. NanoCeO<sub>2</sub>, synthesized by this method, was subsequently coated to make glucose-, levan- and pullulan-coated nanoCeO<sub>2</sub> (G-CeO<sub>2</sub>, L-CeO<sub>2</sub> and P-CeO<sub>2</sub>). Suspensions of these nanoparticles (200 mg/L) were prepared in water, and characterized by X-ray diffraction (XRD) and transmission electron microscopy (TEM). After the treatment the aboveground parts of plants were cut off and phenols were isolated by the procedure<sup>7</sup>.

The physiochemical properties of the synthesized nanoCeO<sub>2</sub> were analyzed using XRD and HRTEM methods. The XRD patterns of obtained nanoCeO<sub>2</sub> are shown in Figure 1. Samples exhibited typical peaks corresponding to planes which are the typical of face centered. All samples showed broad peaks, explained due their synthesis procedure at low temperature, but no shift was found following synthesis and coating process.

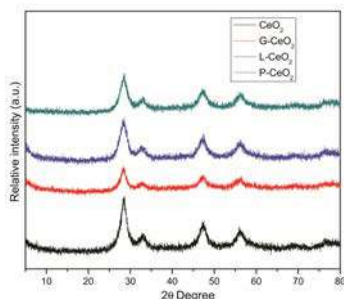


**Figure 1.** XRD pattern of uncoated nanoCeO<sub>2</sub> and coated G-, L- and P-CeO<sub>2</sub>

For uncoated nanoCeO<sub>2</sub> HRTEM images (Figure 2) demonstrated an average size between 8-13 nm, which is slightly increased for the coated systems. This can be explained by the obviously coating effect which apparently aggregates them, especially in L-CeO<sub>2</sub>. In all nanoCeO<sub>2</sub> was found a crystalline structure with a spacing of 0.333 nm (Figure 2E), which indicate face-centered cubic crystallographic structure<sup>8</sup>. Treatment of wheat with four different nanoCeO<sub>2</sub>, uncoated and coated, did not show statistically significant differences in total phenol content of the aboveground plant parts, regardless of the timing of its application (during germination or growth in hidroponics). On the other hand, it can be observed (Figure 3) that total phenol content increased in pea plants treated with L-CeO<sub>2</sub> and P-CeO<sub>2</sub> during germination. Between the other treatments in pea plants there were no statistically significant differences, as well as in comparison with control.

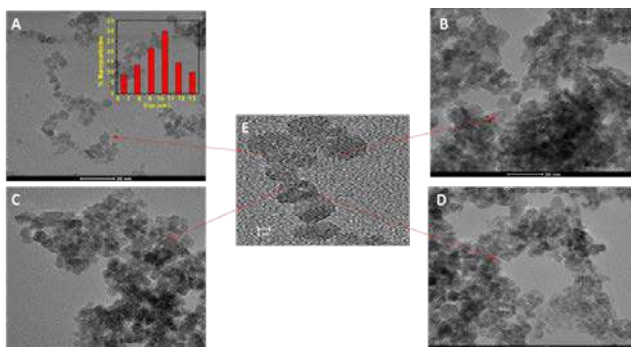


**Figure 2.** HRTEM images of the obtained nanoCeO<sub>2</sub> (A) Uncoated nanoCeO<sub>2</sub>, (B) L-CeO<sub>2</sub>, (C) G-CeO<sub>2</sub> and (D) P-CeO<sub>2</sub>. Histogram of nanoparticles size distribution is shown as inset in (A).

These results show that the treatment with different nanoCeO<sub>2</sub> has stronger effect on plant metabolism when applied during germination compared to its application during growth in hydroponics. Although different coating of selected nanoparticles improves their biocompatibility, the results show that it can influence the difference in plant response.

L-CeO<sub>2</sub> and P-CeO<sub>2</sub> nanoparticles had positive effects on pea phenol content, while there was no effect on wheat phenols, in the aboveground plant parts. This indicates that the effect of nanoparticles depends on plant species and of particle coating, meaning that their toxicity may vary for different plant species. The impact of nanoparticles on morphological parameters, total antioxidative activity and changes in phenolic profile, remains to be investigated.

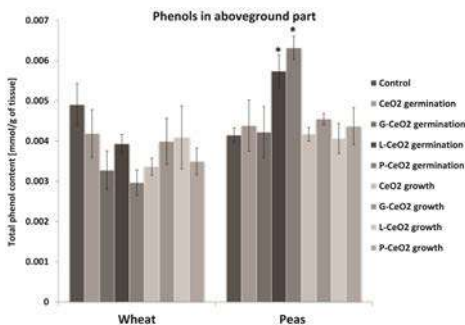


**Figure 3.** Effect of nanoCeO<sub>2</sub>, G-CeO<sub>2</sub>, L-CeO<sub>2</sub> and P-CeO<sub>2</sub> treatment during germination/growth on phenol content in the aboveground parts of wheat and pea plants (Mean±SE; \* indicates statistically significant differences in comparison with control, p<0.05)

## Acknowledgements

This study was supported by the Ministry of Education, Science and Technological Development of the Republic of Serbia, Grant No. 45012

## References

1. Majumdar S, Peralta-Videa RJ, Bandyopadhyay S, Castillo-Michel H, Hernandez-Viezcas J-A, Sahi S, Gardea-Torresdey LJ. Exposure of cerium oxide nanoparticles to kidney bean shows disturbance in the plant defense mechanisms. *J Haz Mater* 2014;278:279-87.
2. Majumdar S, et al. Environmental effects of nanoceria on seed production of common bean (*Phaseolus vulgaris*): A proteomic analysis. *Environ Sci Technol* 2015;49:13283-93.
3. Zhao L, et al. Effect of surface coating and organic matter on the uptake of CeO<sub>2</sub> NPs by corn plants grown in soil: Insight into the uptake mechanism. *J Haz Mater* 2012;225-226:131-8.
4. Mazid M, Khan TA, Mohammad F. Role of secondary metabolites in defense mechanisms of plants. *Biol Med* 2011;3:232-49.
5. Schützendübel A, Polle A. Plant responses to abiotic stresses: heavy metal-induced oxidative stress and protection by mycorrhization. *J Exp Bot* 2002;53:1351-65.
6. Matović B, Dukić J, Babić B, Bučevac D, Dohčević-Mitrović Z, Radović M, Bošković S. Synthesis, calcination and characterization of Nanosized ceria powders by self-propagating room temperature method. *Ceram Int* 2013;39:5007-12.
7. Singleton VL, Rossi JA. Colorimetry of total phenolics with phosphomolybdic-phosphotungstic acid reagents. *Amer J Enol Viticult* 1965;16:144-58.
8. Hu C, Zhang Z, Liu H, Gao P, Wang LZ. Direct synthesis and structure characterization of ultrafine CeO<sub>2</sub> nanoparticles. *Nanotechnology* 2006;17:5983-7.



---

# Newly designed soluble hemagglutinin-Der p 2 chimera is a potential candidate for allergen specific immunotherapy

---

Ivan Mrkić<sup>1\*</sup>, Rajna Minić<sup>2</sup>, Marija Gavrović Jankulović<sup>3</sup>

<sup>1</sup>*Innovation Centre of Faculty of Chemistry, University of Belgrade, Belgrade Serbia*

<sup>2</sup>*Torlak Institute of Virology, Vaccines and Sera, Belgrade, Serbia*

<sup>3</sup>*Faculty of Chemistry, University of Belgrade*

\**e-mail: mrkicivan@gmail.com*

Dust mite allergen Der p 2 contributes to the pathogenesis of respiratory allergic diseases, and is one of the primary targets for allergen specific immunotherapy. In this study a newly created chimera H1sD2, composed of the receptor-binding site of hemagglutinin 1 (H1) from Influenza virus and recombinant Der p 2 (D2), was produced by genetic engineering in *E. coli*. CD spectra of both antigens revealed well defined secondary structures. The chimera preserved IgE reactivity in ELISA and immunoblot with serum of house dust mite allergic persons. Immunogenicity of H1sD2 or D2 antigens was tested in Balb/c mice by intramuscular injection. Levels of D2 specific IgG were determined by ELISA. Spleen leukocytes from injected mice were stimulated with the H1sD2 and D2 antigens and H1sD2 immunization yielded qualitatively different response in comparison to D2 immunization, evidenced by secreted cytokine profile. Unstimulated cells from all groups produced no IL-6, IFN- $\gamma$  or IL-5 with the exception of H1sD2 injected mice whose cells even unstimulated produced a certain amount of IL-6. The level of IL-4 was lowered by *in vitro* stimulation with D2 and even more by stimulation with H1sD2. The expression of IFN- $\gamma$  was notable only in H1sD2 injected group, upon both stimulation with D2 or H1sD2. Both D2 and H1sD2 stimulation led to the production of IL-6, but only stimulation with H1sD2 led to a significant increase of the production of both IL-10 and IL-17. The results indicate that H1sD2 is a more potent immunostimulant, increasing the activation of the Th1 branch of the immune system, that was coupled with IL-17 and IL-10 production <sup>1</sup>.

## Acknowledgements

This work is supported by Grant No. 172049 Ministry of Education, Science and Technological Development of the Republic of Serbia

## References

1. Mrkić I, et al. Modulation of the specific immune response in Balb/c mice by intranasal application of recombinant H1D2 chimera. *J Chem Technol Biotechnol* 2017;92:1328-35.



---

## Chemical composition and antioxidant potential of hydromethanolic extracts of celery (*Apium graveolens* L.) cultivated at different locations in Vojvodina

---

Ivana Nemeš<sup>1\*</sup>, Nataša Simin<sup>1</sup>, Emilija Svirčev<sup>1</sup>, Dejan Orčić<sup>1</sup>, Danijela Arsenov<sup>2</sup>, Nataša Nikolić<sup>2</sup>, Neda Mimica-Dukić<sup>1</sup>

<sup>1</sup>Department of Chemistry, Biochemistry and Environmental Protection, Faculty of Sciences, University of Novi Sad, Novi Sad, Serbia

<sup>2</sup>Department of Biology and Ecology, Faculty of Sciences, University of Novi Sad

\*e-mail: ivanan@dh.uns.ac.rs

Celery (*Apium graveolens* L.) is a plant from the Apiaceae family, cultivated as a popular vegetable all over the world. As a plant with antihypertensive, anticoagulant, hepatoprotective, anti-inflammatory and antioxidant activity, it has been used in traditional medicine since ancient times <sup>1</sup>. Numerous reports confirm that health-promoting benefits of plants could be attributed to their phenolic composition, which can be affected by factors such as: genetic makeup, geographical location, type of soil, climate conditions and agricultural practices <sup>2</sup>.

Since this species is widely grown in Province of Vojvodina in Serbia, the aim of this study was to determine the phenolic profile, as well as to evaluate the antioxidant activity of extracts obtained from celery cultivated at seven different geographical locations within this province. The extracts were prepared by the extraction of dry celery roots with 80% methanol. The total phenolic and total flavonoid contents were determined by standard spectrophotometric assays. The presence and content of 44 selected phenolic compounds were investigated by LC-MS/MS technique <sup>3</sup>. Antioxidant activity was evaluated by measuring the 2,2-diphenyl-1-picrylhydrazyl (DPPH) radical scavenging potential and ability to inhibit lipid peroxidation <sup>4</sup>.

The total phenolic content (5.13-8.50 mg gallic acid equivalents/g of d.e.) and total flavonoid content (0.348-1.063 mg quercetin equivalents/g of d.e.) varied between the samples from different locations. Phenolic compounds examined by LC-MS/MS included 14 phenolic acids, 25 flavonoids, 3 coumarins and 2 lignans. Flavonoid apiin was the most abundant compound, but its concentration varied greatly between the samples obtained from different locations (82.11-881.8 µg/g of dry extract). The most dominant phenolic acids were chlorogenic acid (4.82-41.1 µg/g of d.e.) and ferulic acid (9.49-29.9 µg/g of d.e.). All three investigated coumarins (umbelliferone, scopoletin and esculetin) were detected. The levels of umbelliferone and scopoletin varied greatly among different samples (1.55-108 and 9.67-57.2 µg/g of d.e., respectively). In comparison to standard antioxidant PG, the extracts exhibited weak antioxidant potential (IC<sub>50</sub>=0.349-0.532

mg/mL vs.  $IC_{50}=0.570$   $\mu\text{g/mL}$  in DPPH assay and  $IC_{50}=1.213-3.352$  mg/mL vs.  $IC_{50}=0.056$  mg/mL in LP assay). There were no significant differences in antioxidant activity between the samples from different locations.

In this research, detailed phenolic profile and antioxidant activity of celery root extracts cultivated in seven different locations in Vojvodina were determined. The results suggest that cropping conditions (soil type and agro-technical practices) have an impact on phenolic composition, particularly quantitative. Additionally, the obtained results showed that celery root is a weak antioxidant, while cropping system does not have considerable influence on the activity.

## Acknowledgements

This study was supported by Provincial Secretariat for Science and Technological Development, Autonomous Province of Vojvodina, Serbia (Grant No. 114-451-2149/2016-03, 2016-2019).

## References

1. Sowbhagya HB. Chemistry, technology, and nutraceutical functions of celery (*Apium graveolens* L.): an overview. *Crit Rev Food Sci Nutr* 2014;54:389-96.
2. Manach C, Scalbert A, Morand C, Rémésy C, Jiménez L. Polyphenols: food sources and bioavailability. *Am J Clin Nutr* 2004;79:727-47.
3. Orčić D, et al. Quantitative determination of plant phenolics in *Urtica dioica* extracts by high-performance liquid chromatography coupled with tandem mass spectrometric detection. *Food Chem* 2014;143:48-53.
4. Simin N, et al. Phenolic profile, antioxidant, anti-inflammatory and cytotoxic activities of small yellow onion (*Allium flavum* L. subsp. *flavum*, Alliaceae). *LWT - Food Sci Technol* 2013;54:139-46.

---

## Effects of the bee products on energy status and relative expression of biotransformation and apoptosis genes in healthy and colon cancer cells

---

Danijela Nikodijević\*, Milena Jovanović, Milena Milutinović, Danijela Cvetković, Maja Čupurdija, Jovana Jovankić, Snežana Marković

*Department for Biology and Ecology, Faculty of Science, University of Kragujevac, Kragujevac, Serbia*

\*e-mail: danijela.nikodijevic@pmf.kg.ac.rs

Colorectal cancer is one of the most widespread cancers in the world. Considering to that, there are great interest in using natural products in prevention and curing cancer. In this study, we investigated antitumor effects of royal jelly (RJ) and bee venom (BV) through their influence on cell viability, energy status, genes for biotransformation and apoptosis in healthy lung fibroblasts MRC-5 and cancer cell lines HCT-116 and SW-480.

Evaluation of tested products effects was determined by MTT assay (cytotoxic activity) <sup>1</sup>, energy status was observed by concentration of lactate dehydrogenase in medium as indicator of necrosis, and in lysate as parameter of glycolysis intensity (determined by LDH colorimetric assay <sup>2</sup>) and concentration of adenosine triphosphate (determined by ATP colorimetric assay). Expression of genes whose proteins included in biotransformation (*CYP1A1*, *GSTP1*, *MRP-2* genes) and apoptosis (*BAX* and *BCL-2* genes), were monitored by qRT-PCR method <sup>3</sup>, and relative genes expression were calculated in relation of *β-actin* as housekeeping gene (endogenous control).

Results showed no cytotoxic effect of royal jelly on all tested cell lines. On the contrary, bee venom has a significant cytotoxic effect, and that is shown through IC<sub>50</sub> values (Table 1). The basal LDH concentration was similar in healthy and cancer cells (Table 2), indicating equal rate of glycolysis. Royal jelly significantly increased LDH level in lysate of cancer cell lines suggesting increased glycolysis rate, while did not change this parameter in healthy MRC-5 cells (Table 2). Bee venom was significantly increased LDH concentration in medium (indicator of necrosis) and in lysate (stimulated glycolysis) of all tested cell lines (Table 2); there is no cell selectivity in this treatment. Royal jelly and bee venom generally increased ATP concentration in all tested cell lines (Table 3).

The relative expression of genes, whose proteins were included in biotransformation of xenobiotics and active substances, were changed after both bee products treatments in all tested cells (Table 4). Treatments suppressed of *CYP1A1* gene expression in all three cell lines, with the exception of HCT-116 cells in which BV did not affect the expression of this gene. After treatment of RJ and BV on healthy and SW-480, the results showed increased expression of *GSTP1* gene, while the opposite effect was observed in HCT-116

cells after these treatments. *MRP-2* gene was increased by royal jelly in all cell lines, while bee venom increased this parameter in cancer cell lines, and in healthy cells are decreased. When it comes to expression analysis of BAX and BCL-2 genes, RJ and BV increase the expression of said genes on all cell lines (Table 4). Royal jelly showed cell selective effects in this case - expression of apoptotic genes was higher in healthy than cancer cells.

**Table 1.** Cytotoxic effects - IC<sub>50</sub> values (µg/ml) of RJ and BV on MRC-5, HCT-116 and SW-480 cell lines, after 24 h.

IC <sub>50</sub> (µg/ml)		
Cell line	Treatment	
	RJ	BV
MRC-5	> 500	2.25 ± 1.82
HCT-116	> 500	4.25 ± 1.88
SW-480	> 500	1.27 ± 0.08

**Table 2.** Effects of RJ and BV on LDH concentration in medium and lysate of MRC-5, HCT-116 and SW-480 cell lines, after 24 h.

LDH (OD 490 nm/nr. of viable cells)							
Cell line		Control	RJ		BV		
		0 µg/ml	100 µg/ml	250 µg/ml	0.1 µg/ml	1 µg/ml	2 µg/ml
MRC-5	Medium	1.19±0.02	0.92±0.01*	0.96±0.04*	1.32±0.05	1.20±0.1	3.03±0.28*
	Lysate	2.16±0.07	1.94±0.02*	2.24±0.05	2.36±0.04	2.46±0.06*	4.89±0.12*
HCT-116	Medium	1.11±0.001	1.34±0.09	1.76±0.13*	1.59±0.26	1.81±0.24*	1.93±0.03*
	Lysate	2.36±0.03	2.85±0.08*	3.75±0.07*	2.80±0.29*	3.33±0.12*	4.37±0.01*
SW-480	Medium	1.10±0.03	0.96±0.04*	1.29±0.03*	1.28±0.04*	1.32±0.31*	1.94±0.05*
	Lysate	2.34±0.05	2.27±0.05	4.11±0.06*	3.04±0.05*	3.27±0.04*	4.42±0.08*

Results are expressed as means ± SE for three independent determinations. \*statistically significant difference (p<0.05) compared to control.

**Table 3.** Effects of RJ and BV on ATP concentration in MRC-5, HCT-116 and SW-480 cell lines, after 24 h.

ATP (nmol ATP/µl /nr. of viable cells)						
Cell line	Control	RJ		BV		
	0 µg/ml	100 µg/ml	250 µg/ml	0.1 µg/ml	1 µg/ml	2 µg/ml
MRC-5	0.03±0.001	0.04±0.002*	0.02±0.001	0.02±0.001	0.03±0.002	0.07±0.003*
HCT-116	0.01±0.001	0.04±0.001*	0.05±0.01*	0.03±0.01	0.05±0.01*	0.08±0.001*
SW480	0.03±0.001	0.04±0.01*	0.06±0.002*	0.05±0.001*	0.03±0.01	0.08±0.01*

Results are expressed as means ± SE for two independent determinations. \*statistically significant difference (p<0.05) compared to control.

In conclusion, bee venom shows stronger cytotoxicity than royal jelly according to the IC<sub>50</sub> values and LDH concentrations in the medium. The both treatments caused changes in energy status, by similar increasing of LDH and ATP concentrations, and bee venom is more effective. According to these results, the process of glycolysis was increased in tumor cells in both investigated treatments, while bee venom increased glycolysis also in the healthy cells. Also, based on the results, the examined treatments affect the expression of the gene whose proteins were included in biotransformation of xenobiotics and active substances. Investigated treatments, generally showed increasing of apoptotic genes expression in all cell lines, BV similar in healthy and tumor cells, while RJ shows more

pronounced effects in healthy cells. Based on these results, the royal jelly and bee venom, with their impact on different signaling pathways in colon cancer cells, can be used for future investigations as the potential antitumor substances.

**Table 4.** Relative expression of *CYP1A1*, *GSTP1*, *MRP-2*, *BAX* and *BCL-2* genes in MRC-5, HCT-116 and SW-480 cell lines, after 24 h of treatment with RJ and BV.

RJ (100 µg/ml)					
	<i>CYP1A1</i>	<i>GSTP1</i>	<i>MRP-2</i>	<i>BAX</i>	<i>BCL-2</i>
Control	1	1	1	1	1
MRC-5	0.86	1.75	1.74	2.5	2.1
HCT-116	0.65	0.58	1.72	1.52	1.42
SW-480	0.86	1.04	1.67	1.02	1.61
BV (1 µg/ml)					
	<i>CYP1A1</i>	<i>GSTP1</i>	<i>MRP-2</i>	<i>BAX</i>	<i>BCL-2</i>
Control	1	1	1	1	1
MRC-5	0.95	1.35	0.98	1.29	1.78
HCT-116	1.01	0.89	1.56	1.18	1.97
SW-480	0.77	1.38	1.8	1.09	1.52

## Acknowledgements

This study was supported by Ministry of Education and Science of the Republic of Serbia for financial support (Projects No. III41010). We are grateful to Jelena Rakobradović for donating royal jelly.

## References

1. Mosmann T. Rapid colorimetric assay for cellular growth and survival: application to proliferation and cytotoxicity assays. *J Immunol Meth* 1983;65:55-63.
2. Ka-Ming Chan F, Morawski K, De Rosa MJ. Detection of necrosis by release of lactate dehydrogenase (LDH) activity. *Methods Mol Biol* 2013;979:65-70.
3. Zhai W, Jeong H, Cui L, Krainc D, Tjian R. In vitro analysis of huntingtin-mediated transcriptional repression reveals multiple transcription factor targets. *Cell* 2005;7:1241-1253.



---

## Comparison of prooxidative properties of four different tyrosine kinase inhibitors

---

**Teodora Obradović<sup>1\*</sup>, Biljana Radišić<sup>1\*</sup>, Milan Cerović<sup>1</sup>, Vesna Spasojević-Kalimanovska<sup>1</sup>, Biljana Jančić-Stojanović<sup>2</sup>, Jelena Kotur-Stevuljević<sup>1</sup>**

<sup>1</sup>*Department of Medical Biochemistry, Faculty of Pharmacy, University of Belgrade, Belgrade, Serbia*

<sup>2</sup>*Department of Drug Analysis, Faculty of Pharmacy, University of Belgrade*

\**e-mails: ooteodora@gmail.com; radisicbiljana307@gmail.com*

Oxidative stress (OS) has been characterized by an imbalance between the production of reactive oxygen species and an organism's capability to maintain adequate redox balance by using antioxidative system resources. Enzyme paraoxonase 1 (PON1) is located at the HDL lipoprotein particles and is a part of specific antioxidative system of our organism. Redox disbalance could cause protein, lipid and DNA damage and further disorders of different cellular functions. OS is important mechanism in pathogenesis of cancer. Moreover, chemotherapeutic drugs could induce oxidative stress in target cells <sup>1</sup>.

We have used four tyrosine kinase inhibitor (TKI) drugs: imatinib, crizotinib, axitinib and nilotinib as 80 mg/L DMSO solutions, which was added to serum pool samples. We aimed to compare prooxidative potential of these four substances in biological material by measuring the PON1 enzymatic activity. In order to combat increased oxidative stress in a separate series of serum samples we have added vitamin E and measured the same parameter activity (PON1). Results are presented at the Figure 1.

Crizotinib and axitinib which are second generation TKI drugs, caused significant decrease in PON1 enzymatic activity as a consequence of their stronger prooxidant activity, compared to imatinib, so as nilotinib. Vitamin E addition leads to very similar pattern in PON1 activity of all 4 drugs, with slightly higher values compared to samples without vitamin E. Samples with crizotinib and axitinib upon the vitamin E addition showed significantly higher PON1 activities than in the samples with the same drug, but without vitamin E. A previous study has shown that second generation TKI drugs has stronger oxidative stress effects, which is just partially showed in our investigation <sup>2</sup>.

Results of several studies showed an increased risk of cardiovascular (atherothrombotic) events in chronic myeloid leukemia patients receiving nilotinib <sup>3,4</sup>.

Having in mind that all four ITK drugs analysed in this current study, could decrease PON1 activity, there is a strong need for further investigation of long-term effects of these drugs.

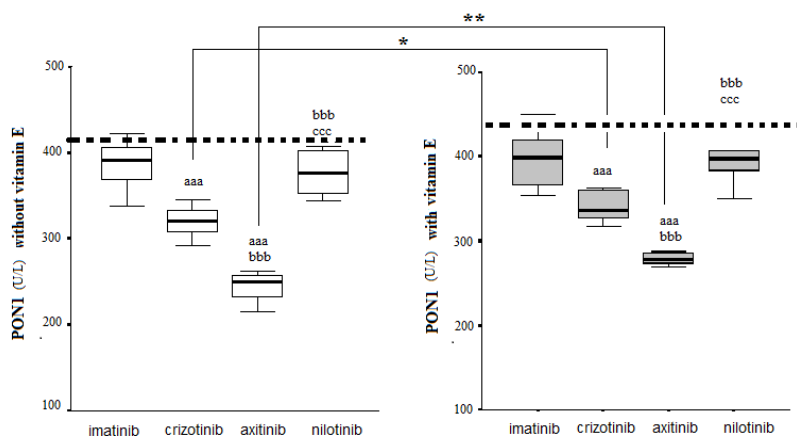


**Figure 1.** Different level of prooxidative activity of four different tyrosine-kinase inhibitors: imatinib, crizotinib, axitinib and nilotinib, measured through the paraoxonase 1 (PON1) activity determination (aaa, bbb, ccc -  $P < 0.001$  vs. imatinib, crizotinib and axitinib, respectively; \*, \*\* -  $P < 0.05, 0.01$  between the same drug with vitamin E: crizotinib, axitinib, respectively); Dashed line - baseline values: serum + DMSO or serum + DMSO + vitamin E.

## References

1. Udensi KU, Tchounwou PB. Dual effect of oxidative stress on leukemia cancer induction and treatment. *J Exp Clin Cancer Res* 2014;33:1-15.
2. Damiano S, et al. Comparison of dasatinib, nilotinib, and imatinib in the treatment of chronic myeloid leukemia. *J Cell Physiol* 2016;231:680-7.
3. Awad MM, Shaw AT. ALK inhibitors in non-small cell lung cancer: crizotinib and beyond. *Clin Adv Hematol Oncol* 2014;12:429-39.
4. Bocchia M, et al. Genetic predisposition and induced pro-inflammatory/prooxidative status may play a role in increased atherothrombotic events in nilotinib treated chronic myeloid leukemia patients. *Oncotarget* 2016;7:72311-21.

---

## Imaging and regional distribution of copper, zinc, manganese and iron in sclerotic hippocampi of patients with mesial temporal lobe epilepsy

---

Miloš Opačić<sup>1\*</sup>, Aleksandar J. Ristić<sup>2</sup>, Danijela Savić<sup>3</sup>, Vid Simon Šelih<sup>4</sup>, Marko Živin<sup>5</sup>, Dragoslav Sokić<sup>2</sup>, Savo Raičević<sup>6</sup>, Vladimir Baščarević<sup>6</sup>, Ivan Spasojević<sup>1</sup>

<sup>1</sup>Department of Life Sciences, Institute for Multidisciplinary Research, University of Belgrade, Belgrade, Serbia

<sup>2</sup>Center for Epilepsy and Sleep Disorders, Neurology Clinic, Clinical Center of Serbia, Belgrade, Serbia

<sup>3</sup>Department of Neurobiology, Institute for Biological Research 'Siniša Stanković', University of Belgrade

<sup>4</sup>Department of Analytical Chemistry, National Institute of Chemistry Slovenia, Ljubljana, Slovenia

<sup>5</sup>Brain Research Laboratory, Institute of Pathophysiology, Medical Faculty, University of Ljubljana, Ljubljana, Slovenia

<sup>6</sup>Neurosurgery Clinic, Clinical Center of Serbia, Belgrade, Serbia

\* e-mail: milos@imsi.bg.ac.rs

Mesial temporal lobe epilepsy (mTLE) represents the most common subtype of human focal epilepsies and perhaps the best-characterized disorder of this type <sup>1</sup>. Hippocampal sclerosis (HS) is the most common histopathologic abnormality found in adults with drug-resistant mTLE <sup>2</sup>. The histopathologic hallmark of HS is segmental pyramidal cell loss, which can affect any field of the *cornu Ammonis* (CA1-4). Hippocampal neuronal cell loss is always associated with a severe pattern of astrogliosis <sup>3</sup>. Therewithal, disturbed homeostasis of metals is implicated in the pathology of mTLE-HS. Zinc has been considered to play a major role in epileptogenesis in relation to its involvement in the modulation of excitability and synaptic plasticity <sup>4,5</sup>. Further, it has been shown that epileptogenic hippocampi are exposed to oxidative stress and that the development of pro-oxidative conditions in the CNS usually involves the loss of homeostasis of iron <sup>6,7</sup>. Low brain levels of copper and manganese have been reported in patients with Menkes disease and in animal models of epilepsy, and linked to seizure development <sup>8,9</sup>. Ristić et al. were the first to conduct a case-control study of total concentration of metals in tissue of human HS, and report lower concentrations of copper and manganese <sup>10</sup>.

We herein applied laser ablation inductively coupled plasma mass spectrometry (LA-ICP-MS) imaging to produce copper, zinc, manganese and iron maps of coronal sections of sclerotic hippocampi of mTLE patients. The aims were to present spatial distribution of

these metals in different fields and layers of the hippocampus and to establish relation between neuron loss and metal concentrations in *stratum pyramidale* (SPy) of the CA1.

The study was performed on hippocampi of four patients with drug-resistant mTLE-HS. The epileptic hippocampi were removed en bloc, in the course of anterior temporal lobe resection and amygdalohippocampectomy. The posterior parts of the head of the sclerotic hippocampi were cryopreserved in liquid N<sub>2</sub> and stored at -80°C. Serial 16 µm thick coronal sections were cut on a cryostat, dried in air, and protected with metal-free foil until further analysis. Adjacent slices were used for LA-ICP-MS imaging and for histological staining with cresyl violet (CV). Analysis was performed in ImageJ image processing software (NIH).

It can be observed that the human hippocampus shows a high degree of spatial organization of metals (Figure 1). The highest Zn levels were found in the regions that contain mossy fibers - CA4, *gyrus dentatus* (GD) and CA3. Comparatively high Fe concentrations were found in the *subiculum* (SUB). LA-ICP-MS images of Fe show several bright spots indicating a high concentration of iron in the tissue. These most likely come from hemoglobin in larger blood vessels. The highest level of Cu is found in the SUB, followed by CA4, the GD, and the SPy in CA1. Mn concentration was significantly higher in regions with neuron somata compared to the regions that contain axons and dendrites. *Alveus* showed the lowest level of all the examined metals.

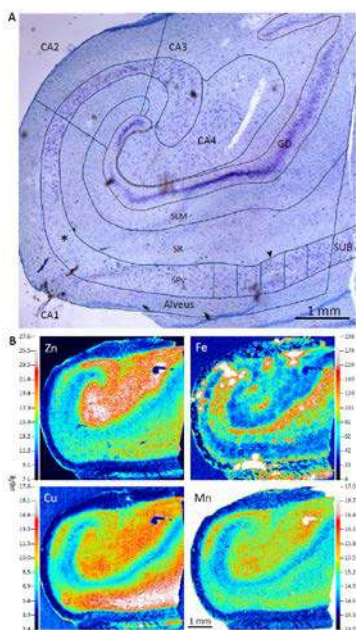


**Figure 1.** LA-ICP-MS images of Cu, Zn, Mn and Fe content of the coronal section of human sclerotic hippocampus. Asterisk - CA1 region of the total neuronal loss.

The concentration of Cu was decreased in the area of total neuronal loss, whereas both the Cu and Mn concentrations showed positive correlation with neuron somata density in the SPy of CA1. This is in line with our previous results showing that the total concentrations of these metals are lower in sclerotic hippocampi compared to controls<sup>10</sup>. The processes behind the decrease of Cu concentration in sclerotic areas remain to be elucidated. A defect in Cu transport is proposed to play an essential role in the development of seizures and neuron loss in Menkes disease<sup>8</sup>. Our next step will be to analyze the regional distribution of copper transporting machinery and copper-containing proteins in order to elucidate the role of this metal in HS and to identify novel viable targets for noninvasive treatment of patients with mTLE-HS.

## Acknowledgements

This study was supported by Slovenian Research Agency (ARRS), project numbers P3-0171 and P1-0034, and by the Ministry of Education, Science and Technological Development of the Republic of Serbia, Grant numbers III41014 and OI173014.

## References

1. Tatum WO 4<sup>th</sup>. Mesial temporal lobe epilepsy. *J Clin Neurophysiol* 2012;29:356-65.
2. Blumcke I, Coras R, Miyata H, Ozkara C. Defining clinic-neuropathological subtypes of mesial temporal lobe epilepsy with hippocampal sclerosis. *Brain Pathol* 2012;22:402-11.
3. Blumcke I, et al. International consensus classification of hippocampal sclerosis in temporal lobe epilepsy: A Task Force report from the ILAE Commission on Diagnostic Methods. *Epilepsia* 2013;54:1315-29.
4. Frederickson CJ, Koh JY, Bush AI. The neurobiology of zinc in health and disease. *Nat Rev Neurosci* 2005;6:449-62.
5. Mitsuya K, Nitta N, Suzuki F. Persistent zinc depletion in the mossy fiber terminals in the intrahippocampal kainate mouse model of mesial temporal lobe epilepsy. *Epilepsia* 2009;50:1979-90.
6. Ristić AJ, et al. Hippocampal antioxidative system in mesial temporal lobe epilepsy. *Epilepsia* 2015;56:789-99.
7. Kell DB. Iron behaving badly: inappropriate iron chelation as a major contributor to the aetiology of vascular and other progressive inflammatory and degenerative diseases. *BMC Med Genomics* 2009;2:2.
8. Schlieff ML, West T, Craig AM, Holtzman DM, Gitlin JD. Role of the Menkes copper-transporting ATPase in NMDA receptor-mediated neuronal toxicity. *Proc Natl Acad Sci USA* 2006;103:14919-24.
9. Gonzalez-Reyes RE, Gutierrez-Alvarez AM, Moreno CB. Manganese and epilepsy: a systematic review of the literature. *Brain Res Rev* 2007;53:332-6.
10. Ristić AJ, et al. Metals and electrolytes in sclerotic hippocampi in patients with drug-resistant mesial temporal lobe epilepsy. *Epilepsia* 2014;55:e34-7.



---

## Environmental effect on metallothionein gene expression in honey bee (*A. mellifera*)

---

Snežana Orčić<sup>1\*</sup>, Tatjana V. Nikolić<sup>1</sup>, Danijela Kojić<sup>1</sup>, Elvira Vukašinić<sup>1</sup>, Dragana Vujanović<sup>2</sup>, Ivan Gržetić<sup>3</sup>, Konstantin Ilijević<sup>3</sup>, Duško P. Blagojević<sup>4</sup>, Jelena Purać<sup>1</sup>

<sup>1</sup>Department of Biology and Ecology, Faculty of Sciences, University of Novi Sad, Novi Sad, Serbia

<sup>2</sup>Faculty of Pharmacy, University of Belgrade, Belgrade, Serbia

<sup>3</sup>Faculty of Chemistry, University of Belgrade

<sup>4</sup>Institute for Biological Research "Siniša Stanković", University of Belgrade

\* e-mail: snezana.orcic@dbe.uns.ac.rs

The molecular basis of the interaction of honey bees with their environment has attracted more attention in recent years because of the global decline of the honey bee populations. It is considered that a better understanding of the mechanisms that mediate the interaction of honey bees with stress factors in the environment contribute to the conservation of this species. Bees are exposed to numerous pollutants contaminating their habitat, either directly from the atmosphere and water or indirectly by consumption of pollen and nectar originating from plants growing in a polluted environment <sup>1</sup>. This study aims to analyze the response of the metallothionein gene (*Mtn*) in honey bees related to the presence of heavy metals in habitats with different degrees of urbanization. Samples of bees were collected during the active season from three different localities in Serbia: rural area on Fruška Gora Mountain (control), urban area of Belgrade, and the surroundings of an industrial facility in Zajača. Concentrations of four metals: copper, zinc, cadmium and lead, were determined in the honey bees using ICP-OES against multi-element standard solutions. In order to determine the relative expression of *Mtn* gene using qPCR method, total RNA was isolated from the abdomen of the bees. The results show that bees from the urban area had significantly higher concentrations of zinc, while bees from the industrial area had elevated concentrations of cadmium and lead, in comparison with bees from the rural area. Furthermore, *Mtn* gene expression was significantly higher in bees from both the urban and industrial area, compared to bees from the rural area. Metallothionein plays a significant role in the response to stress caused by heavy metals and is considered to be a good biomarker in medicine and ecology <sup>1</sup>. Induction of *Mtn* gene in bees from urban and industrial areas could be linked to elevated concentrations of metal ions originated from the environment. However, in natural populations, expression of this gene could be affected by other stressors, such as viral infections, alkylating agents etc., which could induce metallothionein response as well <sup>2</sup>.

## **Acknowledgements**

This study was supported by the Ministry of Education, Science and Technological Development of the Republic of Serbia, Grant No. OI173014.

## **References**

1. Lambert O, Piroux M, Puyo S, Thorin C, Larhantec M, Delbac F, Pouliquen H. Bees, honey and pollen as sentinels for lead environmental contamination. *Env Pol* 2012;170:254-9.
2. Carpena E, Andreani G, Isani G. Metallothionein functions and structural characteristics. *J Trace Elem Med Biol* 2007;21:35-9.

---

## Mechanism of action of novel ruthenium(III) complexes toward cisplatin resistant MDA-MB231 breast cells

---

Marijana Pavlović<sup>1\*</sup>, Sandra Arandelović<sup>1</sup>, Sanja Grgurić-Šipka<sup>2</sup>, Nevzeta Ljubijankić<sup>3</sup>, Siniša Radulović<sup>1</sup>

<sup>1</sup>Department of Experimental Oncology, Institute for Oncology and Radiology of Serbia, Belgrade, Serbia

<sup>2</sup>Faculty of Chemistry, University of Belgrade, Belgrade, Serbia

<sup>3</sup>Department of Chemistry, Faculty of Science, University of Sarajevo, Sarajevo, Bosnia and Herzegovina

\*e-mail: marijana.kajzerberger@gmail.rs

Since the discovery of cisplatin (*cis*-diamminedichloridoplatinum (II), CDDP) as a successful chemotherapeutic <sup>1</sup>, a great challenge came out for medicinal chemists regarding design of the less toxic anticancer agents, with fewer side-effects and greater cytoselectivity. Ruthenium compounds have received much attention lately because of their promising anticancer activity. Two compounds named KP1019 and NAMI-A have already been evaluated in clinical trials <sup>2</sup>. Here we report the evidence of *in vitro* cytotoxic activity of the four newly synthesized ruthenium(III) complexes with bidentate anionic schiff base derived from 5-methylsalicylaldehyde and methylamine: (SB10), (SB13), (SB14), (SB15). Cisplatin was used in this study, as a referent compound. *In vitro* antitumor activity of complexes was determined on human cancer cell lines derived from myelogenous leukemia (K562), alveolar basal adenocarcinoma (A549), umbilical vein endothelium (EA.hy926), breast adenocarcinoma (MDA-MB231), and on non-tumor human fetal lung fibroblast cell line (MRC-5), after 48 h of continuous drug action, by using MTT assay. The average IC<sub>50</sub> values, obtained from cell survival diagrams, were in the low micromolar range 2-23 μM, depending on cell line (Table 1). Investigated complexes displayed an apparent cytoselective profile, as they reduced the viability of tested tumor cell lines more efficiently than of the non-tumor MRC-5 cells. SB10 and SB13 exhibited higher cytotoxicity comparing to SB14 and SB15. Interestingly, cisplatin resistant MDA-MB231 cells showed significantly greater sensitivity to all tested complexes. Complex Na[RuLCl<sub>2</sub>], L=N-propyl-5-chlorosalicylaldiminato, SB10, appeared to be the most potent against MDA-MB231 cells (IC<sub>50</sub>=2μM), and is ten times more active than cisplatin (IC<sub>50</sub>=21.9 μM). The biggest problem in the successful treatment of triple-negative breast cancer is how to manage the drug resistance after the treatment with cancer therapeutics such as cisplatin <sup>3</sup>. Interesting cytotoxicity of tested complexes raised a demand to further examine their mechanism of action. Being the most cytotoxic of all four tested complexes, SB10 is selected for further analyses of molecular mechanisms underlying its activity toward MDA-MB231 cells.

**Table 1.** IC<sub>50</sub> [μM] values obtained after 48 h of continuous drug action.

Compound	K562	A549	EA.hy926	MDA-MB231	MRC-5
SB10	3.89±0.35	4.50±1.35	2.97±0.53	2.0±0.3	13.63±6.43
SB13	6.81±2.45	10.83±6.08	6.84±1.29	3.83±1.53	17.69±0.48
SB14	8.85±2.29	10.89±0.56	10.7±2.62	6.32±1.55	13.35±0.80
SB15	7.18±1.01	13.17±7.46	8.29±1.85	4.77±2.2	23.02±0.06
CDDP	11.0±1.2	17.0±0.6	11.08±2.71	21.9±2.3	15.0±1.7

\* IC<sub>50</sub> [μM] values are presented as the mean ± SEM of three independent experiments.

The capability of SB10 complex and cisplatin to induce cell cycle alterations in MDA-MB231 cells, was examined by flow-cytometry after 24 h and 48 h of continual drug treatment and staining with PI. Results are presented in Figure 1. 24h treatment with SB10 complex with IC<sub>50</sub> and 2xIC<sub>50</sub> values, induced cell cycle alterations, in manner different to cisplatin and characterized by minor increase in the Sub-G1 fraction of cells (4.8% and 5.2%, respectively, comparing to 2.4% in control cells), and slight decrease in the S phase. Prolonged incubation (48 h) of MDA-MB231 cells with SB10, induced major changes in cell cycle phases, characterized by substantial accumulation of cells in Sub-G1 region, up to 22.4% (IC<sub>50</sub>) and 76.5% (2xIC<sub>50</sub>), comparing to control (4.8%). These results showing accumulation of cells in Sub-G1 region, indicate that possible mechanism by which SB10 display cytotoxic activity toward MDA-MB231 cells could be by activation of apoptotic machinery through the interactions of this metal complex with DNA<sup>4</sup>.

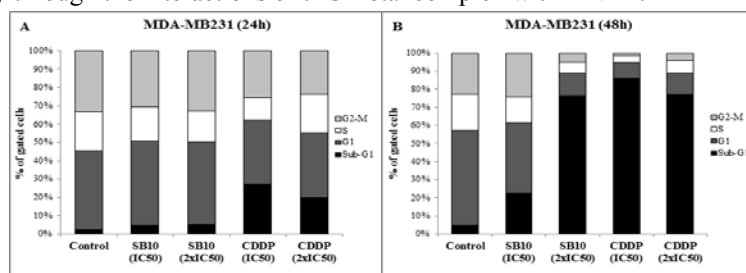


**Figure 1.** Diagrams of cell cycle phase distribution of MDA-MB-231 cells after 24 h (A) and 48 h (B) of treatment with SB10 complex or CDDP, at concentrations corresponding to IC<sub>50</sub> and 2xIC<sub>50</sub>.

Morphological characteristics of cell death of MDA-MB231 cells, induced by SB10 complex or cisplatin, were analyzed by fluorescent microscopy and acridine orange/ethidium bromide (AO/EtBr) dual staining, after 24 h and 48 h of continuous drug treatment, with concentrations corresponding to IC<sub>50</sub> (Figure 2). After 24 h of treatment with SB10 (IC<sub>50</sub>), cell number is reduced; cells became rounded with morphology of early apoptosis with condensed peri-nuclear chromatin (green fluorescence). 48 h treatment with SB10, induced more reduction in cell number and occurrence of apoptotic bodies. Same treatment conditions, also induced morphological changes characteristic for secondary apoptosis and necrosis (red fluorescing nuclei), more condensed chromatin and disrupted cell membrane. According to these results, it cannot be distinguished whether SB10 cause

apoptosis or necrosis of MDA-MB231 cells. To closely characterize type of cell death, MDA-MB231 cells were incubated with SB10, in the presence of caspase inhibitor Z-VAD-FMK (Calbiochem) or necrosis inhibitor IM-54 (Calbiochem), applied in concentration of 10  $\mu$ M, and viability of cells was evaluated by MTT assay. SB10 treated MDA-MB231 cells displayed enhanced survival in the presence of IM-54 ( $IC_{50}$ =3.65  $\mu$ M) and Z-VAD-FMK ( $IC_{50}$ =4.2  $\mu$ M) inhibitors. This indicates that SB10 complex could at least partially induce caspase-dependent cell death in MDA-MB231 cells, which is in concordance with the previous results gained by fluorescent microscopy.

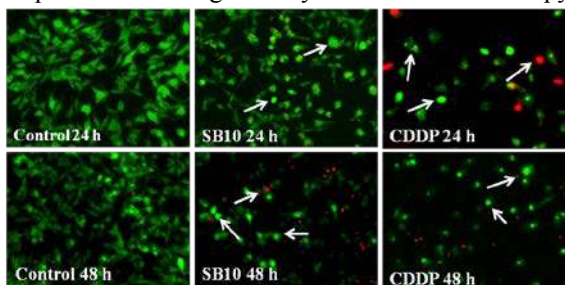


**Figure 2.** Micrographs of acridine orange/ethidium bromide-stained MDA-MB231 control cells and cells exposed for 24 h and 48 h to SB10 or CDDP, at concentrations corresponding to  $IC_{50}$ . Arrows indicate characteristic changes in cell morphology after the treatment with tested compounds.

These results may be considered promising for additional biological studies and further investigation of mechanism of action of this type of ruthenium(III) complexes.

## Acknowledgements

This work was supported by the grant from the Ministry of Education and Science of the Republic of Serbia (Grant number III 41026).

## References

1. Rosenberg B, Van Camp L, Krigas T. Inhibition of cell division in *Escherichia coli* by electrolysis products from a platinum electrode. *Nature* 1965;205:698-9.
2. Bergamo A, Gaiddon C, Schellens JH, Beijnen JH, Sava G. Approaching tumour therapy beyond platinum drugs: status of the art and perspectives of ruthenium drug candidates. *J Inorg Biochem.* 2012;106:90-9.
3. Liu J, Chen X, Ward T, Pegram M, Shen K. Combined niclosamide with cisplatin inhibits epithelial-mesenchymal transition and tumor growth in cisplatin-resistant triple-negative breast cancer. *Tumor Biol* 2016;37:9825-35.
4. Nikolić S, Oспенica DM, Filipović V, Dojčinović B, Arandjelović S, Radulović S, Grgurić-Šipka S. Strong in vitro cytotoxic potential of new ruthenium-cymene complexes. *Organometallics* 2015;34:3464-73.



---

## Direct effects of $\gamma$ -rays in MCF-7 breast cancer cells

---

Vladana Petković, Otilija Keta\*, Marija Vidosavljević, Ivan Petrović, Aleksandra Ristić Fira

<sup>1</sup>*Vinča Institute of Nuclear Sciences, University of Belgrade, Belgrade, Serbia*

\**e-mail: otijak@vin.bg.ac.rs*

DNA damage is considered as the crucial outcome of ionizing radiation, since the destabilisation of DNA can alter cellular functions and lead to cell death. Radiation damages DNA directly or indirectly, through radiolysis of water. As the result, different types of DNA damages arise, such as DNA strand breaks, base modifications and protein-DNA crosslinks. Among them, the DNA double strand breaks (DSB) are considered as the most dangerous, as failure to repair these lesions can induce cell death<sup>1</sup>. In response to DSB, DNA repair mechanisms are activated. One of the earliest signal molecules involved in DSB repair is histone H2AX. When DSB occur, H2AX becomes phosphorylated ( $\gamma$ H2AX) near the site of lesion and attracts other molecules that will regulate DSB repair. Due to its role,  $\gamma$ H2AX has been used as a marker of the DNA DSB<sup>2</sup>.

The aim of the present study is to test direct effects of  $\gamma$ -rays on human cancer cell lines, to be compared with the direct action of radiation with high energy particles (therapeutic protons and carbon ions). In order to obtain proper experimental conditions, free radical scavengers (DMSO or glycerol) are applied.

The present study was carried out on MCF-7 breast adenocarcinoma cells that were obtained from the ATCC and cultured in standard conditions in humidified atmosphere at 5% CO<sub>2</sub> and 37°C. One hour before irradiation, cells were incubated with DMSO (1, 100, 250, 500 mM) or glycerol (2, 200 mM). The irradiations were performed with <sup>60</sup>Co  $\gamma$ -rays in air at room temperature. Dose range was from 0.1 to 2 Gy at the dose rate of ~1 Gy/min. For analyses of the cell survival, clonogenic assay was performed as described previously<sup>3</sup>. Immunocytochemical analyses of  $\gamma$ H2AX was carried out to observe DSB formation 0.5 h after irradiation, the time point when it reaches the peak of expression<sup>3,4</sup>.

Clonogenic cell survival revealed that MCF-7 are radio-resistant. The analyses of cell survival at 2 Gy (SF2) also show protective effect of DMSO. Pre-treatment with DMSO increases SF2 from 0.52 in only irradiated cells to 0.56 in cells pre-treated with 100 mM DMSO. With the rise of DMSO concentration up to 250 or 500 mM, SF2 values reach 0.65 and 0.67, respectively. The same protective effect is observed with 2 and 200 mM glycerol (0.77 and 0.79 respectively). The number of  $\gamma$ H2AX foci increases in MCF-7 cells in the dose dependent manner. With the administration of DMSO or glycerol, the number of  $\gamma$ H2AX is lower as compared to only irradiated cells, as presented in Figure 1. The best protective effect is attained in 100 mM DMSO pre-treated cells. The scavenging effect of DMSO is related to the decrease of DNA damage caused by indirect actions of radiation.

The same effects are observed with both concentrations of glycerol. These results are in accordance with our previously published data <sup>3</sup>.

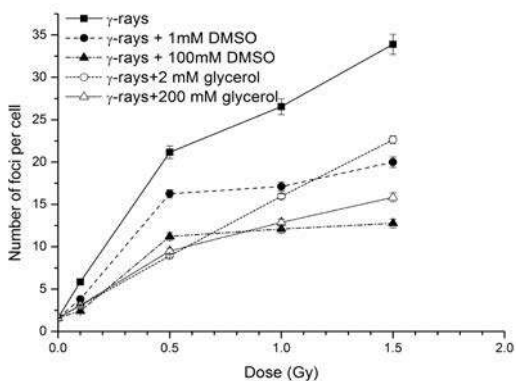


**Figure 1.** Immunocytochemical analyses of  $\gamma$ H2AX foci in MCF-7 cells 0.5 h after irradiation with  $\gamma$ -rays. Irradiation doses were 0.1, 0.5, 1 and 1.5 Gy, at the dose rate of  $\sim 1$  Gy/min. Results are presented as mean number of  $\gamma$ H2AX foci  $\pm$  SEM.

DMSO and glycerol show protective effect in  $\gamma$ -irradiated MCF-7 cells, which is related to their free radical scavenging role. These results will serve for comparison of direct effects in therapeutic proton and carbon ion radiation.

## Acknowledgements

This work was financially supported by the Ministry of Education, Science and Technological Development of Serbia (Grant No. 173046 and 171019).

## References

1. Goodhead DT. Initial events in the cellular effects of ionizing-radiations: clustered damage in DNA. *Int J Radiat Biol* 1994;65:7-17.
2. Stiff T, O'Driscoll M, Rief N, Iwabuchi K, Löbrich M, Jeggo PA. ATM and DNA-PK function redundantly to phosphorylate H2AX after exposure to ionizing radiation. *Cancer Res* 2004;64:2390-6.
3. Petković V, Keta O, Vojnović N, Incerti S, Petrović I, Ristić Fira A. Radioprotective effect of DMSO and glycerol in human non-small cell lung cancer irradiated with gamma rays. 13th International Conference on Fundamental and Applied Aspects of Physical Chemistry, Belgrade, September 26-30, 2016.
4. Rogakou EP, Pilch DR, Orr AH, Ivanova VS, Bonner WM. DNA double-stranded breaks induce histone H2AX phosphorylation on serine 139. *J Biol Chem* 1998;273:5858-68.

---

## Is wine price a guarantee for its healthful properties?

---

Diandra Pintac\*, Nataša Simin, Dejan Orčić, Neda Mimica-Dukić, Marija Lesjak

<sup>1</sup>*Department of Chemistry, Biochemistry and Environmental Protection, Faculty of Sciences, University of Novi Sad, Novi Sad, Serbia*

\**e-mail: diandra.pintac@dh.uns.ac.rs*

Wine phenolics influence the colour, bouquet, astringency, and bitterness of the wine, and represent chemotaxonomic markers for distinguishing different grape varieties <sup>1</sup>. Besides contributing to the quality of wine by affecting the organoleptic properties, phenolic compounds are also mainly responsible for the health benefits associated with wine, thanks to their strong antioxidant activity <sup>2</sup>. In this study a quality assessment was made by comparing the market price, biological activity and phenolic content of six commercially available Cabernet Sauvignon wines from the region of Fruška Gora, Serbia. Wines were divided into two groups based on the price range - lower (manufacturers: Podrum Petrović, MK Kosović, Dulka) and higher (manufacturers: Bajilo, Mrđanin, Živanović) priced products. The antioxidant potential of the samples was determined through the scavenging of diphenylpicrylhydrazyl and nitric oxide radicals, and Ferric Reducing Antioxidant Power assay (FRAP), while the neuroprotective effect was estimated through a potential inhibition of acetylcholinesterase. Also, total phenolic and flavonoid contents of Cabernet Sauvignon wines were determined spectrophotometrically. Generally, two out of three higher priced wines did exert a better biological activity and higher phenolic and flavonoid content, compared with lower priced products, with Cabernet Sauvignon Živanović being the most representative sample. However, Cabernet Sauvignon Podrum Petrović did not only express the best activity amongst the lower priced wines, it also proved to be the most active sample to scavenge nitric oxide, with the highest flavonoid content compared to all the tested wines. Novel data on commercial Cabernet Sauvignon wines from Fruška Gora presented here show a good correlation between the biological activity and the total phenolic and flavonoid content of the samples, suggesting that these compounds do influence the health benefits of wine and contribute to its quality. However, a clear correlation between the price and biological activity was not observed.

### Acknowledgements

This study was supported by the Ministry of Education, Science and Technological Development of the Republic of Serbia (Grant No. 172058).

## References

1. Seabra RM, et al. Principal components of phenolics to characterize red Vinho Verde grapes: Anthocyanins or non-coloured compounds? *Talanta* 2008;75:1190-202.
2. Villaño D, Fernández-Pachón MS, Troncoso AM, García-Parrilla C. Comparison of antioxidant activity of wine phenolic compounds and metabolites in vitro. *Anal Chim Acta* 2005;538: 391-8.

---

## Identification of potential inhibitors of AKR1C3 and preparation for structural analyses

---

Jovana J. Plavša<sup>1</sup>, Jovana Ajduković<sup>2</sup>, Anđelka Čelić<sup>1</sup>, Marija Sakač<sup>2</sup>, Edward T. Petri<sup>1\*</sup>

<sup>1</sup>*Department of Biology and Ecology, Faculty of Sciences, University of Novi Sad, Novi Sad, Serbia*

<sup>2</sup>*Department of Chemistry, Biochemistry and Environmental Protection, Faculty of Sciences, University of Novi Sad*

\**e-mail: Edward.Petri@dbe.uns.ac.rs*

Aldo-keto reductase family 1 member C3 is an important enzyme in steroidogenesis and redox homeostasis in humans. This enzyme uses NADH and/or NADPH as cofactors to catalyze conversion of aldehydes and ketones to alcohols. Overexpression of AKR1C3 contributes to tumor development and inhibition of AKR1C3 activity represents a promising target for development of new therapies<sup>1</sup>. To understand how inhibitors bind to AKR1C3, we are planning to test recombinant AKR1C3 protein for crystallization in complex with new ligands.

Tested compounds have steroid core with modification that include heterocyclic systems as a part of their A-rings. These and other modifications display a range of biological properties such as anti-inflammatory, antimicrobial, anticancer, hypotensive, hypocholesterolemic and diuretic activities<sup>2</sup>. An *in vitro* spectrophotometric assay for measuring enzyme activity was developed. Phenanthrenequinone (PQ) was used as a positive control and ibuprofen (IBU) as a known inhibitor. According to the enzyme activity plot (Figure 1) compound 3 have good inhibitory potential, compared to IBU.

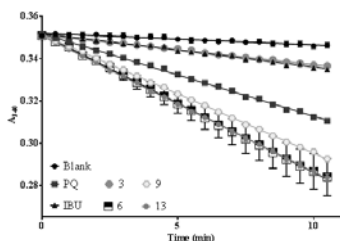


**Figure 1.** AKR1C3 activity plot. Graphic shows relation between time and change in absorbance of NADPH on 340 nm in the presence of AKR1C3 and different tested compounds.

We are optimizing docking system for AKR1C3 with these compounds, and now we are in position to test potent new inhibitors or to explain differences between binding different substrates. At the moment, according to docking results, compound 3 has most fixed orientation almost without any changes in position, compound 13 has fixed orientation but position of group on C17 position occupies different orientations.

There are several published crystal structures of AKR1C3 with different substrates (PDB code: 1XF0, 1ZQ5, 1S1P etc.) solved by the use of X-ray crystallography. Crystallization conditions and protocols of these, has been used for the initial crystallization screening and we got first crystals with 1.5Å (Figure 2), however further optimization is needed.

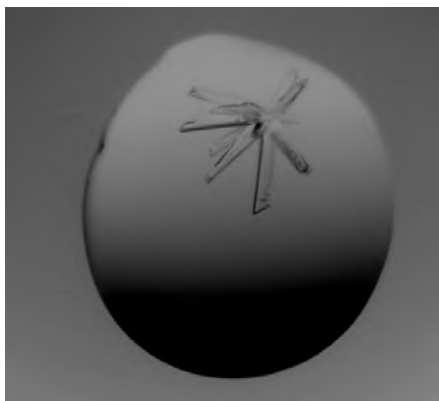


**Figure 2.** Crystals of AKR1C3.

## **Acknowledgements**

This study was supported by Ministry of Education, Science and Technological Development, Republic of Serbia (Project ON172021 and ON173014).

## **References**

1. Adeniji AO, Chen M, Penning TM. AKR1C3 as a target in castrate resistant prostate cancer. *J Steroid Biochem* 2013;137:136-49.
2. Aiduković JJ, et al. 17 (E)-Picolinylidene androstane derivatives as potential inhibitors of prostate cancer cell growth: antiproliferative activity and molecular docking studies. *Bioorgan Med Chem* 2013;21:7257-66.

---

## **Whole grain of peanut digestomics according to harmonized static digestion protocol suitable for solid food and characterization of short digestion resistant fragments.**

---

**Ivana Prodić<sup>1\*</sup>, Dragana Stanić-Vučinić<sup>2</sup>, Danijela Apostolović<sup>3</sup>, Jelena Mihailović<sup>2</sup>, Jelena Radosavljević<sup>2</sup>, Katarina Smiljanić<sup>2</sup>, Tanja Ćirković Veličković<sup>2,4</sup>**

*<sup>1</sup>Faculty of Chemistry - Innovation Centre Ltd., University of Belgrade, Belgrade, Serbia*

*<sup>2</sup>Faculty of Chemistry - CoE for Molecular Food Sciences, University of Belgrade,*

*<sup>3</sup>Department of Medicine Solna, Karolinska Institute, Stockholm, Sweden*

*<sup>4</sup>Ghent University Global Campus, Incheon, South Korea and Faculty of Bioscience Engineering, Ghent University, Ghent, Belgium*

*\*e-mails: [iprodic@chem.bg.ac.rs](mailto:iprodic@chem.bg.ac.rs); [ivana.prodic@gmail.com](mailto:ivana.prodic@gmail.com)*

Most allergens are considered to sensitize an individual via GIT, so digestibility represents an important factor in food allergenicity. Studies of digestion were carried out on purified proteins <sup>1</sup>, using aqueous extracts of defatted food proteins, paying no attention to the impact of food matrix. General standardized static digestion method <sup>2</sup>, based on physiologically relevant conditions were proposed within the COST Infogest network for digestion of solid foods.

The aim of our work was to investigate the digestibility of whole grain of raw peanut, and searched for stable large and small peptide fragments formed during the gastric digestion. Sensitizing capacity of those peptides was analyzed, which should be considered as a risk factor for allergenicity.

Whole grain of grounded raw peanut was incubated with human  $\alpha$ -amylase and pepsin, mimicking the effects of oral and gastric phase digestion, in total duration of 2h. Proteins were extracted from the mixture and analyzed by 1D and 2D SDS-PAGE, followed by mass spectrometry (MS) identification. Using size-exclusion chromatography we separated short digestion-resistant peptides (SDRP) obtained after digestion and analyzed by MS. IgE-binding was quantified using inhibition ELISA and immunoblots with pooled sera from peanut-allergic patients. Structural properties of control and pepsin digested peanut proteins sample were examined by circular dichroism (CD).

We analyzed the standard peanut extract (SPE) prepared from non-digested, defatted peanuts, control peanut sample (CPS) treated under the same conditions of digestion, without addition of pepsin, and digested peanut sample (DPS), which can be observed in Figure 1. Ara h 1 was detected as an almost full length protein, shortened at the N-terminal and C-terminal in DPS. Ara h 3, acidic subunit, was identified in DPS and, compared to

the CPS spots showed a remarkably lower intensity suggesting intensive proteolysis by pepsin. Almost intact basic subunit of Ara h 3 in different isoforms was found, with intensities similar to control, suggesting that the basic Ara h 3 subunit is more resistant to pepsin. Intact Ara h 2 and 6 in the digesta were identified in the protein spots of SPE, CPS and DPS 2D SDS PAGE. Ara h 1 and 3 were also identified in SDRPs fraction and the obtained peptides matched with peanut linear epitopes (IEDB database search). CD of digested peanut showed no changes in the secondary structure compared with the control sample. In IgE ELISA inhibition obtained for control and digested sample suggests that partly digested peanut allergens mainly retained their allergenic potential, and that pepsin proteolysis only slightly reduced the IgE binding potential of peanut proteins extracted during digestion. IgE-binding properties were analyzed on the solid phase for peanut rAra h 1, rAra h 2, and rAra h 3 with patients' sera. Binding of IgE to rAra h 2 in all patients was markedly inhibited by peptides released during digestion, suggesting the presence of potent functional Ara h 2 epitopes in low-molecular mass fractions.

Our data indicate that oral and gastric phase digestion products of raw peanut are both intact proteins and large digestion resistant peptides, suggesting that processes of protein extraction from the matrix and their enzymatic digestion occur simultaneously. We demonstrated that the most potent allergens, Ara h 2 and Ara h 6 remained mostly intact to proteolysis by pepsin, and SDRPs originating from Ara h 2 were the most potent in inhibiting IgE binding.

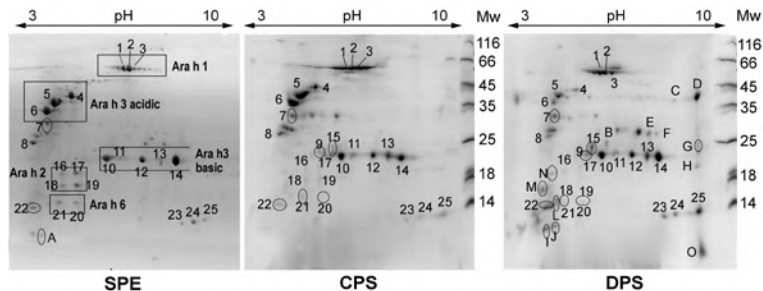


**Figure 1.** 2D SDS-PAGE of standard peanut extract (SPE), control peanut sample (CPS) and digested peanut sample (DPS) in reducing conditions. Protein spots labelled with numbers are matched, while non-matched spots are labelled with capitalized letters; all of them were trypsin digested and subjected to MS/MS analyses for identification. Mw - Molecular weight protein markers in kDa.

## Acknowledgements

This study was partially funded by a project 172024 of Ministry of Education, Science and Technological Development of the Republic of Serbia. This study was supported by Center of Excellence for Molecular Food Sciences, FCUB.

## References

1. Astwood JD, Leach JN, Fuchs RL. Stability of food allergens to digestion *in vitro*. Nat Biotechnol 1996;14:1269-73.
2. Minekus M. A standardised static in vitro digestion method suitable for food - an international consensus. Food Funct 2014;5:1113-24.



---

## Minor depolarization mediates magnesium suppression of nonsynaptic epileptiform activity

---

Marija Stanojević<sup>1\*</sup>, Srđan Lopičić<sup>1</sup>, Svetolik Spasić<sup>1</sup>, Vladimir Nedeljkov<sup>1</sup>, Milica Prostran<sup>2</sup>

<sup>1</sup>*Institute for Pathological Physiology, Faculty of Medicine, University of Belgrade, Belgrade, Serbia*

<sup>2</sup>*Institute for Pharmacology, Clinical Pharmacology and Toxicology, Faculty of Medicine, University of Belgrade*

\**marijastanojevic2002@yahoo.com*

Nonsynaptic mechanisms are long known to play a role in the pathogenesis of epileptiform activity in the mammalian central nervous system (CNS) <sup>1</sup>. Cellular bases of epilepsy have also been shown on computer models of hippocampal pyramidal cells <sup>2</sup>. General principles of basic mechanisms of epilepsy are considered to be universal in humans and animals, including invertebrate model systems <sup>3</sup>. Leech CNS represents a useful experimental model for basic research in epileptology <sup>4</sup>. Magnesium is a cation bioessential for the function of excitable membranes both in health and disease. As an anticonvulsant, Mg<sup>2+</sup> is used to control specific seizure types, but its antiepileptic potential is greater than its actual therapeutic use <sup>5</sup>. Neuroprotective action of Mg<sup>2+</sup> is experimentally and clinically proven to be beneficial in a number of neurological and psychiatric conditions <sup>6</sup>. However, the mechanisms underlying these salutary effects of simple Mg<sup>2+</sup> ions are still a matter of controversy. On the other hand, the incidence of dietary Mg<sup>2+</sup> deficiency is nowadays unfortunately increasing and hypomagnesaemia is considered the most frequent clinically unrecognized electrolyte dysbalance.

Experiments were performed *in vitro* on Retzius neurons of the free segmental ganglia of the leech *H. sanguisuga* using classical electrophysiological technique of intracellular recording. To induce epileptiform activity, Ringer saline containing 3 mM NiCl<sub>2</sub> (Ni<sup>2+</sup> Ri) was applied. A series of Mg<sup>2+</sup> containing Ni<sup>2+</sup> Ri salines with increasing concentrations of MgCl<sub>2</sub> (1 mM, 3 mM, 7 mM, 10 mM and 20 mM) were applied in separate trials of experiments. All data are represented as mean ± SEM. Statistical comparisons were made using Student's *t*-test. The present research was performed on an established experimental model of epileptiform activity induced in Retzius neurons by Ni<sup>2+</sup>. It is considered to be of nonsynaptic mechanism, since Ca<sup>2+</sup> channel blockade by Ni<sup>2+</sup> abolishes chemical synaptic neurotransmission. It was previously shown that Na<sup>+</sup> influx is mandatory for its generation <sup>7</sup>. This study investigates some of the features of the effect of Mg<sup>2+</sup> on this model.

Resting membrane potential (RMP) of Retzius cells in standard solution was -43.17±0.79 mV. Application of Ni<sup>2+</sup> reversibly caused the induction of stable oscillatory activity of

Retzius nerve cell membrane, which was considered epileptiform due to its bursting nature. It was characterized by the repetitive generation of rhythmic membrane potential oscillations in a form of paroxysmal depolarization shifts (PDSs). In control  $\text{Ni}^{2+}$  Ri saline RMP was  $-41.91 \pm 1.02$  mV. Several quantitative parameters were measured to describe the developed and stabilized  $\text{Ni}^{2+}$ -induced epileptiform activity. Mean values of PDS parameters were as follows:  $5.92 \pm 0.28$   $\text{min}^{-1}$  of PDS frequency,  $12.35 \pm 0.43$  mV of PDS amplitude,  $4.81 \pm 0.14$  s PDS duration, with an average number of  $7.17 \pm 0.50$  action potentials (APs) per PDS ( $n=28$ ).

**Table 1.** Introducing increasing concentrations of  $\text{Mg}^{2+}$  into the superfusing  $\text{Ni}^{2+}$  Ringer saline in separate trials of experiments slightly depolarizes Retzius nerve cell membrane potential during the induced epileptiform activity suppression.

[ $\text{Mg}^{2+}$ ] (mM)	MP in $\text{Ni}^{2+}$ Ri (mV)	MP in $\text{Mg}^{2+}$ - $\text{Ni}^{2+}$ Ri (mV)	MP difference (mV)	n	p
1	$-42.53 \pm 2.31$	$-41.07 \pm 2.63$	$1.47 \pm 0.56$	5	<0.05
3	$-36.76 \pm 4.11$	$-34.72 \pm 4.28$	$2.04 \pm 0.40$	5	<0.01
7	$-41.60 \pm 1.82$	$-39.44 \pm 1.50$	$2.16 \pm 0.51$	5	<0.01
10	$-41.47 \pm 1.36$	$-38.33 \pm 1.71$	$3.13 \pm 0.84$	6	<0.05
20	$-42.63 \pm 1.33$	$-39.26 \pm 0.87$	$3.37 \pm 0.66$	7	<0.01

Data shown as mean $\pm$ SEM; MP - membrane potential, Ri - Ringer, n - number of trials, p - level of significance.

Next, the effects of  $\text{Mg}^{2+}$  (in concentrations from 1 mM to 20 mM) were examined on this model of nonsynaptic epileptiform discharge. Introducing  $\text{Mg}^{2+}$  into the superfusing  $\text{Ni}^{2+}$  Ri saline caused a significant reversible suppression of the induced epileptiform activity in a dose-dependent manner. Magnesium suppression was of rapid onset, reversible and prolonged, and followed by an incomplete recovery<sup>8</sup>. Dose dependency analysis has shown that within the range of concentrations tested  $\text{Mg}^{2+}$  significantly reduced all PDS parameters of interest. Mean inhibitory concentration ( $\text{IC}_{50}$ ) was 8.29 mM  $\text{Mg}^{2+}$  for PDS frequency, 10.73 mM  $\text{Mg}^{2+}$  for PDS amplitude, for PDS duration it was 11.71 mM  $\text{Mg}^{2+}$  and finally 11.80 mM  $\text{Mg}^{2+}$  for the number of APs/PDS. The effect of  $\text{Mg}^{2+}$  on membrane potential during  $\text{Ni}^{2+}$ -induced epileptiform activity was also tested for. We have found that the described antiepileptic  $\text{Mg}^{2+}$  action was accompanied by a minor membrane depolarization. Although mild, it was always present and significant and itself dose-dependent. Table 1 shows that small depolarization mediates  $\text{Mg}^{2+}$  suppression of nonsynaptic epileptiform discharge on our cell model.

These results form part of a broader research project on the effects of  $\text{Mg}^{2+}$  as a potential antiepileptic agent against nonsynaptic epileptiform activity. Our findings report of generally neurodepressive  $\text{Mg}^{2+}$  effects under both standard (nonepileptogenic) and epileptogenic conditions, including an increase in free nerve cell membrane resistance, i.e. a decrease in membrane conductance caused by  $\text{Mg}^{2+}$ <sup>9,10</sup>. Concomitant  $\text{Mg}^{2+}$ -induced depolarization reported here is most probably mediated by  $\text{Mg}^{2+}$  influx into the neurons after exposure to  $\text{Mg}^{2+}$  containing perfusing saline. We suppose that a reverse function of

1Na<sup>+</sup>/1Mg<sup>2+</sup> exchanger of Retzius neurons, activated by the intraneuronal Na<sup>+</sup> overaccumulation during the Na<sup>+</sup>-dependent Ni<sup>2+</sup>-induced bursting, is also involved<sup>11</sup>. Mild depolarizing Mg<sup>2+</sup> action on our experimental model represents another important feature speaking in favor of the assumed mechanism responsible of antiepileptic magnesium effect against nonsynaptic epileptiform activity, which is considered to be Na<sup>+</sup> channel blockade by Mg<sup>2+</sup> ions, at least partially due to Mg<sup>2+</sup> influx into the neuron and rising intracellular Mg<sup>2+</sup> concentration. We conclude that increasing extracellular Mg<sup>2+</sup> concentration can protect against nonsynaptic Na<sup>+</sup>-dependent epileptic activity. This finding could have a broader significance, referring to a number of paroxysmal epileptic and nonepileptic neurological conditions, with Na<sup>+</sup>-dependent neuronal hyperexcitability as an important mechanism of pathogenesis (migraine headaches, neuralgias, etc).

## Acknowledgements

This work was supported by the Ministry of Education, Science and Technological Development of Republic of Serbia, Grant No. 175023.

## References

1. Jefferys JG, Haas HL. Synchronized bursting of CA1 hippocampal pyramidal cells in the absence of synaptic transmission. *Nature* 1982;300:448-50.
2. Heilman AD, Quattrochi J. Computational models of epileptiform activity in single neurons. *Biosystems* 2004;78:1-21.
3. Altrup U. Epileptogenicity and epileptic activity: mechanisms in an invertebrate model nervous system. *Curr Drug Targets* 2004;5:473-84.
4. Hahn E, Burrell B. Pentylentetrazol-induced seizure-like behavior and neural hyperactivity in the medicinal leech. *Invert Neurosci* 2015;15:1-9.
5. James MF. Magnesium in obstetrics. *Best Pract Res Clin Obstet Gynaecol* 2010;24:327-37.
6. Ghabriel MN, Vink R. Magnesium transport across the blood-brain barriers. In: Vink R, Nechifor M. (eds) *Magnesium in the Central Nervous System*, University of Adelaide Press, Adelaide, 2011, pp 59-74.
7. Pathak D, et al. Ethanol and magnesium suppress nickel-induced bursting activity in leech Retzius nerve cells. *Gen Physiol Biophys* 2009;28:9-17.
8. Stanojević M. et al. Incomplete recovery from Mg<sup>2+</sup> suppression of nonsynaptic epileptiform activity on an invertebrate model system. *Epilepsia* 2016;57:4950.
9. Stanojević M, Lopicic S, Spasic S, Aleksic I, Nedeljkov V, Prostran M. Effects of high extracellular magnesium on electrophysiological properties of membranes of Retzius neurons in leech *Haemopsis sanguisuga*. *J Elem* 2016;21:221-30.
10. Stanojević M, et al. Magnesium effects on nonsynaptic epileptiform activity in leech Retzius neurons. *Folia Biol Kraków* 2015;63:301-06.
11. Günzel D, Schlue WR. Sodium-magnesium antiport in Retzius neurones of the leech *Hirudo medicinalis*. *J Physiol* 1996;491.3:595-608.



---

## The effects of ibogaine on uterine redox homeostasis and contractility

---

Nikola Tatalović<sup>1\*</sup>, Zorana Oreščanin Dušić<sup>1</sup>, Jelena Nestorov<sup>2</sup>, Teodora Vidonja Uzelac<sup>1</sup>, Ana Mijušković<sup>1</sup>, Aleksandra Nikolić Kokić<sup>1</sup>, Mihajlo Spasić<sup>1</sup>, Roman Paškulin<sup>3</sup>, Maja Bresjanac<sup>4</sup>, Duško Blagojević<sup>1</sup>

<sup>1</sup>*Department of Physiology, Institute for Biological Research “Siniša Stanković”, University of Belgrade, Belgrade, Serbia*

<sup>2</sup>*Department of Biochemistry, Institute for Biological Research “Siniša Stanković”, University of Belgrade*

<sup>3</sup>*OMI Institute, Ljubljana, Slovenia*

<sup>4</sup>*Institute of Pathophysiology, University of Ljubljana, Ljubljana, Slovenia*

\**e-mail: nikola.tatalovic@ibiss.bg.ac.rs*

The ibogaine drug is originated from the rainforest shrub *Tabernanthe iboga*, which grows in West Africa. The tribes of the Gabon have used the iboga plant root bark for centuries as a stimulant, for medicinal purposes, and in rite of passage ceremonies. In the western world ibogaine is mostly known for its ability to inspire a sense of wellbeing both mentally and physically. Ibogaine has also been used for the treatment of substance abuse because it interrupts drug addiction, relieves withdrawal symptoms, and significantly decreases the desire for cocaine, heroin, alcohol and most other mind altering drugs. Now it is known that the pharmacology of ibogaine is quite complex and affects many different neurotransmitter systems simultaneously. Ibogaine binds to several types of receptors: 5-hydroxytryptamine (5-HT), opioid, nicotinic and N-methyl-D-aspartate (NMDA) receptors, dopaminergic and 5-HT transporters and monoamine oxidase enzyme (MAO) <sup>1</sup>. Although the mechanisms of ibogaine action in neural tissue are well studied, the effects on peripheral tissues are poorly understood.

Paskulin et al. have shown that ibogaine causes a sharp and transient fall in cellular ATP level in yeast, which was followed by an immediate increase in respiration and CO<sub>2</sub> production, in a time and concentration dependent manner <sup>2,3</sup>. Increased respiration leads to increase of ROS production and subsequent activation of antioxidant enzymes. These effects of ibogaine are not mediated by receptor binding and are not tissue and species specific <sup>2,4</sup>. It was previously shown that ibogaine-induced fall in cellular ATP level was caused by increased ATP consumption. The process in which the consumption of ATP is increased remains unclear. The proteome changes (induction of energy metabolism enzymes, antioxidant enzymes and numerous low abundance proteins) are responsible for at least a part of initial energy expenditures in ibogaine-treated yeast <sup>2,5</sup>. Study on human blood erythrocytes showed that ibogaine leads to release of ATP in the blood plasma <sup>4</sup>.

Ibogaine doesn't have any significant in vitro antioxidant properties per se but it influences physiological oxidative stress defence system in pro-antioxidant manner<sup>3,4</sup>.

In this study, we examined the effects of ibogaine on the model of the isolated rat uterus. Contractile tissues are sensitive to ATP levels and the depletion of energetics could lead to the impairment of regular rhythms and reversible relaxation. Extracellular ATP is known to stimulate uterine contractions in different species but the exact underlying mechanisms are poorly investigated. Furthermore, different contractile tissues, including uterus, are also sensitive to ROS, especially hydrogen peroxide (H<sub>2</sub>O<sub>2</sub>)<sup>6</sup>. Antioxidant enzyme cytosolic copper-zinc containing superoxide dismutase (SOD1) can also affect the contractility of uterine smooth muscles<sup>7</sup>. All these make the isolated contractile tissues a good model for examining the effects of ibogaine on both redox homeostasis and pharmacodynamics.

Unlike isolated arteries and ileum<sup>8</sup>, the uterus may have a wide range of different types and intensities of contractile activity depending on the properties of the isotonic solution. This allows us to register not only the relaxant but also the stimulatory effect of the tested substance. The aim of this study was to investigate the effects of ibogaine on both contractile properties of uterus and redox homeostasis and explore the possible link between the two.

Overall, ibogaine treatment has altered redox homeostasis and affected contractile properties of uterus. Ibogaine had the opposite effects on spontaneously active rat uteri depending on the applied concentration. Lower concentrations increased force of contraction, amplitude, frequency and duration of individual contractions. Higher concentrations caused concentration dependent relaxation of spontaneously active uteri. On the other hand, when the uterus is contracting with a high intensity (when exposed to higher Ca<sup>2+</sup> concentration) ibogaine showed only a relaxant effect.

The increase in uterine contractile activity after treatment with low doses of ibogaine could be partly attributed to possible increase in the extracellular concentration of ATP. However, the ATP leads only to a moderate increase in the intensity of uterine contractility, without affecting the character of contractions (i.e. their regularity), whereas ibogaine has a pronounced pace making effect.

Ibogaine also had a concentration dependant effect on the activity of antioxidant enzymes suggesting a vast, increase in cellular respiration and H<sub>2</sub>O<sub>2</sub> level. Ibogaine mediated relaxation found in the present study can be attributed to the influence of H<sub>2</sub>O<sub>2</sub>. However, the other possible mechanisms of ibogaine induced smooth muscle relaxation cannot be eliminated, regarding to its wide range of interaction with different receptors and signal transduction pathways.

The results regarding energy metabolism and redox homeostasis are in accordance with the previous observations in different experimental models. Research on an isolated uterus has allowed us to further examine the mechanism of this phenomenon: whether the increase in the intensity of cellular respiration is the result of an increased contractile activity that is caused by ibogaine? Only partially, because ibogaine leads to an increase that is several times greater compared to the uterus with phasic contractile activity of maximal intensity,

induced by extracellular  $\text{Ca}^{2+}$ , indicating the existence of ibogaine tissue non-specific ways of energy metabolism induction.

## Acknowledgements

This work was supported by a grant from the Ministry of Education, Science and Technological Development of the Republic of Serbia, project No. 173014: “Molecular mechanisms of redox signalling in homeostasis, adaptation and pathology”.

## References

1. Alper KR. Ibogaine: A review. *Alkaloids Chem Biol* 2001;56:1-38.
2. Paskulin R, Jamnik P, Obermajer N, Slavic M, Strukelj B. Induction of energy metabolism related enzymes in yeast *Saccharomyces cerevisiae* exposed to ibogaine is adaptation to acute decrease in ATP energy pool. *Eur J Pharmacol* 2010;627:131-5.
3. Paskulin R, et al. Metabolic plasticity and the energy economizing effect of ibogaine, the principal alkaloid of *Tabernanthe iboga*. *J Ethnopharmacol* 2012;143:319-24.
4. Nikolić-Kokić A, et al. Ex vivo effects of ibogaine on the activity of antioxidative enzymes in human erythrocytes. *J Ethnopharmacol* 2015;164:64-70.
5. Paskulin R, Jamnik P, Zivin M, Raspor P, Strukelj B. Ibogaine affects brain energy metabolism. *Eur J Pharmacol* 2006;552:11-4.
6. Appiah I, et al. Hydrogen peroxide affects rat uterine contractile activity and endogenous antioxidative defence. *Br J Pharmacol* 2009;158:1932-41.
7. Nikolić-Kokić A, Oreščanin-Dušić Z, Spasojević I, Blagojević D, Stević Z, Andjus P, Spasić M. The Effects of Wild-Type and Mutant SOD1 on Smooth Muscle Contraction. *Arch Biol Sci* 2015;67,187-92.
8. Tatalovic N, et al. Ibogaine relaxes rat arteries: the role of endothelium. FEBS3+ Meeting - Molecules of Life, September 2015, Slovenia, Abstract Book, pp 194.



---

## Serum redox-homeostasis in half-marathons

---

Tamara Uzelac<sup>1\*</sup>, Vesna Jovanović<sup>1</sup>, Jelena Aćimović<sup>1</sup>, Nevena Kardum<sup>2</sup>, Vuk Stefanović<sup>2</sup>, Ana Jelenković<sup>2</sup>, Marija Glibetić<sup>2</sup>, Ljuba Mandić<sup>1</sup>

<sup>1</sup> Faculty of Chemistry, University of Belgrade, Belgrade, Serbia

<sup>2</sup> Center of Research Excellence in Nutrition and Metabolism, Institute for Medical Research, University of Belgrade

\*e-mail: tamarauzelac31@gmail.com

Strenuous physical exercise is known to result in the formation of Reactive Oxygen Species (ROS) in the body <sup>1</sup>. Mitochondrial electron transport chain, hemoglobin and myoglobin, NADPH oxidase and catecholamine autoxidation are the main sources of ROS <sup>2</sup>. When the formation of ROS is higher than antioxidant defense, oxidative stress occurs which leads to damage of macromolecules such as proteins, lipids and nucleic acids. During the evolution, two main antioxidant systems (enzyme and non-enzyme system) were developed. Beside the high activities of antioxidant enzymes, glutathione is the most important intracellular antioxidant. Extracellular fluids contain only small amounts of antioxidant enzymes, so human serum albumin (HSA) is proposed as a major extracellular (intravascular and extravascular compartment) antioxidant <sup>3</sup>. Because HSA is the most abundant extracellular protein which has one free Cys34 thiol group in 75 % reduced form, it contributes 80% to the total thiol serum content. The property of molecule HSA to bind different endogenous (free fatty acids, hormones, bilirubin and hem) and exogenous (polyphenols, drugs and metal anions) substances, also contributes to the antioxidative role of HSA.

The aim of this study was to examine how oxidative stress caused by intense physical activity, affects serum redox-homeostasis. Total serum thiol content, and content and reactivity of HSA-SH groups were determined before the start of the race (control) and 15 min, 60 min and 24 h after the end of the race. Participants were amateur half-marathon racers (n = 10), ages between 20 and 30 years old, who ran the half-marathon (21.1 km). The total thiol content in serum was statistically significantly (p<0,05) higher after 15 min from the end of the race ( $0.425 \pm 0.019$  mM) compared to control ( $0,400 \pm 0,029$  mM). After 60 min it gradually decreases ( $0.416 \pm 0.037$  mM) and after 24h it is almost equal to the value obtained before the start of the race ( $0.401 \pm 0.025$  mM). Mean value of the content of HSA-SH groups in HSA preparations (isolated from the serum by precipitation with saturated ammonium sulfate solution in two steps) was  $0.564 \pm 0.025$  mol SH/mol HSA, which is in agreement with published claims that about 60 % of HSA-SH groups in healthy people are in a reduced state <sup>4</sup>. A statistically significant (p <0.05) decrease in the HSA-SH group content was found 15 min after the end of the race ( $0.519 \pm 0.039$  mol SH/mol HSA) compared to control. After 60 min the content of HSA-SH groups ( $0.562 \pm$

0.043 mol SH/mol HSA) corresponds to the initial value and remains constant for 24 hours ( $0.561 \pm 0.052$  mol SH/mol HSA). The pseudo first order rate constant ( $k'$ ), for the reaction of HSA-SH with DTNB, was  $49.91 \pm 9.8 \times 10^{-3} \text{ s}^{-1}$  before the race. In HSA samples, taken 15 min after the race, statistically significant ( $p < 0.05$ ) increase of  $k'$  values was found ( $56.24 \pm 5.57 \times 10^{-3} \text{ s}^{-1}$ ) compared to the control. As time passes from the end of the race, there is a gradual decrease in the  $k'$  value (Figure 1).

Intense physical work leads to dehydration of the body, which is reflected in the transient increase in total serum thiol content immediately after the race. However, these conditions don't affect the total serum thiol content in the samples taken 60 min and 24 h after the race which indicates that the total thiols are not a sensitive marker for the evaluation of oxidative stress in intense physical activity. The oxidative stress, which is most intense during the race and immediately after it, leads to a statistically significant ( $p < 0.05$ ) decrease in the content of the Cys34 thiol group. The results obtained show that the molar ratio -SH / HSA is a more sensitive indicator of oxidative stress than the content of total serum thiols as well as that in healthy people, the drop of the content of the HSA-SH group returns to the initial level very fast. Also, statistically significant ( $p < 0.05$ ) increase in the reactivity of the HSA-SH group during intense physical work indicates that this effect is important in efficient antioxidant defense.

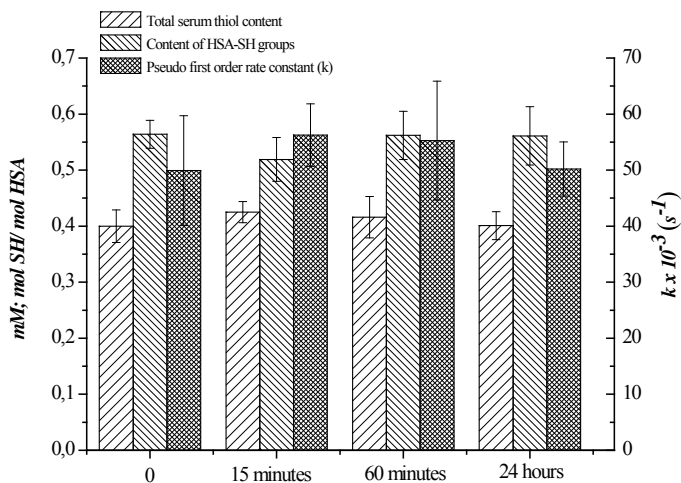


**Figure 1.** Total serum thiol content, and content and reactivity of HSA-SH groups before the start of the race (control) and 15 min, 60 min and 24 h after the end of the race.

## References

1. Nikolaidis MG, Kyparos A, SpanouC, Paschalis V, Theodorou AA, Vrabas IS. Redox biology of exercise: an integrative and comparative consideration of some overlooked issues. J Exp Biol 2012;215:1615-25.

2. Turner JE, Hodges NJ, Bosch JA, Aldred S. Prolonged depletion of antioxidant capacity after ultraendurance exercise. *Med Sci Sports Exerc* 2011;43:1770-6.
3. Quinlan GJ, et al. Albumin influences total plasma antioxidant capacity favorably in patients with acute lung injury. *Crit Care Med* 2004;32:755-9.
4. Turell L, Radi R, Alvarey B. The thiol pool in human plasma: The central contribution of albumin to redox processes. *Free Radic Biol Med* 2013;65:244-53.



---

## Ibogaine redox potential - the effects on antioxidant enzymes after ingestion

---

**Teodora Vidonja Uzelac<sup>1\*</sup>, Nikola Tatalović<sup>1</sup>, Gordana Koželj<sup>2</sup>, Zorana Oreščanin Dušić<sup>1</sup>, Aleksandra Nikolić Kokić<sup>1</sup>, Mihajlo Spasić<sup>1</sup>, Roman Paškulin<sup>3,4</sup>, Maja Bresjanac<sup>4</sup>, Duško Blagojević<sup>1</sup>**

<sup>1</sup>*Department of Physiology, Institute for Biological Research "Siniša Stanković", University of Belgrade, Belgrade, Serbia*

<sup>2</sup>*Institute of Forensic Medicine, Faculty of Medicine, University of Ljubljana, Ljubljana, Slovenia*

<sup>3</sup>*OMI Institute, Ljubljana, Slovenia*

<sup>4</sup>*Institute of Pathophysiology, Faculty of Medicine, University of Ljubljana*

\**e-mail: teodora.vidonja@ibiss.bg.ac.rs*

For centuries, plant *T. iboga* was used in African tribal communities for different ritual purposes. Beseades its stimulant effects in the last few decades ibogaine has been used as antiaddiction substance against nicotine, alcohol, stimulants and opiates <sup>1</sup>. Ibogain is not registered as a cure, but it is possible to purchase capsule with ibogaine through websites <sup>2</sup>. Ibogaine binds to different types of receptors and neurotransmitter transporters in brain <sup>3</sup>. It also influences cellular energy, redox state and antioxidant capacity in a dose- and time-dependent manner. In yeast, ibogaine decreases cellular ATP level and increases CO<sub>2</sub> production in the first hour after exposure, followed by increased cellular respiration and the production of reactive oxygen species (ROS) after 5 h <sup>4-6</sup>. Ibogain is metabolized in the liver by CYP2D6, and its pharmacologically active metabolite noribogaine is formed by demethylation. Both are excreted via gastrointestinal and renal tracts within 24 h <sup>3</sup>.

In this experiment 30 male Wistar rats, 3 months old, 200-250 g body weight (b.w.) were treated *per os* once with either 1 or 20 mg/kg b.w. of ibogaine. After 6 h and 24 h from treatments, the concentrations of ibogaine and noribogaine were measured in the blood plasma, as well as the activity of antioxidant enzymes: catalase (CAT), glutathione peroxidase (GPx), glutathione reductase (GR) and superoxide dismutase 1 (SOD1) in erythrocytes and liver. In liver, the activity of SOD2 and glutathione S transferase (GST) were also measured. The control group was treated with dH<sub>2</sub>O. All studies were approved by the Local Animal Care Committee.

Measurement of ibogaine and noribogaine concentrations in the blood plasma showed dominant presence of noribogaine against ibogaine 6 h after treatment, while after 24 h only noribogaine was present in traces. The concentration of ibogaine and noribogaine was higher in the group treated with 20 mg/kg b.w. The presence of noribogaine in higher concentrations than ibogaine 6 h after treatment is consistent with pharmacokinetics of

ibogaine. Our results showed that ibogaine treatment with both doses did not change the activity of antioxidant enzymes in erythrocytes and liver after neither 6 nor 24 h.

After entering the circulation, ibogaine quickly becomes available to tissues. After the first pass in liver, it is metabolized to noribogaine that is also pharmacologically active<sup>3</sup>. However, despite liver activity in ibogaine metabolism and transformation that additionally produce ROS and ibogaine redox potential, no changes of the activity of antioxidant enzymes were measured in the liver. It is possible that ibogaine in applied doses is not so effective or liver has large antioxidant potential and resolve ibogaine-mediated redox disequilibrium much earlier than 6 or 24 h.

Ibogaine in vitro affected the activity of SOD1 and GR in erythrocytes, but in higher concentration and for 1 h period<sup>6</sup>. Treatment with ibogaine in this experiment yielded lower amount of ibogaine in the blood plasma that could influence erythrocytes antioxidant enzymes and the activity measurements were performed after 6 and 24 h. That's are some of possible explanations for the lack of changes in the activity of antioxidant enzymes in erythrocytes in this experiment.

Our previous results on ileum (where changes of the activity of antioxidant enzymes were measured) suggests tissue specific ibogaine influence and a combination of its pharmacological and redox mediated effects<sup>7</sup>.

## Acknowledgements

This study was supported by a grant from the Ministry of Education, Science and Technological Development of the Republic of Serbia, project No: 173014: "Molecular mechanisms of redox signalling in homeostasis, adaptation and pathology".

## References

1. Paškulin R, Jamnik P, Živin M, Raspor P, Štrukelj B. Ibogaine affects brain energy metabolism. *Eur J Pharmacol* 2006;552:11-4.
2. O'Connell C, Gerona R, Friesen M, Ly B. Internet-purchased ibogaine toxicity confirmed with serum, urine, and product content levels. *Am J Emerg Med* 2015;33:985.e5-6.
3. Alper K. Ibogaine: A Review. *Alkaloids Chem Biol* 2001;56:1-38.
4. Paškulin R, Jamnik P, Obermajer N, Slavić M, Štrukelj B. Induction of energy metabolism related enzymes in yeast *Saccharomyces cerevisiae* exposed to ibogaine is adaptation to acute decrease in ATP energy pool. *Eur J Pharmacol* 2010;627:131-5.
5. Paškulin R, et al. Metabolic plasticity and the energy economizing effect of ibogaine, the principal alkaloid of *Tabernanthe iboga*. *J Ethnopharmacol* 2012;143:319-24.
6. Nikolić-Kokić A, et al. *Ex vivo* effects of ibogaine on the activity of antioxidative enzymes in human erythrocytes. *J Ethnopharmacol* 2015;164:64-70.
7. Vidonja Uzelac T, et al. Ibogaine affects the redox status in rat ileum. Joint Meeting of National Physiological Societies, New Perspectives in Physiological Research - Young Investigator Forum, 2017 May 25-27, Subotica, Serbia, p. 113.

---

## **Estimation of the overall cardiovascular risk in patients with acute myocardial infarction, stroke and polycystic ovary syndrome by DOI score (dyslipidemia, oxidative stress and inflammation) calculation**

---

**Sanja Vujčić<sup>1</sup>, Azra Guzonjić<sup>1\*</sup>, Aleksandra Vukašinić<sup>1</sup>, Iva Perović-Blagojević<sup>2</sup>, Nataša Bogavac-Stanojević<sup>1</sup>, Jelena Vekić<sup>1</sup>, Vesna Spasojević-Kalimanovska<sup>1</sup>**

<sup>1</sup>*Department of Medical Biochemistry, Faculty of Pharmacy, University of Belgrade, Belgrade, Serbia*

<sup>2</sup>*Biochemical Laboratory, Clinical Health Center "Dr. Dragiša Mišović", Belgrade, Serbia*

\**e-mail: kundab6@gmail.com*

Cardiovascular diseases (CVDs) take the lives of 17.7 million people every year, 31% of all global deaths. Triggering these diseases, which manifest primarily as heart attacks and strokes, are tobacco use, unhealthy diet, physical inactivity and the harmful use of alcohol. Estimation of cardiovascular health status on an individual level can be performed by using Total Damaging Scale (DOI score), which includes dyslipidemia, oxidative stress and inflammation. Considering the significance of above-mentioned CV risk factors and the fact that these three processes are mutually dependent and overlapping, the DOI score can be an important marker of the patient's condition, perhaps more potent than the application of individual parameters <sup>1</sup>.

An increased level of LDL-cholesterol (LDL-C) leads to the onset of atherosclerosis that increases the risk of acute myocardial infarction (AMI) and stroke. HDL-cholesterol (HDL-C) reduces the risk of developing CVDs. On the development of atherosclerosis, triglycerides have a major effect as well. In patients with PCOS (polycystic ovary syndrome), dyslipidemia is also present. Insulin resistance and hyperandrogenemia in PCOS may cause increased levels of the small, low-density lipoprotein-cholesterol (sdLDL-C), which are a particularly atherogenic form of lipoprotein <sup>2</sup>.

Experimental and clinical studies suggest that oxidative stress contributes to the development and progression of CVDs by influencing the endothelial function. Reactive oxygen species can cause direct cardiac injury by oxidizing cellular constituents. In patients with AMI, stroke, as well as PCOS, production of free radicals is increased, while the serum level of total antioxidants is decreased; also, serum malondialdehyde (MDA) is increased which indicates on a high degree of lipid peroxidation <sup>3</sup>.

The pathogenesis of CVDs and PCOS has been thought of as an inflammation-mediated process with increased levels of inflammatory markers. Chronic inflammation is closely

related to endothelial inflammation and consequent endothelial dysfunction, which plays a key role in CVDs. PCOS is also associated with endothelial dysfunction and an increase in markers of endothelial inflammation <sup>4</sup>.

We have included a total of 606 subjects: 54 with AMI, 179 stroke patients, 124 patients with PCOS and 303 healthy persons (CG). In our previous studies we have determined for all these subjects parameters of oxidative status (total oxidative status - TOS, rate of superoxide anion generation, MDA, advanced oxidation protein products (AOPP), prooxidative-antioxidative balance (PAB), total antioxidative status (TAS), superoxide dismutase activity, total SH groups, paraoxonase activity), inflammation marker (hsCRP) and lipid status components (total cholesterol, LDL-C, HDL-C and triglycerides concentration). Using these concentrations and z-score statistics calculation we have calculated distinct risk scores: Inflammation Score as a z-score value for hsCRP for every person, Dyslipidemia Score as a difference between Lipid Risk Score (average value between LDL-C and TG z-score values) and Lipid Protective Score (HDL-C z-score value), and Oxy Score as a difference between Prooxidative Score (average value of the z-scores of the measured prooxidants) and Antioxidative Scores (z-score values of the measured antioxidants). Population z-score values for all parameters were calculated from the control group values.

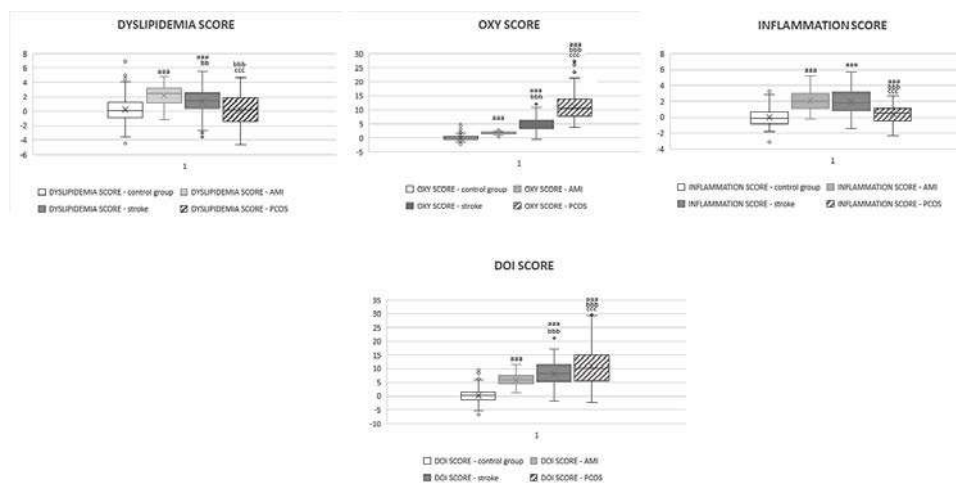


**Figure 1.** Comparison of risk scores between control group and patients. a - Significantly different from the first group  $a < 0.05$ ;  $aa < 0.01$ ;  $aaa < 0.001$  (control group); b - Significantly different from the second group  $b < 0.05$ ;  $bb < 0.01$ ;  $bbb < 0.001$  (AMI group); c - Significantly different from the third group  $c < 0.05$ ;  $cc < 0.01$ ;  $ccc < 0.001$  (stroke group)

Comparisons between groups were made by Kruskal-Wallis test, since the data was not normally distributed. These statistical tests were followed with Mann-Whitney U test. As Figure 1 shows, all the groups of patients (patients with AMI, stroke and PCOS) had

significantly higher risk scores (dyslipidemia score, oxy score, inflammation score, as well as DOI score) compared with the control group. Patients with stroke had significantly higher dyslipidemia score, oxy score and DOI score compared with the patients with AMI, while the similar level of inflammation was observed in both groups. Patients with PCOS had significantly higher all risk scores compared with both groups (patients with AMI and stroke). Relationship between CV scores was examined by using a nonparametric correlation statistical test - the Spearman test. As Figure 2 shows, all subjects (CG, AMI, stroke and PCOS) have positive correlation between dyslipidemia score and oxy score ( $P<0.001$ ), oxy score and inflammation score ( $P<0.001$ ), also between dyslipidemia score and inflammation score ( $P<0.001$ ).

Patients with AMI and high dyslipidemia score have higher level of oxidative stress in their bodies, this relationship was with marginal significance ( $P=0.070$ ). On the other hand, in a stroke group results showed higher oxy score in those who have high dyslipidemia score ( $P<0.01$ ) and higher dyslipidemia score in those who have high inflammation score ( $P<0.05$ ). As for the patients with PCOS the results were similar. These patients have higher dyslipidemia score owing to the fact that their oxy score is high ( $P<0.001$ ), higher inflammation score also because their high oxy score ( $P<0.01$ ) and higher inflammation score due to high dyslipidemia score ( $P<0.001$ ).

The fact that the DOI score includes parameters of lipid status, inflammation and oxidative stress leads to conclusion that the DOI score represents the parameter of the overall health risk of the patients. Furthermore, the DOI score can be used in making prognosis of CVDs, while individual parameters, which show just one aspect of these complex atherosclerosis connected diseases, showed less satisfying results.

## References

1. Veglia F, Cighetti G, De Franceschi M, Zingaro L, Boccotti L, Tremoli E, Cavalca V. Age- and gender-related oxidative status determined in healthy subjects by means of OXY-SCORE, a potential new comprehensive index. *Biomarkers* 2006;11:526-73.
2. Kotur-Stevuljevic J, et al, Correlations of oxidative stress parameters and inflammatory markers in coronary artery disease patients; *Clin Biochem* 2007;40:181-7.
3. Manninen V, Tenkanen L, Koskinen P, Huttunen J, Mänttari M, Heinonen O, Frick M. Joint effects of serum triglyceride and LDL cholesterol and HDL cholesterol concentrations on coronary heart disease risk in the Helsinki Heart Study. Implications for treatment. *Circulation* 1992;85:37-45.
4. Griendling KK, FitzGerald GA. Oxidative stress and cardiovascular injury, Part 1: Basic mechanisms and in vivo monitoring of ROS. *Circulation* 2003;108:1912-1916.
5. Kotur-Stevuljevic J, et al. Oxidative stress and paraoxonase 1 status in acute ischemic stroke patients. *Atherosclerosis* 2015;241:192-8.



---

## DOI score - novel biomarker for cardiovascular diseases

---

**Aleksandra Vukašinović<sup>1</sup>, Srđan Kafedžić<sup>2</sup>, Milica Stefanović<sup>2</sup>, Ivan Ilić<sup>2</sup>, Saša Hinić<sup>3</sup>, Lidija Memon<sup>3</sup>, Vesna Spasojević-Kalimanovska<sup>1</sup>, Nataša Bogavac-Stanojević<sup>1</sup>, Biljana Putniković<sup>2</sup>, Marija Zdravković<sup>3,4</sup>, Jelena Kotur-Stevuljević<sup>1\*</sup>, Aleksandar N. Nešković<sup>2,4</sup>**

<sup>1</sup>*Department of Medical Biochemistry, Faculty of Pharmacy, University of Belgrade, Belgrade, Serbia*

<sup>2</sup>*Department of Cardiology, Clinical Hospital Center Zemun, Belgrade*

<sup>3</sup>*Department of Cardiology, University Hospital Medical Center Bezanijska Kosa, Belgrade*

<sup>4</sup>*Faculty of Medicine, University of Belgrade*

\* *e-mail: jkotur@pharmacy.bg.ac.rs*

Oxidative stress stands for condition where precise balance between prooxidants and antioxidative compounds is disturbed in a favour of prooxidants. It is considered that it takes place in many pathophysiologic processes like cardiovascular diseases <sup>1</sup>. Cardiovascular disease development support endothelial dysfunction as well, a state where physiological endothelial role is transformed by many inflammation and oxidative stress factors. Most common event of cardiovascular diseases is atherosclerosis. As a consequence of its progress coronary artery disease appears. Endothelial dysfunction and cell senescence are considered to be in its base as well <sup>2</sup>. One of several coronary artery disease manifestations is acute coronary syndrome which entity is acute myocardial infarct with ST elevation (STEMI). Its basic pathophysiologic event is rupture of atherosclerotic plaque and occlusive thrombus formation which at the end leads to acute myocardial infarct. Suggested treatment for these patients was percutaneous coronary intervention (PCI) or mechanic opening of thrombus occluded coronary artery with or without stent implement <sup>3</sup>. By now, there are a lot of markers that correlate with appearance of acute myocardial events, but still cardiovascular diseases are leading cause of death worldwide. A total of 81 healthy volunteers were included, all negative for cardiovascular disease, and 83 patients with cardiovascular disease. In the group of patients 70 of them had acute myocardial infarct (STEMI patients) without previous cardiovascular events and were candidates for percutaneous coronary intervention treatment. Blood from patients was collected in different time points: at the time of angiography procedure in AP patients, for STEMI patients at the time of the admission to the hospital due to acute myocardial infarction and after the PCI procedure and in the morning from fasting healthy volunteers. For evaluation of oxidative stress status in sera, we have assessed several prooxidative and several antioxidative species <sup>4,5</sup>. As markers of oxidative stress we have measured level of: rate of superoxide anion (O<sub>2</sub><sup>-</sup>) generation, total oxidative status (TOS), prooxidative-

antioxidative balance (PAB) and advanced oxidation protein products (AOPP). From the parameters which represent antioxidative status we have chosen paraoxonase 1 activity (PON), total sulfhydryl groups content (tSHG), total antioxidative status (TAS) and activity of superoxide dismutase enzyme (SOD). Calculated risk scores were: Inflammation Score, Oxidative Score that represent difference between prooxidative and antioxidative score, Score of Dyslipidemia as the difference between lipid risk score and protective lipid score and DOI score which combined the three mentioned scores <sup>6</sup>.

Table 1 reports basic demographic and biochemical characteristics of subjects included in the research. Parameters of oxidative stress and comprehensive scores are show in Figure 1. tSHG was significantly higher in healthy person comparing to STEMI patients at admission. SOD activity had significantly higher activity in group of patients comparing to healthy patients, but STEMI patient at the admission and after the procedure did not show significant difference in spite of higher values after the procedure. Controls had statistically higher values of total antioxidative status than STEMI patient at the admission. TOS concentrations significantly decrease after the PCI procedure comparing to the time of admission. Score of Inflammation was significantly lower in control group that at STEMI patients as well as Oxidative-stress Score.

**Table 1.** Basic characteristics of characteristics of subjects included in study.

Parameter	Group of patients		
	Healthy individuals (n=81)	Cardiovascular patients (n=70)	p <sup>a</sup>
Age, years	49.9±10.46	60.7±11.86	p<0.05
Body mass index, kg/m <sup>2</sup>	25.87±3.758	26.78±4.395	ns <sup>aa</sup>
Blood pressure, mmHg	125/80 ± 18.9/10.8	135/84 ± 23.5/14.5	p<0.05
Smokers	16/81	38/83	/
Total cholesterol, mmol/L	5.29 ± 4.469	6.31 ± 1.29	p<0.05
Triglycerides, mmol/L	1.29±0.590	1.83±1.057	p<0.05
HDL cholesterol, mmol/L	1.52 ± 0.328	1.19 ± 0.421	p<0.05
LDL Cholesterol, mmol/L	3.19±0.809	3.32±1.212	p<0.05
CRP, mg/L	2 - 7.7*	0 - 290*	p<0.05

<sup>a</sup>Mean difference is significant at the level of 0.05, AVONA test; <sup>aa</sup>ns - non significant

Based on these three scores, we formed comprehensive DOI score that includes dyslipidemia, oxidative stress and inflammation. DOI score showed significantly higher values in STEMI patient comparing to group of healthy subjects (Figure 1). ROC analysis evaluated the ability of DOI score to separate cardiovascular patients from healthy persons and it showed strong predictive capability, with AUC=0.835. Comparing the calculated scores between various subgroups of patients based on age, smoking habit, blood pressure, body mass index and glucose levels, significant difference was reported for protective lipid score and lipid risk score. Results showed statistically higher lipid risk score for patient in middle age comparing to elderly and young patients (Figure 2). On the other side, protective lipid score was tightly attached to body mass index.

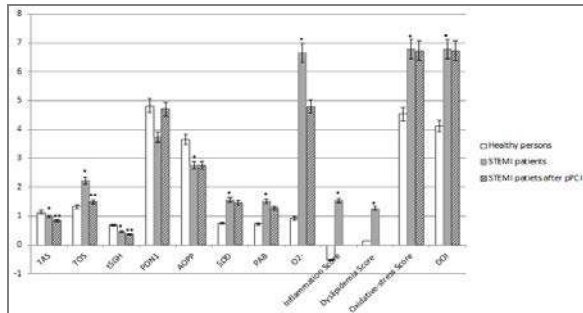


**Figure 1.** Parameters of oxidative stress and comprehensive risk scores evaluated at patients with AIM; (\*) Mean values significant comparing to healthy persons at the level 0.05, Post-Hoc test; (\*\*) Mean values significant comparing to mean values of patient at the admission at the level 0.05.

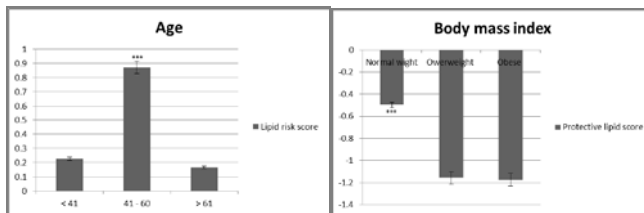


**Figure 2.** Risk scores at subgroup of patients with AIM, divided by age (left) and by body mass index (right); (\*\*\*) Mean values significant at the level 0.05.

Our results strongly supported earlier investigation about oxidative stress and its role in the pathophysiology of cardiovascular diseases. Besides, acute events specifically mark condition of oxidative stress which means low antioxidative defense and increase of prooxidative harmful compounds. This was supported by our results, patients at admission had higher levels of oxidative stress and various levels of antioxidative defence, while after the PCI procedure prooxidative levels decreased slightly. Our new parameter, DOI score, takes in consideration inflammation, lipid status and oxidative stress status, and could be a reliable marker to indicate cardiovascular process in patients without clinical signs.

## References

1. Griending KK, FitzGerald GA. Oxidative stress and cardiovascular injury, Part 1: Basic mechanisms and in vivo monitoring of ROS. *Circulation* 2003;108:1912-1916.
2. Versari D., Daghini E., Viridis A., Ghiadoni L., Taddei S. The aging endothelium, cardiovascular risk and disease in man. *Exp Physiol* 2009;94:317-321.
3. Keeley EC, Boura JA, Grines CL. Primary angioplasty versus intravenous thrombolytic therapy for acute myocardial infarction: a quantitative review of 23 randomised trials. *Lancet* 2003;361:13-20.
4. Kotur-Stevuljević J, et al. PON1 status is influenced by oxidative stress and inflammation in coronary heart disease patients. *Clin Biochem* 2008;41:1067-73.
5. Kotur-Stevuljević J, et al. Oxidative stress and paraoxonase 1 status in acute ischemic stroke patients. *Atherosclerosis* 2015;241:192-8.
6. Veglia F, et al. Age- and gender-related oxidative status determined in healthy subjects by means of OXY-SCORE, a potential new comprehensive index. *Biomarkers* 2006;11:526-73.



---

## Telomerase stability study using Real-Time telomeric repeat amplification protocol

---

Aleksandra Vukašinić<sup>1</sup>, Barbara Ostanek<sup>2\*</sup>, Vid Mlakar<sup>2</sup>, Miron Sopić<sup>1</sup>, Zorica Cvetković<sup>3</sup>, Vesna Spasojević-Kalimanovska<sup>1</sup>, Nataša Bogavac-Stanojević<sup>1</sup>, Janja Marc<sup>2</sup>, Jelena Kotur-Stevuljević<sup>1\*</sup>

<sup>1</sup>Department of Medical biochemistry, Faculty of Pharmacy, University of Belgrade, Belgrade, Serbia

<sup>2</sup>Department of Clinical biochemistry, Faculty of Pharmacy, University of Ljubljana, Ljubljana, Slovenia

<sup>3</sup>Department of Haematology, Clinical Hospital Center Zemun, Belgrade, Serbia; Faculty of Medicine, University of Belgrade

\*e-mails: Barbara.Ostanek@ffa.uni-lj.si; jkotur@pharmacy.bg.ac.rs

Telomerase is a ribonucleic complex that adds short d(TTAGGG) tandem repeats at 3' end of telomeric DNA. Active enzyme consists of a catalytic subunit (human telomerase reverse transcriptase) and RNA template placed in the core of the enzyme, and helper proteins necessary for *in vivo* telomerase activity<sup>1</sup>. Its activity is strictly regulated and it is expressed in proliferating cells like healthy hematopoietic, stem and especially cancer cells while in healthy, non-dividing ones, telomerase activity is usually inhibited during gestational period<sup>2</sup>. Although telomerase activity is undetectable in nonproliferating cells, it is highly active after fertilization and remains active in embryonic stem and germinative cells during intrauterine growth. In growing phase telomerase activity is decreasing slowly and finally completely disappears in most somatic cells<sup>3</sup>. Telomerase activity in hematopoietic cells increases in response to cytokine induced proliferation in certain states<sup>4</sup>. Besides its diagnostic potential, telomerase is recognized as a powerful therapeutic goal for cancers, it is considered that its specific inactivation would be strong tool for therapy of these patients<sup>5</sup>. Because of that, there is a need to develop a reliable method for measurement of telomerase activity and determine the sample storage conditions the time frame in which the samples should be analysed.

Samples were collected from healthy volunteers and patients with diagnosed cancer. Three healthy persons and three patients with diagnosed carcinoma (acute myeloid leukaemia, oesophaguscarcinoma with metastasis and diffuse large B-cell lymphoma) were included. Cell lines used in this study were HeLa cells, Ramos Blue cells and Human osteosarcoma (ATCC). All cell lines were grown using standard laboratory techniques and protocols. Telomerase enzyme was extracted from blood samples and cell line samples using ice cold CHAPS protocol. Telomerase activity was measured using real-time telomeric repeat amplification protocol (TRAP).

In order to evaluate sample stability we performed study by analysing samples stored for different time intervals and at different temperatures. Results are presented as Threshold cycle value (Ct) for easier comparison and as telomerase indexes, where each telomerase index value represents reciprocal value of telomerase Ct value.

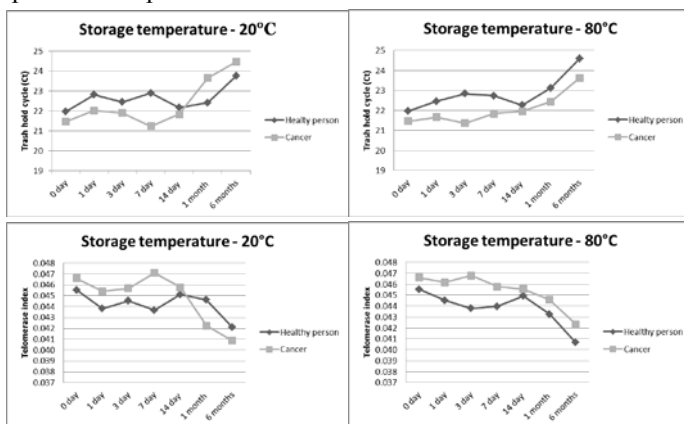


**Figure 1.** Telomerase sample stability.

Our TRAP method showed good linearity. Standard curve covered wide ranges of protein extracts concentrations, 700 $\mu\text{g/ml}$  to 6.25 $\mu\text{g/ml}$  ( $R=0.9915$ ), with efficacy of reaction of 90%. Figure 1 shows the results of sample stability study. As was expected, telomerase activity that originates from patients with cancer shows higher activity of telomerase comparing to telomerase from healthy subjects. Storage at  $-20^\circ$  was more acceptable for telomerase with high activity from cancer patients and it could be seen at figure 1A that activity decreased with time, but the difference became statistically significant after 1 month ( $23.67 \pm 0.253$ ,  $p=0.000$ ). In human samples with initially lower telomerase activity the statistically significant lower value appeared already after 14 days of storage at  $-20^\circ\text{C}$  ( $22.17 \pm 0.252$ ,  $p=0.018$ ). Regarding storage at  $-80^\circ\text{C}$  telomerase activity from cancer patients did not show statistically different lowering after 6 months of storage, while in low telomerase activity samples the decrease was noted between 1<sup>st</sup> and 6<sup>th</sup> month of storage ( $24.59 \pm 0.253$ ,  $p=0.024$ ). These results indicate that samples which are supposed to have lower telomerase activity should be handled more carefully. Besides, buffy coat for telomerase isolation was kept for 14 day at  $+4^\circ\text{C}$  and isolation were repeated in the same time intervals as the points of storage evaluations. Telomerase activity was confirmed even after 14 days without significant difference which indicate a way of short term storage of samples. Further evaluation of buffy coat stability at  $+4^\circ\text{C}$  was not performed, since it is not common in routine laboratory practice.

As can be seen from Table 1 repeated thawing also affects telomerase activity regardless of origin. Telomerase samples with low activity could be thawed two times without significant impact on its activity, while telomerase sample with higher activity could be

thawed even up to four times, which again supports higher stability of samples with more active enzyme.

**Table 1.** Sample stability study - Repeated thawing of samples

Number of thawing	Healthy person	p*	Cancer	p*
0	21.96 ± 0.107	/	21.46 ± 0.135	/
1	22.8 ± 0.356	ns	21.59 ± 0.543	ns
2	22.66 ± 0.395	ns	21.21 ± 0.447	ns
3	24.07 ± 0.151	0.032	20.95 ± 0.217	ns
4	24.91 ± 0.439	0.000	20.86 ± 0.224	ns
5	25.32 ± 0.046	0.000	23.09 ± 0.316	0.010
6	27.03 ± 0.187	0.000	24.09 ± 0.315	0.000

Recent researches indicate the connection between telomerase and various diseases, especially in cancer development and maintenance<sup>9</sup>. This emerging role in pathogenesis lead telomerase to become potential target of cancer therapy, although still it is not in common use<sup>6,10</sup>. However, all these fact declared telomerase activity as a novel biomarker of great clinical significance, especially for patients with various cancers, where it can demonstrate the presence of illness<sup>10,11</sup>. Because of that, there is a need for adequate sample and precisely defined storage condition in order to obtain valid result. Here we presented results of sample stability testing. Telomerase enzyme showed great stability, but still for samples of supposed lower values, we strong recommend storage at deeper temperatures.

## Acknowledgements

This study was supported by Bilateral project with Republic of Slovenia, number 17/2016.

## References

1. Gomez ED, et al. Telomere structure and telomerase in health and disease (Review). *Int J Oncol* 2012;41:1561-9.
2. Hiyama K, Hiyama E. Telomere and telomerase in stem cells. *Br J Cancer* 2007;96:1020-4.
3. Saeed H, Iqtedar M. Stem cell function and maintenance - ends that matter: Role of telomeres and telomerase. *J Biosci* 2013;38:641-9.
4. Chung SS, et al. Proinflammatory cytokines IL-6 and TNF- $\alpha$  increased telomerase activity through NF- $\kappa$ B/STAT1/STAT3 activation, and with aferin A inhibited the signaling in colorectal cancer cells. *Mediators Inflamm* 2017;2017:5958429.
5. Jäger K, Walter M. Therapeutic targeting of telomerase. *Genes* 2016;7:39.
6. Jafri MA, Ansari SA, Alqahtani MH, Shay JW. Roles of telomeres and telomerase in cancer, and advances in telomerase-targeted therapies. *Genome Medicine* 2016;8:69.
7. Gomez DLM, Armando RG, Cerrudo CS, Ghiringhelli PD, Gomez DE. Telomerase as a cancer target. Development of new molecules. *Curr Top MedChem* 2016;16:2432-440.
8. Lui L, et al. TERT promoter hypermethylation in gastrointestinal cancer: A potential stool biomarker. *Oncologist* 2017;22:1178-88.



---

## Directed evolution of cellulase from *Trichoderma reesei* for higher activity and development of microtiter plate assay based on cellobiose dehydrogenase

---

Nevena Zelenović<sup>1\*</sup>, Raluca Ostafe<sup>2</sup>, Rainer Fischer<sup>2</sup>, Radivoje Prodanović<sup>3</sup>

<sup>1</sup>*Institute for Chemistry, Technology and Metallurgy, University of Belgrade, Belgrade, Serbia*

<sup>2</sup>*Institute for Molecular Biotechnology, RWTH Aachen University, Aachen, Germany*

<sup>3</sup>*Faculty of Chemistry, University of Belgrade*

\**e-mail: zelenovic@ihmt.bg.ac.rs*

Cellulase (EC 3.2.1.4) are important enzymes in food, paper, textile, detergent and biofuel industries. Most cellulases have low activity and stability. Improving these properties would have substantial impact on numerous industrial processes. Enzymatic properties can be improved by directed evolution, but the screening process is the limiting step. Coupled cellulase assay has been developed in order to improve the screening process. This method does not require boiling samples and allows rapid screening of mutants in a microtiter plate. The aim of this study was to establish enzyme coupled assay where cellulase first hydrolyzes carboxymethylcellulose (CMC), and cellobioses dehydrogenase (CBDH) and dichlorophenolindophenol (DCPIP) is used subsequently for detection of reducing ends<sup>1,2</sup>. Cellulase gene (wt) derived from *Trichoderma reesei* was cloned in the pESC-TRP vector, and expressed in the yeast *S. cerevisiae*. Obtained heterologous protein is used to optimize enzymatic assay conditions, including pH optimum, CMC concentration, and CBDH amount. Libraries were obtained using semi-rational design and mutations were introduced in catalytic site of cellulase<sup>3</sup> as can be observed in the Figure 1.

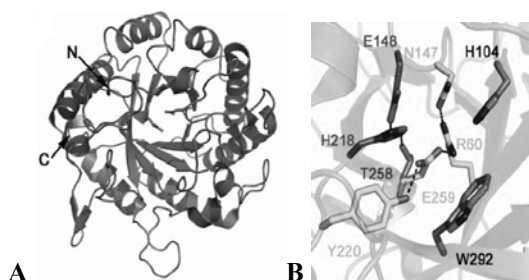


**Figure 1.** A: 3D structure of cellulase; B: Catalytic site of cellulase.

Libraries were screened for mutants by previously optimized assay. Selected mutants showed increased cellulase activity as can be observed in the Figure 2.

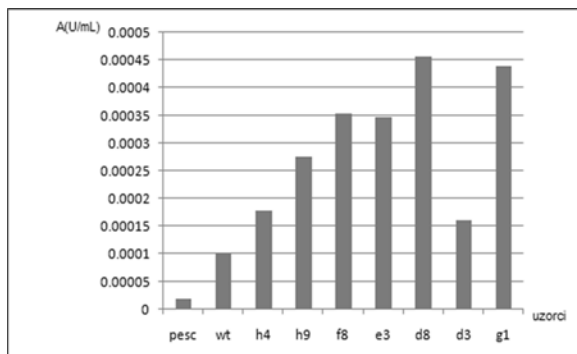


**Figure 2.** The activity of wild-type cellulase and selected mutants.

Cellulase gene (wt) has been recloned in pCTcon2 vector because it allows for expression on the yeast surface. Also, the library was created in this vector by introducing random mutations using error prone PCR. The gene library was screened with the aforementioned assay and mutants with higher cellulase activity were selected. The aim of this study was to obtain cellulase expressed on the yeast surface in order to develop fluorescent assay applied in flow cytometry.

Cellulase was successfully produced in *S. cerevisiae*, and libraries yielded mutants with increased cellulase activity. Developed assay allowed us a quick and efficient way of scanning aforementioned gene libraries.

## Acknowledgements

This work was supported by Grant No. III46010 and Grant No.43009, sponsored by the Ministry of Education and Science, Republic of Serbia and the Fraunhofer Institute in Chile.

## References

1. Ostafe R, Prodanovic R, Lloyd Ung W, Weitz DA, Fischer R. A high-throughput cellulase screening system based on droplet microfluidics. *Biomicrofluidics* 2014;8:041102.
2. Canevascini G. A cellulase assay coupled to cellobiose dehydrogenase. *Anal Biochem* 1985;147:419-27.
3. Lee TM, Farrow MF, Arnold FH, Mayo SL. A structural study of *Hypocrea jecorina* Cel5A. *Protein Sci* 2011;20:1935-40.

---

## Structural characterization of EPS produced by *Brachybacterium paraconglomeratum* sp. CH-KOV3

---

Aleksandra Žeradjanin<sup>1,2\*</sup>, Gordana Gojgić-Cvijović<sup>1</sup>, Dragica Jakovljević<sup>1</sup>, Branka Lončarević<sup>1</sup>, Miroslav M. Vrvic<sup>2</sup>, Vladimir P. Beškoski<sup>2</sup>

<sup>1</sup>Department of Chemistry, Institute of Chemistry, Technology and Metallurgy, University of Belgrade, Belgrade, Serbia

<sup>2</sup>Department of Biochemistry, Faculty of Chemistry, University of Belgrade

\*e-mail: adjuric@chem.bg.ac.rs

Microorganisms isolated from polluted environments can be used for bioremediation<sup>1</sup>. However, some of microbial isolates can synthesize various exopolysaccharides (EPSs)<sup>2,3</sup>. This non-toxic, natural, and biodegradable polymers can be used in different industries such as food and cosmetic as water-binding and gelling agents, as probiotics, sweeteners, thickeners, stabilizers. In waste water treatment today they are used as heavy metal removal agents<sup>4</sup>. In medicine EPS have a potential antiviral, immunostimulatory and antitumor activities<sup>5,6</sup>.

The aim of this work was structural characterization of EPS produced by *Brachybacterium paraconglomeratum* sp. CH-KOV3. For the structural instrumental analysis of EPS, the following methods were applied: GC-MS (gas chromatography mass spectrometry) and correlated two-dimensional NMR (nuclear magnetic resonance) techniques - DEPT 135 (distortionless enhancement by polarization transfer), COSY (correlation spectroscopy), and HSQC (heteronuclear single quantum coherence). Methylation was performed by the method which described earlier<sup>7</sup>. The permethylated EPS was subjected to reductive cleavage as described by Rolf and Gray<sup>8</sup>. Cleaved monomer units were acetylated. Obtained acetylated, methylated products were analyzed by GC-MS. These analyses were performed on a GCxGC-MS (Shimadzu, Kyoto, Japan). NMR spectra of the isolated EPS were measured on a Bruker AVANCE III 500 spectrometer.

GC-MS analysis - three sets of two peaks were identified<sup>8,9</sup>. First set represented fructofuranoses with (2,6)-linkages and referred to the main chain. Second set of peaks corresponded to the nonreducing terminal units of the glycan molecules. Third set also had two retention times. The identified peaks corresponded to the fructosyl residues that indicate the (2,1) branching of the polysaccharide chain. GC-MS analysis of methylation products suggest that the units in the main chain are (2,6)-linked, the main chain was substituted with single d-fructofuranoses at position O-1. Polysaccharide was of moderate branching.

DEPT 135 spectrum which was used to determine the degree of hydrogenation of each carbon showed intense signals corresponded to CH protons of C-5, C-3 and C-4; CH2

protons of C-6 and C-1. The part of the COSY spectrum of isolated EPS, showed cross peaks H6a/H6b, H5/H6b, H4/H5 and H3/H4 and the absence of any correlation peaks in the region 3.6-3.8 ppm<sup>10</sup>. HSQC spectrum indicates direct correlations between carbons of the sugar units and skeleton protons. Diagnostic cross peaks H5/C5, and H6a, H6b/C6 were detected, and their values are similar to the values of another levan-type fructan<sup>11</sup>.

In conclusion, EPS produced by *Brachy bacterium paraconglomeratum* sp. CH-KOV3 is a levan-type polysaccharide.

## Acknowledgements

This work was supported by the Ministry of Education and Science, Republic of Serbia, Project No. III 43004, and Japan International Cooperation Agency (JICA) grassroot project "Capacity building for analysis and reduction measures of persistent organic pollutants in Serbia".

## References

1. Bertrand JC, et al. Applied microbial ecology and bioremediation. In: Bertrand JC, Caumette P, Lebaron P, Matheron R, Normand P, Sime-Ngando T (eds) Environmental Microbiology: Fundamentals and Applications, Springer Netherlands, Dordrecht, 2015, pp 659-753.
2. Uzoigwe C, Grant Burgess J, Ennis CJ, Rahman PKSM. Bioemulsifiers are not biosurfactants and require different screening approaches. *Front Microbiol* 2015;6:245-50.
3. Kılıç NK, Donmez G. Environmental conditions affecting exopolysaccharide production by *Pseudomonas aeruginosa*, *Micrococcus* sp., and *Ochrobactrum* sp. *J Haz Mater* 2008;154:1019-24.
4. Öner ET. Microbial production of extracellular polysaccharides from biomass. In: Fang Z (ed) Pretreatment Techniques for Biofuels and Biorefineries: Green Energy and Technology, Springer, Berlin, 2013, pp 35-56.
5. Kang SA et al. Levan: applications and perspectives. In: Rehm BHA (ed) Microbial Production of Biopolymers and Polymer Precursors: Applications and Perspectives, Caister Academic Press, Norfolk, 2009, pp 145-61.
6. Liu C, Lu J, Lu L, Liu Y, Wang F, Xiao M. Isolation, structural characterization and immunological activity of an exopolysaccharide produced by *Bacillus licheniformis* 8-37-0-1. *Bioresour Technol* 2010;101:5528-33.
7. Ciucanu I, Kerek F. A simple and rapid method for the permethylation of carbohydrates. *Carbohydr Res* 1984;131:209-17.
8. Rolf D, Gray GR. Analysis of the linkage positions in D-fructofuranosyl residues by the reductive-cleavage method. *Carbohydr Res* 1984;131:17-28.
9. Simms PJ, Boyko WJ, Edwards JR. The structural analysis of a levan produced by *Streptococcus salivarius* SS2. *Carbohydr Res* 1990;208:193-98.
10. Tajima K, Uenishi N, Fujiwara M, Erata T, Munekata M, Takai M. The production of a new water-soluble polysaccharide by *Acetobacter xylinum* NCI 1005 and its structural analysis by NMR spectroscopy. *Carbohydr Res* 1997;305:117-22.
11. Matulová M, Husárová S, Čapek P, Sancelme M, Delort AM. NMR structural study of fructans produced by *Bacillus* sp. 3B6, bacterium isolated in cloud water. *Carbohydr Res* 2011;346:501-7.

## Notes

## Notes

## When protein stability matters.

---

Prometheus precisely characterizes thermal unfolding, chemical denaturation and aggregation with the most flexibility a system has to offer.



## When binding affinity matters.

---

Swiftly measure binding interactions using very little sample with the Monolith.

